POPULATION BIOLOGY OF THE TAN SPOT PATHOGEN OF PYRETHRUM

by

Tamieka Lee Pearce

B Agr Sc (Hons)

School of Land and Food

Submitted in fulfilment of the requirements for the

Degree of Doctor of Philosophy

University of Tasmania January 2016

This thesis contains no material which has been accepted for a degree or diploma by the University or any other institution, except by way of background information and duly acknowledged in the thesis, and to the best of my knowledge and belief no material previously published or written by another person except where due acknowledgement is made in the text of the thesis, nor does the thesis contain any material that infringes copyright.

This thesis may be made available for loan. Copying and communication of any part of this thesis is prohibited for two years from the date this statement was signed; after that time limited copying and communication is permitted in accordance with the Copyright Act 1968.

The publishers of the papers comprising chapters three and four hold the copyright for that content, and access to the material should be sought from the respective journals. The remaining non published content of the thesis may be made available for loan and limited copying and communication in accordance with the Copyright Act 1968.

The research associated with this thesis abides by the international and Australian codes on human and animal experimentation, the guidelines by the Australian Government's Office of the Gene Technology Regulator and the rulings of the Safety, Ethics and Institutional Biosafety Committees of the University.

Tamieka Lee Pearce

University of Tasmania

January 2016

Signed:

Date: 20-01-2016

TABLE OF CONTENTS

LIST OF TABLES

CHAPTER 3 TAN SPOT OF PYRETHRUM IS CAUSED BY A *DIDYMELLA* SPECIES COMPLEX

CHAPTER 4 MATING-TYPE GENE STRUCTURE IN *DIDYMELLA TANACETI* AND THEIR SPATIAL DISTRIBUTION IN PYRETHRUM FIELDS

CHAPTER 5 FINE SCALED POPULATION GENETIC ANALYSIS OF *DIDYMELLA TANACETI*

LIST OF FIGURES

CHAPTER 2 LITERATURE REVIEW

CHAPTER 3 TAN SPOT OF PYRETHRUM IS CAUSED BY A *DIDYMELLA* SPECIES COMPLEX

CHAPTER 4 MATING-TYPE GENE STRUCTURE IN *DIDYMELLA TANACETI* AND THEIR SPATIAL DISTRIBUTION IN PYRETHRUM FIELDS

CHAPTER 5 FINE SCALED POPULATION GENETIC ANALYSIS *OF DIDYMELLA TANACETI*

CHAPTER 6 CHARACTERISATION OF BOSCALID SENSITIVITY IN *DIDYMELLA TANACETI*

ACKNOWLEDGEMENTS

Firstly I must thank Drs Sarah Pethybridge and Jason Scott for introducing me to molecular plant pathology when I was an impressionable third year undergraduate student. As a student, who at that stage, disliked plant pathology I am still somewhat bemused by the fact that I have completed and thoroughly enjoying both an honours and PhD project in this area.

I would like to gratefully acknowledge the funding provided by Botanical Resources Australia and pyrethrum growers through the Pyrethrum R & D Committee and from the Commonwealth Government through the Australian Research Councils Linkage funding scheme to undertake the projects included in this thesis. I am further grateful to the pyrethrum growers for access to their fields for sampling and Mr Tim Groom for his support as an industry supervisor and assistance with any agronomical queries. I would also like to thank the University of Tasmania for financial support through an Australian Postgraduate Award and the Cuthbertson Elite Tasmania Graduate Research Scholarship, both which supported me throughout my candidature. In addition, the University of Tasmania's Conference and Research Travel Funding scholarship allowed me to present aspects of my research at the joint American Phytopathological Society and Canadian Phytopathological Society conference in Minneapolis in August 2014.

I am extremely grateful to my supervisory team of Drs Jason Scott, Frank Hay, Sarah Pethybridge and A/Prof. Calum Wilson. Jason, as the only supervisor on site in the past 18 months, you have had the "pleasure" of being the first call for enquires, good news, bad news and the odd R related question. I sincerely thank you for all your guidance and support throughout my candidature. Frank and Sarah, the knowledge that you have both brought to

my research, from over 20 years of plant pathology research in the pyrethrum industry is invaluable. I have enjoyed being able to work alongside you both. I am further grateful for your comments and suggested improvements of manuscript and thesis drafts. Calum, thankyou for joining my supervisory team in 2014 following the relocation of Frank and Sarah to Cornell University. I appreciate the input you provided for the structure of the experimental chapter examining fungicide resistance. In addition, your comments on manuscripts and thesis drafts chapters were much appreciated.

I am further thankful to Prof. Dr. Pedro Crous for all his assistance with the phylogenetic analyses that was undertaken, as well as his comments on the draft manuscript of the first experimental chapter.

I would like to thank all the staff from the Tasmanian Institute of Agriculture (TIA) at the University of Tasmania's Cradle Coast campus for creating such a positive and supportive environment to work in. Our plant pathology department may be only made up of a small group of people, but I think we are able to accomplish a great deal (quality not quantity!). I would like to especially thank Craig Palmer and Phil Beveridge for their assistance in the collection of field samples, and Stacey Pilkington and Pattie Weichelt for assistance with fungal isolations and laboratory work.

Finally, I could not have completed this thesis without the constant support of my wonderful family and friends. I would like to especially thank Stacey for all your support, encouragement and friendship. However, my greatest thanks must go to Lachy, who has

always encouraged me and never doubted my ability to complete my PhD even when things weren’t going my way.

ABBREVIATIONS

a.i	active ingredient
aa	amino acid
ACT	actin
AFLP	Amplified fragment length polymorphism
AGRF	Australian Genome Research Facility
AIC	Akaike Information Criterion
AMOVA	Analysis of molecular variance
APN2	apurinic/apyrimidinic endonuclease 2 protein
BI	Bayesian Inference
BOC	British Oxygen Company
bp	base pair
BRA	Botanical Resources Australia
CADM	Congruence Among Distance Matrices
CDD	conserved domain database
CDS	coding sequence
CIG	Commonwealth Industrial Gases
cm	centimetre
CT	cycling threshold
d	days
D/G	genotypic diversity
DLP	DNA lyase-like protein
DNA	deoxyribonucleic acid
dNTP	deoxyribonucleotide triPhosphate
E_5	genotypic evenness
eMLG	number of expected genotypes
ENA	effective number of alleles
FDR	false discovery rate

FRAC	Fungicide Resistance Action Committee
GAP	GTPase activator-like protein
GAPDH	glyceraldehyde-3-phosphate-dehrydogenase
GTR+G	general time reversible nucleotide substitution model with gamma distribution rates
GTR+I	general time reversible nucleotide substitution model with a proportion of invariable sites
GTR+I+G	general time reversible nucleotide substitution model with a proportion of invariable sites and a gamma distribution
h	Nei's genetic diversity
HMG	high mobility group
hr	hour
HRM	high resolution melt
ICBN	International Code of Botanical Nomenclature
ITS	internal transcribed spacer unit of the ribosomal nucleic acid
kb	kilo-base
LDA	linear discriminant analysis
LOBF	line of best fit
LSU	large subunit 28S of nuclear ribosomal DNA
MAFFT	Multiple Alignment using Fast Fourier Transform
MAT/*MAT*	mating-type/mating-type genes
MAT1-1	individual with a *MAT1-1-1* mating-type gene
MAT1-1(II)	haplotype II of *MAT1-1*
MAT1-1-1	mating-type gene encoding an alpha domain
MAT1-2	individual with a *MAT1-2-1* mating-type gene
MAT1-2-1	mating-type gene encoding a high mobility group domain
MCMC	Markov chain Monte Carlo
Mbp	mega base pair
MEA	malt extract agar
MEB	malt extract broth

min	minute
MLGs	multilocus genotypes
m	meter
mg	milligram
ml	millilitre
mm	millimetre
mM	millimolar
MP	maximum parsimony
MSN	minimum spanning network
NA	not applicable
NC	not calculated
NCBI	National Centre of Biotechnological Information
ng	nanogram
NT	not tested
OA	oatmeal agar
ORF1	protein with a pyridoxamine 5'-phosphate oxidase
PAM	partitioning around medoids
PCA	principle components analysis
PCR	polymerase chain reaction
PCs	principle components
PDA	potato dextrose agar
PIC	polymorphic informative content
RAPD	Random Amplified Polymorphic DNA
$\bar{r}_d$	standardized index of association
RNA	ribonucleic acid
rpm	revolutions per minute
R_{xy}	Mantel’s correlation coefficient

S1	field sampled in Sassafras
S2	field sampled in Sassafras
SDHA/*SDHA*	succinate dehydrogenase subunit A/gene encoding succinate dehydrogenase subunit A
SDHB/*SDHB*	succinate dehydrogenase subunit B/ gene encoding succinate dehydrogenase subunit B
SDHC/*SDHC*	succinate dehydrogenase subunit C/ gene encoding succinate dehydrogenase subunit C
SDHD/*SDHD*	succinate dehydrogenase subunit D/ gene encoding succinate dehydrogenase subunit D
SDHI	succinate dehydrogenase inhibitor
SE	standard error
s	seconds
SNPs	single nucleotide polymorphisms
SSR	simple sequence repeat/microsatellite
SSU	small subunit 18S of nuclear ribosomal DNA
SYM+I+G	symmetrical nucleotide substitution model with a proportion of invariable sites and a gamma distribution
TAE	tris-acetate-EDTA
TAS	Tasmania
TC1	field sampled in Table Cape
TC2	field sampled in Table Cape
TIA	Tasmanian Institute of Agriculture
TUB2	β-tubulin
uh	Nei's unbiased gene diversity
µL	microlitre
µM	micromolar
UV	ultraviolet
WA	water agar
WT	wild type

ABSTRACT

Tan spot is one of the most significant foliar diseases of pyrethrum (*Tanacetum cinerariifolium*) in Tasmania, Australia. It is associated with tan coloured, necrotic lesions on leaves, stems and flower buds which result in a loss of green leaf area. Severe outbreaks can lead to plant death and termination of crops. Phylogenetic and morphological analysis of the causal pathogen, originally described as *Microsphaeropsis tanaceti,* resulted in reclassification of the pathogen as two closely related species of *Didymella,* namely *D. tanaceti* and *D. rosea*. Molecular differences between the two species were evident for four of the five genome regions examined. Furthermore, morphological differences in culture pigmentation and conidial size allowed rapid identification of the two species.

To elucidate explanations for the shift from a minor disease in 2001 to one of the most frequent and severe diseases of pyrethrum, the reproductive strategy and population structure of the dominant tan spot pathogen, *D. tanaceti* were investigated. Two first harvest fields in each of two regions, were intensively sampled in July/August 2012, using two 50 m transects in each field, to provide field populations of *D. tanaceti* for analysis. Tan spot incidence in these fields was high, with 325 isolates obtained from 800 sampling units.

Analysis of the structure and arrangement of mating-type (*MAT*) genes identified a putative heterothallic mode of reproduction for *D. tanaceti*, with either a single *MAT1-1-1* or *MAT1-2-1* gene occurring in *D. tanaceti* isolates. A multiplex *MAT*-specific PCR assay was developed and validated. This assay was utilised to quantify the number of *D. tanaceti* isolates of each *MAT* gene within the field populations. Isolates with a *MAT1-1-1* gene occurred in equal frequencies with isolates containing a *MAT1-2-1* gene. Significant spatial structure of isolates of each *MAT* gene in the fields was absent. Additionally, two haplotypes

of the *MAT1-1-1* gene, sharing 99.6% sequence homology, were identified. Isolates of the two haplotypes were differentiated using a restriction enzyme digest of the *MAT1-1-1* amplicon. Within the field populations, haplotype I was dominant, occurring in 95.6% of isolates with a *MAT1-1-1* gene. These results suggested that the occurrence of a cryptic sexual reproduction cycle in Tasmanian pyrethrum fields could not be dismissed. However, *in vitro* crosses between compatible isolates failed to produce ascospores, suggesting that specific environmental conditions and temporal requirements were necessary.

To assess the genetic structure of *D. tanaceti*, a set of polymorphic microsatellite (SSR) markers were identified based on sequence data obtained from genomic sequencing. The *D. tanaceti* field populations were genotyped using eight SSR markers, with alleles determined by high resolution melt analysis. Within the 317 isolates genotyped, 127 multilocus genotypes were identified, with 82 represented by a single isolate. Furthermore, high average genetic and genotypic diversity were identified within the field populations. However, genotypic spatial structure between regions, fields and within transects in each field were absent. Similar frequencies of alleles were observed for each marker in each of the fields. Evidence of high levels of genotypic migration between fields was also detected. These results suggested that individuals within these populations may have originated from a common genetic source, such as an alternative host or seed crop. Linkage disequilibrium was detected within fields. Thus, long distance dispersal of inoculum via ascospores may have only minimally contributed to disease incidence in these fields.

Control of tan spot has relied, mostly, on the use of boscalid, a succinate dehydrogenase inhibitor fungicide. Boscalid has been used widely in pyrethrum for control of multiple

pathogens. To initiate the characterisation of the molecular mechanisms associated with the observed boscalid resistant phenotypes, the succinate dehydrogenase subunit B (*SDHB*) gene of *D. tanaceti* was sequenced. The *SDHB* gene sequences of isolates with varied *in vitro* growth responses to boscalid (different resistant phenotypes) were compared. The results revealed that a decreased sensitivity to boscalid was associated with the substitution of a highly conserved histidine residue at codon 277 with either tyrosine (H277Y) or arginine (H277R). These two substitutions have been shown to cause boscalid resistance in other fungal species. In addition, an isoleucine to valine (I279V) substitution occurred at codon 279, but was not correlated with a decreased sensitivity to boscalid. Both the H277Y and H277R substitutions were associated with isolates exhibiting moderately resistant (EC_{50} 0.5 – 5.0 µg a.i/mL), resistant (EC_{50} 5.0 – 50.0 µg a.i/mL) and highly resistant (EC_{50} 50.0 – 250.0 µg a.i/mL) phenotypes. No isolates with a boscalid susceptible phenotype (EC_{50} 0.0 – 0.5 µg a.i/mL) were associated with these substitutions. However, the association of isolates with a WT *SDHB* gene for each of the moderately resistant, resistant and highly resistant phenotypes restricted the ability to correlate the H277Y and H277R substitutions with the resistant phenotypes. This indicated that mutations in the succinate dehydrogenase subunit C (*SDHC*) and D *(SDHD*) genes, or other regions may also occur in *D. tanaceti*. To evaluate the extent of *SDHB g*ene mutations in the 2012 field populations, a high resolution melt analysis assay was developed and its ability to identify mutations in codons 277 and 279 of the *SDHB* gene verified. The majority of *D. tanaceti* isolates within the field populations contained a mutation in the *SDHB* gene. The H277Y substitution was the most dominant, occurring in 52.3% of isolates, while the H277R substitution occurred in 9.3%.

Overall this thesis has identified and characterised the pathogens associated with tan spot of pyrethrum in Australia; establishing them as two species (*D. tanaceti* and *D. rosea*) from the

genus *Didymella*. It has developed a collection of SSR markers and assays for the rapid identification of mating-type for use in future studies. Furthermore, it has initiated the characterisation of the molecular mechanisms associated with boscalid resistance and developed an assay for the rapid identification of *SDHB* alleles. Moreover, it has provided a greater understanding of population biology and structure of the dominant tan spot pathogen; *D. tanaceti* by the characterisation of intensively sampled field populations. While the specific reasons for the rapid increase in tan spot incidence and severity remain unclear, this study has identified possible factors which could be associated with it. Despite evidence against a frequent sexual cycle in the field populations, the high genotypic diversity within populations suggests *D. tanaceti* individuals have a high adaptive ability. The adaptive ability of the pathogen population was demonstrated by the development of insensitivity to the fungicide boscalid. However, it may have also provided *D. tanaceti* individuals with a competitive advantage (e.g. increased virulence) over other pyrethrum pathogens. Furthermore, the decreased efficiency of disease control from boscalid, due to the moderately high incidence of fungicide resistance, has undoubtedly played a significant role in increasing disease incidence. Thus, efficient long term control of the disease will need to be delivered from an integrated approach, incorporating methods to decrease inoculum loads and strategies based on alternation of fungicides in different resistance groupings with regular evaluation of the pathogen population for fungicide resistance.

INTRODUCTION

1.1 THE AUSTRALIAN PYRETHRUM INDUSTRY

Pyrethrum (*Tanacetum cinerariifolium)* is a perennial plant cultivated for the extraction of pyrethrins, which are concentrated within achenes on the surface of the seed (Grdiša et al., 2009). The pyrethrins are a collection of six naturally occurring esters which have insecticidal properties active against a large range of arthropods (Crombie, 1980, Crombie, 1995). The Australian pyrethrum industry currently supplies the majority of the world market demand for pyrethrins. However, as the global demand for pyrethrin based products increases, the Australian industry will need to increase production while remaining economically and environmentally sustainable. High yields are obtained through a highly mechanised production system and cultivar selection of high performing genotypes (Greenhill, 2007). Historically, due to its perennial nature, a typical pyrethrum crop would return four to five annual harvests before crop termination due to decreased productivity and economic returns. However, in more recent years, increased disease severity and resultant plant loss and regrowth decline in subsequent seasons has meant many crops provide only a single economic harvest before crop termination.

1.2 TAN SPOT OF PYRETHRUM

There are several fungal pathogens that cause root, foliar and flower diseases of pyrethrum (Hay et al., 2015, Pethybridge et al., 2003, Pethybridge et al., 2008a). Pyrethrum fields are monitored periodically to quantify the level of known pathogens and identify potential threats. During routine surveying in 2001, an unidentified pathogen was isolated at a low frequency from necrotic spots on stems, leaves and buds (Pethybridge et al., 2003). In subsequent years,

the isolation frequency of the unidentified pathogen increased in terms of the number of fields and the number of diseased leaves per field from which it was isolated (Pethybridge et al., 2008a). Morphological and limited molecular characterisation was used to identify the pathogen as a new species within the genus *Microsphaeropsis* (*Microsphaeropsis tanaceti*), and the disease associated with it was termed tan spot (Pethybridge et al., 2008b).

Tan spot is currently one of the major fungal diseases affecting pyrethrum in Tasmania, Australia (Hay et al., 2015). The disease has progressed from a predominately spring associated disease to one which also occurs at high frequency throughout autumn and winter (Hay et al., 2015, Pethybridge et al., 2008b). Several explanations for the shift from a minor disease to one of the most frequent and severe diseases of pyrethrum have been hypothesised. These included increased virulence or adaptive ability of the pathogen and increased disease transmission via infected seed or airborne sexual spores. Other means, such as a lack of efficacy of control due to the development of pathogen fungicide resistance have also been suggested. By examining various aspects of population structure and biology of the tan spot pathogen, alternative control options or improvements to the implementation of current practices could be identified.

1.3 THESIS AIMS

The research in this thesis aimed to further characterise the taxonomic identification of the pathogen associated with tan spot by incorporating new data that was not available at the time of the original identification. Furthermore, the reproductive strategy and genetic population

structure of the pathogen were evaluated. The genetic mechanisms governing sensitivities to the fungicide boscalid (Filan®; Nufarm Ltd.) and the prevalence of boscalid sensitivities within field populations were also examined.

1.3.1 Taxonomic classification of the tan spot pathogen

The original taxonomic description of the causal pathogen of tan spot as a member of the genus *Microsphaeropsis* was based on a limited number of isolates collected in 2004 and sequences from a single gene region; the internal transcribed spacer unit of the ribosomal nucleic acid (ITS) (Pethybridge et al., 2008b). Accuracy of identification was restricted at the time by the limited number of fungal species with gene sequence data available for nucleotide comparison. However, due to the decreased cost and increased performance of DNA sequencing platforms, and an increase in the number of deposits in nucleotide sequence databases such as GenBank (National Centre of Biotechnological Information) (Benson et al., 2015), the ability to access or produce reliable sequence data has dramatically improved. This has resulted in a large increase in the taxonomic revision of fungal groups, via the use of specific gene regions and a phylogenetic approach, rather than the historical approach based largely on morphological and host range characteristics, which have been shown to produce artificial classifications (Aveskamp et al., 2010, de Gruyter et al., 2009, Woudenberg et al., 2013). Taxonomic re-assessment of the tan spot pathogen (chapter 3) was undertaken for two reasons. Firstly, the ITS sequence data used for the initial pathogen identification recognised two haplotypes attributed to three single nucleotide polymorphisms (SNPs) (Pethybridge et al., 2008b). This variation questioned the classification of the two haplotypes as the same species (Nilsson et al., 2008, Schoch et al., 2012). It also questioned whether genetic differences identified in the ITS were consistent within other gene regions and if the

polymorphisms correlated to morphological differences *in vitro*. Secondly, the genus *Microsphaeropsis* is known to contain species which can be morphologically confused with species belonging to the genus *Coniothyrium* (Summerell et al., 2006, Verkley et al., 2014, Verkley et al., 2004). Recent studies have shown that molecular data provided a distinct separation of *Microsphaeropsis* and *Coniothyrium* species, with the genus *Microsphaeropsis* taxonomically situated within the family *Didymellaceae* (Aveskamp et al., 2010, Verkley et al., 2014). Phylogenetic analysis in this thesis aimed to confirm the taxonomic identity of the tan spot pathogen within the 18 representative groups of the *Didymellaceae* (Aveskamp et al., 2010), and examine the phylogenetic relationship between the haplotypes. In addition, morphological differences were recorded to identify specific phenotypic characteristics which would discriminate the two haplotypes in culture.

1.3.2 Population structure of the tan spot pathogen

Despite the rapid increase in infection frequency within pyrethrum fields, there is little knowledge of the diversity of the tan spot pathogen. Characterising pathogen populations could identify aspects which have contributed to the observed increase in disease frequency. Population studies require a sufficient number of isolates that adequately represent the populations they characterise. However, sufficient intensive sampling of field populations had not been conducted prior to the work in this thesis. Therefore, a large scale and intensively sampled population of the tan spot pathogen was collected. To allow regional and field comparisons, the population was collected under a hierarchical structure. Two 12-month-old, first harvest fields in each of two geographically separated pyrethrum growing regions were selected. To permit spatial analyses, the populations were collected along two 50 m transects in each field. Whilst not providing a temporal comparison, this population

and subsequent analyses provided a “snap shot” in time of the pathogen population. Moreover, it provided the ability to make inferences on the relative contribution of seed borne and localised plant to plant spread of disease inoculum.

1.3.3 Reproductive strategy of the tan spot pathogen

The complete reproductive cycle of the tan spot pathogen is unknown. Asexual reproduction, via the production of conidia, is known to occur frequently *in vitro* and within pyrethrum tissue (Pethybridge et al., 2008b). Conidia serve as an inoculum source allowing local disease spread via splash dispersal. However, the sexual morph has not been observed. The occurrence of a sexual cycle may provide the tan spot pathogen with a potentially advantageous method of long distance inoculum dispersal via airborne ascospores. Furthermore, recombination of beneficial alleles may produce individuals with increased fitness including, decreased susceptibility to fungicides, the ability to survive previously adverse conditions or increased virulence (McDonald & Linde, 2002). Thus, the occurrence and frequency of a sexual cycle in the tan spot pathogen could have a dramatic impact on the incidence and distribution of disease and implications for the timing of management methods. The potential for sexual reproduction was examined via three independent methods. The first identified the occurrence and arrangement of two of the genes necessary for sexual reproduction and their distribution within the 2012 field populations (chapter 4), the second examined the ability for the production of ascospores (chapter 4), and the third used statistical analysis to assess the probability of recombination within the 2012 field populations (chapter 5).

In ascomycetes, such as the tan spot pathogen, two mating-type (*MAT*) genes (*MAT1-1-1* and *MAT1-2-1*) exist that need to be concurrently expressed for the sexual cycle to be initiated. This thesis aimed to identify the mating-type genes and their arrangement within the tan spot pathogen, using a combination of published and newly designed polymerase chain reaction (PCR) primers. The structural arrangement of the *MAT* genes identifies the heterothallic or homothallic nature of the species, which has implications on the potential frequency and genetic outcomes of sexual reproduction. Furthermore, it aimed to develop a PCR based assay to allow rapid identification of the mating-type genes in isolates of the tan spot pathogen. Use of this assay to screen the 2012 population allowed the ratio and spatial distribution of isolates of each mating-type within each field and region to be examined. It also allowed the potential for interactions between isolates of each mating-type, which is required for sexual reproduction, to be analysed.

Although the ability to detect the two mating-type genes would provide partial evidence of sexual reproduction, identification of a sexual morph that produced fertile ascospores would be definitive evidence. Despite the lack of field observation of the sexual stage, it was hypothesised that under adequate controlled conditions *in vitro* the sexual morph could be induced. This experiment was designed to identify the specific environmental cues and time periods required for the initiation of a sexual reproduction cycle. Identification of such cues would allow the likelihood of sexual reproduction occurring in the field to be inferred.

1.3.4 Genetic characterisation of the tan spot pathogen

As an alternative approach to observing physical evidence of sexual reproduction, populations were examined for the historical occurrence of recombination using molecular markers. A range of molecular markers are available for such analysis. As a molecular marker set for the tan spot pathogen had not been developed, this thesis aimed to produce a set of markers which would allow discrimination of individuals. Microsatellite (SSR) markers were selected as they are highly polymorphic, abundant within genomes, species specific and well suited to analyses of recombination and genotypic diversity (Sunnucks, 2000). For discrimination of microsatellite alleles, this research tested the capability of high resolution melt (HRM) technology to detect alleles. Traditionally, microsatellite alleles are determined by fragment length analysis, in which the length of the amplified fragment is used to determine the number of repeats. One of the limitations of fragment length analysis is that it does not allow the presence of SNPs or combined insertion/deletion of nucleotides within the amplified regions to be differentiated, such that genetically different individuals are not always correctly identified. HRM analysis uses real-time PCR technology and the melting temperature profile of the PCR product, which is dependent on the nucleotide sequence. HRM is commonly used to detect SNPs within sequence data, as the presence of the SNP changes the melting profile of the DNA segment (Liew et al., 2004). It was hypothesised that the same concept could be applied to identify varying numbers of SSR repeats. Use of the SSR markers to screen the 2012 population and the subsequent analyses undertaken aided in answering questions regarding pathogen transmission, sexual reproduction and the amount and distribution of genotypic variation. It also addressed the degree of relatedness and the genetic structure of individuals and populations at regional, field and transect scales, and estimated the magnitude of gene flow between populations.

1.3.5 Fungicide resistance in the tan spot pathogen

Phenotypic diversity within the tan spot pathogen population, specifically differential susceptibility to fungicides, has been detected in isolates from various locations and sampling years (Hay et al., 2015, Pethybridge et al., 2008b). Since 2005 boscalid has been one of the main spring fungicides applied for controlling foliar diseases of pyrethrum. Boscalid is a succinate dehydrogenase inhibitor fungicide and inhibits respiration by binding to the succinate dehydrogenase enzyme (Hägerhäll, 1997, Fraaije et al., 2012). Boscalid resistant isolates of the tan spot pathogen were first identified in 2009, by examining the *in vitro* growth response of isolates to varying boscalid concentrations (Hay et al., 2015). High levels of fungicide resistance may have contributed to the recent increase in disease frequency and severity.

This research aimed to identify the extent of boscalid resistance within the 2012 population (chapter 6). However, *in vitro* fungicide testing is laborious, which limits the number of isolates which can be examined. Therefore, to facilitate this and allow the entire 2012 population to be tested, this thesis aimed to initiate the identification of the molecular basis of boscalid insensitive and develop a PCR based assay to identify the expected boscalid phenotype of isolates. A PCR based method allows high throughput analysis of isolates and discrimination of singular and compound mutations, which may result in similar resistant phenotypes. Such discrimination cannot be made from *in vitro* growth response testing. The succinate dehydrogenase enzyme is constructed from four protein subunits; SDHA – SDHD (Horsefield et al., 2006). Mutations within each of the subunits have been correlated with boscalid resistance in different fungal species (Avenot & Michailides, 2010, Sierotzki & Scalliet, 2013). However, mutations governing resistance in the *SDHB* gene have been well

documented (Avenot et al., 2012, Veloukas et al., 2011, Yin et al., 2011). Therefore, this thesis examined the *SDHB* gene of boscalid susceptible and resistant isolates to identify the mutations associated with resistance. Examining this gene region also identified if there was a need to examine the additional subunits for mutations (i.e. identification of isolates with a wild-type *SDHB* gene but a boscalid resistant phenotype).

1.4 THESIS STRUCTURE

The thesis is structured as a "thesis by publication" according to the guidelines provided by the School of Land and Food, University of Tasmania. It contains a literature review, followed by four experimental chapters, each encompassing a theme identified above. The experimental chapters have been formatted as journal manuscripts and are at various stages of submission and acceptance. Chapter 3 has been accepted for publication in *Plant Pathology*. Chapter 4 has been accepted for publication in *Phytopathology*. Chapter 5 is also intended to be submitted to *Phytopathology*. Chapter 6 has been formatted as a journal manuscript. For consistency, due the published/unpublished nature of different chapters, where work completed in previous chapters requires reference it has been cited as the thesis chapter it occurs in. Statements of co-authorship for each chapter are located in the appendices. The results of each experimental chapter are put into overall context in the General Discussion of this thesis. For consistency, a formatting theme based on *Plant Pathology* has been implemented throughout this thesis.

1.5 CONCLUSION

Overall the research presented in this thesis aimed to examine some key aspects which may have contributed to the increase in frequency of tan spot observed over the past decade. The collection and analysis of an intensively sampled population for multiple aspects, including the ratio and distribution of mating-type genes, genetic diversity and fungicide insensitivity allowed the implications and interactions between these aspects to be investigated.

1.6 REFERENCES

Avenot HF, Michailides TJ, 2010. Progress in understanding molecular mechanisms and evolution of resistance to succinate dehydrogenase inhibiting (SDHI) fungicides in phytopathogenic fungi. *Crop Protection* **29**, 643-51.

Avenot HF, Thomas A, Gitaitis RD, Langston Jr DB, Stevenson KL, 2012. Molecular characterization of boscalid and penthiopyrad resistant isolates of *Didymella bryoniae* and assessment of their sensitivity to fluopyram. *Pest Management Science* **68**, 645-51.

Aveskamp M, De Gruyter J, Woudenberg J, Verkley G, Crous PW, 2010. Highlights of the *Didymellaceae*: A polyphasic approach to characterise *Phoma* and related pleosporalean genera. *Studies in Mycology* **65**, 1-60.

Benson DA, Clark K, Karsch-Mizrachi I, Lipman DJ, Ostell J, Sayers EW, 2015. GenBank. *Nucleic Acids Research* **43**, 30-5.

Crombie L, 1980. Chemistry and biosynthesis of natural pyrethrins. *Pesticide Science* **11**, 102-18.

Crombie L, 1995. Chemistry of pyrethrins. In: Casida JE, Quistad G, eds. *Pyrethrum Flowers: Chemistry, Toxicology and Uses.* New York: Oxford University Press, 123-92.

De Gruyter J, Aveskamp MM, Woudenberg JHC, Verkley GJM, Groenewald JZ, Crous PW, 2009. Molecular phylogeny of *Phoma* and allied anamorph genera: Towards a reclassification of the *Phoma* complex. *Mycological Research* **113**, 508-19.

Fraaije BA, Bayon C, Atkins S, Cools HJ, Lucas JA, Fraaije MW, 2012. Risk assessment studies on succinate dehydrogenase inhibitors, the new weapons in the battle to control Septoria leaf blotch in wheat. *Molecular Plant Pathology* **13**, 263-75.

Grdiša M, Carović-Stanko K, Kolak I, Šatović Z, 2009. Morphological and biochemical diversity of Dalmatian pyrethrum (*Tanacetum cinerariifolium* (Trevir.) Sch. Bip.). *Agriculturae Conspectus Scientificus* **74**, 73-80.

Greenhill M, 2007. Pyrethrum production: Tasmanian success story. *Chronica* **47**, 5-8.

Hägerhäll C, 1997. Succinate: quinone oxidoreductases: variations on a conserved theme. *Biochimica et Biophysica Acta* **1320**, 107-41.

Hay FS, Gent DH, Pilkington SJ, Pearce TL, Scott JB, Pethybridge SJ, 2015. Changes in distribution and frequency of fungi associated with a foliar disease complex of pyrethrum in Australia. *Plant Disease* **99**, 1227-35.

Horsefield R, Yankovskaya V, Sexton G, *et al.*, 2006. Structural and computational analysis of the quinone-binding site of complex II (succinate-ubiquinone oxidoreductase) - A mechanism of electron transfer and proton conduction during ubiquinone reduction. *Journal of Biological Chemistry* **281**, 7309-16.

Liew M, Pryor R, Palais R, *et al.*, 2004. Genotyping of single-nucleotide polymorphisms by high-resolution melting of small amplicons. *Clinical Chemistry* **50**, 1156-64.

Mcdonald BA, Linde C, 2002. Pathogen population genetics, evolutionary potential, and durable resistance. *Annual Review of Phytopathology* **40**, 349-79.

Nilsson RH, Kristiansson E, Ryberg M, Hallenberg N, Larsson K-H, 2008. Intraspecific ITS variability in the kingdom fungi as expressed in the international sequence databases and its implications for molecular species identification. *Evolutionary Bioinformatics Online* **4**, 193.

Pethybridge S, Hay F, Groom T, 2003. Seasonal fluctuations in fungi associated with pyrethrum foliage in Tasmania. *Australasian Plant Pathology* **32**, 223-30.

Pethybridge SJ, Hay FS, Esker PD, *et al.*, 2008a. Diseases of pyrethrum in Tasmania: challenges and prospects for management. *Plant Disease* **92**, 1260-72.

Pethybridge SJ, Jones SJ, Shivas RG, Hay FS, Wilson CR, Groom T, 2008b. Tan spot: A new disease of pyrethrum caused by *Microsphaeropsis tanaceti* sp. nov. *Plant Pathology* **57**, 1058-65.

Schoch CL, Seifert KA, Huhndorf S, *et al.*, 2012. Nuclear ribosomal internal transcribed spacer (ITS) region as a universal DNA barcode marker for fungi. *Proceedings of the National Academy of Sciences* **109**, 6241-6.

Sierotzki H, Scalliet G, 2013. A review of current knowledge of resistance aspects for the next-generation succinate dehydrogenase inhibitor fungicides. *Phytopathology* **103**, 880-7.

Summerell BA, Groenewald JZ, Carnegie AJ, Summerbell RC, Crous PW, 2006. Eucalyptus microfungi known from culture. 2. *Alysidiella*, *Fusculina* and *Phlogicylindrium* genera nova, with notes on some other poorly known taxa. *Fungal Diversity* **23**, 323-50.

Sunnucks P, 2000. Efficient genetic markers for population biology. *Trends in Ecology & Evolution* **15**, 199-203.

Veloukas T, Leroch M, Hahn M, Karaoglanidis GS, 2011. Detection and molecular characterization of boscalid-resistant *Botrytis cinerea* isolates from strawberry. *Plant Disease* **95**, 1302-7.

Verkley G, Dukik K, Renfurm R, Göker M, Stielow J, 2014. Novel genera and species of coniothyrium-like fungi in *Montagnulaceae* (*Ascomycota*). *Persoonia: Molecular Phylogeny and Evolution of Fungi* **32**, 25.

Verkley GJ, Da Silva M, Wicklow DT, Crous PW, 2004. Paraconiothyrium, a new genus to accommodate the mycoparasite *Coniothyrium minitans*, anamorphs of *Paraphaeosphaeria*, and four new species. *Studies in Mycology* **50**, 323-36.

Woudenberg J, Groenewald J, Binder M, Crous P, 2013. *Alternaria* redefined. *Studies in Mycology* **75**, 171-212.

Yin YN, Kim YK, Xiao CL, 2011. Molecular characterization of boscalid resistance in field isolates of *Botrytis cinerea* from apple. *Phytopathology* **101**, 986-95.

LITERATURE REVIEW

2.1 PYRETHRUM

2.1.1 Botany

Tanacetum cinerariifolium (Trevir.) Sch. Bip. is an herbaceous perennial plant of the *Asteraceae* family (Compositae) (Grdiša et al., 2009). It is more commonly referred to as pyrethrum and is an economically important plant which is grown and harvested for the extraction of secondary metabolites called pyrethrins (Khater, 2012). Pyrethrum is tufted, slender and typically 30 to 100 cm high (Fig. 2.1). Leaves are alternate and pinnately lobed/narrowly lanceolate to oblong lanceolate (Pethybridge et al., 2008c). Flower buds are produced, following a period of vernalisation, on the terminal ends of multiple stems under a compound inflorescence (Brown & Menary, 1994). Each daisy-like flower comprises 2 types of sessile florets. Between 40 and 100 bisexual yellow disk florets are encircled by a ring of 18 to 22 white ray florets to produce the capitulum (Fig. 2.1). Each of the ray florets contains a white strap corolla which has three teeth at the terminus (Grdiša et al., 2009). Self-fertilisation is biologically discouraged by the discharge of ripe pollen prior to the unfolding of the receptive surface of the bi-lobed style (Grdiša et al., 2009). Outcrossing is further encouraged by a rapid decrease in germination of pollen following anthesis and sporophytic self-incompatibility inhibiting germination or tube growth of the tri-nucleated pollen on the stigma (Grdiša et al., 2009, Bhat, 1995). Pollination is carried out predominately via *Hymenoptera* insect vectors (Grdiša et al., 2009). These mechanisms result in pyrethrum populations that are genetically and morphologically diverse (Grdisa et al., 2014). Fertilisation results in fruit containing a single achene, within the solitary inferior ovary, of the ray and disk florets (Bhat, 1995). The fruits are pale brown, cylindrical or semi-cuneiform, 3.5 to 4.0 × 1.2 to 1.4 mm. Each achene has 5 to 7 ridges, containing secretary

lacunae (Bojnanský & Fargašová, 2007), in which the pyrethrins accumulate at high concentrations.

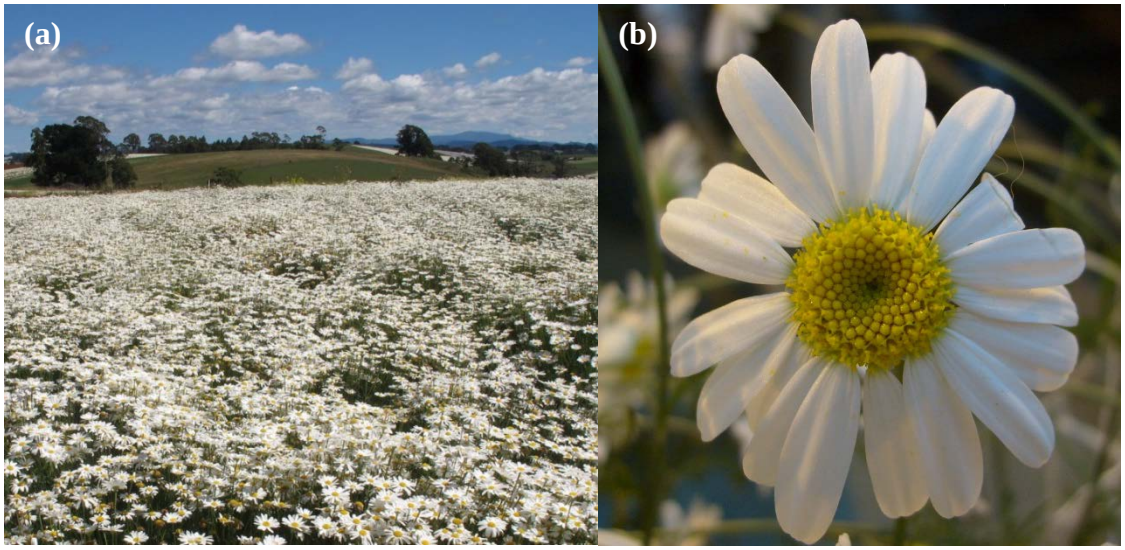

Fig. 2.1. (a) Pyrethrum field in full flower; (b) pyrethrum capitulum.

2.1.2 Pyrethrins

The pyrethrins collectively comprise six closely related esters (Fig. 2.2). Each ester differs only in the terminal substituent on the side chain of their alcohol and acid component (Casida, 1980). The pyrethrins, cinerins and jasmolins contain the alcohols pyrethrolone, cinerolone and jasmonoline, respectively (Casida, 1980). The acid component is used to group the esters into two fractions. Pyrethrin I, cinerin I and jasmolin I are esters of chrysanthemic acid and are collectively termed the pyrethrins I fraction. Pyrethrin II, cinerin II and jasmolin II are

esters of pyrethric acid and are collectively termed the pyrethrins II fraction (Grdiša et al., 2009).

Pyrethrins are localised within secretory lacunae on the surface of the achenes. However, they also accumulate throughout the aerial components of the plant, but are intensified in the achenes at concentrations 10 to 20 times higher than in the leaves (Head, 1966). Within the flower, 93.7% of pyrethrins accumulate within the achenes, with 2.6% in the ray florets and receptacles and 2.0% in the disk florets (Grdiša et al., 2009). The biochemical pathways of pyrethrin production and genetic control of these mechanisms in *T. cinerariifolium* have been examined (Ramirez et al., 2012). Results indicated that the biosynthesis of the pyrethrins begins within trichomes on the pericarps of the achenes. Pyrethrin intermediates produced in the trichomes are exported and used in the pericarps to synthesize the pyrethrins. These accumulate in the intercellular spaces and are absorbed by the desiccating embryo (Ramirez et al., 2012).

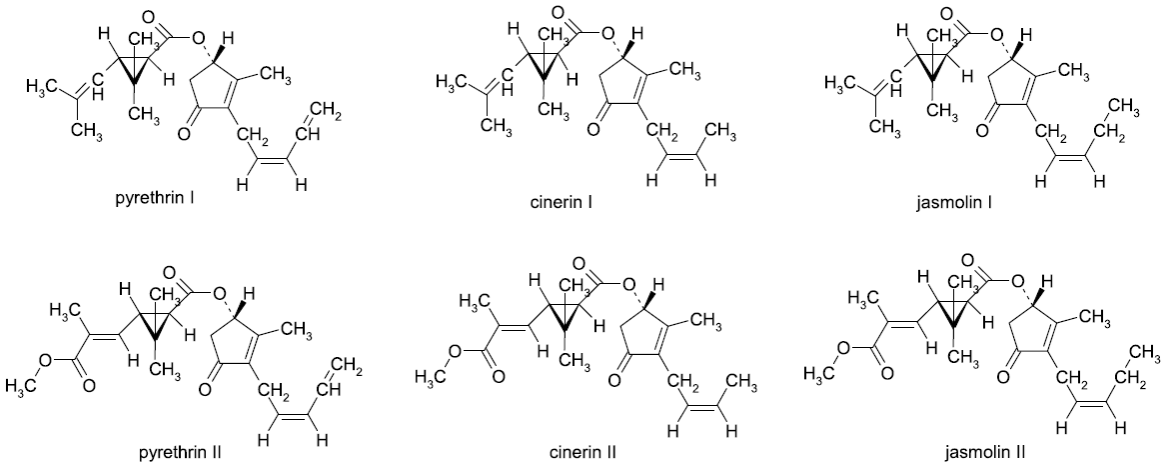

Fig. 2.2 Chemical structure of pyrethrin I, pyrethrin II, cinerin I, cinerin II, jasmolin I and jasmolin II. Reproduced from Grdiša et al. (2009).

The pyrethrins act as an anoxic poison, acting on the sodium channels of the synapses and affecting both the peripheral and central nervous symptoms of arthropods (Soderlund, 1995, Khater, 2012). The structure and stereo chemical characteristics of the alcohol and acid components result in the pyrethrins I fraction having a lethal kill effect and the pyrethrins II fraction a knockdown (repellent) effect against a large range of arthropod insects (Grdiša et al., 2009, Casida, 1980). Furthermore, the pyrethrin I and pyrethrin II components occur at a higher concentration, and are more active, than the jasmolin and cinerin components (Crombie, 1995, Head, 1966). Thus, the ratio of pyrethrin I to pyrethrin II is important as it determines the quality (kill effect) of the extract. A typical extract contains 38% pyrethrin I, 35% pyrethrin II, 7.3% cinerin I, 11.7% cinerin II, 4% jasmolin I, and 4% jasmolin II (Crombie, 1995). However, the ratio vary depending on the geographical source, plant type and time of harvest (Crombie, 1995). In a study of 25 natural pyrethrum populations from Croatia, Grdiša et al. (2009) found the pyrethrin I:pyrethrin II ratio ranged from 0.64 to 3.33 and the total pyrethrins content was positively correlated with the percentage of pyrethrin I, and negatively correlated with cinerin II.

The commercial use of insecticides containing pyrethrins has increased in recent years, with many consumers and industries preferring a natural bio insecticide over more common synthetic chemicals. Pyrethrum is currently the predominant botanical used in the world (Khater, 2012, Isman et al., 2005). This preference can be attributed to a range of characteristics, including the breakdown of the pyrethrins in ultra-violet light and a low level of mammalian toxicity when in its commercial form compared to other chemical products, including the synthetic pyrethroids (Casida & Quistad, 1995). Studies have shown that following application of pyrethrins, low residues were detected in both soil and water run-off

(Antonious et al., 2004, Antonious et al., 1997). Furthermore, the half-life of pyrethrins applied on field grown tomato and bell pepper was less than 2 hours (Antonious, 2004). While the rapid breakdown may potentially limit their use in agriculture and forestry, the decreased environmental persistence also decreases the chance of insect resistance developing. Very few cases of specific resistance to pyrethrins have been described, and many insect populations which are resistant to the synthetic pyrethroids remain susceptible to pyrethrins (Duchon et al., 2009, Cochran, 1995). Additionally, pyrethrins are one of the few insecticides permitted for pest control on certified organic farms (Jordan, 2004, Kuhne et al., 2013).

2.1.3 History and current production regions

The first historical record of pyrethrum dates back over 2000 years to the time of China's Chou dynasty (Greenhill, 2007). From the late 19th century until World War I, pyrethrum was predominately grown in Dalmatia (current day Croatia). It's insecticidal properties were recognised and it was traded under the name of "Dalmatian flea powder" in Europe for the control of mosquitos and body lice on humans and animals (Grdiša et al., 2009, Glynne-Jones, 2001). Commercial cultivation of pyrethrum spread globally following World War I. Pyrethrum was introduced into highland areas of East Africa, including Kenya, Tanzania, Zaire and Rwanda in the late 1920s (Wainaina, 1995). The cool climate, high altitude, well drained soils and even rain distributed throughout the year in these regions resulted in high flower and pyrethrin yields. By 1940, Kenya became the main global producer of pyrethrum and remained so for just over 60 years.

The production system in Eastern African is made up of 50 – 60,000 small scale farms (Greenhill, 2007). The majority of these farms are less than an acre in size and the growers rely on the pyrethrum as their main source of income. Growing pyrethrum in these regions is labour intensive. Crops are established by hand via vegetative propagation of pyrethrum seedlings. In addition, flower heads are manually harvested by hand over a 10 month flowering period. Flowers are air dried in the sun and transferred to factories for processing. Throughout the past 60 years Kenya has been unable to maintain a consistent supply of pyrethrum (MacDonald, 1995). Periodic shortages in the world supply of pyrethrum provided the opportunity for the establishment of commercial pyrethrum production in several other countries (Greenhill, 2007). Currently, pyrethrum is produced in ten countries including: Kenya, Australia, Papua New Guinea, Tanzania, Rwanda, France, Chile and Ecuador (Grdiša et al., 2009).

The pyrethrum supply market is currently dominated by pyrethrum produced in Kenya and Australia, by the Pyrethrum Board of Kenya (PBK) and Botanical Resources Australia Pty Ltd., respectively (Greenhill, 2007). While production in Australia was originally based on the Kenyan system, over 40 years of research and development has resulted in a substantially different commercial operation. In Australia, a highly mechanised system is implemented which has increased the sustainability of a continuous supply of pyrethrum on the global market and opened additional markets to increase demand for the product.

2.1.4 Production in Australia

The earliest report of pyrethrum production in Australia was in the lower Latrobe River Valley in Victoria prior to 1895 (MacDonald, 1995). Attempts to cultivate pyrethrum as a commercial crop began in 1932 and continued until 1952. Trials were conducted in Canberra, New South Wales and Tasmania by the Commonwealth Scientific and Industrial Research Organisation (CSIRO). However, the high cost of production restricted the ability of Australian grown commercial pyrethrum to compete with pyrethrum exported from the East African countries. The turning point for the formation of a commercial pyrethrum industry in Australian began with the establishment of a pyrethrum breeding program in the late 1970s by Drs R. Menary and K. Bhat at the University of Tasmania (MacDonald, 1995). The research from this program overcame previous issues derived from the introduction of inferior planting material, such as low flower and pyrethrin yields. High yielding, uniform plants which were able to be mechanically harvested were developed by selecting clones which exhibited several traits including synchronous flowering, even and upright presentation and high yields of pyrethrins per plant (Bhat & Menary, 1984, Bhat, 1995). Momentum during this period for the continued perseverance of a commercial industry in Australia was encouraged by a global shortage and increased demand for pyrethrins from the United States of America (MacDonald, 1995). The Australian pyrethrum industry progressed from trial status to a commercial industry in 1988 under the control of the Commonwealth Industrial Gases (CIG); a subsidiary of the British Oxygen Company (BOC) (Mac Donald 2005). By 1992, Australia had become the second largest global producer of pyrethrum behind Kenya. The ownership of the Tasmania pyrethrum industry was sold in 1996 to Botanical Resources Australia (BRA) (Greenhill, 2007). Botanical Resources Australia continued to expand and evolve the industry and by 2010 Australia was producing 60% of the world's pyrethrum demand (Pethybridge et al., 2010). Among their research accomplishments was a doubling of

pyrethrum yields, measured in kilograms of pyrethrins per hectare, from 1994 to 2007 (Greenhill 2007).

The majority of Australia's pyrethrum production occurs in the north west of Tasmania (Fig. 2.3a), where it provides a perennial component of many mixed farming systems. In Tasmania, pyrethrum is predominately (80%) grown between Deloraine (41° 31' S; 146° 3' E) and Table Cape (40° 56' S; 145° 43' E) in the north-west of Tasmania (Pethybridge *et al.*, 2008b) (Fig. 2.3b). However, when Tasmania's pyrethrum growing area began to reach full capacity in 2002 – 2003, BRA began investigating the potential of pyrethrum production in Ballarat, Victoria (37° 56' S; 143° 87' E), to ensure a stable supply of product in the medium to long term. Trial production was successful and 300 hectares of pyrethrum were planted in Ballarat in 2009 to combat an increase in world pyrethrum demand. An additional 275 hectares were planted in Ballarat in 2010 (BRA, 2010). Pyrethrin produced in Ballarat is partially processed and transported to BRA's processing plant in Tasmania for extraction of the pyrethrins.

2.1.5 Cultivation in Tasmania

A standard pyrethrum production cycle in Tasmania begins with precision direct seeding, from July to September (Pethybridge et al., 2008c). Prior to the initiation of floral buds a period of vernalisation is required. Night temperatures of less than 18°C are required to provide the vernalisation stimulus (Brown, 1992). Brown (1992) demonstrated that two weeks at 6°C or three weeks at 12°C was the minimum vernalisation requirement under short days, where day temperatures remained between 20 and 30°C (Brown, 1992). Following

germination, pyrethrum plants undergo a juvenile growth stage until these requirements are obtained by the winter of the following season (June to August). Bud initiation and flowering occurs in the subsequent spring (September to November). Therefore, the crop is first harvested in December to January of the following year (15-17 months after sowing). Once the crop is visibly senescing, it is cut and windrowed. Crops are mechanically harvested once the crops reach 10% moisture using a specially designed combine harvester (Greenhill, 2007, Morris et al., 2006). The period between cutting and harvesting is typically 2 weeks, with the pyrethrins remaining stable *in planta* during this period (Morris et al., 2006). The harvested material is processed at BRA's processing plant at Ulverstone, Tasmania. The material is passed through a hammer mill prior to pelletising (Greenhill, 2007). Botanical Resources Australia uses a two-step process to extract the pyrethrins from the pelletised material. A hexane extraction is undertaken, followed by a refining process which uses carbon dioxide as

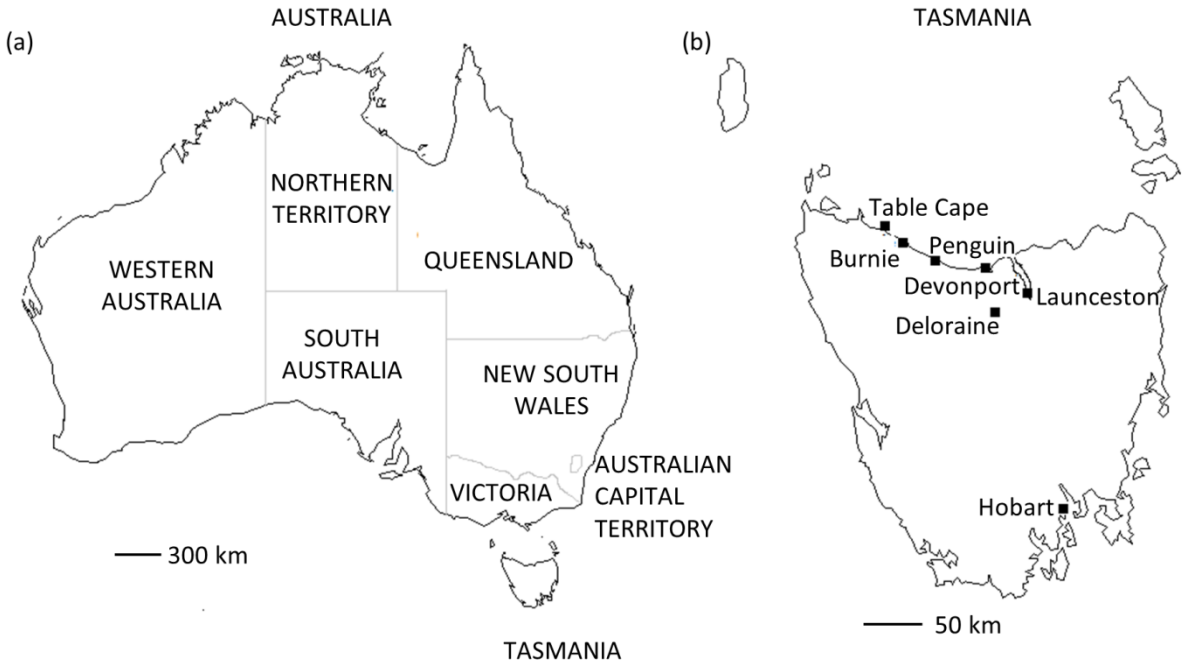

Fig. 2.3. Geographical map of (a) Australia and (b) Tasmania. Scale bars indicate distance.

viscous oleoresin containing approximately 30% pyrethrins. The carbon dioxide refining process produces a final refined pyrethrum extract which is a clear light amber/yellow liquid with a faint flowery fragrance (Ryan et al., 2002). The refined product is standardised to 50% pyrethrins using a deodorised solvent as the diluent (Greenhill, 2007).

Following the first harvest, pyrethrum plants regrow into compact bushes and remain semi-dormant until the following spring, at which time multiple stems are produced from each plant and bud initiation develops, followed by flowering (Pethybridge et al., 2008c). Historically, Tasmania pyrethrum crops typically yielded up to four harvests under optimal conditions. However, in many instances crops are terminated after first harvest due to weed and disease pressure. It is hoped that identification of the key drivers of yield will allow increases in yield and therefore gross margin, allowing pyrethrum to remain competitive with other agricultural crops in Tasmania.

2.2 AGRONOMICAL ISSUES AFFECTING PYRETHRUM

Two agronomical issues that remain problematic for pyrethrum production systems are weed and disease control. High incidence of either in crops result in a decreased yield and can lead to early crop termination. Management strategies to control weed and disease issues are complex and dependent on a range of integrated factors and are therefore designed on a “per field” basis.

2.2.1 Weed management

The perennial nature of pyrethrum has two issues for weed control. Firstly, following seedling establishment and during crop regrowth following harvest, there is an increased opportunity for competition between pyrethrum and weed species. This can be controlled, in part, by pyrethrum sowing densities. However, high planting densities can create microclimatic conditions within the crop canopy which are conducive for disease.

Following planting, there is a limited ability to control weeds with cultivation (Rawnsley et al., 2006). Weed removal by hand remains common practice, but is labour intensive. Thus, weed control in pyrethrum is mainly chemical based. A number of herbicides are registered for use in pyrethrum. However, due to the physiological nature of pyrethrum, some herbicides have a negative impact on pyrethrum health (Hocombe & Kroll, 1962), which limits the chemical control options. Additionally, for crops which have a high incidence of weeds at harvest, the cutting, windrowing and harvest processes can aid in dissemination of weed seeds throughout the crop, causing weed issues in subsequent seasons. Additional non-chemical control options are being investigated, as are mechanisms of herbicide application, which may increase the number of herbicides which can be used in pyrethrum to combat weeds (T. Groom, per. comms.). Plant death due to disease also provides opportunities for weeds to outcompete the pyrethrum. Subsequently, weeds within pyrethrum can act as alternative hosts for pathogens (Pethybridge et al., 2008c).

2.2.2 Diseases

Pathogens cause a complex of root, foliar and flower diseases in pyrethrum. The prevalence of specific diseases varies temporally and affects pyrethrum at different stages of plant development (Pethybridge et al., 2008c, Hay et al 2015). Furthermore, the perennial nature allows pathogens to undergo polyetic disease epidemics throughout the life of the crop and the potential to build up large amounts of inoculum for infection in subsequent seasons.

Root diseases of pyrethrum are poorly understood. However, lesion nematodes (*Pratelenchus* spp. including *P. crenatus*, *P. penetrans*) have been associated with damaged pyrethrum roots (Hay et al., 2001, Hay et al., 2009). The damage caused by these species results in a decrease in the yield of roots, foliage and pyrethrins (Hay et al., 2001).

Pyrethrum is deleteriously affected by a complex of foliar diseases, including ray blight caused by *Stagonosporopsis tanaceti* (Pethybridge & Wilson, 1998, Vaghefi et al., 2012); tan spot caused by *Microsphaeropsis tanaceti* (Pethybridge et al., 2008e); crown rot caused by *Sclerotinia minor* and *Sclerotinia sclerotiorum* (Scott et al., 2014, Pethybridge et al., 2008c); anthracnose caused by *Colletotrichum tanaceti* (Barimani et al., 2013); pink spot caused by *Stemphylium botryosum* (Pethybridge et al., 2004, Pethybridge et al., 2008c) and winter blight caused by *Alternaria* spp. (Pethybridge et al., 2004, Pethybridge et al., 2008c). In addition, *Paraphoma chrysanthemicola* and *Itersonilia perplexans* cause un-named foliar diseases (Hay et al., 2015). Furthermore, several other fungi, including *Cladosporium cladosporioides* and *Ulocladium atrum* are also commonly isolated from pyrethrum tissue, but are proposed to be saprophytes (Pethybridge et al., 2003, Pethybridge et al., 2004).

Flower disease cause significant annual losses of flowers, resulting in a subsequent decrease in pyrethrum yield. The two most common flower diseases are Sclerotinia flower blight caused by *Sclerotinia sclerotiorum* and Botrytis flower blight caused by *Botrytis cinerea* (Pethybridge et al., 2008c, Pethybridge et al., 2010). However, in recent years, *Sclerotinia minor* (O'Malley et al., 2015), *M. tanaceti*, *Stagonosporopsis tanaceti* and *Itersonilia perplexans* have also been isolated at low frequencies from flowers (J. Scott and F. Hay, unpublished data).

A number of pathogens have also been identified as seed borne. Pethybridge et al. (2006) identified 14 fungal species regularly associated with non-sterilised and surface sterilised pyrethrum seed. These included a number of known foliar pathogens: *Stagonosporopsis tanaceti*, *Microsphaeropsis tanaceti*, *Stemphylium botryosum* and *Alternaria tennuissima.* Transmission of the pathogen from the seed to the seedling has only been minimally examined for *Stagonosporopsis tanaceti* (O'Malley, 2007) and *Microsphaeropsis tanaceti* (J. Scott, unpublished data), with results suggesting that seedlings produced from infected seed are often asymptomatic. However, the frequency of isolation of *Stagonosporopsis tanaceti* and severity of defoliation from ray blight have been significantly correlated with the incidence of seed contamination (Pethybridge et al., 2011). It has been proposed that the *Stagonosporopsis tanaceti* infected seed contributes indirectly to ray blight through directly increasing the overwintering frequency of the pathogen.

2.2.3 Disease management

Management of pyrethrum disease relies on integrated approaches developed from extensive research, development and evaluation. The focus has been on the use of disease biology and epidemiology to implement successful disease management systems that allow control of diseases before damage is substantial. However, as limited alternatives are available the pyrethrum industry strongly relies on fungicides for disease control. Due to the destructive nature of many pyrethrum diseases, and their detrimental effect on pyrethrins yield (Pethybridge & Hay, 2001, Pethybridge et al., 2007a, Pethybridge et al., 2008a, Pethybridge et al., 2007b) chemical control sprays are generally applied as preventatives throughout the season to minimise disease epidemics.

As the most dominant disease over the past two decades, considerable effort has been invested to identify factors affecting the severity of ray blight. This has resulted in the development of integrated management strategies for its control in spring and summer. Identifying the influence of environmental and site specific factors on the severity of ray blight have assisted in the selection of fields and/or identified high risk sites which may need additional monitoring (Pethybridge & Hay, 2001, Pethybridge et al., 2009). Knowledge of the host range (Pethybridge et al., 2008b), genetic diversity (Pethybridge et al., 2012, Vaghefi et al., 2015b) and mating system (Vaghefi et al., 2015a) of *Stagonosporopsis tanaceti* have assisted in identifying inoculum sources and assessing the genetic adaptive ability of the pathogen. Quantification of the amount of seed infected with *Stagonosporopsis tanaceti* (Pethybridge et al., 2006, O'Malley, 2007), and the subsequent development of fungicide seed treatment options minimised the disease potential from seed borne inoculum (Pethybridge et al., 2006). The development of logistic regression modelling algorithms for

ray blight assist in estimating the probability of severe ray blight epidemics (Pethybridge et al., 2011). Furthermore, mechanisms to accurately quantify losses due to ray blight have been developed (Pethybridge et al., 2007a, Pethybridge et al., 2007b , Pethybridge et al., 2008a). Such mechanisms have been used to quantify the effects of different rates and timing of applications of different fungicides (Jones et al., 2007, Pethybridge et al., 2005a, Pethybridge et al., 2008d, Pethybridge et al., 2005b).

A number of fungicides have been registered for use in pyrethrum in Australia. Fungicide applications are structured into three distinct programs, which target specific disease risks at different stages of crop development.

The autumn/winter program is applied while plants are in their winter dormancy phase. The program is designed to control crown rot and to a lesser extent to decrease inoculum loads for tan spot, ray blight and anthracnose. Historically it has involved applications of procymidone (Sumsiclex®; Sumitomo; FRAC code 2)/(Fortress®; Crop Care Australasia). Currently it involves applications of fluazinam (Emblem®; Crop Care Australasia; FRAC code 29).

The spring fungicide program is applied during the rapid spring growth phase and subsequent bud initiation. The program is slightly modified, depending on if crops are in the first or subsequent harvests. It is targeted to control spring dieback from ray blight, tan spot and to a lesser extent crown rot, but also provides control of additional foliar diseases such as anthracnose. It includes applications of a fludioxonil + cyprodinil mix (Switch®; Syngenta; FRAC code 12 + 9), azoxystrobin (Amistar®; Syngenta; FRAC code 11), cyprodinil (Chorus®;

Syngenta; FRAC code 9) and a tebuconazole + prothioconazole mix (Prosaro®; Bayer CropScience; FRAC code 3). Chlorothalonil (Bravo®; Syngenta; FRAC code M5), a multi-site protectant, is applied with Amistar®, Chorus® and Prosaro®. Historically, boscalid (Filan®; Nufarm Ltd.; FRAC code 7) and difenoconazole (Score®; Syngenta; FRAC code 3) were used in the spring fungicide program, but were removed due to decreased efficiency.

The flowering fungicide program is applied during periods of flower maturation (typically late spring-summer) to control yield loss by the flower blights. It currently involves applications of penthiopyrad (Fontellis®; DuPont; FRAC code 7) and tebuconazole (Folicur®; Bayer CropScience; FRAC code 3). Historically the flowering fungicide program has also used carbendazim (Spin Flo® or Bavistin®; Nufarm Ltd./Biostadt India Ltd.; FRAC code B1) and ipriodione (Rovral®; Bayer CropSciene; FRAC code 2.).

There are a number of management strategies implemented which aim to delay the development of fungicide resistance in pyrethrum. These include restricting the number of individual fungicide applications to a maximum of two per season and tank mixing of some fungicides with single-site modes of action (e.g. Chorus®) with the multi-site protectant Bravo®. In addition, caution is taken when using two different chemicals with the same FRAC code in the same season. For example, first year crops which receive Switch®, do not receive applications of Chorus® unless disease severity is severe, as they both contain cyprodinil (T. Groom, pers. comm.)

2.3 TAN SPOT OF PYRETHRUM

2.3.1 Symptoms and characterisation

Tan spot, caused by *Microsphaeropsis tanaceti* R.G. Shivas, S.J. Pethybridge and S.J. Jones, results in tan coloured necrotic spots on leaves, stems and buds (Fig. 2.4b & Fig. 2.4c), which coalesce to form lesions leading to a loss of green leaf area (Pethybridge et al., 2008e). The pathogen was characterised in 2008 as a member of the genus *Microsphaeropsis,* following confirmation that the pathogen was pathogenic to pyrethrum. Identification and characterisation of *M. tanaceti* was undertaken using 15 isolates collected in 2004/2005 from various regions in Tasmania. It was based on culture morphology and nucleotide sequence data of the nuclear ribosomal internal transcribed spacer (ITS) locus (Pethybridge et al., 2008e). Comparison of 540 base pair (bp) of the ITS sequence identified two haplotypes (I and II) differentiated by three single nucleotide polymorphisms (SNPs). However, only one isolate (BRIP 50785) was of the second haplotype. Despite the genetic differences there was no significant difference in disease severity, measured by the number and area covered by lesions, following inoculation of leaves of two pyrethrum cultivars with conidial suspensions of the two haplotypes. Phylogenetic analysis supported the pathogen as genetically similar, but distinct from other *Microsphaeropsis* spp., and the name *M. tanaceti* was proposed (Pethybridge et al., 2008e). However, at the time there was limited nucleotide data available for comparison to other species.

Microsphaeropsis tanaceti produces conidia within a pycnidium, *in vivo* on plant material and profusely *in vitro* on potato dextrose agar (PDA) and oatmeal agar (OA). The conidia of *M. tanaceti* are 3.5 to 6.2 µm × 2.5 to 3.3 µm. and 3.5 to 8.0 µm × 2.0 to 3.5 µm on OA and

PDA, respectively (Fig. 2.4a). The proportion of aseptate to septate conidia is isolate and media dependant (Pethybridge et al., 2008e). A sexual morph has not been identified and thus, *M. tanaceti* is proposed to reproduce via clonal means.

Fig. 2.4. (a) *Microsphaeropsis tanaceti* conidia and the outer pycnidial wall; (b) tan spot lesions 18 days after inoculation of a pyrethrum leaf with a conidial suspension of *M. tanaceti*; (c) discrete and coalescing tan spot lesions caused by *M. tanaceti*, on a pyrethrum leaf (40× magnification). Reproduced from Pethybridge et al. (2008e).

2.3.2 Isolation history

The first report of the association of *M. tanaceti* with pyrethrum was during assessment of the mycoflora of surface-sterilized or non-treated commercial pyrethrum seed harvested in 2000 (Pethybridge et al., 2006). *Microsphaeropsis tanaceti* was not associated with necrotic

lesions on pyrethrum until 2001, during routine field sampling. The pathogen was highly prevalent, occurring in 63 – 75% of fields (n = 8) sampled monthly from April to November. However, isolation frequencies were low, with *M. tanaceti* associated with 10.5% of leaf spots and 4.3% of stem lesions and buds (Pethybridge et al., 2003). Between 2004 and 2006, the isolation frequency from necrotic leaf spots in spring (September to October) substantially increased to 65% (Pethybridge et al., 2008e). Between 2009 and 2011, severity of necrosis and defoliation of fields over autumn and winter and apparent control failures of the spring fungicide program (high disease severity despite standard fungicide application) were identified. Sampling of these fields identified a high incidence of *M. tanaceti* (F. Hay, pers. comm.). Furthermore, a study evaluating temporal fluctuations in the isolation frequency of pathogens throughout 2012 and 2013, in the absence of fungicides, identified *M. tanaceti* as the dominant species associated with foliar disease in both winter and spring. *Microsphaeropsis tanaceti* was isolated from 96 and 92% of fields sampled in 2012 (n = 83) and 2013 (n = 136), respectively (Hay et al., 2015). In 2012, *M. tanaceti* had a mean isolation frequency of 40.8, 55.5, and 53.3% in winter (April to July), spring (August to September) and summer (November), respectively. Furthermore, 25% of fields sampled in spring and summer had isolation frequencies greater than 81.9 and 73.2%, respectively (Hay et al., 2015). In 2013, the isolation frequency in winter (June to July) and spring (September to October) decreased slightly to 18 and 38.3%, respectively (Hay et al., 2015).

An increased prevalence of *M. tanaceti* within commercial pyrethrum seed lines has also been identified. In seed lines from multiple cultivars harvested between 2000 and 2005 (200 seeds tested at a maximum of 30 days post-harvest), *M. tanaceti* was sporadically identified from surface sterilised and non-treated seeds. It ranged in incidence between 0 and 7.5% of

seed, with a mean frequency of 1% (Pethybridge et al., 2006). The occurrence of the pathogen was not greatly affected by surface sterilisation, indicating that it may be present on both the outer pericarp tissue and within the seed (Pethybridge et al., 2006). However, during routine testing of 2012 harvested seed, *M. tanaceti* was identified in 14 of 18 seed lines with a mean and a maximum incidence of 4.9 and 26.0%, respectively (F. Hay, pers. comm.).

2.4 GENUS *MICROSPHAEROPSIS*

2.4.1 *Microsphaeropsis* spp.

Microsphaeropsis spp. have a global distribution (Wang et al., 2002, Kluger et al., 2004, Hall et al., 2013, Crous et al., 2011). Although many have been identified as plant pathogens (Ortiz-Ribbing & Williams, 2006, Mintz et al., 1992), some species have proven to be antagonists to fungal pathogens (Carisse & Bernier, 2002), etiological agents of soft tissue disease in mammals (Pendl et al., 2004, Krockenberger et al., 2010, Kluger et al., 2004) and have potential biotechnological roles (Luo et al., 2013, Sommart et al., 2012, Xiao et al., 2010).

Phytopathogenic *Microsphaeropsis* species can attack a wide range of plant hosts. *Microsphaeropsis callista* and *M. conielloides* have been isolated in Australia from leaves of *Eucalyptus haemastoma* and *E. pauciflora*, respectively (Sutton, 1971). In addition, *M. proteae* causes disease on *Proteae* spp. (including. *P. nitida*) (Crous et al., 2011), *M. arundinis* is a plant inhabitant first described in Pakistan from *Arundo donax* (Ahmad, 1960)

and *M. amaranthi* causes disease of *Amarthaceae* spp.. *Microsphaeropsis olivacea* (Bonord) Höhnel, the type species of the genus, has been isolated from many plant genera worldwide (Sutton, 1980).

Within the genera, *M. ochracea* and *M. amaranthi* have been reported as being antagonistic to fungal and plant species, respectively. *Microsphaeropsis ochracea* (Carisse & Bernier, 2002, Bernier et al., 1996), has been shown to control ascospore production of the apple scab pathogen *Venturia inaequalis.* Application of *M. ochracea* on naturally infected apple leaves that overwintered on the orchard floor, reduced ascospore production in the following spring by 76 to 84% (Carisse et al., 2000). Furthermore, inoculation of sclerotia of *Botrytis squamosa* with *M. ochracea in vitro* decreased conidia production by 75.5%. Consistent results were also obtained in the field with *M. ochracea* reducing the production of conidia on senescent or necrotic leaves on average by 82% (Carisse et al., 2006). In addition, *M. ochracea* has also been shown to be an antagonist of *Giberella zeae* which causes Fusarium head blight of cereals, by reducing ascospore production *in vitro* on corn and wheat (Bujold et al., 2001) and of *Rhizocotonia solani,* by reducing germination and production of sclerotia both *in vitro* and on stored potato tubers (Carisse et al., 2001). Thus, *M. ochracea* could serve as a broad-spectrum biological control agent, as an alternative to fungicides, for control of these pathogens (Carisse et al., 2001, Carisse et al., 2006). *Microsphaeropsis amaranthi* is a candidate as a bio-herbicide for weedy *Amarthaceae* spp. (Mintz et al., 1992). However, its ability to cause plant death is dependent on environmental conditions (Moran & Showler, 2007, Ortiz-Ribbing & Williams, 2006, Smith et al., 2006, Smith & Hallett, 2006).

Microsphaeropsis arundinis has been identified in association with mammalian tissue infection. The first report was in a 7 year old cat in 2003 (Kluger et al., 2004). In addition, an 11 year old spayed crossbred cat in Australia developed dew claw and nasal bridge lesions attributed to localised infections of *M. arundinis* (Krockenberger et al., 2010). In Australia, two cases of subcutaneous soft tissue infections caused by *M. arundinis* have been reported in diabetic human patients (Pendl et al., 2004). Additionally, a case of cutaneous infection was diagnosed in an immunosuppressed human patient in the United States of America (Hall et al., 2013).

From a biotechnology aspect *Microsphaeropsis* spp. have been shown to produce useful fungal metabolites, which have been isolated and identified (Luo et al., 2013, Sommart et al., 2012, Krohn et al., 2009). *Microsphaeropsis arundinis* strains produced modiolin and phthalide derivatives (microsphaerophthalides) (Sommart et al., 2012) and arundinols and arundinones (Luo et al., 2013), which exhibited antifungal, antimalarial and antibacterial activity, and algicidal properties. Other biotechnology aspects include the potential use of *Microsphaeropsis* spp. to produce single cell oil in solid state fermentation from steam exploded wheat straw and wheat bran (Peng & Chen, 2008, Peng & Chen, 2007). Additionally, a fungal endophyte identified as a *Microsphaeropsis* species based on 26S RNA sequences has been shown to have a high bio-sorption capacity of cadmium (Xiao et al., 2010).

2.4.2 Current taxonomic state

The genus *Microsphaeropsis* Höhn was established by von Höhnel (1917) and placed in *Montagnulaceae (Pleosporales, Dothideomycetes).* It was proposed by Sutton (1971) to be utilised for species described as *Coniothyrium* which were non-congeneric with the type species, *Coniothyrium palmarum*. *Microsphaeropsis* was restricted to pycnidial species with small pigmented unicellular conidia produced from phialides with periclinal thickening (Morgan-Jones, 1974, Sutton, 1971, Sutton, 1980). Species characterized by small, often septate conidia produced from phialidic annellides were retained in *Coniothyrium* (Sutton, 1980). The dichotomous key for separation of species within the genus *Microsphaeropsis* is based on conidia formation, shape and size (Sutton, 1980). However, there are some discrepancies in the described measurements for some *Microsphaeropsis* species. For example, the original description of the holotype of *M. arundinis* by Ahman (1971), differs in several features from the description of *M. arundinis* in Sutton's key (Sutton, 1980). These features include conidia shape and size, described as oblong and 6.5 to 7.8 × 1.8 to 2.5 µm by Ahman (1971), and cylindrical and 4.0 to 4.5 × 1.5 µm by Sutton's key (Sutton, 1980). Furthermore, some morphological features characteristic of *Microsphaeropsis* are exhibited by species in other genera, which can impede accurate identification. For example, the brown colouration of conidia, characteristic for *Microsphaeropsis* spp., is also observed in pycniospores within old pycnidia of members of the genus *Peyronellaea* (Boerema et al., 2004, Aveskamp et al., 2010).

The present state of taxonomy of the *Microsphaeropsis* and *Coniothyrium* genera is confused (Someya, 1997, Sutton, 1980, Morgan-Jones, 1974). Some fungal species have been placed in *Microsphaeropsis* as an interim measure, following similar morphological characteristics

to *Microsphaeropsis* spp., without further reclassification (Sutton, 1980). While morphologically, a large number of species have been combined in *Microsphaeropsis,* very few of these have been confirmed via genetic or phylogenetic analyses. In some instances identification has been further limited by a lack of nucleotide sequence data of *Microsphaeropsis* species in nucleotide databases for comparison (Pendl et al., 2004, Pethybridge et al., 2008e).

Phylogenetic analyses incorporating *M. olivacea* (strains: CBS 401.84, 442.83 and 336.78), based on sequenced data of the small subunit 18S nrDNA (SSU), phylogenetically embedded *Microsphaeropsis* within the *Pleosporales* (Verkley et al., 2004) which is congruent with the initial genus description by von Höhnel (1917). Clades associated with *Microsphaeropsis* in the *Pleosporales* were of the genus *Coniothyrium* and *Coniothyrium*-like genera including *Paraconiothyrium* and *Paraphaeosphaeria* (Verkley et al., 2004). In a subsequent analysis, providing more resolution by utilising SSU sequence data in combination with sequence data from the large subunit 28S nrDNA (LSU), *M. olivacea* (CBS 442.83 and CBS 116669) clustered in the new proposed family *Didymellaceae* (de Gruyter et al., 2009). In comparison, *Coniothyrium palmarum* (the type species of *Coniothyrium*) clustered within the *Leptosphaerisacea* (de Gruyter et al., 2009). The *Didymellaceae* includes *Phoma* and allied genera such as *Peyronellaea*, *Stagonosporopsis* and *Boeremia* (Aveskamp et al., 2010). Further examination of the *Didymellaceae* with sequence data of the LSU, ITS and β-tubulin (*TUB2*) loci, in concatenation, provided sufficient resolution to identify 19 groups representing taxonomic units of species (Aveskamp et al., 2010). *Microsphaeropsis,* represented by the type species *M. olivacea*, was retained as a separate genus, but formed a basal clade paraphyletically associated with the 19 groups. The placement of

Microsphaeropsis within the *Didymellaceae* was also supported by studies by Crous et al. (2011) and Verkley et al. (2014).

Currently, *Microsphaeropsis proteae* is the only species shown to be phylogenetically associated with *M. olivacea* within the *Didymellaceae* (Crous et al 2011). A phylogenetic analysis with the LSU, *TUB2* and ITS sequences identified a number of misclassified *Microsphaeropsis* spp.. Verkley et al. (2014) found that *M. pseudaspera* (CBS 113682), *M. ruguspora* (CBS 638.93) (Someya, 1997), a strain of *M. olivacea* (CBS 305.68) and two *Microsphaeropsis* sp. strains (CBS 638.93 and 978.95) were phylogenetically embedded in the family *Montagulaceae*, which is distantly related to the *Didymellaceae.* These species were recombined into the genera/division *Paraconiothyrium* sp. 1, *Paraconiothyrium variabile*, *Paraphaeosphaeria* sp. and *Paraphaeosphaeria sporulosa.* In addition, *M. arundinis* (CBS 100243) was also identified in the *Montagulaceae*, (Verkley et al., 2014) but was not reclassified, and thus still retains its association with the genus *Microsphaeropsis*, despite not being phylogenetically associated with the type species.

These phylogenetic studies indicate that the morphological characteristics used to identify *Microsphaeropsis* spp. exhibit plasticity among multiple genera and thus classifications based solely on these characters may be artificial (Verkley et al., 2014). Phylogenetic analysis of *Phoma* also identified that the nine sections of *Phoma* defined by Boerema et al. (2004), based solely on morphological and host range characteristics, failed to reflect the evolutionary history among the species, with the *Phoma* sections being paraphyletic within the *Didymellaceae* (Aveskamp et al., 2010, Aveskamp et al., 2008). These results suggest that the confirmation of members of the genus *Microsphaeropsis* can be identified via a

phylogenetic approach. Further evaluation of economic and environmentally important *Microsphaeropsis* species needs to be undertaken to delimit the genus.

2.5 FUNGICIDE RESISTANCE

2.5.1 Overview and mechanisms

Fungicide resistance refers to the decreased sensitivity of strains of a pathogen to a particular inhibitor (Sierotzki & Gisi, 2003). In agricultural industries, resistance becomes problematic when the proportion of resistance strains within a population reach a level which results in a decrease in effectiveness of the particular inhibitor for disease control (Beckerman, 2013). Studies have shown that fungicide efficacy decreased substantially when frequencies of resistant individuals exceeded 10% of the population (Ishii et al., 2007, Lacombe, 2003). However, van den Bosch et al. (2011) proposed that a frequency of resistant strains as low as 1% represents a large proportion within a population.

Several mechanisms of resistance have been identified to date. These include: a reduced binding efficiency of the inhibitor due to mutations in the inhibitor target site; a reduction in the uptake of the inhibitor; overproduction of the gene that the inhibitor targets and active efflux of the inhibitor (Ghannoum & Rice, 1999, Hollomon et al., 1997, Deising et al., 2008, Beckerman, 2013). Fungicide resistance can be described as qualitative or quantitative. Qualitative resistance is usually mutation-based, with individuals in a population either sensitive or highly resistant to the inhibitor (Reddy, 2012, Brent & Hollomon, 1995). With

quantitative resistance, resistant individuals exhibit a range of sensitivities to the inhibitor compared to sensitive individuals. Many different mechanisms can result in quantitative resistance (Deising et al., 2008). In some instances, the resistant individuals can be controlled with a higher dose rate or more frequent applications (Reddy, 2012). However, repeated fungicide treatments can also result in a shift of the population, and over time individuals with increasing levels of resistance are selected, until eventually the entire population consists of almost completely resistant individuals (Brent & Hollomon, 1995).

2.5.2 Development

Fungicide resistance can be described as a two-step process, encompassing an emergence and selection phase (van den Bosch & Gilligan, 2008, van den Bosch et al., 2011). Resistance develops from genetic changes within individuals (i.e. mutation) which are heritable. The emergence phase relates to both the development of the resistant individual and the ability for it to increase in frequency (i.e. develop a sub population), such that it is unlikely to die out by random chance. Initially, the resistant individual occurs at a very low frequency. Stochastic processes determine both when resistant mutants arise and whether they survive (Hobbelen et al., 2014).

In some cases the mutation governing resistance can subsequently result in individuals with an associated decreased fitness. This may include decreased virulence, mycelial growth, and spore production and germination compared to sensitive individuals (Dekker, 1988). Such costs of resistance prevent the individual from building up large population numbers through drift (Hobbelen et al., 2014). An example of this is the G143A mutation in the cytochrome *b*

gene that confers high levels of resistance in many fungal pathogens to Quinone outside inhibitor (Q_oI) compounds (Gisi et al., 2002, Sierotzki et al., 2000, Ma & Michailides, 2005). This mutation (GGT to GCT) has not been reported for species which harbour an intron immediately adjacent to codon 143 of of the *cytochrome b* gene (Grasso et al., 2006). In these species, the G143A mutation hinders the splicing of the intron resulting in significantly lower levels of cytochrome *b* expression and a severe decrease in respiratory growth, resulting in counter selection of these individuals in the field (Vallieres et al., 2011, Grasso et al., 2006). Reports of the fitness costs associated with fungicide resistance vary. Sclerotia from dicarboximide resistant *Botrytis cinerea* strains had lower survival rates than sclerotia from sensitive strains (Raposo et al., 2000). Additionally, boscalid resistant *Sclerotinia sclerotiorum* resistant strains were more sensitive to osmotic stress than sensitive strains and lacked the ability to produce sclerotia (Wang et al., 2015a). However, in some species no differences in fitness between resistance and susceptible strains have also been reported (Veloukas et al., 2014, Avenot & Michailides, 2007, LaMondia & Douglas, 1997). Furthermore, positive correlations between virulence and fungicide tolerance have been reported in *Mycosphaerella graminicola* (Yang et al., 2013).

Resistant individuals can be introduced into new geographic regions via migration of resistant individuals from one population to another population (Hollomon & Brent, 2007). The reproductive strategy of the pathogen can influence the migration of individuals. Species with a sexual stage may have a greater dissemination capacity than those with a solely asexual reproductive cycle, due to more sophisticated dispersal mechanisms. The prolificacy of reproduction will also determine the relative increase in population size during the emergence phase and the rate at which resistance spreads. If mutations arise or resistant individuals are introduced during periods conducive for profuse asexual or sexual

reproduction, then the probability of the frequency of the mutation reaching a critical frequency is increased (Milgroom, 1990a). However, such timings also needs to coincide with infectible plant growth stages or the pathogen needs to produce adequate survival structures (e.g. sclerotia), to allow the disease cycle of resistant strains to continue. An additional benefit of sexually reproducing species is that recombination can allow genes harbouring resistant alleles to be combined with novel genes, resulting in increased fitness of resistant individuals (McDonald & Linde, 2002). Furthermore, differential fungicide responses to boscalid of ascospores and conidia produced from the same isolate have been noted in *Didymella bryoniae* (*Stagonosporopsis cucurbitacearum*) (Keinath, 2012).

Following the emergence phase, a selection phase begins in which the application of the fungicide provides a selection pressure and increases the frequency of resistant individuals in the population (Hobbelen et al., 2014). In comparison to the emergence phase, which is largely governed by the number of "daughter lesions" produced per "mother" lesion (i.e. absolute number of offspring), the selection phase is governed by the rate of increase of resistant individuals relative to sensitive individuals in the population (Milgroom & Fry, 1988, Milgroom, 1990b, van den Bosch et al., 2011). Fungicide resistance management strategies aim to decrease the rate at which fungicide resistant strains are selected for in populations. As the number of resistant individuals in the population increase, the efficiency of disease control from the fungicide declines. Following the increase in the number of resistant individuals, adjustment of management program will be necessary, by changing dose rates or active chemical components, to maintain sufficient control (van den Bosch et al., 2014a). The frequency of selection of the resistant individuals in the pathogen population will generally increase faster for higher dose rates of the fungicide (van den Bosch et al., 2011).

However, it can be reduced by tank mixing of the at-risk fungicide with both multi- and single-site fungicides with other modes of action to limit the effectiveness of the selection phase (van den Bosch et al., 2014b).

2.5.3 Managing the development of resistance

Management strategies for fungicide resistance aim to delay the evolution and spread of resistance, while ensuring effective disease control. The management strategy utilised may differ between the emergence and the selection phase. However, it is very difficult to identify and quantify the effectiveness of management strategies during the emergence phase (Hobbelen et al., 2014). There are a number of inherent risk factors that relate to the use of fungicides for disease control. These relate to the fungicide, biology of the target pathogen and the management of fungicide applications (Staub & Sozzi, 1984). Each of these aspects requires separate evaluations, which can then be integrated to estimate the overall risk factor of resistance (Hollomon & Brent, 2007).

2.5.3.1 Fungicide associated risks

To assist with the development of fungicide resistance strategies, fungicides are designated into different fungicide group codes (FRAC codes) according to their mode of action (FRAC, 2015). The FRAC code, which also reflects the fungicide chemical class, can assist in estimating the relative risk of developing resistance to the fungicide (Hollomon & Brent, 2007). The risk can be low (decrease in effectiveness or occurrence of resistant isolates not detected or very rare after many years of use); moderate (decrease of effectiveness detected in a few situations, or to a limited extent, and/or resistant isolates obtained from field samples of

target pathogens); or high (widespread and severe decrease of effectiveness due to resistance development has occurred in one or more target pathogens, in certain regions, within a few years of introduction) (Hollomon & Brent, 2007). Individuals with resistance to one fungicide in a FRAC code have an increased risk of developing cross resistance to other fungicides in the FRAC code, due to sharing the same mode of action. For example, many fungal strains resistant to Q_oI fungicides (FRAC code 11) exhibit cross-resistance to other Q_oI fungicides (Vincelli, 2002). However, pathogens which are resistant to fungicides in one FRAC code class should be able to be controlled with fungicides from a different FRAC code class (Brent et al., 1998). However, there are some reported cases of resistance to multiple FRAC code classes in *Botrytis cinerea* (Veloukas et al., 2014, Fernández-Ortuño et al., 2012). In addition, fungicides which have single-site modes of action (e.g. some FRAC code 7 and 9 fungicides) fungicide are more susceptible to the development of resistance than those with multi-site modes of action (e.g. FRAC code M1 – M11 fungicides) (Deising et al., 2008).

2.5.3.2 Pathogen associated risks

Knowledge of pathogen biology can identify the pathogen-associated risk of resistance developing and assist the development of pathogen-specific management strategies (Brent et al., 1998). The influence of the reproductive strategy of the pathogen, in terms of generation time, recombination and migration, has already been discussed. In addition, pathogens with high genetic diversity and/or the ability to mutate or express mutant genes have an increased risk of developing resistant strains (McDonald & Linde, 2002). Prior to the introduction of a new fungicide, the resistance of the pathogen in other crops or pathosystems to the particular fungicide or fungicides in the same FRAC group should be evaluated. If the chance of resistance is high, and application is necessary, then specific management practices such as

application of the fungicide as a mix with other fungicides and constant field monitoring may be necessary (Brent et al., 1998).

The pathogen-associated risk can also be partially inferred from the mechanisms governing resistance (or potentially governing resistance) in the target pathogen. This can include identification and sequencing of the target gene/s and characterising the specific mutations conferring resistance. Characteristics of the target gene in sensitive strains can identify if it shares conserved amino acids within which mutation has occurred in species with known resistance. In addition, the structural and biological characteristics of the target gene can also be used to identify the resistance risk. For example, heteroplasmy and the location of an intron after codon 143 of the cytochrome *b* gene (Vallieres et al., 2011, Grasso et al., 2006, Ishii et al., 2009) can be used to determine the resistance risk to QoI inhibitor fungicides. Potential mutations can also be identified from sequencing the target gene of isolates produced *in vitro* from mutagenesis and subsequent selection on fungicide amended media (Laleve et al., 2014). While the specific mutations identified may not occur in the field, these analyses can identify the potential mutations which could occur, and allow the relative fitness associated with the mutations to be evaluated. The stability of the mutations governing resistance in the absence of the fungicide varies for different species and mutations. If the stability is short lived, then removal of the fungicide may decrease the proportion of resistant isolates in a population. For example, reversion of QoI sensitivity in the absence of the fungicide has been identified in *Botrytis cinerea* (Ishii et al., 2009, Ishii et al., 2007). However, Kim and Xiao (2011) found that the mutations in *Botrytis cinerea* isolates conferring resistance to boscalid and pyraclostrobin were stable, through multiple generations, in the absence of the fungicides.

2.5.3.3 Management associated risks

Management practices to prevent or at least delay the onset of the development of fungicide resistance have been proposed. These include, restricting the number of applications per season and using the recommended dose rate of fungicides within any one FRAC code (van den Bosch et al., 2011) (especially those with a single site mode of action), alternating fungicides with different FRAC codes (Deising et al., 2008) and incorporating multi-site protectants with the application of single-site mode of action fungicides (Deising et al., 2008). Mixing single-site acting fungicide with multi-site acting fungicide can delay the emergence of resistance to the single-site component (Hobbelen et al., 2014).

2.5.4 Detection and monitoring

Identifying the occurrence of fungicide resistance requires monitoring and subsampling of populations. Identifying a decreased efficiency of the fungicide (i.e. disease control failures) is usually the first justification for the need to sample the pathogen population. However, if the applied fungicide has a high risk of developing resistance or the target pathogen is resistant to chemicals in the same FRAC code, then sub-sampling to detect the level of control in populations, following application, may be warranted. Such detection may allow counter measures to slow down resistance development to be implemented (Dekker, 1988).

The identification of fungicide resistant strains requires knowledge of the baseline response of sensitive strains (Dekker, 1988). Such data is usually collected prior to large scale applications of the fungicide. A number of different methods, *in vitro* and *in vivo*, have been used to detect resistant strains. These include: measurement of the radial growth of

mycelium and spore germination on fungicide amended agar and spore germination and growth in liquid fungicide solutions (Dekker, 1988). Fungicide amended agar testing can use multiple agar plates of varying concentrations or a single plate in which the concentration of the fungicide is applied under a spiral gradient dilution. The advantage of spiral gradient dilution plates is that they allow a wide range of concentrations to be evaluated on a single plate (Forster et al., 2004). In addition, the use of microtiter-based assays combined with alamar blue provides quantifiable and detection within hours for fast growing pathogens like *Mondinia fructicola*, *Alternaria alternata* and *Verticillium dahliae* (Cox et al., 2009, Vega et al., 2012, Rampersad, 2011). Individuals can also assessed by inoculation onto living plant material treated with fungicide, followed by assessment of disease severity. The benefits of this method are that it confirms that the resistant strains can cause disease and it can be used on economically important fungi, such as rusts, powdery mildews and downy mildews, which cannot be cultured *in vitro* (Dekker, 1988). However, each of these methods can be labour intensive when a large number of strains need to be tested.

Where resistance can be linked to a mutation in a specific gene (i.e. quantitative resistance), molecular techniques can be used to assess the proportion of populations which have developed resistance (van den Bosch et al., 2011). Such methods have the potential to provide rapid and reliable assessment of fungicide resistance within populations. However, it is important that the expected genetic profile being screened correlates to the phenotype of resistance for each species (Beckerman, 2013).

Several molecular techniques, such as PCR, PCR-restriction fragment length polymorphism (PCR-RFLP), allele-specific PCR (Yin et al., 2011), allele-specific real-time PCR and high

resolution melt (HRM) (Chatzidimopoulos et al., 2014, Curvers et al., 2015) have been used successfully to detect fungicide-resistant genotypes of several plant pathogens (Capote et al., 2012). The use of real-time PCR allows quantification of resistant alleles in populations, while HRM can allow unknown mutations to be identified.

2.5.5 Fungicide resistance in pyrethrum pathogens

Fungicides are relied on for control of many fungal pathogens in pyrethrum, as outlined in section 2.2.3. Extensive research has been undertaken to quantify the effects of different rates and timing of applications of different fungicides on disease severity and pyrethrum yield and quality to identify efficient management programs (Hay et al., 2015, Pethybridge et al., 2005a, Pethybridge et al., 2005b). In addition, *in vitro* fungicide testing of pathogen isolates collected from pyrethrum are used to identify the occurrence of resistance and allow management strategies to be altered. For example, *in vitro* testing identified reduced sensitivity among *Stagonosporopsis tanaceti* isolates to difenoconazole, and of *Botrytis cinerea* and *Sclerotinia sclerotiorum* isolates to carbendazim (Jones et al., 2007, Pethybridge et al., 2008c, O'Malley, 2012). Subsequently, both of these fungicides were removed from the fungicide programs and replaced with alternatives.

In addition, *M. tanaceti* has been reported as developing a decreased sensitivity to fungicides used in the pyrethrum fungicide program (Hay et al., 2015, Pethybridge et al., 2008e). Seven isolates collected in 2004/5 had a mean EC_{50} value against difenoconazole of 2.33 μg/ml, (range = 0.31 – 4.99 μg/ml,), despite only being exposed to only one or two applications of the fungicide (Pethybridge et al., 2008e). Boscalid replaced difenoconazole in the spring

fungicide program in 2005. However, *in vitro* testing of *M. tanaceti* field isolates collected in 2009 identified a boscalid resistant phenotype. Furthermore, a control failure of the spring fungicide program was identified in 2011 (Hay et al., 2015). Fields were identified with high levels of disease despite receiving the commercial fungicide program. Fungal isolations from leaves sampled from these field identified a high frequency of *M. tanaceti*. *In vitro* testing of isolates isolated from these fields to each of the fungicides used within the spring fungicide program identified a high proportion of isolates with resistance to boscalid (Hay et al., 2015). The majority of *M. tanaceti* isolates exhibited boscalid EC_{50} values in excess of 50.0 µg a.i./mL boscalid (Hay et al., 2015). *In vitro* fungicide testing of field isolates of *M. tanaceti* identified that isolates remained sensitive to azoxystrobin and cyprodinil (Hay et al., 2015, Pethybridge et al., 2008e). It has been proposed that the observed increased incidence of *M. tanaceti* as a component of spring disease in recent years, in comparison to *Stagonosporopsis tanaceti*, appears to be related to the selection of reduced sensitivity in *M. tanaceti* to boscalid (Hay et al., 2015).

2.5.6 Boscalid

Boscalid is a pyridine-carboxamide fungicide that acts as a succinate dehydrogenase inhibitor (SDHI; FRAC code 7). It was commercially released in 2003. Succinate dehydrogenase (succinate-ubiquinone oxidoreductase or complex II) is an enzyme with roles in the tricarboxylic acid (TCA) cycle and the mitochondrial transport chain, and thus is necessary for cellular respiration (Hägerhäll, 1997). The enzyme is constructed from four nuclear encoded protein subunits. The SDHA (flavoprotein) and SDHB (iron-sulfur protein) subunits form the soluble component which catalyses the oxidation of succinate to fumarate (TCA cycle). The SDHB contains three iron-sulphur clusters (2Fe-2S, 4Fe-4S and 3Fe-4S) which

transfer electrons for the reduction of ubiquinone. The amino acid sequences of these clusters are highly conserved among fungal species (Avenot et al., 2008). The SDHC and SDHD subunits are hydrophobic membrane proteins which anchor the SDHA and SDHB subunits within the mitochondrial membrane and reduce ubiquinone to ubiquinol (mitochondrial electron transport chain) (Horsefield et al., 2006, Avenot & Michailides, 2010, Huang & Millar, 2013). The ubiquinone binding site (Q-site) is formed by residues of the SDHB, SDHC and SDHD subunits (Hägerhäll, 1997, Horsefield et al., 2006, Scalliet et al., 2012, Fraaije et al., 2012). Boscalid inhibits ubiquinone reduction by binding to the Q-site, restricting cellular respiration and resulting in cell death. Due to its single-site mode of action boscalid has been classified as having moderate to high risk of resistance by the FRAC (FRAC, 2015).

2.5.7 Molecular characterisation of boscalid resistance

Mutations within each of the genes encoding the subunits have been correlated with boscalid resistance within field isolates and laboratory-induced mutants of different fungal species (Avenot & Michailides, 2010, Sierotzki & Scalliet, 2013). Within the gene encoding the SDHB subunit (*SDHB*), a conserved histidine (H) residue in the third iron-sulphur complex (3Fe-4S) was proposed to play a central role in ubiquinone binding and reduction and is essential for the attachment of boscalid (Avenot & Michailides, 2010, Fraaije et al., 2012, Horsefield et al., 2006, Sierotzki & Scalliet, 2013). Boscalid resistance has been associated with mutations resulting in the substitution of this conserved histidine residue with tyrosine (Y) or arginine (R) in *Stagonosporopsis cucurbitacearum* (syn: *Didymella bryoniae*) (H277Y and H277R) (Avenot et al., 2012), *Corynespora cassiicola* (H278Y and H278R) (Miyamoto et al., 2010), *Alternaria alternata* (H277Y and H277R) (Avenot et al., 2008) and *Botrytis*

cinerea (H272Y and H272R). Furthermore, substitution with leucine (L) also confers resistance in *Botrytis cinerea* (H272L) (Fernández-Ortuño et al., 2012, Veloukas et al., 2011, Yin et al., 2011). Boscalid resistance in *Botrytis cinerea* has also been associated with substitutions in the second iron-sulphur complex (4Fe-4S). These include a proline (P) to phenylalanine (F) substitution at codon 225 and an asparagine (N) to isoleucine (I) substitution at codon 230 (Veloukas et al., 2011, Yin et al., 2011). Furthermore, resistance in *Sclerotinia sclerotiorum* has been associated with substitution of alanine (A) with valine (V) at codon 11, which is not situated within any of the three iron-sulphur clusters (Wang et al., 2015b, Wang et al., 2015a).

Boscalid resistance associated with mutations in the *SDHC* and *SDHD* are less well characterised. Mutations in the *SDHC,* conferring boscalid resistance, result in substitution of histidine (H) with arginine (R) at codon 134 in *Alternaria alternata* (Avenot et al., 2009) and serine (S) with proline (P) at codon 73 in *Corynespora cassiicola* (Glattli et al., 2009, Miyamoto et al., 2010). Mutations in the *SDHD,* conferring boscalid resistance, result in substitution of aspartic acid (D) with glutamic acid (E) and argine (R) at codons 123 and 133, respectively in *Alternaria alternata* (Avenot et al., 2009), histidine (H) for arginine (R) at codons 133 and 132, in *Alternaria solani* and *Sclerotinia sclerotiorum*, respectively (Glattli et al., 2009, Miles et al., 2014), and serine (S) with proline (P) at codon 89 and glycine (G) for valine (V) at codon 109 in *Corynespora cassiicola* (Glattli et al., 2009, Miyamoto et al., 2010).

Several studies have shown that mutations in the succinate dehydrogenase complex can result in differential cross-resistance to other SDHI fungicides (FRAC code 7) (Sierotzki & Scalliet,

2013). For example, Avenot et al. (2012) identified boscalid resistant isolates of *Stagonosporopsis cucurbitacearum* with SDHB H277Y and H277R substitutions, to be as sensitive to the SDHI fungicide penthiopyrad as isolates with a wild type SDHB. However in *Alternaria alternata*, a H134R substitution in the SDHC has been shown to confer cross-resistance to all tested SDHI fungicides (Sierotzki et al., 2011). For *Botrytis cinerea*, SDHB P225 and N230 substitutions conferred resistance to boscalid, fluopyram, carboxin and bixafen. Furthermore, substitution of the histidine at codon 272 in the SDHB of *B. cinerea* had differential effects. The substitution H272L affected susceptibility to all four SDHI fungicides identified above; H272R conferred resistance to all except fluopyram, and H272Y conferred hypersensitivity to fluopyram

Initial testing of *M. tanaceti* strains exhibiting boscalid resistance has identified that they remain sensitive to the SDHI fungicide fluopyram (F. Hay, pers. comm.). Such information may be used to identify which specific SDH substitutions may occur in *M. tanaceti* by evaluating which SDH substitutions result in combined boscalid resistance and fluopyram sensitivity or hyper-sensitivity in other species. For example, if boscalid resistance in *M. tanaceti* is due to substitutions in the *SDHB* gene, then a substitution corresponding with P225, N230 and H272L of *B. cinerea SDHB* may not occur, but substitutions corresponding with H272R/Y may occur (Laleve et al., 2014).

The molecular mechanisms of boscalid resistance in *M. tanaceti* have not been identified. Identification of the specific mechanism resulting in resistance may allow for, the development of molecular protocols to accurately assess the frequency of resistance in

populations, the stability of boscalid resistance to be examined and the potential cross resistance to other SDHIs to be identified

2.6 FUNGAL REPRODUCTION

2.6.1 Modes of reproduction

The ability to successfully reproduce is vital to the survival of fungi at an individual and species level. At an individual level it provides a means to increase fungal biomass, produce inoculum for dispersal and introduce genetic variation. Within the fungal kingdom reproduction varies from simple asexual cellular division via mitosis, to complex sexual reproductive strategies involving specialised reproductive structures and meiosis.

2.6.1.1 Asexual reproduction

Asexual reproduction refers to all reproductive modes in which a new individual is derived from only one parental source. It maintains the vegetative haploid (N) lifecycle phase (asexual morph) in ascomycetes by increasing fungal biomass and producing survival structures (Souza et al., 2003). Additionally, asexual reproduction can result in the production of asexual spores (conidia, macroconidia, microconidia and chlamydospores) from conidiophores within structures such as a pycnidium or acervuli, which germinate to produce mycelium (Pöggeler, 2001, Kiffer & Morelet, 1999). Asexual spores can provide species with short range dissemination mechanisms via rain or wind mediated spore dispersal. Both these mechanisms allow pathogens the potential to exploit additional environments.

The production of asexual spores occurs under specific genetic cues and environmental conditions (Leeder et al., 2011, Shi & Leung, 1995). Asexual reproduction can be advantageous as it uses less energy than sexual reproduction and for many species provides their only means of reproduction (Reece et al., 2014). Indicators of asexual reproduction in populations include significant linkage disequilibrium, occurrence of genetic subpopulations within species and congruent phylogenies between genes (Xu, 2006).

2.6.1.2 Sexual reproduction

Sexual reproduction in filamentous ascomycetes results in diploid sexual structures and/or cells within which meiosis occurs to produce haploid sexual spores (ascospores). The spores are formed within an ascus or sac like structure (Pöggeler, 2001). A single fertilisation event can produce hundreds of asci (Coppin et al., 1997). Sexual reproduction has some potential biological and ecological advantages over asexual reproduction. Firstly, it allows recombination of favourable mutations that have arisen in separate lineages within a single individual. This may result in increased fitness, evolution and adaptation to the environment (Xu, 2006). Secondly, in some species the spores can be discharged with sufficient force, allowing them to become airborne and providing a mechanism for long range inoculum dispersal (Hind et al., 2003). Additionally, sexual species tend to be more genotypically diverse than asexual species (Milgroom 1996). Indicators of recombination include linkage equilibrium, a lack of subpopulations within species and incongruence between phylogenies constructed using different genes (Geiser et al., 1998, Xu, 2006). However, sexual reproduction also requires significantly more energy than asexual reproduction in both the finding of mating partners and spore production (Metzenberg & Glass, 1990, Billiard et al., 2012). In addition, recombination can break apart beneficial gene combinations.

Not all species are able to undergo both asexual and sexual stages of reproduction. Approximately 20,000 fungal species are believed to reproduce only via an asexual means (Reece et al., 2014). There are a number of reasons for the loss of the sexual reproductive cycle in these species. These include, loss of functional mating-type genes, loss of one mating-type from populations (via drift or introduction of single strains into new environments) and non-conducive environmental conditions for the transition from asexual to sexual reproduction (Souza et al., 2003). For *M. tanaceti* the sexual morph has not been observed.

2.6.2 Genetics of sexual reproduction

2.6.2.1 Mating-type genes

Sexual reproduction is governed on a genetic level by mating-type (*MAT*) genes and the biochemical products and pathways associated with them (Billiard et al., 2011). *MAT* genes determine haploid cell identity, enable compatible mating partners to attract each other, and prepare cells for sexual reproduction after fertilisation (Casselton, 2008). The *MAT* locus refers to a region of a chromosome at which the *MAT* genes reside. It varies in size depending on the number and arrangement of the *MAT* gene components (Arie et al., 1997, Souza et al., 2003, Turgeon & Yoder, 2000). In most filamentous ascomycetes, two mating-types or idiomorphs can be found at the *MAT* locus. The two idiomorphs are termed *MAT1-1* and *MAT1-2* (also termed: *MAT1*/*MAT2* (Hsiang et al., 2003), *MAT-*/*MAT+* and *MATa*/*Matα* (Souza et al., 2003, Turgeon & Yoder, 2000)). The term idiomorph is used, rather than alleles due to the lack of similarity between the sequence data (Coppin et al., 1997) and the inability to determine that the two idiomorphs have a common hereditary origin (Metzenberg & Glass, 1990). Molecular analyses of the *MAT* genes suggest they encode transcriptional

regulators, with DNA-binding motifs found in the proteins encoded by each *MAT* gene (Arie et al., 1997). The *MAT1-2* idiomorph appears to be conserved within all genera with one gene per idiomorph and a single opening reading frame encoding a high mobility group (HMG) motif (Coppin et al., 1997). In comparison, the *MAT1-1* idiomorph can contain up to 4 genes. The *MAT1-1-1* gene encodes an alpha domain protein; the *MAT1-1-2* gene encodes an amphipathic alpha helix protein, the *MAT1-1-3* gene encodes a HMG domain protein and the *MAT1-1-4* encodes a metallothionein protein (Groenewald et al., 2007). However, all *MAT1-1* idiomorphs examined to date contain a *MAT1-1-1* gene (Turgeon & Yoder, 2000). The role of the *MAT* genes and their regulation mechanisms on other genes is known with considerable detail in the unicellular hemiascomycete yeast *Saccharomyces cerevisiae* and is well reviewed by Souza et al. (2003). However, in other ascomycetes little is known about the genes under the control of mating-type proteins.

In 1988, Glass *et al.*, cloned and sequenced *MAT1-1-1* and *MAT1-2-1* in the filamentous ascomycete *Neurospora crassa.* Subsequently, in the past 15 years the *MAT* genes of a large range of ascomycete species have been identified, including species which were presumed asexual (Cozijnsen & Howlett, 2003, Groenewald et al., 2006, Woudenberg et al., 2012). Despite differences in arrangement and sequence dissimilarity between different genera, and in many cases between species of the same genus, there are regions of the *MAT* loci that are conserved among species. These include regions of the alpha box (Cozijnsen & Howlett, 2003, Bennett et al., 1999), the HMG domain (Woudenberg et al., 2012, Hsiang et al., 2003, Bennett et al., 1999, Barve et al., 2003, Arie et al., 1997), and the regions flanking the *MAT* idiomorph (Turgeon et al., 1993, Dyer et al., 2001, Cozijnsen & Howlett, 2003, Woudenberg et al., 2012).

The arrangement of the *MAT* idiomorphs within individuals of a species has implication on their requirement for a mating partner for sexual reproduction (Coppin et al., 1997). Depending on this requirement species are classified as heterothallic or homothallic. This classification can be inferred by the ability of a single strain, or the requirement of the interaction of two strains, to produce a sexual morph *in vitro* and/or via detecting the arrangement of the *MAT* genes.

In heterothallic species, syngamy is restricted by the *MAT* loci, with fusion occurring between haploids containing different mating-type idiomorphs (Billiard et al., 2011). Most heterothallic ascomycete fungi present a uni-factorial system, in which they contain a single mating-type locus, containing either a *MAT1-1* or *MAT1-2* idiomorph (Turgeon & Yoder, 2000, Glass et al., 1988, Coppin et al., 1997). Therefore, for a compatible sexual reaction to occur, strains require a male donor cell from an individual containing an opposite mating-type, forcing them to outcross with genetically different individuals. Thus, heterothallic species are likely to be more genetically diverse due to outcrossing between individuals (which are genetically different). Individuals which are heterothallic are commonly characterised by which mating-type they contain. Morphologically heterothallic individual of each mating-type of the same species will appear indistinguishable (Pöggeler, 2001).

In comparison, homothallic species exhibit a lack of discrimination at fertilisation and are able to self-fertilise and complete the sexual cycle without the need for a partner (Billiard et al., 2011). However, they aren't restricted to self-fertilisation and can reproduce with other genetically different individuals (Burnett, 2003). The most frequent cause of homothalism is that each haploid possess the two idiomorphs in its genome (Billiard et al., 2011), allowing it

to undergo sexual reproduction when a single strain is present (Turgeon, 1998). The arrangement of the *MAT* idiomorphs in homothallic ascomycetes varies. Tightly linked *MAT1-1-1* and *MAT1-2-1* genes at the same loci occur in homothallic *Aspergillus sp*. (Ramirez-Prado et al., 2008), *Petromyces alliaceus* (Ramirez-Prado et al., 2008), *Didymella clematidis* and *Peyronellaea pinodes* (Woudenberg et al., 2012). Unlinked *MAT* genes have been observed in *Aspergillus nidualns* (sexual morph: *Emericella nidulans*) (Paoletti et al., 2007, Galagan et al., 2005) and *Neosartorya fischeri* (Rydholm et al., 2007). In these species the *MAT1-1* and *MAT1-2* idiomorphs are located on separate chromosomes. However homothallic fungi have also been identified in which only one of the two mating-type loci can be detected (Pöggeler, 1999, Glass et al., 1990, Debuchy & Turgeon, 2006). This observation may be due to the inability of degenerate primers to detect the second idiomorph.

While there is some confusion in the literature on the role of *MAT* genes in homothallic fungi, gene deletion studies have demonstrated the importance of both *MAT1-1-1* and *MAT1-2-1* genes for sexual reproduction in homothallic fungi. In these studies deletion of the *MAT* genes resulted in self-sterility (Poggeler et al., 2006, Paoletti et al., 2007, Lee et al., 2003). In addition, Paoletti et al. (2007) crossed homothallic mutants of *Aspergillus nidulans* containing a single *MAT1-1-1* or *MAT1-2-1* gene and produced non-sterile cleoistotheica. Furthermore, *MAT* genes from homothallic species have been shown to be functional in heterothallic species (Yun et al., 1999, Debuchy & Turgeon, 2006).

The genetic implications of sexual reproduction in homothallic species are dependent on the ratio of selfing to outcrossing. When a homothallic individual undergoes self-fertilisation the genetic outcomes are the same as if it were reproducing clonally, as the entire genome is

effectively linked (Xu, 2006). This results in linkage disequilibrium, where the haplotype frequencies within the population deviate from those expected if the genes at each locus were randomly combined (as would occur in a randomly outcrossing population) (Griffiths et al. 2008).

Recent studies have examined mating-types loci of species within the *Didymellaceae* (de Gruyter et al., 2009). *MAT* genes have been analysed in *Didymellaceae* species including: *Ascochyta lentis* (Cherif et al., 2006), *Didymella rabiei* (Barve et al., 2003), *Didymella zeae-maydis* (Yun et al., 2013), *Didymella vitalbina, Didymella clamatidis, Peyronellaea pinodes, Peyronellaea pinodella, Phoma herbarum, Phoma clematidina* (Woudenberg et al., 2012), *Stagonosporopsis tanaceti, Stagonosporopsis chrysanthemi, Stagonosporopsis inoxydabilis* (Vaghefi et al., 2015a), and *Phoma dennissi* (Voigt et al., 2005). In the homothallic species, *Didymella clamatidis, Peyronellaea pinodes, Stagonosporopsis chrysanthemi, Stagonosporopsis inoxydabilis* and *Didymella zeae-maydis* the *MAT1-1* and *MAT1-2* idiomorphs co-occurred at same locus, but the order of the arrangement of the two genes varied (Woudenberg et al., 2012, Vaghefi et al., 2015a, Yun et al., 2013),

2.6.2.2 Distribution of mating-types

For heterothallic species co-location of individuals of each mating-type is required for crossing. Thus, the frequency and spatial distribution of individuals of each mating-type within populations impacts the occurrence/frequency of sexual reproduction. Negative frequency-dependant selection is expected to retain equilibrium of the mating-type idiomorphs present in a heterothallic population that is sexually reproducing. In comparison,

in populations undergoing predominately asexual reproduction, the ratio becomes skewed. Therefore, statistical testing for equilibrium can be used to determine if mating-type frequencies reflect those expected in a sexually outcrossing species.

Molecular techniques are commonly used to genotype populations for mating-type. The mating-type of isolates can be determined using *MAT1-1-1*- and *MAT1-2-1*-specific PCR primers (Stergiopoulos et al., 2007, Zhan et al., 2002). However, for heterothallic species in which the two *MAT* idiomorphs occur at the same location within the genome, and which share high similarity in the regions flanking the idiomorphs, multiplex PCRs can be developed. This technique has been used in *Leptosphaeria maculans* (Cozijnsen & Howlett, 2003), *Ascochyta rabiei* (Barve et al., 2003), *Tapesia yallundae* (Dyer et al., 2001) and *Cercospora sp.* (Groenewald et al., 2007), allowing fast screening for both *MAT* idiomorphs within a single PCR reaction, with the *MAT1-1* and *MAT1-2* isolates differentiated by the length of the PCR product.

Analysing the distributions of mating-type idiomorphs within a geographical area is a common second step following idiomorph identification for heterothallic species. The geographical area (i.e population) over which this is examined varies. Analysis of a collection of isolates from multiple global locations was used to identify both *MAT* idiomorphs in the presumed asexual ascomycete *Cladosporium fulvum* (Stergiopoulos et al., 2007). Comparisons between geographical regions can also be used to identify explanations for differences in the observed frequency of sexual reproduction observed. For example, distribution studies in *Dothistroma septosporum* showed that only *MAT1-2* isolates were present in Australia and New Zealand, where only asexual reproduction had been identified.

However, isolates of both mating-type were found in isolates from Canada and Europe, where the sexual stage is known to occur (Groenewald et al., 2007). Furthermore, the lack of sexual reproduction observed for *Stagonosporopsis tanaceti* in Tasmanian pyrethrum fields has been proposed to be due to a lack of isolates containing the *MAT1-2-1* gene (Vaghefi et al., 2015a). In comparison, mating-type segregation studies can also eliminate the lack of a *MAT* idiomorph as the cause for lack of observation of a sexual stage. Dyer et al. (2001) showed that despite the low frequency of field observations of the sexual stage of *Tapesia acuformis*, the reason for the rare detection in the heterothallic fungi was not due to a lack of a particular mating-type idiomorph. In addition to identifying the frequency and ratio of mating-types, the spatial distribution of mating-types is also important, as physical interaction between isolates of the opposite mating type are required for sexual reproduction. Such analyses require sampling on a smaller spatial scale, such as within fields or plants. A study of *Stagonosporopsis nodorum*, which undergoes regular sexual reproduction, found that 23% of lesions on leaves of wheat (*Triticum aestivum* L.) contained isolates of both mating-type (Sommerhalder et al., 2006). In addition, Zhan et al. (2002) studied the mating-type ratios of *Mycosphaerella graminicola* isolates, isolated from two different pycnidia collected from each of 16 leaf lesions. They found that the two different pycnidia from 6 of the lesions contained isolate of different mating types. Furthermore, for the lesions for which isolates from the pycnidia had the same mating-type, the RFLP genotype profile of the two isolates was different (Zhan et al., 2002).

2.6.2.3 Environmental effects

Sexual reproduction is often induced in response to changes in environmental conditions, providing that the genetic requirements are concurrently meet. This can include changes in

temperature, pH, relative humidity, aeration, moisture or nutrient levels (Hawker, 1957). The conditions necessary for sexual reproduction are generally narrower than required for vegetative mycelial growth (Hawker, 1957). The specific conditions required are species specific and can vary for geographical populations of the same species (Dyer et al., 1992). For example, the homothallic species *Sclerotinia minor* and *Sclerotinia sclerotiorum* sexually reproduce via carpogenic germination of sclerotia. The sclerotia possess constitutive and exogenous dormancy, which must be overcome prior to carpogenic germination and subsequent ascospore production (Garg et al., 2010). This requires combinations of light, temperature and moisture for specific time periods (Sun & Yang, 2000). Despite being closely related, the temperature range for carpogenic germination of *Sclerotinia minor* is much narrower than *Sclerotinia sclerotiorum* (Ekins et al., 2002, Clarkson et al., 2007, Hawthorne, 1973). In addition, to the effects of temperature, light and moisture, the size of the sclerotia can also impact carpogenic germination, with smaller sclerotia unable to produce apothecia initials (Hao et al., 2003, Dillard et al., 1995). The size of sclerotia can be impacted by the nutrient source available during their production and thus, environmental conditions during sclerotia development may also impact the ability of these species to sexually reproduce.

Furthermore, the environmental factors required to induce the change from asexual to sexual reproduction often have ecological importance, such that they ensure sexual reproduction occurs when conditions are favourable (Dyer et al., 1992). For example, in *Sclerotinia minor* and *Sclerotinia sclerotiorum*, the stipes, produced during carpogenic germination, are positively phototrophic and will not differentiate into disks until they are exposed to light

(Willetts & Wong, 1980). This ensures they will not produce and disseminate ascospores prior to the apothecial disks being above the soil surface.

Identification of the environmental requirements for sexual reproduction for specific plant pathogens in agricultural systems is beneficial to allow the development of disease models, which can be used to identify periods conducive for disease epidemics (Clarkson et al., 2007). This may allow effective management strategies to be implemented during periods in which they will have the greatest impact on decreasing disease inoculum.

2.7 POPULATION GENETICS

Population genetics is a growing discipline which focuses on the processes that lead to genetic change in pathogen populations over time and space (McDonald, 2004). It attempts to investigate evolutionary forces such as mutation, migration, genetic drift, selection and recombination, and their effect on changes in gene frequencies in populations. These forces interact to shape the overall genetic structure of populations (Linde, 2010). The space over which is it evaluated is dependent on the specific biological questions being investigated, but can range from the smallest geographical distance, such as from within lesions on plants or between neighbouring plants, to the largest geographical distance, such as globally between and within continents (Goss et al., 2009, Lee & Neate, 2007, Zhan et al., 2003).

2.7.1 Genetic structure of populations

The genetic structure refers to the amount and distribution of genetic variation within and among populations (McDonald, 1997). It further reflects the evolutionary history of populations and their potential to evolve (McDonald & Linde, 2002). Mutation is one of the main sources of introduction of new alleles into populations. However, it does not have sufficient power to change the frequencies of alleles within populations (McDonald, 2004). Combinations of selection, genetic drift and migration affect the frequency of alleles in populations. Additionally, the mating and reproductive systems affect the way that alleles are combined in individuals in a population. Gene flow, or migration, is a key driver in limiting population divergence into sub populations. Isolation between populations, due to factors such as geographic separation or mating behaviour, which impede gene flow for multiple generations, will lead to populations genetically diverging via genetic drift or selection of specific alleles which allow the populations to better adapt to their environmental niches (McDonald, 2004). For comparison of populations a number of different descriptive parameters can be calculated or estimated. These include: the number of alleles per loci, percentage of polymorphic loci, relative occurrence of recombination and the amount of genetic diversity (Xu, 2006). Genetic diversity is composed of both gene and genotypic diversity (McDonald, 2004).

2.7.1.1 Gene diversity

Gene diversity refers to the number and frequency of alleles at each individual loci in a population (Burnett, 2003). It is not affected by the mating system, but is largely dependent

on the genetic marker used, mutation rate and the size and age of the population. Larger populations are expected to have higher gene diversity as they contain more alleles and undergo less genetic drift. Additionally, older populations have had a greater period to acquire mutations and for genetic drift to act (Burnett, 2003). The most commonly used measure of gene diversity is Nei's measure of gene diversity (Nei, 1973).

2.7.1.2 Genotypic diversity

Genotypic diversity is dependent on both the number and distribution of genotypes within a population. Common indices of genotypic diversity are Stoddart and Taylor's *G* (Stoddart & Taylor, 1988), Shannon-Weavers *H'* (Shannon & Weaver, 1963) and Simpson's index *D* (Simpson, 1949). Genotypic diversity is composed of richness and evenness, which refer to the number and distribution of genotypes in a population, respectively (Grunwald et al., 2003). Genotypic diversity increases as the number of genotypes (richness) increases and as the frequencies of genotypes become more evenly distributed (evenness) (McDonald, 2004). As richness tends to increase with population size (and therefore so does genotypic diversity), when genotypic indices of populations of different sizes are compared caution should be taken. A number of scaling methods for calculating the genotypic diversity indices have been examined by Grunwald et al. (2003) to allow comparisons of populations with different sample numbers.

Genotypic diversity is affected by the mating system (Burnett, 2003). Recombination provides the key mechanism to form new combinations of genes, which creates new

genotypes and generates high genotypic diversity. Thus, high genotypic diversity is generally considered to be a signature of sexual reproduction (Halkett et al., 2005). However, in some instances where populations exhibit low gene diversity (i.e. it originated from a small number of individuals), genotypic diversity may be low even if the population is randomly outcrossing (McDonald, 2004). Pathogens that undergo asexual reproduction tend to maintain old combinations of genes/alleles, resulting in lower genotypic diversity in populations (Burnett, 2003). This can result in the occurrence of clones, or clonal lineages within populations, which are all genetically identical. An increase in frequency of particular clones in a population (due to selection) results in a decrease in the genotypic diversity of the population (McDonald, 2004).

2.7.1.3 Assessing recombination

In addition to identifying populations with high genotypic diversity, a number of indices can be calculated to support the occurrence of recombination within populations. Linkage disequilibrium is a measure of the associations among alleles at different loci. It can be tested between loci pairs or over all loci examined (Xu, 2006). Random association between alleles at different loci is an indicator of recombination (Milgroom, 1996). Multilocus linkage disequilibrium can be measured by the index of association (I_a) (Brown et al., 1980) or the standardised index of association ($\bar{r}_d$) (Agapow & Burt, 2001). For fungal species with a mixed mode of reproduction, in which a sexual cycle is followed by multiple rounds of asexual reproduction, clonal lineages can develop within populations. The infrequent occurrence of recombination in these populations contributes to population structure by generating genetic variation. In some instances this can be identified by analysing clone corrected populations, which contain only a single copy of each genotype for each population

(Xu, 2006, Kamvar et al., 2014). However, as linkage disequilibrium between unlinked loci can only decay by a maximum of 50% with recombination from each sexual generation, it may take several sexual recombination events for the disequilibrium to be eliminated (Ardlie et al., 2002). In addition, for homothallic species, which undergo recombination following self-fertilisation, the entire genome is effectively linked (Xu, 2006). Therefore, linkage disequilibrium may persist even in populations that are randomly mating. Thus it should be used predominately as an indicator for the occurrence of sexual recombination, rather than to exclude its occurrence (Milgroom, 1996, Brewer et al., 2012).

2.7.2 Genetic markers for population analysis

Population genetics utilises polymorphic markers to determine the frequency and distribution of alleles within populations (Schurko et al., 2009). In most instances, it is best to use genetic markers which are selectively neutral, highly informative and relatively easy to assay (McDonald, 1997, Michelmore & Hulbert, 1987). Though, in some instances markers in specific genes are required (Xu, 2006). Markers can be phenotypic (i.e. mycelial compatibility groups) or based on DNA characteristics (D'Surney et al., 2001, Xu, 2006, Michelmore & Hulbert, 1987). DNA markers are advantageous over phenotypic markers in that they are highly heritable, easy to assay and not affected by environmental factors (Duran et al., 2009). A number of DNA based markers are available for the study of fungal population genetics. DNA makers are classified as either binary (alleles are present or absent) or polymorphic (multiple alleles at each loci). In addition, they can be defined as dominant or co-dominant. Co-dominant markers are able to distinguish heterozygotes from homozygotes, whereas dominant markers cannot distinguish the two (Kosman & Leonard, 2005). However, in haploid genomes, such as occurs for many ascomycetes in their asexual

morph, there is only one set of the chromosomes and thus one allele for each locus (Xu, 2006). Therefore, a wider range of markers are available for use in haploid species.

Historically, restriction fragment length polymorphism (RFLP) (Botstein et al., 1980), random amplified polymorphic DNA (RAPD) (Welsh & McClelland, 1990), and amplified fragment length polymorphism (AFLP) (Vos et al., 1995) makers have been commonly used for studying population genetics. These DNA-based binary markers utilise restriction enzyme digestion, PCR amplification and a combination of the two, respectively (Xu, 2006). These markers are beneficial for use in species for which genomic information is limited, as they do don't require any prior genome knowledge. While, RFLP and RAPD makers have issues with reproducibility of results, AFLP markers are more sensitive and reproducible (Singh et al., 2013, Abdel-Mawgood, 2012).

More recently the use of microsatellite and single nucleotide polymorphism (SNP) markers for analysing plant pathogens has become more popular due to the decreased cost of their development, ease of use and ability to automate allele calls. (Singh et al., 2013). Microsatellites, or simple sequence repeats (SSRs), are DNA sequences that generally consist from 5 – 40 tandem repeats of a 2 – 6 base pair nucleotide sequence (Selkoe & Toonen, 2006). Microsatellite loci are proposed to evolve via a stepwise mutation model, such that variation in the number of repeats (which occurs during DNA replication or repair) is incremental, changing one step at a time going up or down (Valdes et al., 1993, Levinson & Gutman, 1987). Over many generations these accumulate leading to individuals containing different microsatellite variants (Cunningham & Meghen, 2001). The number of repeats of the SSR motif can be scored using fragment length analysis, in which the length of the

amplified fragment is used to determine the number of repeats (Xu, 2006). However, high resolution melt (HRM) analysis has been employed as an efficient, accurate and cost-effective alternative to fragment length electrophoresis based methods for differentiating alleles of SSR markers (Arthofer et al., 2011, Distefano et al., 2012). (Atallah & Subbarao, 2012). Their popularity as genetic markers include their co-dominance, abundance within genomes, high level of polymorphism, requirement of low quantities of DNA and high within-population and within-individual variability. They can further be analysed as single alleles, genotypic arrays and as gene genealogies. These characteristics result in SSR markers being versatile to address many ecological questions (Selkoe & Toonen, 2006).

In comparison, SNP markers (Singh et al., 2013) represent the most widespread source of sequence variation in genomes (Brumfield et al., 2003, Abdel-Mawgood, 2012). The frequency of occurrence of SNPs in a genome is generally one SNP in every 100 – 3000 bp (Singh et al., 2013). They are co-dominant, but are restricted to four character states. While this might make SNPs less informative than microsatellites for detecting fine-scale geographic structure this limitation can be offset by scoring more loci (Brumfield et al., 2003, Atallah & Subbarao, 2012). SNP markers are becoming increasingly popular for population genetics. Genotyping SNP data can be done by comparing sequence data, or if the SNP occurs in a known DNA region, it can be amplified by PCR and differentiated by HRM. Only a few studies have reported on the use of SNP data in fungi, though its use is increasing as genomic sequencing services increase in performance and decrease in cost (Xu et al., 2007, Sha et al., 2008, Abbott et al., 2010, Leboldus et al., 2015, Akamatsu et al., 2007, Amend et al., 2010).

Developing SSR and SNP markers can often be challenging and expensive, as they often need to be identified *de novo* for each species (Selkoe & Toonen, 2006). However, in some instances, SSR markers can be cross-amplified in closely related species (Barbara et al., 2007). However, this species specificity also minimises issues with contamination by cross-amplification of the SSR loci in non-target organisms (Selkoe & Toonen, 2006). Microsatellite and SNP loci can be detected via sequencing and screening DNA libraries of the target species.. However, the increased ability to sequence the full genome of non-model fungal species has simplified the process, allowing the whole genome to be analysed for SSR motifs and SNP regions (Duran et al., 2009, Atallah & Subbarao, 2012). A number of search algorithms can be used to detect SSR motifs and SNPs within genomic data (Meglécz et al., 2010, Benson, 1999, Liu et al., 2010)

2.8 SUMMARY

Studies evaluating population biology of the tan spot pathogen of pyrethrum have not been conducted. The genus *Microsphaeropsis* appears to be paraphyletic and thus phylogenetic evaluation of the tan spot pathogen is warranted. Therefore, one of the objectives of this research was to evaluate the taxonomic placement of the two identified ITS-haplotypes of *M. tanaceti* within the *Didymellaceae*. Additionally, it aimed to assess the relationship between the two ITS-haplotypes via identifying genetic and morphological differences between the two. The complete reproductive strategy of *M. tanaceti* is unresolved, with only the occurrence of asexual reproduction confirmed. Therefore an objective of this research was to identify the molecular potential of sexual reproduction in *M. tanaceti* via examining the structure and arrangement of the mating-type genes in individuals. Following this, if appropriate, it aimed to undertake population analysis of the distribution of mating-types

within field populations and test for ascospore production *in vitro*. Understanding the genetic population structure of pathogen populations can aid in identifying their evolutionary history and adaptive ability. Therefore this research aimed to analyse the amount and structure of genetic diversity within geographically separated field populations of *M. tanaceti*. However, molecular markers for analysing *M. tanaceti* populations have not been developed. Therefore one of the objectives of this research was to develop a set of polymorphic SSR markers for population genetic analysis. Disease control failures have been identified which have been associated with the isolation of *M. tanaceti* isolates with a phenotype inferring resistance to boscalid. The underlying molecular mechanisms resulting in this phenotype remain unknown. In a number of other pathosystems boscalid resistance has been shown to be caused by/correlated with mutations in the SDHI subunits. An objective of this research was to initiate the identification of the molecular mechanism causing a boscalid resistant phenotype by examining the *SDHB* gene of *M. tanaceti* isolates with varying *in vitro* boscalid growth responses, to identify mutations which correlated with reduced boscalid sensitivity. A secondary objective was to develop a molecular screen to identify the distribution of individuals with specific mutations in commercial fields. By fulfilling the objectives outlined above, it is envisioned that some of the current knowledge gaps within this pathosystems will be filled.

2.9 REFERENCES

Abbott C, Gilmore S, Lewis C, *et al.*, 2010. Development of a SNP genetic marker system based on variation in microsatellite flanking regions of *Phytophthora infestans*. *Canadian Journal of Plant Pathology* **32**, 440-57.

Abdel-Mawgood AL, 2012. DNA based techniques for studying genetic diversity. In: Caliskan M, ed. *Genetic Diversity in Microorganisms.* InTech, 95-122.

Agapow P-M, Burt A, 2001. Indices of multilocus linkage disequilibrium. *Molecular Ecology Notes* **1**, 101-2.

Ahmad S, 1960. Further contributions to the fungi of West Pakistan, I. *Biologia, Lahore* **6**, 117-36.

Ahman S, 1971. Contributions to the fungi of West Pakistan. X. *Biologia, Lahore* **17**, 1-26.

Akamatsu HO, Grünwald NJ, Chilvers MI, Porter LD, Peever TL, 2007. Development of codominant simple sequence repeat, single nucleotide polymorphism and sequence characterized amplified region markers for the pea root rot pathogen, *Aphanomyces euteiches*. *Journal of Microbiological Methods* **71**, 82-6.

Amend A, Garbelotto M, Fang Z, Keeley S, 2010. Isolation by landscape in populations of a prized edible mushroom *Tricholoma matsutake*. *Conservation Genetics* **11**, 795-802.

Antonious GF, 2004. Residues and half-lives of pyrethrins on field-grown pepper and tomato. *Journal of Environmental Science and Health, Part B* **39**, 491-503.

Antonious GF, Byers ME, Kerst WC, 1997. Residue levels of pyrethrins and piperonyl butoxide in soil and runoff water. *Journal of Environmental Science and Health Part B-Pesticides Food Contaminants and Agricultural Wastes* **32**, 621-44.

Antonious GF, Patel GA, Snyder JC, Coyne MS, 2004. Pyrethrins and piperonyl butoxide adsorption to soil organic matter. *Journal of Environmental Science and Health Part B-Pesticides Food Contaminants and Agricultural Wastes* **39**, 19-32.

Ardlie KG, Kruglyak L, Seielstad M, 2002. Patterns of linkage disequilibrium in the human genome. *Nature Reviews Genetics* **3**, 299-309.

Arie T, Christiansen S, Yoder O, Turgeon B, 1997. Efficient cloning of ascomycete mating type genes by PCR amplification of the conserved MAT HMG box. *Fungal Genetics and Biology* **21**, 118-30.

Arthofer W, Steiner FM, Schlick-Steiner BC, 2011. Rapid and cost-effective screening of newly identified microsatellite loci by high-resolution melting analysis. *Molecular Genetics and Genomics* **286**, 225-35.

Atallah ZK, Subbarao KV, 2012. Population biology of fungal plant pathogens. *Methods in Molecular Biology* **835**, 333-63.

Avenot H, Sellam A, Karaoglanidis G, Michailides T, 2008. Characterization of mutations in the iron-sulphur subunit of succinate dehydrogenase correlating with boscalid resistance in *Alternaria alternata* from California pistachio. *Phytopathology* **98**, 736-42.

Avenot H, Sellam A, Michailides T, 2009. Characterization of mutations in the membrane-anchored subunits AaSDHC and AaSDHD of succinate dehydrogenase from *Alternaria alternata* isolates conferring field resistance to the fungicide boscalid. *Plant Pathology* **58**, 1134-43.

Avenot HF, Michailides TJ, 2007. Resistance to boscalid fungicide in *Alternaria alternata* isolates from pistachio in California. *Plant Disease* **91**, 1345-50.

Avenot HF, Michailides TJ, 2010. Progress in understanding molecular mechanisms and evolution of resistance to succinate dehydrogenase inhibiting (SDHI) fungicides in phytopathogenic fungi. *Crop Protection* **29**, 643-51.

Avenot HF, Thomas A, Gitaitis RD, Langston Jr DB, Stevenson KL, 2012. Molecular characterization of boscalid and penthiopyrad resistant isolates of *Didymella bryoniae* and assessment of their sensitivity to fluopyram. *Pest Management Science* **68**, 645-51.

Aveskamp M, De Gruyter J, Woudenberg J, Verkley G, Crous PW, 2010. Highlights of the *Didymellaceae*: A polyphasic approach to characterise *Phoma* and related pleosporalean genera. *Studies in Mycology* **65**, 1-60.

Aveskamp M, Gruyter DJ, Crous P, 2008. Biology and recent developments in the systematics of Phoma, a complex genus of major quarantine significance. *Fungal Diversity* **31**, 1-18.

Barbara T, Palma-Silva C, Paggi GM, Bered F, Fay MF, Lexer C, 2007. Cross-species transfer of nuclear microsatellite markers: potential and limitations. *Molecular Ecology* **16**, 3759-67.

Barimani M, Pethybridge S, Vaghefi N, Hay F, Taylor P, 2013. A new anthracnose disease of pyrethrum caused by *Colletotrichum tanaceti* sp. nov. *Plant Pathology* **62**, 1248-57.

Barve M, Arie T, Salimath S, Muehlbauer F, Peever T, 2003. Cloning and characterization of the mating type (MAT) locus from *Ascochyta rabiei* (teleomorph: *Didymella rabiei*) and a MAT phylogeny of legume-associated *Ascochyta* spp. *Fungal Genetics and Biology* **39**, 151-67.

Beckerman JL, 2013. Detection of fungicide resistance. In: Nita M, ed. *Fungicides - Showcase of Integrated Plant Disease Management from Around the World.* 281-310.

Bennett R, Yun S, Lee T, *et al.*, 1999. Mating type-specific PCR primers for *Stagonospora nodorum* field studies. In. *Septoria and Stagonospora Diseases of Cereals: A Compilation of Global Research: Proceedings of the Fifth International Septoria Workshop, September 20-24, CIMMYT*. Mexico, 90-3.

Benson G, 1999. Tandem repeats finder: a program to analyze DNA sequences. *Nucleic Acids Research* **27**, 573.

Bernier J, Carisse O, Paulitz TC, 1996. Fungal communities isolated from dead apple leaves from orchards in Quebec. *Phytoprotection* **77**, 129-34.

Bhat BK, Menary RC, 1984. Pyrethrum production in Australia - its past and present potential. *Journal of the Australian Institute of Agricultural Science* **50**, 189-92.

Bhat K, 1995. Breeding methodologies applicable to pyrethrum. In: Casida JE, Quistad G, eds. *Pyrethrum Flowers: Chemistry, Toxicology and Uses.* New York: Oxford University Pres, 67-94.

Billiard S, Lopez-Villavicencio M, Devier B, Hood ME, Fairhead C, Giraud T, 2011. Having sex, yes, but with whom? Inferences from fungi on the evolution of anisogamy and mating types. *Biological Reviews* **86**, 421-42.

Billiard S, Lopez-Villavicencioi M, Hood M, Giraud T, 2012. Sex, outcrossing and mating types: unsolved questions in fungi and beyond. *Journal of Evolutionary Biology* **25**, 1020-38.

Boerema GH, Gruyter JD, Noordeloos M, Hamers ME, 2004. *Phoma identification manual. Differentiation of specific and infra-specific taxa in culture*. Wallingford, United Kingdom: CABI Publishing.

Bojnanský V, Fargašová A, 2007. *Atlas of seeds and fruits of Central and East-European Flora: the Carpathian Mountains region*. Netherlands: Springer.

Botstein D, White RL, Skolnick M, Davis RW, 1980. Construction of a genetic linkage map in man using restriction fragment length polymorphisms. *American Journal of Human Genetics* **32**, 314.

Brent KJ, Hollomon DW, 1995. *Fungicide resistance in crop pathogens: How can it be managed?* Brussels, Belgium: Fungicide Resistance Action Committee.

Brent KJ, Hollomon DW, Federation GCP, 1998. *Fungicide resistance: the assessment of risk*. Brussels, Belgium: Fungicide Resistance Action Committee

Brewer MT, Frenkel O, Milgroom MG, 2012. Linkage disequilibrium and spatial aggregation of genotypes in sexually reproducing populations of *Erysiphe necator*. *Phytopathology* **102**, 997-1005.

Brown A, Feldman M, Nevo E, 1980. Multilocus structure of natural populations of *Hordeum spontaneum*. *Genetics* **96**, 523-36.

Brown P, 1992. *Morphological and physiological aspects of flower initiation and development in Tanacetum cinerariaefolium L*. University of Tasmania: University of Tasmania, Doctor of Philosophy.

Brown PH, Menary RC, 1994. Flowering in pyrethrum (*Tanacetum cinerariaefolium* L) .1. Environmental requirements. *Journal of Horticultural Science* **69**, 877-84.

Brumfield RT, Beerli P, Nickerson DA, Edwards SV, 2003. The utility of single nucleotide polymorphisms in inferences of population history. *Trends in Ecology & Evolution* **18**, 249-56.

Bujold I, Paulitz TC, Carisse O, 2001. Effect of *Microsphaeropsis* sp. on the production of perithecia and ascospores of *Gibberella zeae*. *Plant Disease* **85**, 977-84.

Burnett JH, 2003. *Fungal populations & species*. New York: Oxford University Press on Demand.

Capote N, Pastrana AM, Aguado A, Sánchez-Torres P, 2012. Molecular tools for detection of plant pathogenic fungi and fungicide resistance. In: Cumagun CJ, ed. *Plant Pathology*. European Union: InTech, 151-202.

Carisse O, Bernier J, 2002. *Microsphaeropsis ochracea* sp. nov. associated with dead apple leaves. *Mycologia* **94**, 297-301.

Carisse O, El Bassam S, Benhamou N, 2001. Effect of M*icrosphaeropsis* sp. strain P130A on germination and production of sclerotia of *Rhizoctonia solani* and interaction between the antagonist and the pathogen. *Phytopathology* **91**, 782-91.

Carisse O, Philion V, Rolland D, Bernier J, 2000. Effect of fall application of fungal antagonist on spring ascospore production of the apple scab pathogen, *Venturia inaequalis*. *Phytopathology* **90**, 31-7.

Carisse O, Rolland D, Tremblay DM, 2006. Effect of *Microsphaeropsis ochracea* on production of sclerotia-borne and airborne conidia of *Botrytis squamosa*. *BioControl* **51**, 107-26.

Casida JE, 1980. Pyrethrum flowers and pyrethroid insecticides. *Environmental Health Perspectives* **34**, 189-202.

Casida JE, Quistad GB, 1995. *Pyrethrum flower: production, chemistry, toxicology, and uses.* New York: Oxford University Press.

Casselton LA, 2008. Fungal sex genes - searching for the ancestors. *Bioessays* **30**, 711-4.

Chatzidimopoulos M, Ganopoulos I, Madesis P, Vellios E, Tsaftaris A, Pappas A, 2014. High-resolution melting analysis for rapid detection and characterization of *Botrytis cinerea* phenotypes resistant to fenhexamid and boscalid. *Plant Pathology* **63**, 1336-43.

Cherif M, Chilvers MI, Akamatsu H, Peever TL, Kaiser WJ, 2006. Cloning of the mating type locus from *Ascochyta lentis* (teleomorph : *Didymella lentis*) and development of a multiplex PCR mating assay for *Ascochyta* species. *Current Genetics* **50**, 203-15.

Clarkson JP, Phelps K, Whipps JM, Young CS, Smith JA, Watling M, 2007. Forecasting Sclerotinia disease on lettuce: a predictive model for carpogenic germination of *Sclerotinia sclerotiorum* sclerotia. *Phytopathology* **97**, 621-31.

Cochran DG, 1995. Insect resistance to pyrethrins and pyrethroids. In: Casida JE, Quistad G, eds. *Pyrethrum Flowers: Chemistry, Toxicology and Uses.* New York: Oxford University Pres, 234-48.

Coppin E, Debuchy R, Arnaise S, Picard M, 1997. Mating types and sexual development in filamentous ascomycetes. *Microbiology and Molecular Biology Reviews* **61**, 411-28.

Cox KD, Quello K, Deford RJ, Beckerman JL, 2009. A rapid method to quantify fungicide sensitivity in the brown rot pathogen *Mondinia fructicola*. *Plant Disease* **93**, 328-31.

Cozijnsen AJ, Howlett BJ, 2003. Characterisation of the mating-type locus of the plant pathogenic ascomycete *Leptosphaeria maculans*. *Current Genetics* **43**, 351-7.

Crombie L, 1995. Chemistry of pyrethrins. In: Casida JE, Quistad G, eds. *Pyrethrum Flowers: Chemistry, Toxicology and Uses.* New York: Oxford University Press, 123-92.

Crous PW, Summerell BA, Swart L, *et al.*, 2011. Fungal pathogens of *Proteaceae*. *Persoonia: Molecular Phylogeny and Evolution of Fungi* **27**, 20-45.

Cunningham EP, Meghen CM, 2001. Biological identification systems: genetic markers. *Scientific and Technical Review Of The Office International Des Epizooties* **20**, 491-9.

Curvers K, Pycke B, Kyndt T, Vanrompay D, Haesaert G, Gheysen G, 2015. A high-resolution melt (HRM) assay to characterize CYP51 haplotypes of the wheat pathogen *Mycosphaerella graminicola*. *Crop Protection* **71**, 12-8.

D'surney S, Shugart L, Theodorakis C, 2001. Genetic markers and genotyping methodologies: an overview. *Ecotoxicology* **10**, 201-4.

De Gruyter J, Aveskamp MM, Woudenberg JHC, Verkley GJM, Groenewald JZ, Crous PW, 2009. Molecular phylogeny of *Phoma* and allied anamorph genera: Towards a reclassification of the *Phoma* complex. *Mycological Research* **113**, 508-19.

Debuchy R, Turgeon B, 2006. Mating-type structure, evolution, and function in euascomycetes. In: Kües U, Fischer R, eds. *Growth, Differentiation and Sexuality.* Berlin Heidelberg: Springer, 293-323.

Deising HB, Reimann S, Pascholati SF, 2008. Mechanisms and significance of fungicide resistance. *Brazilian Journal of Microbiology* **39**, 286-95.

Dekker J, 1988. How to detect and measure fungicide resistance. In. *Experimental Techniques in Plant Disease Epidemiology.* Berlin, Germany: Springer, 153-63.

Dillard H, Ludwig J, Hunter J, 1995. Conditioning sclerotia of *Sclerotinia sclerotiorum* for carpogenic germination. *Plant Disease* **79**, 411-5.

Distefano G, Caruso M, La Malfa S, Gentile A, Wu S-B, 2012. High resolution melting analysis is a more sensitive and effective alternative to gel-based platforms in analysis of SSR – An example in citrus. *PLoS One* **7**, e44202.

Duchon S, Bonnet J, Marcombe S, Zaim M, Corbel V, 2009. Pyrethrum: a mixture of natural pyrethrins has potential for malaria vector control. *Journal of Medical Entomology* **46**, 516-22.

Duran C, Edwards D, Batley J, 2009. Molecular marker discovery and genetic map visualisation. In. *Bioinformatics.* New York: Springer, 165-89.

Dyer P, Furneaux P, Douhan G, Murray T, 2001. A multiplex PCR test for determination of mating type applied to the plant pathogens *Tapesia yallundae* and *Tapesia acuformis*. *Fungal Genetics and Biology* **33**, 173-80.

Dyer PS, Ingram DS, Johnstone K, 1992. The control of sexual morphogenesis in the Ascomycotina *Biological Reviews of the Cambridge Philosophical Society* **67**, 421-58.

Ekins M, Aitken E, Goulter K, 2002. Carpogenic germination of *Sclerotinia minor* and potential distribution in Australia. *Australasian Plant Pathology* **31**, 259-65.

Fernández-Ortuño D, Chen F, Schnabel G, 2012. Resistance to pyraclostrobin and boscalid in *Botrytis cinerea* isolates from strawberry fields in the Carolinas. *Plant Disease* **96**, 1198-203.

Forster H, Kanetis L, Adaskaveg JE, 2004. Spiral gradient dilution, a rapid method for determining growth responses and 50% effective concentration values in fungus-fungicide interactions. *Phytopathology* **94**, 163-70.

Fraaije BA, Bayon C, Atkins S, Cools HJ, Lucas JA, Fraaije MW, 2012. Risk assessment studies on succinate dehydrogenase inhibitors, the new weapons in the battle to control Septoria leaf blotch in wheat. *Molecular Plant Pathology* **13**, 263-75.

Frac, 2015. FRAC Code List 2015: Fungicides sorted by mode of action. In.: Fungicide Resistance Action Committee.

Galagan JE, Calvo SE, Cuomo C, *et al.*, 2005. Sequencing of *Aspergillus nidulans* and comparative analysis with *A. fumigatus* and *A. oryzae*. *Nature* **438**, 1105-15.

Garg H, Sivasithamparam K, Barbetti MJ, 2010. Scarification and environmental factors that enhance carpogenic germination of sclerotia of *Sclerotinia sclerotiorum*. *Plant Disease* **94**, 1041-7.

Geiser DM, Pitt JI, Taylor JW, 1998. Cryptic speciation and recombination in the aflatoxin-producing fungus *Aspergillus flavus*. *Proceedings of the National Academy of Sciences* **95**, 388-93.

Ghannoum MA, Rice LB, 1999. Antifungal agents: mode of action, mechanisms of resistance, and correlation of these mechanisms with bacterial resistance. *Clinical Microbiology Reviews* **12**, 501-17.

Gisi U, Sierotzki H, Cook A, Mccaffery A, 2002. Mechanisms influencing the evolution of resistance to Qo inhibitor fungicides. *Pest Management Science* **58**, 859-67.

Glass NL, Grotelueschen J, Metzenberg RL, 1990. *Neurospora crassa* A mating-type region. *Proceedings of the National Academy of Sciences* **87**, 4912-6.

Glass NL, Vollmer SJ, Staben C, Grotelueschen J, Metzenberg RL, Yanofsky C, 1988. DNAs of the 2 mating-type alleles of *Neurospora crassa* are highly dissimilar. *Science* **241**, 570-3.

Glattli A, Stammler G, Schlehuber S. Mutations in the target proteins of succinate-dehydrogenase inhibitors (SDHI) and 14alpha-demethylase inhibitors (DMI) conferring changes in the sensitivity - structural insights from molecular modelling. *Proceedings of the French Association of Plant Protection, 9th international conference on plant diseases, 8 - 9 December 2009*. Tours, France, 670-81.

Glynne-Jones A, 2001. Pyrethrum. *Pesticide Outlook* **12**, 195-8.

Goss EM, Larsen M, Chastagner GA, Givens DR, Gruenwald NJ, 2009. Population genetic analysis infers migration pathways of *Phytophthora ramorum* in US nurseries. *PLoS Pathogens* **5**, e1000583.

Grasso V, Palermo S, Sierotzki H, Garibaldi A, Gisi U, 2006. Cytochrome b gene structure and consequences tor resistance to Qo inhibitor fungicides in plant pathogens. *Pest Management Science* **62**, 465-72.

Grdiša M, Carović-Stanko K, Kolak I, Šatović Z, 2009. Morphological and biochemical diversity of Dalmatian pyrethrum (*Tanacetum cinerariifolium* (Trevir.) Sch. Bip.). *Agriculturae Conspectus Scientificus* **74**, 73-80.

Grdisa M, Liber Z, Radosavljevic I, Carovic-Stanko K, Kolak I, Satovic Z, 2014. Genetic diversity and structure of Dalmatian pyrethrum (*Tanacetum cinerariifolium* Trevir./Sch./Bip., Asteraceae) within the Balkan Refugium. *PLoS One* **9**.

Greenhill M, 2007. Pyrethrum production: Tasmanian success story. *Chronica* **47**, 5-8.

Groenewald M, Barnes I, Bradshaw RE, *et al.*, 2007. Characterization and distribution of mating type genes in the *Dothistroma* needle blight pathogens. *Phytopathology* **97**, 825-34.

Groenewald M, Groenewald JZ, Harrington TC, Abeln EC, Crous PW, 2006. Mating type gene analysis in apparently asexual *Cercospora* species is suggestive of cryptic sex. *Fungal Genetics and Biology* **43**, 813-25.

Grunwald NJ, Goodwin SB, Milgroom MG, Fry WE, 2003. Analysis of genotypic diversity data for populations of microorganisms. *Phytopathology* **93**, 738-46.

Hägerhäll C, 1997. Succinate: quinone oxidoreductases: variations on a conserved theme. *Biochimica et Biophysica Acta* **1320**, 107-41.

Halkett F, Simon J-C, Balloux F, 2005. Tackling the population genetics of clonal and partially clonal organisms. *Trends in Ecology & Evolution* **20**, 194-201.

Hall MR, Brumble LM, Mayes MA, Snow JL, Keeling JH, 2013. Cutaneous *Microsphaeropsis arundinis* infection initially interpreted as squamous cell carcinoma. *International Journal of Dermatology* **52**, 84-6.

Hao J, Subbarao K, Duniway J, 2003. Germination of *Sclerotinia minor* and *S. sclerotiorum* sclerotia under various soil moisture and temperature combinations. *Phytopathology* **93**, 443-50.

Hawker LE, 1957. The effect of environment on sporulation. In. *The physiology of reproduction in fungi*. Cambridge: The University Press, 24-47.

Hawthorne B, 1973. Production of apothecia of *Sclerotinia minor*. *New Zealand Journal of Agricultural Research* **16**, 559-60.

Hay F, Stirling G, Chung B. Plant-parasitic nematodes associated with pyrethrum in Tasmania. *Proceedings of the Proceedings of the 13th Biennial Australian Plant Pathology Society conference, 2001*. Cairns, Queensland, Australia, 208

Hay F, Stirling G, Pethybridge S, Chung B, 2009. A survey of nematodes associated with pyrethrum in Tasmania, Australia, and the susceptibility of pyrethrum cultivars to root-lesion nematode. *Australasian Plant Pathology* **38**, 1-5.

Hay FS, Gent DH, Pilkington SJ, Pearce TL, Scott JB, Pethybridge SJ, 2015. Changes in distribution and frequency of fungi associated with a foliar disease complex of pyrethrum in Australia. *Plant Disease* **99**, 1227-35.

Head SW, 1966. A study of the insecticidal constituents in *Chrysanthemum cinerariaefolium.* (1) Their development in the flower head. (2) Their distribution in the plant. *Pyrethrum Post* **8**, 32-7.

Hind TL, Ash GJ, Murray GM, 2003. Prevalence of Sclerotinia stem rot of canola in New South Wales. *Australian Journal of Experimental Agriculture* **43**, 163-8.

Hobbelen PHF, Paveley ND, Van Den Bosch F, 2014. The emergence of resistance to fungicides. *PLoS One* **9**, e91910.

Hocombe S, Kroll U, 1962. The effects of overall herbicide treatments on established East African pyrethrum. *International Journal of Pest Management C* **8**, 319-27.

Hollomon D, Brent K, 2007. Fungicide resistance: the assessment of risk. In. *FRAC Monograph No.2 second (revised) editition.* Brussels, Belgium: Fungicide Resistance Action Committee 53.

Hollomon D, Butters J, Kendall S, 1997. Mechanism of resistance to fungicides. In: Sjut V, ed. *Molecular Mechanisms of Resistance to Agrochemicals.* New York: Springer, 1-20.

Horsefield R, Yankovskaya V, Sexton G, *et al.*, 2006. Structural and computational analysis of the quinone-binding site of complex II (succinate-ubiquinone oxidoreductase) - A mechanism of electron transfer and proton conduction during ubiquinone reduction. *Journal of Biological Chemistry* **281**, 7309-16.

Hsiang T, Chen F, Goodwin PH, 2003. Detection and phylogenetic analysis of mating type genes of *Ophiosphaerella korrae*. *Canadian Journal of Botany* **81**, 307-15.

Huang S, Millar AH, 2013. Succinate dehydrogenase: the complex roles of a simple enzyme. *Current Opinion in Plant Biology* **16**, 344-9.

Ishii H, Fountaine J, Chung W-H, *et al.*, 2009. Characterisation of Qol-resistant field isolates of *Botrytis cinerea* from citrus and strawberry. *Pest Management Science* **65**, 916-22.

Ishii H, Yano K, Date H, *et al.*, 2007. Molecular characterization and diagnosis of QoI resistance in cucumber and eggplant fungal pathogens. *Phytopathology* **97**, 1458-66.

Isman M, Regnault-Roger C, Philogène B, Vincent C, 2005. Problems and opportunities for the commercialization of botanical insecticides. *Biopesticides of Plant Origin*, 283-91.

Jones S, Pethybridge S, Hay F, Groom T, Wilson C, 2007. Baseline sensitivity of Australian *Phoma ligulicola* isolates from pyrethrum to azoxystrobin and difenoconazole. *Journal of Phytopathology* **155**, 377-80.

Jordan CF, 2004. Organic farming and agroforestry: Alleycropping for mulch production for organic farms of southeastern United States. *Agroforestry Systems* **61-2**, 79-90.

Kamvar ZN, Tabima JF, Grünwald NJ, 2014. Poppr: an R package for genetic analysis of populations with clonal, partially clonal, and/or sexual reproduction. *PeerJ* **2**, e281.

Keinath AP, 2012. Differential sensitivity to boscalid in conidia and ascospores of *Didymella bryoniae* and frequency of boscalid-insensitive isolates in South Carolina. *Plant Disease* **96**, 228-34.

Khater HF, 2012. Prospects of botanical biopesticides in insect pest management. *Pharmacologia* **3**, 641-56.

Kiffer E, Morelet M, 1999. *The deuteromycetes. Mitosporic fungi: classification and generic keys*. Florida, USA: Science Publishers, Inc.

Kim YK, Xiao CL, 2011. Stability and fitness of pyraclostrobin- and boscalid-resistant phenotypes in field isolates of *Botrytis cinerea* from apple. *Phytopathology* **101**, 1385-91.

Kluger EK, Della Torre PK, Martin P, Krockenberger MB, Malik R, 2004. Concurrent *Fusarium chlamydosporum* and *Microsphaeropsis arundinis* infections in a cat. *Journal of Feline Medicine and Surgery* **6**, 271-7.

Kosman E, Leonard K, 2005. Similarity coefficients for molecular markers in studies of genetic relationships between individuals for haploid, diploid, and polyploid species. *Molecular Ecology* **14**, 415-24.

Krockenberger MB, Martin P, Halliday C, Rothwell TLW, Clarke K, Malik R, 2010. Localised *Microsphaeropsis arundinis* infection of the subcutis of a cat. *Journal of Feline Medicine and Surgery* **12**, 231-6.

Krohn K, Kouam SF, Kuigoua GM, *et al.*, 2009. Xanthones and oxepino[2, 3-b]chromones from three endophytic fungi. *Chemistry - A European Journal* **15**, 12121-32.

Kuhne S, Priegnitz U, Hummel B, Ellmer F, 2013. Colorado potato beetle (*Leptinotarsa decemlineata* Say) - control strategies in organic farming using biological insecticides (azadirachtin, *Bacillus thuringiensis* var. *tenebrionis*, pyrethrum and spinosad). *Interantional Organisation Biological Control/West Palaearctic Regional Section Bulletin* **90**, 253-6.

Lacombe JP, 2003. Behaviour of the association of fenamidon and fosetyl-al in relation to Qol-resistant downy mildew. *Phytoma*, 45-50.

Laleve A, Gamet S, Walker A-S, Debieu D, Toquin V, Fillinger S, 2014. Site-directed mutagenesis of the P225, N230 and H272 residues of succinate dehydrogenase subunit B from *Botrytis cinerea* highlights different roles in enzyme activity and inhibitor binding. *Environmental Microbiology* **16**, 2253-66.

Lamondia JA, Douglas SM, 1997. Sensitivity of *Botrytis cinerea* from Connecticut greenhouses to benzimidazole and dicarboximide fungicides. *Plant Disease* **81**, 729-32.

Leboldus JM, Kinzer K, Richards J, *et al.*, 2015. Genotype-by-sequencing of the plant-pathogenic fungi *Pyrenophora teres* and *Sphaerulina musiva* utilizing Ion Torrent sequence technology. *Molecular Plant Pathology* **16**, 623-32.

Lee J, Lee T, Lee YW, Yun SH, Turgeon BG, 2003. Shifting fungal reproductive mode by manipulation of mating type genes: obligatory heterothallism of *Gibberella zeae*. *Molecular Microbiology* **50**, 145-52.

Lee SH, Neate SM, 2007. Population genetic structure of *Septoria passerinii* in Northern Great Plains barley. *Phytopathology* **97**, 938-44.

Leeder AC, Palma-Guerrero J, Glass NL, 2011. The social network: deciphering fungal language. *Nature Reviews Microbiology* **9**, 440-51.

Levinson G, Gutman GA, 1987. Slipped-strand mispairing- a major mechanism for DNA-sequence evolution. *Molecular Biology and Evolution* **4**, 203-21.

Linde CC, 2010. Population genetic analyses of plant pathogens: new challenges and opportunities. *Australasian Plant Pathology* **39**, 23-8.

Liu G, Wang Y, Wong L, 2010. FastTagger: an efficient algorithm for genome-wide tag SNP selection using multi-marker linkage disequilibrium. *BMC Bioinformatics* **11**, 1-12.

Luo J, Liu X, Li E, Guo L, Che Y, 2013. Arundinols A-C and arundinones A and B from the plant endophytic fungus *Microsphaeropsis arundinis*. *Journal of Natural Products* **76**, 107-12.

Ma ZH, Michailides TJ, 2005. Advances in understanding molecular mechanisms of fungicide resistance and molecular detection of resistant genotypes in phytopathogenic fungi. *Crop Protection* **24**, 853-63.

Macdonald WL, 1995. Pyrethrum flowers - production in Australia. In: Casida JE, Quistad G, eds. *Pyrethrum Flowers: Chemistry, Toxicology and Uses.* New York: Oxford University Press, 55-66.

Mcdonald BA, 1997. The population genetics of fungi: tools and techniques. *Phytopathology* **87**, 448-53.

Mcdonald BA, 2004. Population genetics of plant pathogens. *The Plant Health Instructor*, doi:10.1094/PHI-A-2004-0524-01.

Mcdonald BA, Linde C, 2002. Pathogen population genetics, evolutionary potential, and durable resistance. *Annual Review of Phytopathology* **40**, 349-79.

Meglécz E, Costedoat C, Dubut V, *et al.*, 2010. QDD: a user-friendly program to select microsatellite markers and design primers from large sequencing projects. *Bioinformatics* **26**, 403-4.

Metzenberg RL, Glass NL, 1990. Mating type and mating strategies in *Neurospora*. *Bioessays* **12**, 53-9.

Michelmore R, Hulbert S, 1987. Molecular markers for genetic analysis of phytopathogenic fungi. *Annual Review of Phytopathology* **25**, 383-404.

Miles TD, Miles LA, Fairchild KL, Wharton PS, 2014. Screening and characterization of resistance to succinate dehydrogenase inhibitors in *Alternaria solani*. *Plant Pathology* **63**, 155-64.

Milgroom M, Fry W, 1988. A simulation analysis of the epidemiological principles for fungicide resistance management in pathogen populations. *Phytopathology* **78**, 565-70.

Milgroom MG, 1990a. A stochastic-model for the initial occurrence and development of fungicide resistance in plant pathogen populations. *Phytopathology* **80**, 410-6.

Milgroom MG, 1990b. A stochastic model for the initial occurrence and development of fungicide resistance in plant pathogen populations. *Phytopathology* **80**, 410-6.

Milgroom MG, 1996. Recombination and the multilocus structure of fungal populations. *Annual Review of Phytopathology* **34**, 457-77.

Mintz A, Heiny D, Weidemann G, 1992. Factors influencing the biocontrol of tumble pigweed (*Amaranthus albus*) with *Aposphaeria amaranthi*. *Plant Disease* **76**, 267-9.

Miyamoto T, Ishii H, Stammler G, *et al.*, 2010. Distribution and molecular characterization of *Corynespora cassiicola* isolates resistant to boscalid. *Plant Pathology* **59**, 873-81.

Moran PJ, Showler AT, 2007. *Phomopsis amaranthicola* and *Microsphaeropsis amaranthi* symptoms on *Amaranthus* spp. under South Texas conditions. *Plant Disease* **91**, 1638-46.

Morgan-Jones G, 1974. Concerning some species of *Microsphaeropsis*. *Canadian Journal of Botany* **52**, 2575-9.

Morris SE, Davies NW, Brown PH, Groom T, 2006. Effect of drying conditions on pyrethrins content. *Industrial Crops and Products* **23**, 9-14.

Nei M, 1973. Analysis of gene diversity in subdivided populations. *Proceedings of the National Academy of Sciences* **70**, 3321-3.

O'malley TB, 2012. *Epidemiology and management of flower diseases of pyrethrum*. University of Tasmania: University of Tasmania, Doctor of Philosophy.

O'malley TB, 2007. *Seed transmission studies of Phoma ligulicola*. University of Tasmania: University of Tasmania, Bachelor of Applied Science (Honours) Honours.

O'malley TB, Hay FS, Scott JB, Gent DH, Shivas RG, Pethybridge SJ, 2015. Carpogenic germination of sclerotia of *Sclerotinia minor* and ascosporic infection of pyrethrum flowers. *Canadian Journal of Plant Pathology* **37**, 179-87.

Ortiz-Ribbing L, Williams MM, 2006. Potential of *Phomopsis amaranthicola* and *Microsphaeropsis amaranthi*, as bioherbicides for several weedy *Amaranthus* species. *Crop Protection* **25**, 39-46.

Paoletti M, Seymour FA, Alcocer MJ, *et al.*, 2007. Mating type and the genetic basis of self-fertility in the model fungus *Aspergillus nidulans*. *Current Biology* **17**, 1384-9.

Pendl S, Weeks K, Priest M, *et al.*, 2004. Phaeohyphomycotic soft tissue infections caused by the coelomycetous fungus *Microsphaeropsis arundinis*. *Journal of Clinical Microbiology* **42**, 5315-9.

Peng X, Chen H, 2008. Single cell oil production in solid-state fermentation by *Microsphaeropsis* sp. from steam-exploded wheat straw mixed with wheat bran. *Bioresource Technology* **99**, 3885-9.

Peng XW, Chen HZ, 2007. Microbial oil accumulation and cellulase secretion of the endophytic fungi from oleaginous plants. *Annals of Microbiology* **57**, 239-42.

Pethybridge S, Hay F, 2001. Influence of *Phoma ligulicola* on yield, and site factors on disease development, in Tasmanian pyrethrum crops. *Australasian Plant Pathology* **30**, 17-20.

Pethybridge S, Hay F, Groom T, 2003. Seasonal fluctuations in fungi associated with pyrethrum foliage in Tasmania. *Australasian Plant Pathology* **32**, 223-30.

Pethybridge S, Hay F, Wilson C, 2004. Pathogenicity of fungi commonly isolated from foliar disease in Tasmanian pyrethrum crops. *Australasian Plant Pathology* **33**, 441-4.

Pethybridge S, Wilson C, 1998. Confirmation of ray blight disease of pyrethrum in Australia. *Australasian Plant Pathology* **27**, 45-8.

Pethybridge SJ, Esker P, Dixon P, *et al.*, 2007a. Quantifying loss caused by ray blight disease in Tasmanian pyrethrum fields. *Plant Disease* **91**, 1116-21.

Pethybridge SJ, Esker P, Hay F, Wilson C, Nutter Jr FW, 2005a. Spatiotemporal description of epidemics caused by *Phoma ligulicola* in Tasmanian pyrethrum fields. *Phytopathology* **95**, 648-58.

Pethybridge SJ, Gent DH, Esker PD, Turechek WW, Hay FS, Nutter Jr FW, 2009. Site-specific risk factors for ray blight in Tasmanian pyrethrum fields. *Plant Disease* **93**, 229-37.

Pethybridge SJ, Gent DH, Hay FS, 2011. Epidemics of ray blight on pyrethrum are linked to seed contamination and overwintering inoculum of *Phoma ligulicola* var. *inoxydabilis*. *Phytopathology* **101**, 1112-21.

Pethybridge SJ, Hay F, Esker P, Groom T, Wilson C, Nutter FW, 2008a. Visual and radiometric assessments for yield losses caused by ray blight in pyrethrum. *Crop Science* **48**, 343-52.

Pethybridge SJ, Hay F, Esker P, Wilson C, Nutter Jr FW, 2007b. Use of a multispectral radiometer for noninvasive assessments of foliar disease caused by ray blight in pyrethrum. *Plant Disease* **91**, 1397-406.

Pethybridge SJ, Hay F, Jones S, Wilson C, Groom T, 2006. Seedborne infection of pyrethrum by *Phoma ligulicola*. *Plant Disease* **90**, 891-7.

Pethybridge SJ, Hay FS, Clarkson RA, Groom T, Wilson CR, 2008b. Host range of Australian *Phoma ligulicola* var. *inoxydablis* isolates from pyrethrum. *Journal of Phytopathology* **156**, 506-8.

Pethybridge SJ, Hay FS, Esker PD, *et al.*, 2008c. Diseases of pyrethrum in Tasmania: challenges and prospects for management. *Plant Disease* **92**, 1260-72.

Pethybridge SJ, Hay FS, Gent DH, 2010. Characterization of the spatiotemporal attributes of Sclerotinia flower blight epidemics in a perennial pyrethrum pathosystem. *Plant Disease* **94**, 1305-13.

Pethybridge SJ, Hay FS, Groom T, Wilson CR, 2008d. Improving fungicide-based management of ray blight disease in Tasmanian pyrethrum fields. *Plant Disease* **92**, 887-95.

Pethybridge SJ, Hay FS, Wilson CR, Groom T, 2005b. Development of a fungicide-based management strategy for foliar disease caused by *Phoma ligulicola* in Tasmanian pyrethrum fields. *Plant Disease* **89**, 1114-20.

Pethybridge SJ, Jones SJ, Shivas RG, Hay FS, Wilson CR, Groom T, 2008e. Tan spot: A new disease of pyrethrum caused by *Microsphaeropsis tanaceti* sp. nov. *Plant Pathology* **57**, 1058-65.

Pethybridge SJ, Scott JB, Hay FS, 2012. Lack of evidence for recombination or spatial structure in *Phoma ligulicola* var. *inoxydabilis* populations from Australian pyrethrum fields. *Plant Disease* **96**, 746-51.

Pöggeler S, 1999. Phylogenetic relationships between mating-type sequences from homothallic and heterothallic ascomycetes. *Current Genetics* **36**, 222-31.

Pöggeler S, 2001. Mating-type genes for classical strain improvements of ascomycetes. *Applied Microbiology and Biotechnology* **56**, 589-601.

Poggeler S, Nowrousian M, Ringelberg C, Loros JJ, Dunlap JC, Kuck U, 2006. Microarray and real-time PCR analyses reveal mating type-dependent gene expression in a homothallic fungus. *Molecular Genetics and Genomics* **275**, 492-503.

Ramirez-Prado JH, Moore GG, Horn BW, Carbone I, 2008. Characterization and population analysis of the mating-type genes in *Aspergillus flavus* and *Aspergillus parasiticus*. *Fungal Genetics and Biology* **45**, 1292-9.

Ramirez AM, Stoopen G, Menzel TR, *et al.*, 2012. Bidirectional secretions from glandular trichomes of pyrethrum enable immunization of seedlings. *The Plant Cell Online* **24**, 4252-65.

Rampersad SN, 2011. A rapid colorimetric microtiter bioassay to evaluate fungicide sensitivity among *Verticillium dahliae* isolates. *Plant Disease* **95**, 248-55.

Raposo R, Gomez V, Urrutia T, Melgarejo P, 2000. Fitness of *Botrytis cinerea* associated with dicarboximide resistance. *Phytopathology* **90**, 1246-9.

Rawnsley RP, Lane P, Brown PH, Groom T, 2006. Occurrence and severity of the weeds *Anthriscus caucalis* and *Torilis nodosa* in pyrethrum. *Animal Production Science* **46**, 711-6.

Reddy PP, 2012. *Recent advances in crop protection*. New York: Springer Science & Business Media.

Reece J, Meyers N, Urry LA, *et al.*, 2014. The evolutionary history of biological diversity: fungi. In. *Campbell Biology Australian and New Zealand.* Australia: Pearson Australia.

Ryan RF, Bishop S, Chung B, Folder I, Krishna H, Lemon A, 2002. Pyrethrum: Nature's Pesticide. In. *9th Asia Pacific Confederation of Chemical Engineering and CHEMICA.* New Zealand

Rydholm C, Dyer P, Lutzoni F, 2007. DNA sequence characterization and molecular evolution of MAT1 and MAT2 mating-type loci of the self-compatible ascomycete mold *Neosartorya fischeri*. *Eukaryotic Cell* **6**, 868-74.

Scalliet G, Bowler J, Luksch T, *et al.*, 2012. Mutagenesis and functional studies with succinate dehydrogenase inhibitors in the wheat pathogen *Mycosphaerella graminicola*. *PLoS One* **7**, e35429.

Schurko AM, Neiman M, Logsdon JM, 2009. Signs of sex: what we know and how we know it. *Trends in Ecology & Evolution* **24**, 208-17.

Scott JB, Gent DH, Pethybridge SJ, Groom T, Hay FS, 2014. Crop damage from Sclerotinia crown rot and risk factors in pyrethrum. *Plant Disease* **98**, 103-11.

Selkoe KA, Toonen RJ, 2006. Microsatellites for ecologists: a practical guide to using and evaluating microsatellite markers. *Ecology Letters* **9**, 615-29.

Sha T, Xu J, Palanichamy MG, *et al.*, 2008. Genetic diversity of the endemic gourmet mushroom *Thelephora ganbajun* from south-western China. *Microbiology* **154**, 3460-8.

Shannon C, Weaver W, 1963. *The mathematical theory of communication*. Urbana and Chicago: University of Illinois Press.

Shi Z, Leung H, 1995. Genetic analysis of sporulation in *Magnaporthe grisea* by chemical and insertional mutagenesis. *Molecular Plant Microbe Interactions* **8**, 949-59.

Sierotzki H, Frey R, Morchoisne M, Olaya G, Mosch M, Scalliet G, 2011. Sensitivity of fungal pathogens to SDHI fungicides. In: Dehne HW, Deising HB, Gisi U, Kuck KH, Russell

PE, Lyr H, eds. *Modern fungicides and antifungal compounds VI. 16th International Reinhardsbrunn Symposium, Friedrichroda, Germany, April 25-29, 2010.* 179-86.

Sierotzki H, Gisi U, 2003. Molecular diagnostics for fungicide resistance in plant pathogens. *Chemistry of Crop Protection: Progress and Prospects in Science and Regulation*, 71-88.

Sierotzki H, Parisi S, Steinfeld U, Tenzer I, Poirey S, Gisi U, 2000. Mode of resistance to respiration inhibitors at the cytochrome bc(1) enzyme complex of *Mycosphaerella fijiensi*s field isolates. *Pest Management Science* **56**, 833-41.

Sierotzki H, Scalliet G, 2013. A review of current knowledge of resistance aspects for the next-generation succinate dehydrogenase inhibitor fungicides. *Phytopathology* **103**, 880-7.

Simpson EH, 1949. Measurement of diversity. *Nature* **163**, 688.

Singh Y, Singh J, Pandey AK, 2013. Molecular markers in diagnosis and management of fungal pathogens: a review. *International Journal of Advanced Biotechnology and Research* **4**, 180-8.

Smith DA, Doll DA, Singh D, Hallett SG, 2006. Climatic constraints to the potential of *Microsphaeropsis amaranthi* as a bioherbicide for common waterhemp. *Phytopathology* **96**, 308-12.

Smith DA, Hallett SG, 2006. Interactions between chemical herbicides and the candidate bioherbicide *Microsphaeropsis amaranthi*. *Weed Science* **54**, 532-7.

Soderlund D, 1995. Mode of action of Pyrethrins and Pyrehtroids. In: Casida J, Quistad G, eds. *Pyrerthrum Flowers: Chemistry, Toxicology and Uses.* New York: Oxford University Press, 217-32.

Someya A, 1997. *Microsphaeropsis rugospora*, a new species from Japanese soil. *Mycoscience* **38**, 429-31.

Sommart U, Rukachaisirikul V, Tadpetch K, *et al.*, 2012. Modiolin and phthalide derivatives from the endophytic fungus *Microsphaeropsis arundinis* PSU-G18. *Tetrahedron* **68**, 10005-10.

Sommerhalder RJ, Mcdonald BA, Zhan J, 2006. The frequencies and spatial distribution of mating types in *Stagonospora nodorum* are consistent with recurring sexual reproduction. *Phytopathology* **96**, 234-9.

Souza C, Silva CC, Ferreira A, 2003. Sex in fungi: lessons of gene regulation. *Genetic Molecular Research* **2**, 136-47.

Staub T, Sozzi D, 1984. Fungicide resistance. *Plant Disease* **68**, 1026-31.

Stergiopoulos I, Groenewald M, Staats M, Lindhout P, Crous PW, De Wit PJ, 2007. Mating-type genes and the genetic structure of a world-wide collection of the tomato pathogen *Cladosporium fulvum*. *Fungal Genetics and Biology* **44**, 415-29.

Stoddart JA, Taylor JF, 1988. Genotypic diversity: estimation and prediction in samples. *Genetics* **118**, 705-11.

Sun P, Yang X, 2000. Light, temperature, and moisture effects on apothecium production of *Sclerotinia sclerotiorum*. *Plant Disease* **84**, 1287-93.

Sutton BC, 1971. *Coelomycetes: The Genus Harknessia, and Similar Fungi on Eucalyptus. IV*. Kew, United Kingdom: Commonwealth Mycological Institute.

Sutton BC, 1980. *The Coelomycetes. Fungi imperfecti with pycnidia, acervuli and stromata*. Kew, United Kingdon: Commonwealth Mycological Institute.

Turgeon BG, 1998. Application of mating type gene technology to problems in fungal biology. *Annual Review of Phytopathology* **36**, 115-37.

Turgeon BG, Bohlmann H, Ciuffetti LM, *et al.*, 1993. Cloning and analysis of the mating type genes from *Cochliobolus heterostrophus*. *Molecular and General Genetics* **238**, 270-84.

Turgeon BG, Yoder O, 2000. Proposed nomenclature for mating type genes of filamentous ascomycetes. *Fungal Genetics and Biology* **31**, 1-5.

Vaghefi N, Ades PK, Hay FS, Pethybridge SJ, Ford R, Taylor PW, 2015a. Identification of the MAT1 locus in *Stagonosporopsis tanaceti*, and exploring its potential for sexual reproduction in Australian pyrethrum fields. *Fungal Biology* **119**, 408-19.

Vaghefi N, Hay FS, Ades PK, Pethybridge SJ, Ford R, Taylor PWJ, 2015b. Rapid changes in the genetic composition of *Stagonosporopsis tanaceti* population in Australian pyrethrum fields. *Phytopathology* **105**, 358-69.

Vaghefi N, Pethybridge S, Ford R, Nicolas M, Crous P, Taylor P, 2012. *Stagonosporopsis* spp. associated with ray blight disease of *Asteraceae*. *Australasian Plant Pathology* **41**, 675-86.

Valdes AM, Slatkin M, Freimer NB, 1993. Allele frequencies at microsatellite loci - the step wise mutation model revisited. *Genetics* **133**, 737-49.

Vallieres C, Trouillard M, Dujardin G, Meunier B, 2011. Deleterious effect of the Q(o) Inhibitor compound resistance-conferring mutation G143A in the intron-containing cytochrome *b* gene and mechanisms for bypassing It. *Applied and Environmental Microbiology* **77**, 2088-93.

Van Den Bosch F, Gilligan CA, 2008. Models of fungicide resistance dynamics. *Annual Review of Phytopathology* **46**, 123-47.

Van Den Bosch F, Oliver R, Van Den Berg F, Paveley N, 2014a. Governing principles can guide fungicide-resistance management tactics. *Annual Review of Phytopathology* **52**, 175-95.

Van Den Bosch F, Paveley N, Shaw M, Hobbelen P, Oliver R, 2011. The dose rate debate: does the risk of fungicide resistance increase or decrease with dose? *Plant Pathology* **60**, 597-606.

Van Den Bosch F, Paveley N, Van Den Berg F, Hobbelen P, Oliver R, 2014b. Mixtures as a fungicide resistance management tactic. *Phytopathology* **104**, 1264-73.

Vega B, Liberti D, Harmon PF, Dewdney MM, 2012. A rapid resazurin-based microtiter assay to evaluate Qol sensitivity for *Alternaria alternata* isolates and their molecular characterization. *Plant Disease* **96**, 1262-70.

Veloukas T, Kalogeropoulou P, Markoglou AN, Karaoglanidis GS, 2014. Fitness and competitive ability of *Botrytis cinerea* field isolates with dual resistance to SDHI and QoI fungicides, associated with several sdhB and the cytb G143A mutations. *Phytopathology* **104**, 347-56.

Veloukas T, Leroch M, Hahn M, Karaoglanidis GS, 2011. Detection and molecular characterization of boscalid-resistant *Botrytis cinerea* isolates from strawberry. *Plant Disease* **95**, 1302-7.

Verkley G, Dukik K, Renfurm R, Göeker M, Stielow J, 2014. Novel genera and species of coniothyrium-like fungi in *Montagnulaceae* (*Ascomycota*). *Persoonia* **32**, 25-51.

Verkley GJ, Da Silva M, Wicklow DT, Crous PW, 2004. Paraconiothyrium, a new genus to accommodate the mycoparasite *Coniothyrium minitans*, anamorphs of *Paraphaeosphaeria*, and four new species. *Studies in Mycology* **50**, 323-36.

Vincelli P, 2002. QoI (Strobilurin) fungicides: benefits and risks. *The Plant Health Instructor*. DOI: 10.1094/PHI-I-2002-0809-02. In.

Voigt K, Cozijnsen AJ, Kroymann R, Poggeler S, Howlett BJ, 2005. Phylogenetic relationships between members of the crucifer pathogenic *Leptosphaeria maculans* species

complex as shown by mating type (MAT1-2), actin, and beta-tubulin sequences. *Molecular Phylogenetics and Evolution* **37**, 541-57.

Von Höhnel F, 1917. *Fungi imperfecti: Beiträge zur kenntnis deraelben*. C. Heinrich.

Vos P, Hogers R, Bleeker M, *et al.*, 1995. AFLP: a new technique for DNA fingerprinting. *Nucleic Acids Research* **23**, 4407-14.

Wainaina J, 1995. Pyrethrum flowers - production in Africa. In: Casida JE, Quistad G, eds. *Pyrethrum Flowers: Chemistry, Toxicology and Uses.* New York: Oxford University Pres, 49-55.

Wang CY, Wang BG, Brauers G, Guan HS, Proksch P, Ebel R, 2002. Microsphaerones A and B, two novel γ-pyrone derivatives from the sponge-derived fungus *Microsphaeropsis* sp. *Journal of Natural Products* **65**, 772-5.

Wang Y, Duan Y, Wang J, Zhou M, 2015a. A new point mutation in the iron-sulfur subunit of succinate dehydrogenase confers resistance to boscalid in *Sclerotinia sclerotiorum*. *Molecular Plant Pathology* **16**, 653-61.

Wang Y, Duan YB, Zhou MG, 2015b. Molecular and biochemical characterization of boscalid resistance in laboratory mutants of *Sclerotinia sclerotiorum*. *Plant Pathology* **64**, 101-8.

Welsh J, Mcclelland M, 1990. Fingerprinting genomes using PCR with arbitrary primers. *Nucleic Acids Research* **18**, 7213-8.

Willetts H, Wong J, 1980. The biology of *Sclerotinia sclerotiorum*, *S. trifoliorum*, and *S. minor* with emphasis on specific nomenclature. *The Botanical Review* **46**, 101-65.

Woudenberg JHC, De Gruyter J, Crous PW, Zwiers L-H, 2012. Analysis of the mating-type loci of co-occurring and phylogenetically related species of *Ascochyta* and *Phoma*. *Molecular Plant Pathology* **13**, 350-62.

Xiao X, Luo S, Zeng G, *et al.*, 2010. Biosorption of cadmium by endophytic fungus (EF) *Microsphaeropsis* sp. LSE10 isolated from cadmium hyperaccumulator *Solanum nigrum* L. *Bioresource Technology* **101**, 1668-74.

Xu J, 2006. Fundamentals of fungal molecular population genetic analyses. *Current Issues in Molecular Biology* **8**, 75-89.

Xu J, Guo H, Yang Z-L, 2007. Single nucleotide polymorphisms in the ectomycorrhizal mushroom *Tricholoma matsutake*. *Microbiology* **153**, 2002-12.

Yang L, Gao F, Shang L, Zhan J, Mcdonald BA, 2013. Association between virulence and triazole tolerance in the phytopathogenic fungus *Mycosphaerella graminicola*. *PLoS One* **8**.

Yin YN, Kim YK, Xiao CL, 2011. Molecular characterization of boscalid resistance in field isolates of *Botrytis cinerea* from apple. *Phytopathology* **101**, 986-95.

Yun S-H, Berbee ML, Yoder O, Turgeon BG, 1999. Evolution of the fungal self-fertile reproductive life style from self-sterile ancestors. *Proceedings of the National Academy of Sciences* **96**, 5592-7.

Yun S-H, Yoder OC, Turgeon BG, 2013. Structure and function of the mating-type locus in the homothallic ascomycete, *Didymella zeae-maydis*. *Journal of Microbiology* **51**, 814-20.

Zhan J, Kema G, Waalwijk C, Mcdonald B, 2002. Distribution of mating type alleles in the wheat pathogen *Mycosphaerella graminicola* over spatial scales from lesions to continents. *Fungal Genetics and Biology* **36**, 128-36.

Zhan J, Pettway RE, Mcdonald BA, 2003. The global genetic structure of the wheat pathogen *Mycosphaerella graminicola* is characterized by high nuclear diversity, low mitochondrial diversity, regular recombination, and gene flow. *Fungal Genetics and Biology* **38**, 286-97.

TAN SPOT OF PYRETHRUM IS CAUSED BY A *DIDYMELLA* SPECIES COMPLEX

Tamieka L. Pearce[a*], Jason B. Scott[a], Pedro W. Crous[bc], Sarah J. Pethybridge[d], Frank S. Hay[d]

[a]Tasmanian Institute of Agriculture (TIA), University of Tasmania, Burnie, Tasmania, 7320, Australia; [b]CBS-KNAW Fungal Biodiversity Centre, Uppsalalaan 8, 3584 CT, Utrecht, Netherlands; [c]Department of Plant Pathology, Faculty of Veterinary and Agricultural Sciences, University of Melbourne, Australia; [d]Cornell University, School of Integrative Plant Science, Section of Plant Pathology and Plant-Microbe Biology, Cornell University, Geneva, NY 14456, USA.

*Corresponding author: Tamieka.Pearce@utas.edu.au

Keywords: *Didymellaceae*, multi-locus, phylogenetics, taxonomy.

This manuscript has been accepted for publication in *Plant Pathology*

Pearce T, Scott J, Crous P, Pethybridge S, Hay F, *in press*. Tan spot of pyrethrum is caused by a *Didymella* species complex. *Plant Pathology*. Doi: 10.1111/ppa.12493

3.1 ABSTRACT

Tan spot is a disease of pyrethrum (*Tanacetum cinerariifolium*) in Australia. Recent increases in the severity and incidence of the disease has prompted a re-evaluation of the pathogen, originally described as *Microsphaeropsis tanaceti*, including its phylogenetic relationships and morphology. Nucleotide comparison of partial sequences of the nuclear ribosomal internal transcribed spacer, β-tubulin, large subunit 28S nrDNA (LSU), actin and glyceraldehyde-3-phosphate dehydrogenase loci identified two distinct haplotypes within the species. Haplotype differentiation was consistent for each locus, except for the LSU, within which sequences were identical across all isolates. Morphological variation, especially culture pigmentation and conidial size, consistently supported the phylogenetic data distinguishing two haplotypes. Phylogenetic comparisons of *M. tanaceti* incorporating 98 *Didymellaceae* species did not associate the *M. tanaceti* haplotypes with the genus *Microsphaeropsis*. The two *M. tanaceti* haplotypes were closely related, and clustered in the *Didymella sensu stricto* clade. Based on these phylogenetic results, supported by their distinct morphology and cultural characteristics, the two haplotypes of *M. tanaceti* are re-classified as two species of *Didymella*, namely *D. rosea* and *D. tanaceti*. The implications of two closely related species causing tan spot of pyrethrum are discussed.

3.2 INTRODUCTION

Pyrethrum (*Tanacetum cineriifolium* trevir. Sch. Bip.) is an economically important perennial of the *Asteraceae* (*Compositae*). The crop is grown for the extraction of six closely related esters, termed pyrethrins, which combined are the most widely used botanical insecticide

worldwide (Khater, 2012). Their popularity is attributed to a rapid kill and knock down effect on a range of insects and a low risk of insect resistance due to rapid breakdown under ultraviolet light (Grdiša et al., 2009). High concentrations of pyrethrins are found in the flower within secretory lacunae on the achenes (Grdiša et al., 2009). The Australian pyrethrum industry produces the majority of worldwide pyrethrum.

Many fungal pathogens contribute to a foliar disease complex affecting the green leaf area in Australian pyrethrum fields (Hay et al., 2015). Tan spot, caused by *Microsphaeropsis tanaceti* R.G. Shivas, S.J. Pethybridge & S.J. Jones, is one of the most common diseases of pyrethrum in Australia (Hay et al., 2015, Pethybridge et al., 2008). Infection results in tan coloured necrotic spots on leaves, stems and buds, which coalesce to form lesions, which can lead to plant death (Pethybridge et al., 2008). The first discovery of *M. tanaceti* associated with necrotic lesions on pyrethrum was during routine sampling in 2001. The fungus was found to be highly prevalent, occurring in 63 – 75% of fields (n = 8) sampled monthly from April to November. However, isolation frequencies were low, with *M. tanaceti* associated with 10.5% of leaf spots and 4.3% of stem lesions and buds (Pethybridge et al., 2003). Between 2004 and 2006, isolation frequencies of *M. tanaceti* from necrotic leaf spots in spring (September to October) substantially increased to 65% (Pethybridge et al., 2008). Furthermore, from 2009 high isolation frequencies (17.6 – 56% of isolations per field), have been associated with an increased severity of necrosis and defoliation over autumn and winter and fungicide control failures in spring (Hay et al., 2015).

Initial identification and characterisation of the pathogen as a member of the genus *Microsphaeropsis* was based on morphology and nucleotide sequence data of the nuclear

ribosomal internal transcribed spacer (ITS) locus (Pethybridge et al., 2008). Comparison of the ITS sequences identified two haplotypes (I and II) differentiated by three single nucleotide polymorphisms (SNPs). Phylogenetic analysis supported the pathogen as genetically similar, but distinct from other *Microsphaeropsis* spp., and the name *M. tanaceti* was proposed (Pethybridge et al., 2008).

Microsphaeropsis spp. have a wide host range and global distribution (Wang et al., 2002, Kluger et al., 2004, Crous et al., 2011). Although many have been identified as plant pathogens (Ortiz-Ribbing & Williams, 2006, Crous et al., 2011), some species have proven to be antagonists to fungal pathogens (Carisse & Bernier, 2002), etiological agents of soft tissue disease in mammals (Kluger et al., 2004) and have potential biotechnological roles (Wang et al., 2002, Xiao et al., 2010).

The genus *Microsphaeropsis* Höhn was proposed by Sutton (1971), to be utilised for species described as *Coniothyrium* that were morphologically non-congeneric with the type species *C. palmarum*. *Microsphaeropsis* was restricted to pycnidial species with small pigmented unicellular conidia produced from phialides with periclinal thickening. Species characterized by small, often septate conidia produced from phialidic annellides were retained in *Coniothyrium* (Sutton, 1980). More recently, nucleotide sequence data of the large subunit 28S and small subunit 18S of nrDNA (LSU and SSU) have been used for rapid delineation of the two genera (de Gruyter et al., 2009).

Additional molecular studies have identified *Microsphaeropsis* as a member of the *Didymellaceae* (*Pleosporales*, *Dothideomycetes)* (de Gruyter et al., 2009, Crous et al., 2011, Aveskamp et al., 2010). This family includes *Phoma* and allied genera including *Boeremia*, *Peyronellaea* and *Stagonosporopsis* (Aveskamp et al., 2010). Based on a three-locus phylogeny the *Didymellaceae* was classified into 19 groups representing several genera (Aveskamp et al., 2010). *Microsphaeropsis*, represented by the type species *M. olivacea*, was retained as a separate taxonomic entity.

As *M. tanaceti* has been identified as an emerging problem within pyrethrum production and the family *Didymellaceae* has undergone recent revision, the classification of the pathogen requires clarification. The objectives of this study were to evaluate the taxonomic placement of *M. tanaceti* based on newly available data from recent revisions of the *Didymellaceae*. Additionally, genetic and morphological variation within *M. tanaceti* was assessed to elucidate the relationship and classification of the two previously observed haplotypes.

3.3 MATERIALS AND METHODS

3.3.1 Isolate collection

Ten isolates of each *M. tanaceti* haplotype were selected for phylogenetic and morphological characterisation (Table 3.1). Individuals were representatives from a collection of strains isolated as previously described (Hay et al., 2015), between 2004 and 2014 from symptomatic pyrethrum leaves within fields in Tasmania, Australia. Individuals of each

haplotype were selected based on the differences observed in colony colour between BRIP 50785 (haplotype I; Table 3.1) and BRIP 50788 (haplotype II; Table 3.1) (Pethybridge et al., 2008), following incubation for 5 d at 21°C in the dark on potato dextrose agar (PDA; Amyl Media). Furthermore, BRIP 50785 and BRIP 50788 were included in all analyses as reference isolates of each haplotype.

In addition, sequence data of 98 fungal species were selected for phylogenetic analysis to study the taxonomic placement of *M. tanaceti* within the *Didymellaceae,* and infer its relationship to representatives of the genus *Microsphaeropsis*. Species were selected to represent the 19 clades identified by Aveskamp et al. (2010) (Table 3.1). Where possible, reference strains of each species were included (according to Boerema et al. (2004)), otherwise ex-type isolates were used. Sequences were retrieved from GenBank (Benson et al., 2015) or Q-bank (Bonants et al., 2013). The genus *Microsphaeropsis* was represented by three isolates of its type species, *M. olivacea* (CBS 233.71, CBS 432.71 and CBS 442.83) and two isolates of *M. proteae* (CPC 1424 and CPC 1425) (Table 3.1).

3.3.2 Molecular characterisation

Genomic DNA was extracted from 20 *M. tanaceti* isolates (10 of each ITS haplotype; Table 3.1) as follows. Isolates were recovered from -80°C storage, plated onto PDA and incubated in the dark at 21°C. Mycelia were scraped from the surface of growing cultures, inoculated in 20 mL of 2% malt extract broth (MEB; Amyl Media) and incubated at ~20°C on an orbital shaker (54 rpm) for 12 d. Excess moisture was removed from the mycelium using a sterile paper towel and ground in liquid nitrogen. DNA was extracted from 100 mg of the

Table 3.1. Fungal species and isolates used in this study for morphological and phylogenetic analysis.

Holomorph	Strain no.[a]	GenBank accession no.[b]					Original substrate	Locality
		TUB2	LSU	ITS	*ACT*	*GAPDH*		
Ascochyta hordei var. *hordei*	CBS 544.74	GU237488	EU754134	GU237887	-	-	*Triticum aevestum*	South Africa
Boeremia diversispora [B]	CBS 102.80	GU237492	GU237930	GU237725	-	-	*Phaseolus vulgaris*	Kenya
Boeremia exigua var. *exigua* [B]	CBS 431.74	FJ427112	EU754183	FJ427001	-	-	*Solanum tuberosum*	Netherlands
Boeremia exigua var. *heteromorpha* [B]	CBS 443.94	GU237497	GU237935	GU237866	-	-	*Nerium oleander*	Italy
Boeremia exigua var. *lilacis* [B]	CBS 569.79	GU237498	GU237936	GU237892	-	-	*Syringa vulgaris*	Netherlands
Boeremia exigua var. *linicola* [B]	CBS 116.76	GU237500	GU237938	GU237754	-	-	*Linum usitatissimum*	Netherlands
Boeremia exigua var. *populi* [T]	CBS 100167	GU237501	GU237939	GU237707	-	-	*Populus (x) euramericana*	Netherlands
Boeremia exigua var. *viburni* [B]	CBS 100354	GU237506	GU237944	GU237711	-	-	*Viburnum opulus*	Netherlands
Boeremia foveata [B]	CBS 341.67	GU237509	GU237947	GU237834	-	-	*Solanum tuberosum*	U.K.
Boeremia noackiana [B]	CBS 100353	GU237514	GU237952	GU237710	-	-	*Phaseolus vulgaris*	Guatemala
Boeremia strasseri	CBS 126.93	GU237518	GU237956	GU237773	-	-	*Mentha* sp.	Netherlands
Boeremia telephii [B]	CBS 760.73	GU237521	GU237959	GU237905	-	-	*Sedum spectabile*	Netherlands
Didymella applanata [T]	CBS 205.63	GU237556	GU237998	GU237798	Q-bank[c]	-	*Rubus idaeus*	Netherlands
Didymella catariae	CBS 102635	GU237524	GU237962	GU237727	Q-bank	-	*Nepeta catenaria*	Netherlands
Didymella exigua [T]	CBS 183.55	GU237525	EU754155	GU237794	Q-bank	-	*Rumex arifolius*	France
Didymella fabae	CBS 524.77	GU237526	GU237963	GU237880	Q-bank	-	*Phaseolus vulgrais*	Belgium
Didymella macropodii	CBS 100190	GU237530	GU237967	GU237708	-	-	*Brassica napus*	Germany
Didymella pisi	CBS 126.54	GU237531	GU237968	GU237772	Q-bank	-	*Pisum sativum*	Netherlands
Didymella rabiei	CBS 581.83a	GU237534	GU237971	GU237894	-	-	*Cicer arietinum*	Syria
Didymella urticicola [T]	CBS 121.75	GU237535	GU237972	GU237761	-	-	*Urtica dioica*	Netherlands
Didymella rosea [d]	TAS 042-0008	KT286965	KT287017	KT287016	KT286964	KT286966	*Tanacetum cinerariifolium*	Forth, Tas[e]
Didymella rosea [d]	TAS 042-0005	KT286962	KT287015	KT287014	KT286961	KT286963	*Tanacetum cinerariifolium*	Kindred, Tas
Didymella rosea [d]	BRIP 61998	KT286957	KT287011	KT287010	KT286956	KT287047	*Tanacetum cinerariifolium*	Penguin, Tas
Didymella rosea [d]	TAS 042-0009	KT286968	KT287019	KT287018	KT286967	KT286969	*Tanacetum cinerariifolium*	Forth, Tas
Didymella rosea [d]	TAS 042-0012	KT286971	KT287021	KT287020	KT286970	KT286972	*Tanacetum cinerariifolium*	Forth, Tas
Didymella rosea [d]	TAS 042-0003	KT286959	KT287012	KT287013	KT286958	KT286960	*Tanacetum cinerariifolium*	Kindred, Tas
Didymella rosea [d]	BRIP 50788	KT286945	KT287003	KT338640	KT286944	KT286946	*Tanacetum cinerariifolium*	Forth ,Tas
Didymella rosea [d]	BRIP 61995	KT286948	KT287005	KT287004	KT286947	KT286949	*Tanacetum cinerariifolium*	Sassafras, Tas

Table 3.1. *continued.*

Holomorph	Strain no.[a]	GenBank accession no.[b]					Original substrate	Locality
		TUB2	LSU	ITS	*ACT*	*GAPDH*		
Didymella rosea [d]	BRIP 61997	KT286954	KT287009	KT287008	KT286953	KT286955	*Tanacetum cinerariifolium*	Sassafras, Tas
Didymella rosea [d]	BRIP 61996	KT286951	KT287007	KT287006	KT286950	KT286952	*Tanacetum cinerariifolium*	Barrington, Tas
Didymella tanaceti [d]	BRIP 61988	KT286977	KT287024	KT287023	KT286976	KT286978	*Tanacetum cinerariifolium*	Sassafras, Tas
Didymella tanaceti [d]	TAS 041-0064	KT286997	KT287038	KT287037	KT286996	KT286998	*Tanacetum cinerariifolium*	Table Cape, Tas
Didymella tanaceti [d]	TAS 041-0071	KT287000	KT287040	KT287039	KT286999	KT287001	*Tanacetum cinerariifolium*	Sassafras, Tas
Didymella tanaceti [d]	BRIP 50785	KT286974	KT287022	KT338641	KT286973	KT286975	*Tanacetum cinerariifolium*	Sassafras, Tas
Didymella tanaceti [d]	BRIP 61992	KT286986	KT287030	KT287029	KT286985	KT286987	*Tanacetum cinerariifolium*	Penguin, Tas
Didymella tanaceti [d]	BRIP 61994	KT286989	KT287032	KT287031	KT286988	KT286990	*Tanacetum cinerariifolium*	Penguin, Tas
Didymella tanaceti [d]	TAS 041-0025	KT286992	KT287034	KT287033	KT286991	KT286993	*Tanacetum cinerariifolium*	Penguin, Tas
Didymella tanaceti [d]	TAS 041-0052	KT286995	KT287036	KT287035	KT286994	KT287002	*Tanacetum cinerariifolium*	Table Cape, Tas
Didymella tanaceti [d]	BRIP 61991	KT286983	KT287028	KT287027	KT286982	KT286984	*Tanacetum cinerariifolium*	Table Cape, Tas
Didymella tanaceti [d]	BRIP 61990	KT286980	KT287026	KT287025	KT286979	KT286981	*Tanacetum cinerariifolium*	Sassafras, Tas
Diplodina coloradensis	CBS 138.25	GU237537	EU754158	GU237784	-	-	*Senecio* sp.	Unknown
Epicoccum nigrum [T]	CBS 173.73	FJ427107	GU237975	FJ426996	-	-	*Dactylis glomerata*	U.S.A.
Epicoccum pimprinum [T]	CBS 246.60	FJ427159	GU237976	FJ427049	-	-	Soil	India
Epicoccum sorghi	CBS 179.80	FJ427173	GU237978	FJ427067	-	-	*Sorghum vulgare*	PuertoRico
Leptosphaerulina arachidicola	CBS 275.59	GU237543	GU237983	GU237820	-	-	*Arachis hypochea*	Taiwan
Leptosphaerulina australis	CBS 317.83	GU237540	EU754166	GU237829	-	-	*Eugenia aromatica*	Indonesia
Leptosphaerulina trifolii	CBS 235.58	GU237542	GU237982	GU237806	-	-	*Trifolium* sp.	Netherlands
Macroventuria anomochaeta [T]	CBS 525.71	GU237544	GU237984	GU237881	Q-bank	-	decayed canvas	South Africa
Macroventuria wentii	CBS 526.71	GU237546	GU237986	GU237884	Q-bank	-	Unidentified plant material	U.S.A.
Microsphaeropsis olivacea	CBS 442.83	GU237547	EU754171	GU237865	Q-bank	-	*Taxus baccata*	Netherlands
Microsphaeropsis olivacea	CBS 432.71	GU237548	GU237987	GU237863	-	-	*Sorothamus* sp.	Netherlands
Microsphaeropsis olivacea	CBS 233.77	GU237549	GU237988	GU237803	-	-	*Pinus laricio*	France
Microsphaeropsis proteae	CPC 1425	JN712650	JN712563	JN712497	-	-	*Protea nitida*	South Africa
Microsphaeropsis proteae	CPC 1424	JN712649	JN712562	JN712496	-	-	*Protea nitida*	South Africa
Peyronellaea americana [B]	CBS 185.85	FJ427088	GU237990	FJ426972	FJ426870	-	*Zea mays*	U.S.A.

Table 3.1. *continued.*

Holomorph	Strain no.[a]	GenBank accession no.[b]					Original substrate	Locality
		TUB2	LSU	ITS	*ACT*	*GAPDH*		
Peyronellaea anserina [B]	CBS 360.84	GU237551	GU237993	GU237839	JN251981	-	Potatoflour	Netherlands
Peyronellaea arachidicola [T]	CBS 333.75	GU237554	GU237996	GU237833	Q-bank	-	*Arachis hypogaea*	South Africa
Peyronellaea aurea [B]	CBS 269.93	GU237557	GU237999	GU237818	Q-bank	-	*Medicago polymorpha*	New Zealand
Peyronellaea australis [T]	CBS 444.81	GU237558	GU238000	GU237867	-	-	*Actinidia chinensis*	New Zealand
Peyronellaea calorpreferens [T]	CBS 109.92	FJ427098	GU238002	FJ426983	FJ426880	-	Undefined food material	Netherlands
Peyronellaea curtisii [B]	CBS 251.92	FJ427148	GU238013	FJ427038	-	-	*Nerine* sp.	Netherlands
Peyronellaea gardeniae [T]	CBS 626.68	FJ427114	GQ387595	FJ427003	FJ426895	-	*Gardenia jasminoides*	India
Peyronellaea glomerata	CBS 464.97	FJ427123	GU238009	FJ427012	FJ426904	-	Indoor environment	Netherlands
Peyronellaea obtusa [B]	CBS 377.93	GU237565	GU238014	GU237847	Q-bank	-	*Daucus carota*	Netherlands
Peyronellaea pinodella [B]	CBS 531.66	FJ427162	GU238017	FJ427052	FJ426942	-	*Trifolium pratense*	U.S.A.
Peyronellaea pinodes	CBS 525.77	GU237572	GU238023	GU237883	Q-bank	-	*Primula auricula*	Switzerland
Peyronellaea pomorum var. *circinata* [T]	CBS 285.76	FJ427163	GU238025	FJ427053	FJ426943	-	*Heracleum dissectum*	Russia
Peyronellaea pomorum var. *pomorum*[B]	CBS 539.66	FJ427166	GU238028	FJ427056	FJ426946	-	*Polygonum tataricum*	Netherlands
Peyronellaea subglomerata [B]	CBS 110.92	FJ427186	GU238032	FJ427080	FJ426966	-	*Triticum* sp.	U.S.A.
Phoma aquilegiicola [B]	CBS 107.96	GU237581	GU238041	GU237735	-	-	*Aconitum pyramidale*	Netherlands
Phoma arachidis hypogaeae [B]	CBS 125.93	GU237583	GU238043	GU237771	-	-	*Arachis hypogaea*	India
Phoma aubrietiae [B]	CBS 627.97	GU237585	GU238045	GU237895	-	-	*Aubrietia* sp.	Netherlands
Phoma bellidis [B]	CBS 714.85	GU237586	GU238046	GU237904	KT287041	KT287042	*Bellis perennis*	Netherlands
Phoma boeremae [T]	CBS 109942	FJ427097	GU238048	FJ426982	FJ426879	-	*Medicago littoralis cv. Harbinger*	Australia
Phoma clematidina [T]	CBS 108.79	FJ427100	FJ515632	FJ426989	-	-	*Clematis* sp.	Netherlands
Phoma clematidis-rectae [T]	CBS 507.63	FJ515624	FJ515647	FJ515606	-	-	*Clematis* sp.	Netherlands
Phoma commelinicola [B]	CBS 100409	GU237593	GU238057	GU237712	-	-	*Tradescantia* sp.	New Zealand
Phoma complanata	CBS 100311	GU237594	EU754181	GU237709	-	-	*Heracleum sphondylium*	Netherlands
Phoma costarricencis [B]	CBS 506.91	GU237596	GU238058	GU237876		-	*Coffea* sp.	Nicaragua
Phoma crystallifera [T]	CBS 193.82	GU237598	GU238060	GU237797	-	-	*Chamaespartium sagittale*	Austria
Phoma dactylitis	CBS 124513	GU237599	GU238061	GU237766	Q-bank		*Dactylis glomerata*	U.S.A.

Table 3.1. *continued.*

Holomorph	Strain no.[a]	GenBank accession no.[b]					Original substrate	Locality
		TUB2	LSU	ITS	*ACT*	*GAPDH*		
Phoma destructiva var. *destructivea* [B]	CBS 378.73	GU237601	GU238063	GU237849	-	-	*Lycopersicon esculentum*	Tonga
Phoma destructiva var. *diversispora*	CBS 162.78	GU237600	GU238062	GU237788	-	-	*Lycopersicon esculentum*	Netherlands
Phoma digitalis [B]	CBS 229.79	GU237605	GU238067	GU237802	KT287044	KT287043	*Digitalis purpurea*	New Zealand
Phoma dimorpha [T]	CBS 346.82	GU237606	GU238068	GU237835	Q-bank	-	*Opuntiae* sp.	Spain
Phoma draconis [B]	CBS 186.83	GU237607	GU238070	GU237795	-	-	*Dracaena* sp.	Rwanda
Phoma eupatorii [B]	CBS 123.93	GU237608	GU238071	GU237764	-	-	*Eupatorium cannabinum*	Netherlands
Phoma fungicola	CBS 633.92	GU237609	EU754127	GU237900	-	-	*Microsphaera alphitoides* on *Quercus sp.*	Ukraine
Phoma glaucii [B]	CBS 114.96	FJ515627	FJ515649	FJ515609	-	-	*Chelidonium majus*	Netherlands
Phoma gossypiicola [B]	CBS 377.67	GU237611	GU238079	GU237845	-	-	*Gossypium hirsutum*	U.S.A.
Phoma henningsii [B]	CBS 104.80	GU237612	GU238081	GU237731	-	-	*Acacia mearnesii*	Kenya
Phoma herbarum [B]	CBS 615.75	FJ427133	EU754186	FJ427022	-	-	*Rosa multiflora*	Netherlands
Phoma herbicola [B]	CBS 629.97	GU237614	GU238083	GU237898	-	-	Water	U.S.A.
Phoma insulana [B]	CBS 252.92	GU237618	GU238090	GU237810	-	-	*Olea europaea*	Greece
Phoma labilis [B]	CBS 124.93	GU237619	GU238091	GU237765	-	-	*Solanum lycopersicum*	Netherlands
Phoma macrostoma var. *macrostoma* [B]	CBS 529.66	GU237625	GU238098	GU237885	Q-bank	-	*Malus sylvestris*	Netherlands
Phoma microchlamydospora	CBS 105.95	FJ427138	GU238104	FJ427028	FJ426918		*Eucalyptus* sp.	United Kingdom
Phoma minor [T]	CBS 325.82	GU237632	GU238107	GU237831	-	-	*Syzygium aromaticum*	Indonesia
Phoma multirostrata [T]	CBS 274.60	FJ427141	GU238111	FJ427031	-	-	Soil	India
Phoma nebulosa [B]	CBS 503.75	GU237634	GU238115	GU237875	-	-	*Urtica dioica*	Austria
Phoma nigripycnidia [B]	CBS 116.96	GU237637	GU238118	GU237756	-	-	*Vicia cracca*	Russia
Phoma paspali [T]	CBS 560.81	FJ427158	GU238124	FJ427048	-	-	*Paspalum dilatatum*	New Zealand
Phoma pedeiae [T]	CBS 124517	GU237642	GU238127	GU237770	Q-bank	-	*Schefflera elegantissima*	Netherlands
Phoma piperis [B]	CBS 268.93	GU237644	GU238129	GU237816	-	-	*Peperomia pereskifolia*	Netherlands
Phoma plurivora [T]	CBS 558.81	GU237647	GU238132	GU237888	-	-	*Setaria* sp.	New Zealand
Phoma poolensis [B]	CBS 116.93	GU237649	GU238134	GU237755	-	-	*Antirrhinum majus*	Netherlands

Table 3.1. *continued.*

Holomorph	Strain no.[a]	GenBank accession no.[b]					Original substrate	Locality
		TUB2	LSU	ITS	*ACT*	*GAPDH*		
Phoma rhei	CBS109177	GU237653	GU238139	GU237743	Q-bank		*Rheum rhaponticum*	New Zealand
Phoma subherbarum [B]	CBS 250.92	GU237659	GU238145	GU237809	Q-bank	-	*Solanum* sp.	Peru
Phoma sylvatica [B]	CBS 135.93	GU237661	GU238147	GU237781	-	-	*Melampyrum pratense*	Netherlands
Phoma senecionis	CBS 160.78	GU237657	GU238143	GU237787	KT287045	KT287046	*Senecio jacobaea*	New Zealand
Phoma xanthina [B]	CBS 383.68	GU237668	GU238157	GU237855	-	-	*Delphinium* sp.	Netherlands
Stagonosporopsis ajacis [T]	CBS 177.93	GU237673	GU238168	GU237791	-	-	*Delphinium* sp.	Kenya
Stagonosporopsis andigena [B]	CBS 101.80	GU237674	GU238169	GU237714	-	-	*Solanum* sp.	Peru
Stagonosporopsis crystalliniformis[T]	CBS 713.85	GU237683	GU238178	GU237903	-	-	*Lycopersicon esculentum*	Colombia
Stagonosporopsis dennisii [B]	CBS 631.68	GU237687	GU238182	GU237899	-	-	*Solidago floribunda*	Netherlands
Stagonosporopsis dorenboschii [B]	CBS 320.90	GU237689	GU238184	GU237830	-	-	*Physostegia virginiana*	Netherlands
Stagonosporopsis heliopsidis [B]	CBS 109182	GU237691	GU238186	GU237747	-	-	*Heliopsis patula*	Netherlands
Stagonosporopsis hortensis [B]	CBS 104.42	GU237703	GU238198	GU237730	-	-	Unknown	Netherlands
Stagonosporopsis chrysanthemi [B]	CBS 500.63	GU237695	GU238190	GU237871	-	-	*Chrysanthemum indicum*	Germany
Stagonosporopsis tanaceti	CBS 131484	JQ897496	JQ897461	JQ897481	-	-	*Tanacetum cinerariifolium*	Australia
Stagonosporopsis trachelii [B]	CBS 379.91	GU237678	GU238173	GU237850	-	-	*Campanula isophylla*	Netherlands
Stagonosporopsis valerianellae [B]	CBS 329.67	GU237706	GU238201	GU237832	-	-	*Valerianella locusta*	Netherlands

[a] CBS: Centraalbureau voor Schimmelcultures, Utrecht, Netherlands; CPC: Culture collection of P.W. Crous, housed at CBS; BRIP: Queensland Plant Pathology herbarium collection, Brisbane, Australia; TAS: Tasmanian Institute of Agriculture fungal collection, Tasmania, Australia.

[b] ITS: Internal transcribed spacers 1 and 2 together with 5.8S nrDNA; LSU: partial 28S nrDNA; *TUB2*: partial β-tubulin gene; *ACT*: partial actin gene; *GAPDH*: partial glyceraldehyde-2-phosphotase dehydrogenase. Accession numbers beginning with KT indicate newly generated sequences in this study.

[c] Bonants *et al.* (2013).

[d] *Didymella tanaceti* = syn. *Microsphaeropsis tanaceti* haplotype I; *D. rosea* = syn. *M. tanaceti* haplotype II.

[e] Tasmania, Australia.

[B] Reference strain according to Boerema *et al.* (2004).

[T] Ex-type strain according to Boerema *et al.* (2004).

ground mycelia using the DNeasy Plant Mini Kit (QIAGEN), according to the manufacturer's instructions. Purified DNA of *Phoma senecionis* (CBS 160.78), *Phoma bellidis* (CBS 714.85) and *Phoma digitalis* (CBS 229.79) was obtained from CBS-KNAW (Utrecht, Netherlands). DNA was quantified using a High Sensitivity Double Stranded DNA QUBIT kit (Life Technologies), diluted to 1 ng uL^{-1} and stored at -20°C before use.

The complete 5.8S nuclear ribosomal loci, including the two flanking internal transcribed spacers (ITS), and partial sequences of the β-tubulin (*TUB2*), LSU, actin (*ACT*) and glyceraldehyde-3-phosphate dehrydogenase (*GAPDH*) loci were sequenced for all *M. tanaceti* isolates. In addition, the *ACT* and GAPDH genes were sequenced in *P. senecionis, P. bellidis* and *P. digitalis*. The regions were amplified using the primers pairs V9G (Hoog & Ende, 1998) and ITS4 (White et al., 1990) for the ITS, BT2Fd and BT4R (Woudenberg et al., 2009), for the *TUB2*, LR0R and LR7 (Rehner & Samuels, 1994) for the LSU, ACT-512F and ACT-783R (Carbone & Kohn, 1999) for the *ACT* and gpd1 and gpd2 (Berbee et al., 1999) for the *GAPDH*. Polymerase chain reactions (PCR) were performed in a C1000 thermocycler (BioRad), in a total volume of 20 µL. The PCR mixture contained 1× TopTaq polymerase (QIAGEN), 1× PCR buffer, 1× CoralLoad, 1.5 mM $MgCl_2$, 0.2 µM (ITS, *TUB2* and *ACT*) or 0.4 µM (LSU and *GAPDH*) of each primer, 200 µM of each dNTP (Bioline) and 2 – 6 ng of genomic DNA.

Conditions for amplification of the ITS, *TUB2*, *ACT* and *GAPDH* loci were an initial denaturation of 5 min at 94°C, followed by 35 cycles of denaturation at 94°C for 30 s, annealing at 56°C (ITS and *TUB2*) or 59°C (*GAPDH* and *ACT*) for 30 s and extension at 72°C for 30 s, followed by a final elongation at 72°C for 7 min. Amplification of the LSU

included an initial denaturation of 10 min at 94°C, followed by 30 cycles of denaturation at 94°C for 30 s, annealing at 50°C for 30 s and extension at 72°C for 75 s, followed by a final elongation at 72°C for 7 min. PCR products were analysed by gel electrophoresis with a 1.5% (w/v) agarose gel containing GelRed™ (Biotium Inc.) in 1× TAE buffer. PCR products were prepared for sequencing using the UltraClean PCR Clean-Up kit (Mo Bio Laboratories Inc.), according to the manufacturer's instructions. The amplicons were sequenced in both directions using the same primer combinations at the Australian Genome Research Facility (Melbourne, Australia) using Big Dye Terminator v3.1 chemistry and capillary separation on an AB 3730xl (Applied Biosystems Inc.). Consensus sequences for each isolate were obtained from pairwise alignment of the forward and reverse sequences in Geneious v7.1.0 (Biomatters). Sequences for each loci were aligned using MAFFT (Katoh et al., 2002), and any interspecific and intraspecific nucleotide variation between the haplotypes for each locus identified. Loci sequences were deposited in GenBank (Table 3.1).

3.3.3 Phylogenetic characterisation

A two-part phylogenetic analysis was conducted. Firstly, the *M. tanaceti* haplotypes were combined with representative species of the genus *Microsphaeropsis* and the 19 clades identified by Aveskamp et al. (2010) to construct a three-locus phylogeny to identify the position of *M. tanaceti* within the *Didymellaceae*. Secondly, to further evaluate the phylogenetic relationship between the *M. tanaceti* haplotypes, a four-locus phylogeny was constructed using a reduced set of isolates for which *ACT* data was available.

The initial phylogenetic analysis was undertaken using the LSU, ITS and *TUB2* loci. Sequences for each loci were aligned using MUSCLE (Edgar, 2004) in Geneious, and manually adjusted where necessary. Prior to concatenation of the three loci to create a combined multilocus sequence, individual loci trees produced using Bayesian Inference (BI) were analysed for congruence. For BI analysis, the best-fit model of nucleotide substitution for each loci region was selected using jModelTests v2.1.4 (Darriba et al., 2012), based on the likelihood scores for 24 models and the Akaike Information Criterion (AIC). The best-fit model for each region was the GTR+I+G model. Bayesian inference was performed in MrBayes v3.2.1 (Ronquist & Huelsenbeck, 2003). The analysis consisted of two runs, each containing three heated chains at a temperature of 0.1 and a cold chain, with data collected once every 1,000 generated trees. The run was stopped once the standard deviation of split frequency ≤ 0.0099 and a potential scale reduction factor of 1 was achieved. Twenty-five percent of the saved trees prior to convergence were discarded as burn-in. A 50% majority rule consensus tree was constructed and posterior probabilities of clades calculate. Topological congruence between the three individual loci trees was tested with the Congruence Among Distance Matrices (CADM) test (Campbell et al., 2011), implemented in R v3.0.1 (R Core Team, 2014) using the package *ape* (Paradis et al., 2004), and 9,999 permutations. The null hypothesis assumed complete incongruence of the phylogenetic trees. The *P* values were adjusted for multiple pairwise comparisons using the Holm correction method.

Phylogenetic analyses of the concatenated loci were conducted using BI and maximum parsimony (MP). *Ascochyta hordei* var. *hordei* (CBS 544.74) was used as the out-group. Bayesian inference analysis was undertaken as previous. Maximum parsimony analysis was

conducted using PAUP v4.0b10 (Swofford, 2003). A heuristic search with 100 replicates, maximum trees set to 1,000, nchuck set to 10 and gaps treated as a fifth state was undertaken. Support for tree topology was calculated by 1,000 bootstrap replicates of the model. A 50% majority rule consensus tree was constructed and the bootstrap percentages of clades calculated. Topological congruence between the 50% majority rule BI and MP trees was tested using CADM. The 50% majority rule tree from BI was visualised in R using the packages *ape* (Paradis et al., 2004) and *phytools* (Revell, 2012). The bootstrapped confidence percentages from MP were overlayed on the nodes of the tree. Tree topology was inspected and the terminal clades of Aveskamp et al. (2010) identified. The tree was lodged with TreeBASE (www.treebase.org/treebase-web/home.html; submission ID = 18003).

To test the observed phylogenetic relationship between the *M. tanaceti* haplotypes and the representative *Microsphaeropsis* spp., steppingstone sampling (Xie et al., 2011), was implemented in MrBayes, to test hypothetical tree topologies by setting constraints on the Markov chain Monte Carlo (MCMC) model topology and calculating the marginal likelihood of opposing models. For each analysis two topologies were tested: H_0 modelled *M. tanaceti* haplotypes forming a monophyletic clade nested within the genus *Microsphaeropsis;* the alternative hypothesis, H_1, modelled the *M. tanaceti* haplotypes constrained to a monophyletic clade distinct from other *Microsphaeropsis* spp. For each topology constraint, the MCMC analysis was run in triplicate, as described for the previous BI analysis, using the concatenated three-locus alignment. Stepping stone analysis consisted of 100 steps spread over 2,000,000 generations, α value of 0.3, relative initial burn-in of one step (20,000 generations), and five samples (5,000 generations) burnt in at the start of each step. Data was collected once every 1,000 generations, sampled from the posterior to the prior. Bayes

factors were calculated from the ratio of the natural log of the marginal likelihood estimate for opposing tree topologies and the interpretation of Bayes factors of Kass and Raftery (1995) used to determine the level of evidence against H_0.

The relationship between the *M. tanaceti* haplotypes and species identified within the branches of the same ancestral node from the three-locus phylogeny was extrapolated in a second phylogenetic analysis. The analysis contained the *M. tanaceti* haplotypes and representatives of the genera; *Peyronelleae, Macroventuria, Microsphaeropsis* and several *Didymella* species with *Ascochyta or Phoma* asexual morphs. A lack of availability of *GAPDH* genes for all strains, limited the analysis to sequence data of the LSU, ITS, *TUB2* and *ACT* loci regions. Loci were aligned using MUSCLE and large indels recoded to minimise bias. For MP large indels were manually recoded as a single nucleotide. For BI large indels were recoded using FastGap v1.2 (Borchsenius, 2009) as binary (1: nucleotide; 0: gap). *Macroventuria wentii* (CBS 526.71) was used as the out-group. The best models of nucleotide substitution, selected according to jModelTest, conducted as described previously, were the GTR+I for the LSU, SYM+I+G for the ITS, GTR+I+G for *TUB2* and GTR+G for *ACT*. Prior to concatenation of the four loci to create a combined multilocus sequence, individual loci trees produced using BI were analysed for congruence using CADM, as previously described. Bayesian inference and MP analysis of the four-locus phylogeny were run as described for the three-locus phylogeny with the exception of a minimum of 5,000,000 generations ran for BI, and no limitation on the nchuck value and maximum trees set to 20,000 for MP. Trees were visualised in R as previously described, and submitted to TreeBASE.

3.3.4 Morphological characterisation

Microsphaeropsis tanaceti isolates (*n* = 20; 10 of each haplotype; Table 3.1), were inoculated in triplicate onto PDA, oatmeal agar (OA) (Boerema et al., 2004), and malt extract agar (MEA; Amyl Media) for culture and morphological comparison. Plates were inoculated with a 4 mm mycelial plug taken from the margin of an actively growing culture on PDA and incubated at 21°C for 7 d in the dark and subsequently incubated in a light box at 20 – 22.5°C with a 13:11 h light:dark cycle under near ultraviolet light for an additional 7 d (Boerema et al., 2004). After 7 and 14 d of incubation, mycelial growth was measured across two perpendicular lines for each isolate on PDA, OA and MEA. In addition, gross morphology, including description of the colony margin and colour of the surface and reverse of cultures (Rayner, 1970) were recorded. Pycnidial diameter, colour and number of necks and ostioles of isolates on OA were recorded at 60× magnification after 14 d incubation. Exuded conidia were harvested from multiple pycnidial ostioles on three replicate plates of OA for each isolate and viewed at 400× magnification. Conidial width and length were measured for 50 conidia per isolate across multiple fields of view. The percentage of septate conidia produced on OA and PDA were respectively calculated by examining 200 conidia over multiple fields of view at 400× magnification. The production of metabolite 'E' was determined by application of a droplet of 1N NaOH to cultures growing on MEA following 14 d incubation (Boerema et al., 2004). Cultures were examined for colour changes (beginning yellow and becoming red/blue/purple) or crystal production within the applied area throughout the hour following application.

To identify morphological variation between the two *M. tanaceti* haplotypes, mean and standard error (SE) of culture diameters after 7 and 14 d incubation and average culture radial

growth on PDA, MEA and OA were calculated. In addition, mean and SE of conidial width, length, and the ratio of length:width were calculated for conidia produced on OA for each haplotype. For each variable 95% confidence intervals of the haplotype mean were calculated from 1,000 bootstrap replicates. Significant differences between haplotypes for the above variables were tested using a permutation *t*-test. Mean culture diameters were calculated as the average of the two perpendicular measurements minus the diameter of the inoculation plug. Average radial growth rate was expressed as the average of the mean radial growth per day under dark conditions and the mean radial growth per day under a 13:11 h light:dark cycle. Statistical analysis were completed in R using the *coin* (Zeileis et al., 2008) and *reshape* (Wickham, 2007) packages.

3.4 RESULTS

3.4.1 Molecular characterisation

Alignment of the ITS (679 base pair (bp)) nucleotide sequence, confirmed the existence of two haplotypes. Ten isolates had an ITS sequence identical to BRIP 50785 (GenBank Acc: KT338641). The remainder contained the three SNPs present in BRIP 50788 (GenBank Acc: KT338640). The two haplotypes shared 99.6% sequence identity for this gene. Consistent differences were found between the haplotypes for the remaining four loci sequenced, except for the LSU locus (1314 bp), which was identical for all isolates. The haplotypes shared 95.8% sequence identity in the *TUB2* (335 bp) attributed to 12 SNPs and a 2 bp insertion/deletion, 98.0% sequence identity in the *ACT* (246 bp) attributed to 5 SNPs, and 97.6% sequence identity in the *GAPDH* (575 bp) attributed to 14 SNPs. In addition, the two haplotypes

shared 89.2 – 89.3% identity in the *TUB2*, 96.5 – 96.7% identity in the ITS locus, and 99.3% identity in the LSU locus with *M. olivacea*. Sequences were 100% identical for all five loci regions within each haplotype. Therefore, one isolate was selected to represent each haplotype in the phylogenetic analysis.

3.4.2 Phylogenetic characterisation

One hundred taxa, including representatives of the two *M. tanaceti* haplotypes, were included in the initial three-locus phylogeny. Analysis of congruence between the three loci regions using CADM identified congruence between each of the three loci (P = 0.0001). Thus, the three regions were combined for further analysis. The composite sequence alignment was 1,713 characters in length (LSU: 869, *TUB2*: 347, ITS: 497). Of those characters 1,380 (LSU: 808, *TUB2*: 187, ITS: 385) were constant and 333 (LSU: 61, *TUB2*: 160, ITS: 112) were variable. The tree obtained through MP supported the tree obtained from BI analysis, (P = 0.0001). The genus *Microsphaeropsis* formed a well-supported (1.0/100; posterior probability/bootstrap percentage), monophyletic clade associated paraphyletically with groups B and C (Fig. 3.1). In contrast, the haplotypes of *M. tanaceti* formed a well-supported (1.0/84) cluster with *Phoma digitalis* and *P. bellidis*, within a monophyletic clade (Groups H and I). This clade also contained the type species of *Didymella, D. exigua* (CBS 183.55) (*Didymella sensu stricto*). Furthermore, the two haplotypes were well supported (0.96 – 0.98) as a separate monophyletic clade in regard to *P. digitalis* and *P. bellidis* and exhibited differing branch lengths. Steppingstone analysis resulted in a mean natural log of the Bayes factor of 25.46, which was considered very strong evidence against the null hypothesis that *M. tanaceti* constituted part of the *Microsphaeropsis* clade.

Analysis of congruence between the four loci used in the second analysis using CADM identified congruence between each loci pair ($P < 0.05$), except for the LSU and *ACT* ($P = 0.51$). Further evaluation identified that the LSU had the lowest correlation scores to each of the other three regions. This was most likely due to the low resolution provided by the LSU, which was expected due to the nature of its evolution within species. To validate the inclusion of the LSU in the concatenated alignment, congruence between concatenated ITS-*TUB2-ACT* and ITS-*TUB2-ACT*-LSU loci was tested. The three- and four-locus concatenated sequences were congruent ($P = 0.0001$) and a Kendall's value (W) of 0.99 indicated a high degree of congruence. Thus, the four loci were combined for further analysis. The concatenated four-locus sequence alignment was 1,960 characters in length, including alignment gaps (LSU: 869, ITS: 485, *TUB2*: 344, *ACT*: 262). Of those characters 1,636 (LSU: 849, ITS: 437, *TUB2*: 212, *ACT*: 138) were constant and 324 (LSU: 20, ITS: 348, *TUB2*: 132, *ACT*: 124), were variable. The tree obtained through MP supported the tree obtained from BI analysis, ($P = 0.0001$). The four-locus tree analysis further supported the haplotypes as clustered in *Didymella sensu stricto* (1.00/87) (Fig. 3.2). Furthermore, the two haplotypes were supported as sharing a recent common ancestor with *P. bellidis*, *P. senecionis* and *P. digitalis* (1.00/98) and a most recent common ancestor with each other (0.66/85). Tree branch lengths of the *M. tanaceti* haplotypes differed (Fig. 3.2).

3.4.3 Morphological characterisation

The two haplotypes varied in colour on PDA and MEA following 7 and 14 d incubation. On PDA and MEA the surface of haplotype I cultures were white and the reverse buff (Fig. 3.3a & 3.3b). Haplotype II cultures on PDA were salmon to saffron on the surface and reverse (Fig. 3.4a & 3.4b). On MEA haplotype II cultures were rosy buff on the surface and buff on

the reverse. On OA, colony morphology was indistinguishable for the two haplotypes (Fig. 3.3c & 3.4c). Culture diameter and average radial growth rate were significantly ($P < 0.05$) greater in haplotype II isolates after 7 and 14 d incubation on each medium (Table 3.2). The largest difference was evident after 14 d incubation on PDA with mean culture diameters of 63.2 mm (95% CI = 60.7 – 65.4 mm) and 67.1 mm (95% CI = 65.8 – 68.4 mm) for haplotype I and II, respectively (Table 3.2). Both haplotypes on OA responded to light by production of pycnidia in concurrent rings, with an associated darkened hyphal pigmentation in pycnidial zones. Pycnidia were produced on the agar surface, submerged within agar and on aerial mycelia for both haplotypes. Pycnidial diameter varied depending on pycnidial age and ranged from 85 – 215 µm and 70 – 220 µm for haplotype 1 and II, respectively (Fig. 3.3d & 3.4d). For both haplotypes 0 – 5 vertical extensions (necks) were produced on mature pycnidia after 7 d under light conditions (Fig. 3.3e & 3.4e) and conidia were released through ostioles on the terminal ends of necks. Conidia of haplotype II were significantly ($P < 0.001$) shorter and wider than conidia of haplotype I (Fig. 3.3f & 3.4f; Table 3.2). The mean conidial dimensions were 2.61 × 5.65 µm (95% CI = 2.59 – 2.64 × 5.59 – 5.71 µm) and 2.74 µm × 5.15 (95% CI = 2.70 – 2.78 × 5.10 – 5.20 µm) for haplotype I and II, respectively (Table 3.2). Secondary conidial septation was present in all isolates of haplotype I and varied with media for haplotype II. The percentage of septate conidia varied for each isolate, ranging from 1 – 7.5% on OA and 1 – 15% on PDA for haplotype I and 0 – 1% on OA and 1 – 2% on PDA for haplotype II. Application of NaOH did not result in colour changes indicative of metabolite "E" production or crystal formation in either haplotype. Morphological variation of the two haplotypes correlated with the genetic differences.

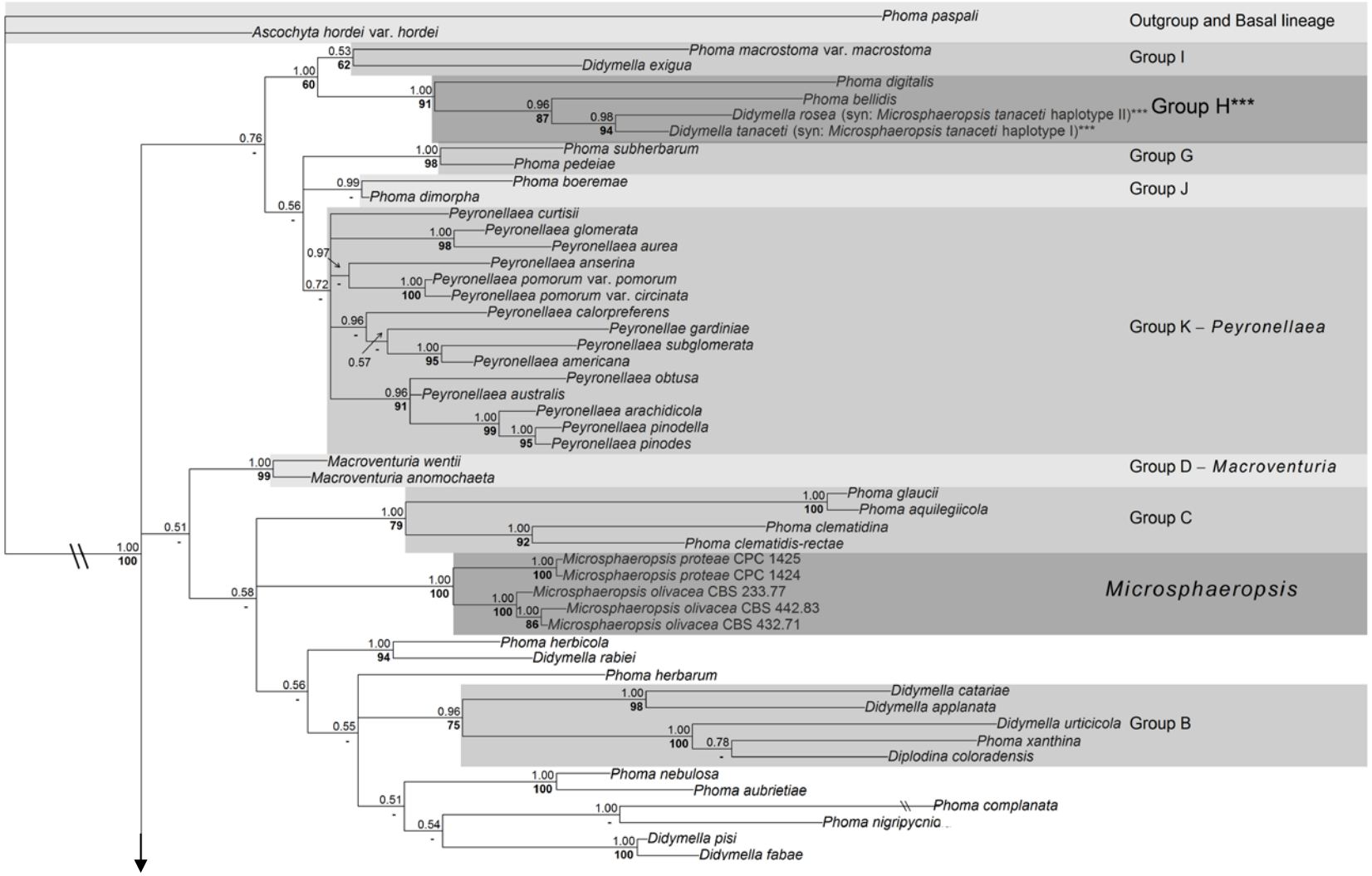

Fig. 3.1. *continued*

Fig. 3.1. *continued*

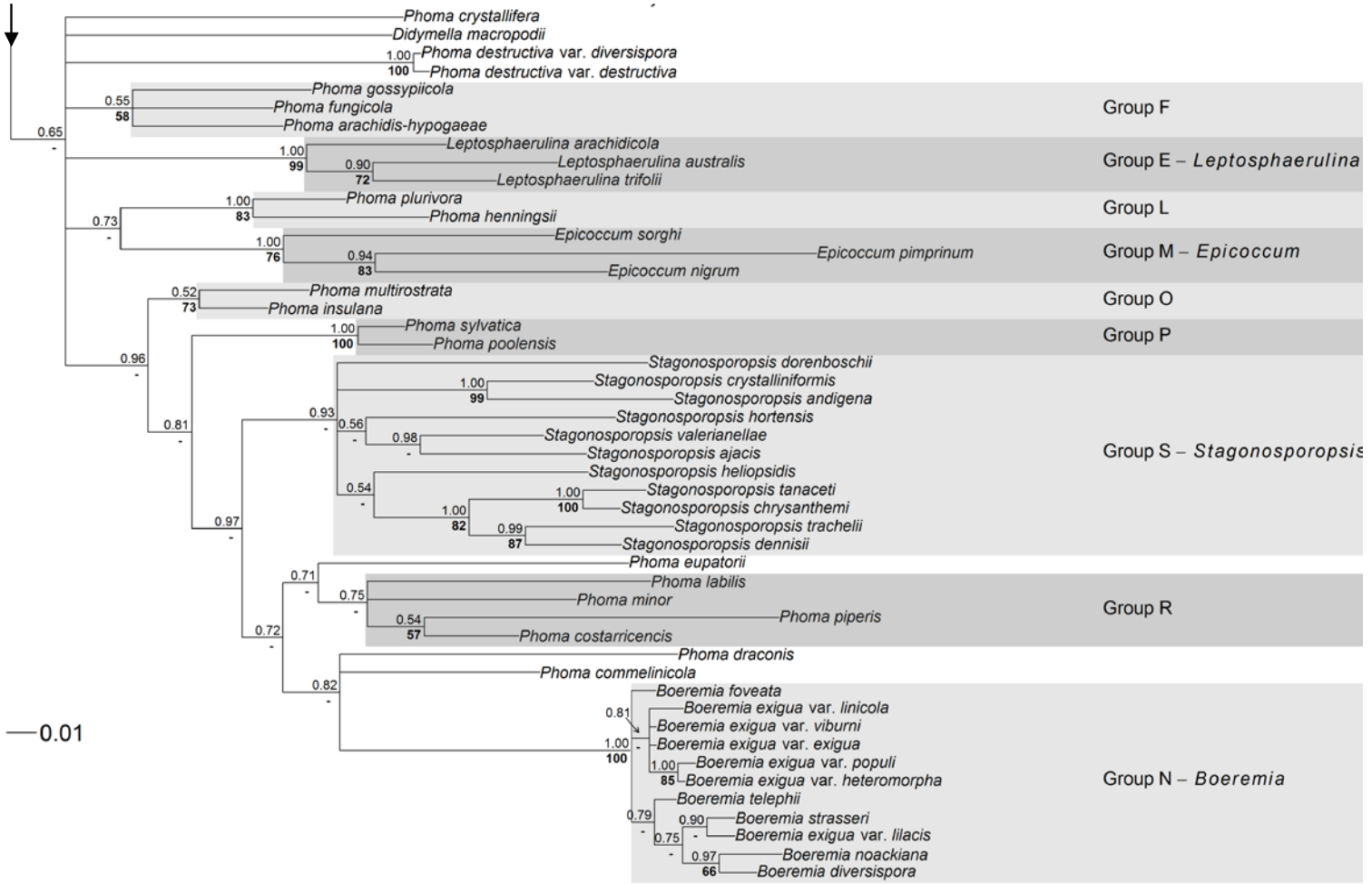

Fig. 3.1. Fifty percent majority rule consensus tree from Bayesian inference (BI) of concatenated nuclear ribosomal internal transcribed spacer β-tubulin and large subunit 28S nrDNA sequence regions of representative isolates of the *Didymellaceae* (*n* = 100). The positions of the *Microsphaeropsis tanaceti* haplotypes are indicated by ***. At the nodes the BI posterior probabilities are presented above the branch and the bootstrap percentages from maximum parsimony (MP) are given below the branch. MP bootstrap percentages <50% are indicated with a dash. Group labels on terminal ends of nodes identify groups within the *Didymellaceae* as indicated by Aveskamp et al. (2010). The tree is rooted to *Ascochyta hordei* var. *hordei* (CBS 544.74). Scale bar indicates branch length.

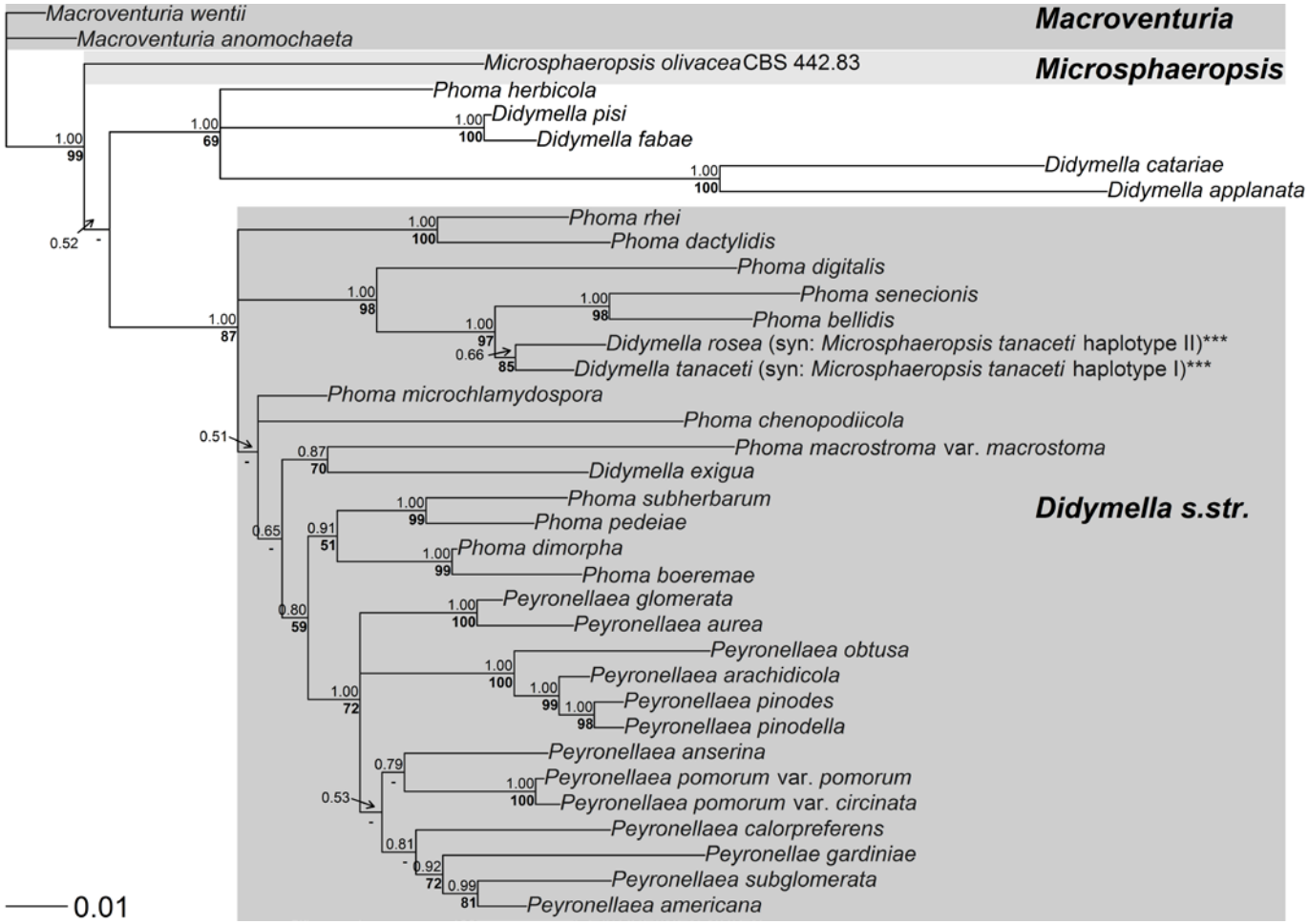

Fig. 3.2. Fifty percent majority rule consensus tree from Bayesian inference (BI) of concatenated nuclear ribosomal internal transcribed spacer, β-tubulin, large subunit 28S nrDNA and actin sequence of the *Microsphaeropsis tanaceti* haplotypes and associated species (*n* = 36). The positions of the *M. tanaceti* haplotypes are indicated by ***. At the nodes the BI posterior probabilities are presented above the branch and the bootstrap percentages from maximum parsimony (MP) are given below the branch. MP bootstrap percentages <50% are indicated with a dash. The tree is rooted to *Macroventuria wentii* (CBS 526.71). Scale bar indicates branch length.

3.4.4 Taxonomy

Phylogenetic analyses demonstrated that the two haplotypes were previously misclassified as a *Microsphaeropsis* species. Furthermore, significant morphological and genetic variation between the two haplotypes indicated that they should be reclassified as two separate species. Re-classification using a phylogenetic analysis based on molecular data identified shared and unique evolutionary relationships between the haplotypes and species within a clade containing the type species of *Didymella* (*D. exigua*) and *Peyronellaea* (*Peyronellaea glomerata*). As *Didymella* is the oldest available name of the two genera, the two haplotypes are herein redescribed as two *Didymella* species.

3.4.4.1 Didymella tanaceti

Didymella tanaceti **(**R.G. Shivas, S.J. Pethybridge & S.J. Jones) T.L. Pearce, J.B. Scott, Crous, S.J. Pethybr. & F.S. Hay, ***comb. nov.*** – MycoBank MB813709 (Fig. 3.3)

Basionym. Microsphaeropsis tanaceti R.G. Shivas, S.J. Pethybridge & S.J. Jones, *Plant Pathology* **57**: 1062 (2008).

Conidiomata pycnidial, brown to black, globose to subglobose and becoming irregular with age, solitary to clustered, 85 – 215 µm diameter, submerged and on agar surface and aerial mycelium; pycnidia develop in concurrent circles following introduction of light source; *conidia* released through ostioles, initially non-papillate but forming an elongated neck in a later stage (some setose), with 0 – 1(–2) or up to 5 necks per pycnidium. Conidial matrix citrine to grey olivaceous. *Conidiogenous cells* phialidic. *Conidia* cylindrical to ellipsoidal with rounded ends, rarely septate, 4.0 – 8.5 × 1.5 – 3.5 µm.

Culture characteristics: On OA: colonies 32 – 47 mm in diameter after 7 d (63 – 77 mm after 14 d), with entire smooth margins, hyphae translucent on plate, hyphal thickening with olivaceous buff to greenish olivaceous pigments extending from centre and in regions of pycnidial production. White tufted mycelium sporadic around plate, reverse, as above. On PDA: colonies 24 – 40 mm in diameter after 7 d (50 – 75 mm after 14 d), with entire smooth margins. Colonies white, reverse buff, sometimes with olivaceous buff to olivaceous extending outwards from centre and olivaceous pigments in regions of pycnidial production. On MEA: colonies 31 – 41 mm in diameter after 7 d (60 – 75 mmm after 14 d), with entire smooth margins. Colonies white, fluffy and raised, reverse buff with olivaceous extending outwards from centre. Crystal formation or colour changes absent on application of NaOH.

Specimen examined: **Australia**, Tasmania, Sassafras, on leaves of *Tanacetum cinerariifolium*, 2004, S.J. Pethybridge (*holotype:* BRIP 50785, *culture ex-type:* TAS72901A = TAS 041-0055).

3.4.4.2 Didymella rosea

Didymella rosea T.L. Pearce, J.S. Scott, Crous, S.J. Pethybr. & F.S. Hay, ***sp. nov.*** – MycoBank MB813698 (Fig. 3.4)

Etymology: Named after gross colony colour on potato dextrose agar following incubation in the dark.

Conidiomata pycnidial, brown to black, glabrous, globose to sub-globose and becoming irregular with age, solitary to clustered, 70 – 220 µm diameter, submerged and on agar surface and aerial mycelium; pycnidia develop in concurrent circles following introduction of light source; *conidia* released through ostioles, initially non-papillate but forming an

elongated neck in a later stage (some setose), with 0 – 2 necks per pycnidium. Conidial matrix citrine to grey olivaceous *Conidiogenous cells* phialidic. *Conidia* short cylindrical with rounded ends, rarely septate, 4 – 7 × 1.5 – 4.5 µm.

Culture characteristics: On OA: colonies 36 – 44 mm in diameter after 7 d (68 – 76 mm after 14 d), with entire smooth margins, hyphae translucent on plate, hyphae thickening with olivaceous buff to greenish olivaceous pigments extending from centre and in regions of pycnidia production. White tufted mycelium sporadic around plate, reverse, as above. On PDA: colonies 33 – 40 mm in diameter after 7 d (58 – 75 mm after 14 d), margin regular but becoming wavy following introduction of light source, colonies salmon to peach with white aerial mycelium, reverse saffron to salmon with honey pigmented hyphae extending from centre. On MEA: colonies 33 – 40 mm in diameter after 7 d (50 – 74 mm after 14 d), with entire smooth margins, colonies rosy buff to buff with dark olivaceous extending from centre underneath, reverse rosy buff to buff with olivaceous extending from centre. Crystal formation or colour changes absent on application of NaOH.

Specimen examined: **Australia**, Tasmania, Forth, on leaves of *Tanacetum cinerariifolium*, 2004, S.J. Pethybridge (*holotype:* BRIP 50788, *culture ex-type:* TAS 46009L = TAS 041-0220).

3.5 DISCUSSION

This study builds on a previous phylogenetic study of *M. tanaceti* which was limited by a relatively small number of available species for phylogenetic comparison (Pethybridge et al., 2008). Further genetic and morphological characterisation and a phylogenetic comparison of

the two recognized haplotypes of *M. tanaceti* to species within the *Didymellaceae* identified that the haplotypes were not associated with the genus *Microsphaeropsis*. Sufficient evidence was found to elevate the two haplotypes to species level within the genus *Didymella* and the new species; *Didymella tanaceti* (previously haplotype I) and *D. rosea* (previously haplotype II) were described. To the best of our knowledge, these species have only been identified as pathogens of pyrethrum in Tasmania, Australia.

Consistent nucleotide differences were evident between the species in four of the five loci examined. The LSU locus shared 100% sequence identify between the species, indicating their close phylogenetic relationship. However, the LSU locus of filamentous fungi is often not sufficient to delimit taxa at the species level (Eberhardt, 2010, Lumbsch et al., 2000). Morphological distinction between the species was most evident when gross culture morphological characteristics, especially culture pigmentation on PDA and the dimensions of conidia produced on OA were examined. The three-locus phylogeny incorporating the LSU, ITS and *TUB2* loci identified 18 of the taxonomic clades previously described by Aveskamp *et al.* (2010) in the 50% majority consensus tree from the BI analysis. Discrepancies occurred between the placement of species within groups obtained in this study and that of Aveskamp et al. (2010) for *Phoma euaptorii, Phoma draconis* and *Phoma commelinicola*. The basal clades (groups B — D) and unresolved species identified by Aveskamp et al. (2010) formed a weakly supported (0.51/-) clade in this analysis. Phylogenetic analysis using a combination of these loci has been used previously to resolve misclassified *Microsphaeropsis* spp. (Verkley et al., 2014). Tree topology provided evidence that the *M. tanaceti* haplotypes were not associated with the genus *Microsphaeropsis*. This was further supported by stepping stone analysis, with the obtained value of the Bayes factors indicating very strong

Table 3.2. Growth dimensions of *Didymella tanaceti* (syn: *Microsphaeropsis tanaceti* haplotype I) isolates (*n* = 10) and *Didymella rosea* (syn: *Microsphaeropsis tanaceti* haplotype II) isolates (*n* = 10) on oatmeal, malt extract and potato dextrose agars, and conidial dimensions on oatmeal agar.

		Growth medium											
		Oatmeal agar (OA)				Malt extract agar (MEA)				Potato dextrose agar (PDA)			
Measurement	Species[a]	Mean ± SE[b]	Min	Max	95% CI[c]	Mean ± SE	Min	Max	95% CI	Mean ± SE	Min	Max	95% CI
Growth[d]													
7 d culture diameter (mm)[e]	*D. tanaceti*	38·1 ± 0·63	32·5	46·5	36·8–39·2	35·3 ± 0·43	31·0	41·0	34·6–36·2	32·4 ± 0·75	24·5	40·0	31.0–33·9
	D. rosea	39·8 ± 0·28	36·5	43·5	39·3–40·4	37·4 ± 0·33	33·0	40·2	36·7–38.0	35·7 ± 0·26	33·0	39·5	35·2–36·2
14 d culture diameter (mm)[e]	*D. tanaceti*	68·9 ± 0·55	63·0	76·8	67·9–70.0	66·2 ± 0·75	59·5	75·0	64·7–67·6	63·2 ± 1·18	49·5	75·0	60·7–65·4
	D. rosea	70·6 ± 0·37	68·0	75·5	69·9–71·4	69·7 ± 0·94	49·5	74·2	67·7–71·3	67·1 ± 0·66	58·0	74·8	65·8–68·4
Average growth rate (mm/day)[f]	*D. tanaceti*	2·46 ± 0·02	2·25	2·74	2·42–2·50	2·36 ± 0·02	1·77	2·65	2·32–2·42	2·26 ± 0·04	1·77	2·68	2·18–2·34
	D. rosea	2·52 ± 0·01	2·43	2·67	2·50–2·55	2·49 ± 0·03	2·21	2·71	2·42–2·55	2·40 ± 0·02	2·07	2·67	2·35–2·44
Conidia[g]													
Width (µm)	*D. tanaceti*	2·61 ± 0·01	1·49	3·75	2·59–2·64	NT[h]	NT	NT	NT	NT	NT	NT	NT
	D. rosea	2·74 ± 0·02	1·60	4·65	2·70–2·78	NT	NT	NT	NT	NT	NT	NT	NT
Length (µm)	*D. tanaceti*	5·65 ± 0·03	3·91	8·40	5·59–5·71	NT	NT	NT	NT	NT	NT	NT	NT
	D. rosea	5·15 ± 0·03	3·67	6·75	5·10–5·20	NT	NT	NT	NT	NT	NT	NT	NT
Length:width ratio	*D. tanaceti*	2·18 ± 0·01	1·49	3·68	2·16–2·20	NT	NT	NT	NT	NT	NT	NT	NT
	D. rosea	1·90 ± 0·01	1·34	2·84	1·88–1·93	NT	NT	NT	NT	NT	NT	NT	NT

[a] *D. tanaceti* = syn. *Microsphaeropsis tanaceti* haplotype I; *D. rosea* = syn. *M. tanaceti* haplotype II.
[b] Mean of measurement ± standard error of the mean.
[c] 95% confidence intervals of mean calculated using 1000 bootstrapped replicates.
[d] Each pairwise comparison was significantly different at $P < 0.05$ for OA and PDA and $P < 0.001$ for MEA based on permutation t-tests.
[e] Calculated as the average of two perpendicular measurements minus the diameter of the plug.
[f] Calculated as the mean of the average radial growth per day in dark conditions and the average radial growth per day in light conditions.
[g] Each pairwise comparison significantly difference at $P < 0.001$ based on permutation t-tests.
[h] NT = not tested.

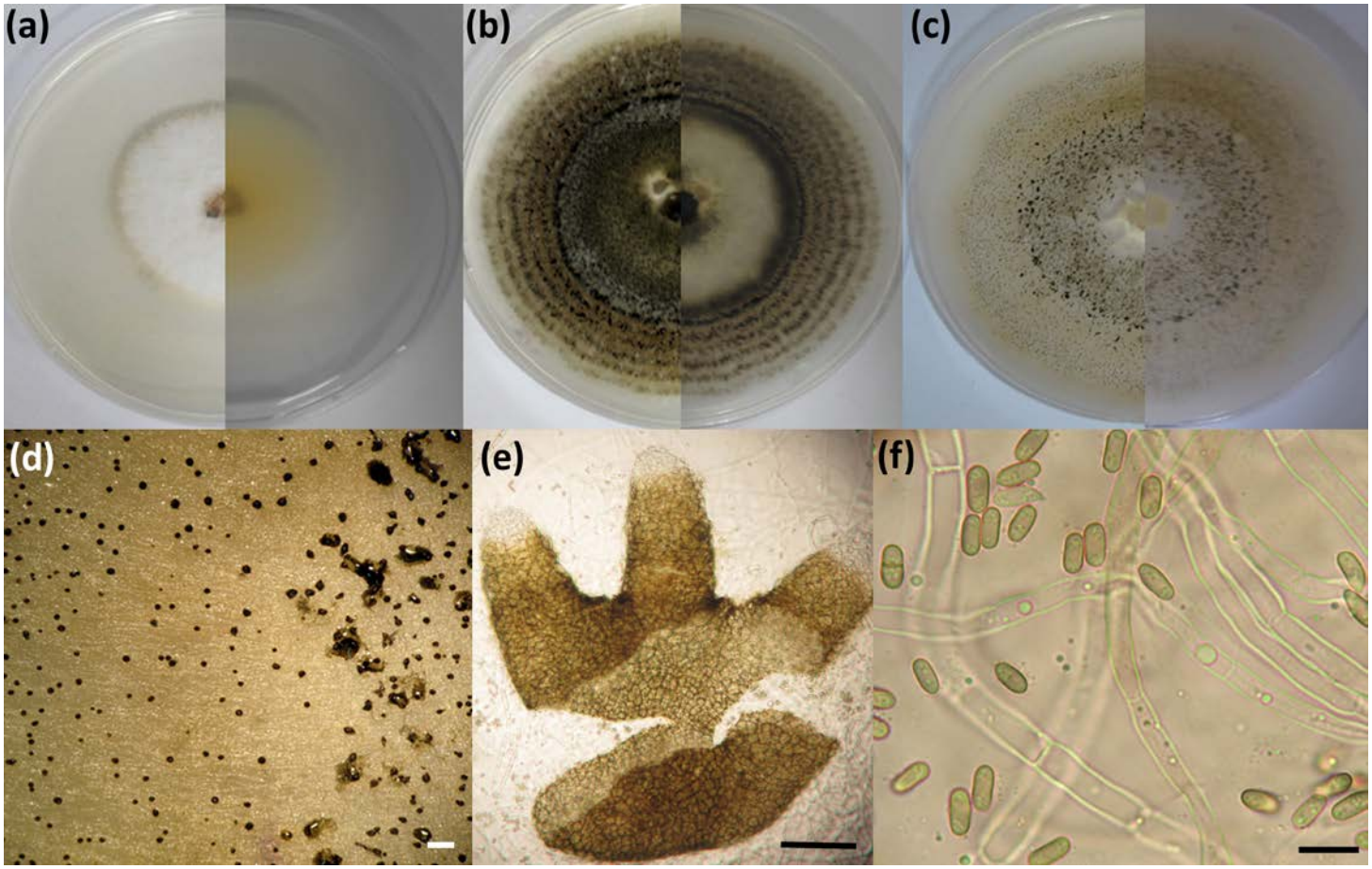

Fig. 3.3. Gross culture, pycnidial and conidial morphology of *Didymella tanaceti* (syn: *Microsphaeropsis tanaceti* haplotype I). (a) Colony on potato dextrose agar (PDA) after 7 d incubation at 21°C in the dark (surface and reverse); (b) colony on PDA after 7 d incubation at 21°C in the dark and 7 d incubation at 20 – 22.5°C with a 13:11 h light:dark cycle under near-ultraviolet light (surface and reverse); (c) colony on oatmeal agar (OA) after 7 d incubation at 21°C in the dark and 7 d incubation at 20 – 22.5°C with a 13:11 h light:dark cycle under near-ultraviolet light (surface and reverse); (d) pycnidia on OA; (e) excised pycnidium with necks; (f) conidia (scale bars: (d) = 500 µm ; (e) = 50 µm; (f) = 10 µm).

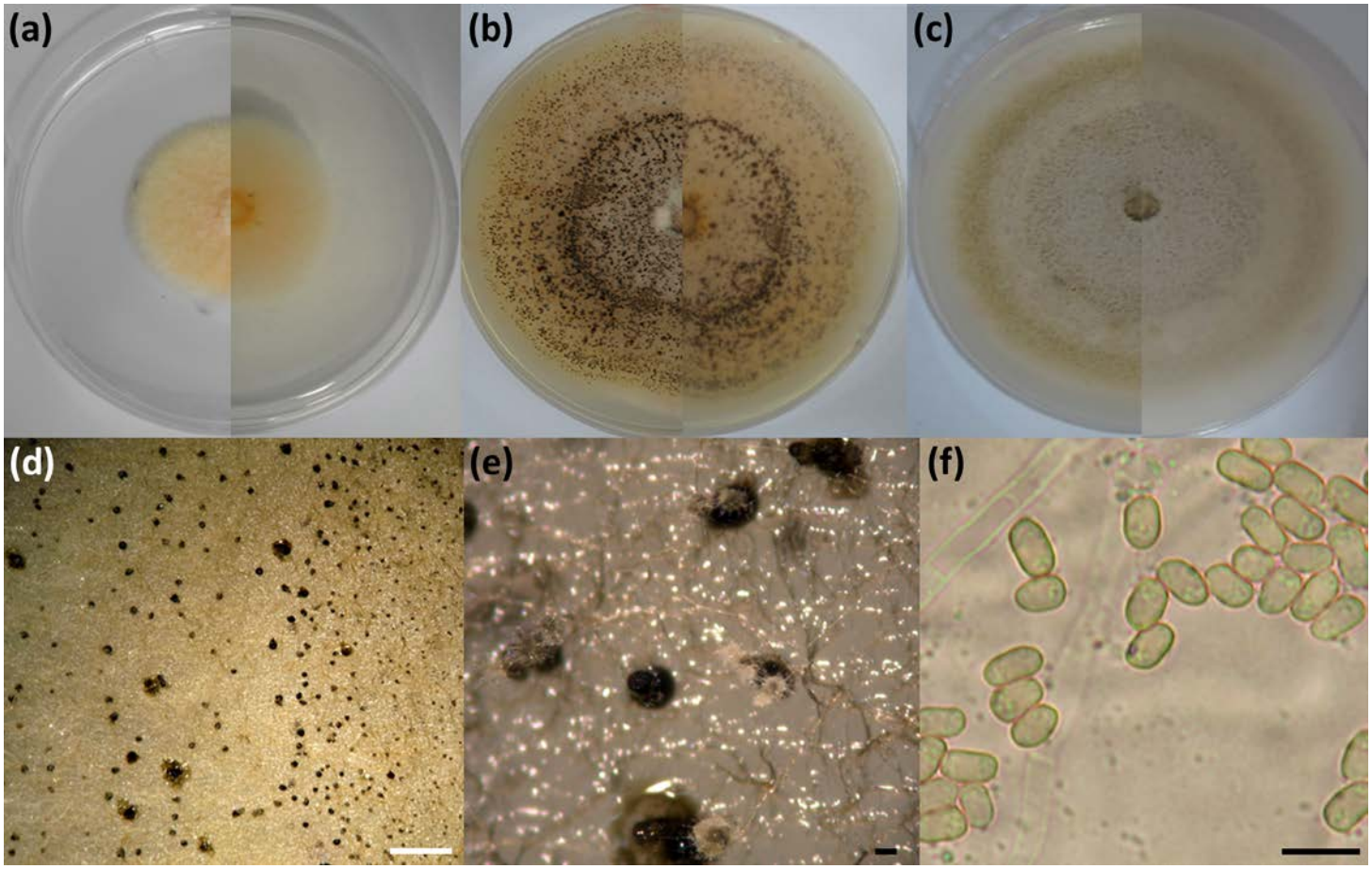

Fig. 3.4. Gross culture, pycnidial and conidial morphology of *Didymella rosea* (syn: *Microsphaeropsis tanaceti* haplotype II). (a) Colony on potato dextrose agar (PDA) after 7 d incubation at 21°C in the dark (surface and reverse); (b) colony on PDA after 7 d incubation at 21°C in the dark and 7 d incubation at 20 – 22.5°C with a 13:11 h light:dark cycle under near-ultraviolet light (surface and reverse); (c) colony on oatmeal agar (OA) after 7 d incubation at 21°C in the dark and 7 d incubation at 20 – 22.5°C with a 13:11h light:dark cycle under near-ultraviolet light (surface and reverse); (d) pycnidia on OA; (e) pycnidia on OA with necks; (f) conidia (scale bars: (d) = 500 µm ; (e) = 50 µm; (f) = 10 µm).

evidence (Kass & Raftery, 1995) against the model which constricted the haplotypes to form a monophyletic clade nested within the *Microsphaeropsis* spp.

Closer examination of these relationships using four loci in a concatenated phylogenetic analysis confirmed the phylogenetic relationship between the haplotypes and identified differing branch lengths, which when combined with the morphological differences; indicated that the two haplotypes should be separate species. In both analyses the haplotypes clustered with strong support with *D. exigua* (CBS 183.55), the type species of the genus *Didymella*, suggesting that the pathogens of pyrethrum would be better accommodated in this genus. Historically, the genus *Didymella* was considered to be the sole sexual morph of *Phoma sensu stricto* (Aveskamp et al., 2010). Prior to the 1st January 2013 mycologists were permitted under the International Code of Botanical Nomenclature (ICBN) to give asexually reproducing fungi (anamorphs) separate names from their sexual morphs (teleomorphs), resulting in dual nomenclature for many species. For *Phoma* the sexual morph was classified in *Didymella* (e.g. *Phoma rabiei* = asexual morph; *Didymella rabiei* = sexual morph) and thus, the inclusion of species within *Didymella* required evidence of a sexual morph. To assist with confusion and clarity the principle of "one fungus, one name" was adopted to resolve the problems associated with dual nomenclature (Wingfield et al., 2012, Crous et al., 2015). This ruling proposes that the genus *Didymella* should no longer only include taxa that solely exhibit a sexual morph. Some *Didymellaceae* genera, including *Stagonosporopsis* and *Boeremia*, already encompass taxa of both morphs (Aveskamp et al., 2010). Furthermore, DNA sequencing and analysis has allowed taxonomists to more easily connect asexual morphs of fungi to sexual morph-typified generic names such as *Didymella*. The genus *Didymella* had previously been identified as paraphyletic within the *Didymellaceae*

(Aveskamp et al., 2010). However, a comprehensive phylogenetic and morphological revision of *Didymella* and related *Phoma* and *Ascochyta* genera has recently been published (Chen et al., 2015). The results of this revision supported the placement of the two tan spot pathogens in the genus *Didymella* in our study. Chen et al. (2015) recombined all of the species identified within the *Didymella sensu stricto* clade in our study into the genus *Didymella.* The *Didymella* species *D. fabae, D. pisi, D. catariae* and *D. applanata,* which clustered outside the *Didymella sensu stricto* clade in our study, were recombined by Chen et al. (2015) into alternative genera.

Within *Didymella sensu stricto, D. tanaceti* and *D. rosea* formed a strongly supported clade with *P. bellidis, P. senecionis* and *P. digitalis.* These *Phoma* spp. were recombined into the genus *Didymella* by Chen et al. (2015) as *D. molleriana* (syn: *P. bellidis*), *D. molleriana* (syn: *P. bellidis*) and *D. senescionicola* (syn: *P. senecionis*). As with *D. tanaceti* and *D. rosea*, *P. bellidis* and *P. senecionis* are pathogens of *Compositae* hosts, causing disease in *Bellidis* and *Senecio* spp., respectively (de Gruyter et al., 2009). In comparison, *P. digitalis* causes leaf spot on *Digitalis* spp. (*Scrophulariaceae*), but shares the characteristic of being a seed pathogen with *P. bellidis* and *D. tanaceti* (Pethybridge et al., 2006). In addition, gross culture morphology of *P. digitalis* on OA and MEA is consistent with that of *D. rosea*.

Despite causing similar symptoms in pyrethrum (Pethybridge et al., 2008), the relative isolation frequency of the two haplotypes varies substantially within infected fields, with *D. tanaceti* the predominately isolated pathogen (T. Pearce; unpublished data). The occurrence of both species in 2004 indicated that they may have been introduced into pyrethrum concurrently. The distinct morphological differences identified in this study between the

species will assist in pathogen identification and allow for more accurate frequency data of the two species to be collected. Identifying differences in virulence between the two species and the contribution of each to seed borne inoculum may assist in establishing the cause of the differential isolation frequency. Furthermore, studies are underway to elucidate the presence of a sexual morph and alternative hosts for both species. In addition, analysis of the amount of genetic diversity with *D. tanaceti* population is also currently underway. Characterising such aspects of the pathogens biology would help infer the potential future impact of the two species on pyrethrum production in Australia.

3.6 ACKNOWLEDGEMENTS

We thank Stacey Pilkington, Pattie Weichelt, Craig Palmer and Phil Gardam (Tasmanian Institute of Agriculture) for technical support. This project was funded by Botanical Resources Australia Agricultural Services Pty. Ltd. and the University of Tasmania's Australian Postgraduate Award and the Cuthbertson Elite Tasmania Graduate Research Scholarship, both awarded to the first author.

3.7 REFERENCES

Aveskamp M, De Gruyter J, Woudenberg J, Verkley G, Crous PW, 2010. Highlights of the *Didymellaceae*: A polyphasic approach to characterise *Phoma* and related pleosporalean genera. *Studies in Mycology* **65**, 1-60.

Benson DA, Clark K, Karsch-Mizrachi I, Lipman DJ, Ostell J, Sayers EW, 2015. GenBank. *Nucleic Acids Research* **43**, 30-5.

Berbee M, Pirseyedi M, Hubbard S, 1999. *Cochliobolus* phylogenetics and the origin of known, highly virulent pathogens, inferred from ITS and glyceraldehyde-3-phosphate dehydrogenase gene sequences. *Mycologia* **91**, 964-77.

Boerema GH, Gruyter JD, Noordeloos M, Hamers ME, 2004. *Phoma identification manual. Differentiation of specific and infra-specific taxa in culture*. Wallingford, United Kingdom: CABI Publishing.

Bonants P, Edema M, Robert V, 2013. Q‐bank, a database with information for identification of plant quarantine plant pest and diseases. *EPPO Bulletin* **43**, 211-5.

Borchsenius F, 2009. *FastGap 1.2* Department of Biological Sciences, University of Aarhus, Aarhus, Denmark.

Campbell V, Legendre P, Lapointe F-J, 2011. The performance of the Congruence Among Distance Matrices (CADM) test in phylogenetic analysis. *BMC Evolutionary Biology* **11**, article no.64.

Carbone I, Kohn LM, 1999. A method for designing primer sets for speciation studies in filamentous ascomycetes. *Mycologia* **91**, 553-6.

Carisse O, Bernier J, 2002. *Microsphaeropsis ochracea* sp. nov. associated with dead apple leaves. *Mycologia* **94**, 297-301.

Chen Q, Jiang JR, Zhang GZ, Cai L, Crous PW, 2015. Resolving the Phoma enigma. *Studies in Mycology* **82**, 137-217.

Crous PW, Hawksworth DL, Wingfield MJ, 2015. Identifying and naming plant pathogenic fungi: past, present, and future. *Annual Review of Phytopathology* **53**, 247-67.

Crous PW, Summerell BA, Swart L, *et al.*, 2011. Fungal pathogens of *Proteaceae*. *Persoonia: Molecular Phylogeny and Evolution of Fungi* **27**, 20-45.

Darriba D, Taboada GL, Doallo R, Posada D, 2012. jModelTest 2: more models, new heuristics and parallel computing. *Nature Methods* **9**, 772.

De Gruyter J, Aveskamp MM, Woudenberg JHC, Verkley GJM, Groenewald JZ, Crous PW, 2009. Molecular phylogeny of *Phoma* and allied anamorph genera: Towards a reclassification of the *Phoma* complex. *Mycological Research* **113**, 508-19.

Eberhardt U, 2010. A constructive step towards selecting a DNA barcode for fungi. *New Phytologist* **187**, 265-8.

Edgar RC, 2004. MUSCLE: multiple sequence alignment with high accuracy and high throughput. *Nucleic Acids Research* **32**, 1792-7.

Grdiša M, Carović-Stanko K, Kolak I, Šatović Z, 2009. Morphological and biochemical diversity of Dalmatian pyrethrum (*Tanacetum cinerariifolium* (Trevir.) Sch. Bip.). *Agriculturae Conspectus Scientificus* **74**, 73-80.

Hay FS, Gent DH, Pilkington SJ, Pearce TL, Scott JB, Pethybridge SJ, 2015. Changes in distribution and frequency of fungi associated with a foliar disease complex of pyrethrum in Australia. *Plant Disease* **99**, 1227-35.

Hoog GD, Ende A, 1998. Molecular diagnostics of clinical strains of filamentous *Basidiomycetes*. *Mycoses* **41**, 183-9.

Kass RE, Raftery AE, 1995. Bayes factors. *Journal of the American Statistical Association* **90**, 773-95.

Khater HF, 2012. Prospects of botanical biopesticides in insect pest management. *Pharmacologia* **3**, 641-56.

Kluger EK, Della Torre PK, Martin P, Krockenberger MB, Malik R, 2004. Concurrent *Fusarium chlamydosporum* and *Microsphaeropsis arundinis* infections in a cat. *Journal of Feline Medicine and Surgery* **6**, 271-7.

Lumbsch H, Lindemuth R, Schmitt I, 2000. Evolution of filamentous ascomycetes inferred from LSU rDNA sequence data. *Plant Biology* **2**, 525-9.

Ortiz-Ribbing L, Williams MM, 2006. Potential of *Phomopsis amaranthicola* and *Microsphaeropsis amaranthi*, as bioherbicides for several weedy *Amaranthus* species. *Crop Protection* **25**, 39-46.

Paradis E, Claude J, Strimmer K, 2004. APE: analyses of phylogenetics and evolution in R language. *Bioinformatics* **20**, 289-90.

Pethybridge S, Hay F, Groom T, 2003. Seasonal fluctuations in fungi associated with pyrethrum foliage in Tasmania. *Australasian Plant Pathology* **32**, 223-30.

Pethybridge SJ, Hay F, Jones S, Wilson C, Groom T, 2006. Seedborne infection of pyrethrum by *Phoma ligulicola*. *Plant Disease* **90**, 891-7.

Pethybridge SJ, Jones SJ, Shivas RG, Hay FS, Wilson CR, Groom T, 2008. Tan spot: A new disease of pyrethrum caused by *Microsphaeropsis tanaceti* sp. nov. *Plant Pathology* **57**, 1058-65.

R Core Team, 2014. *R: A language and environment for statistical computing V. 3.0.1* Vienna, Austria.: R Foundation for Statistical Computing.

Rayner RW, 1970. *A mycological colour chart*. Kew, United Kingdom: Commonwealth Mycological Institute.

Rehner SA, Samuels GJ, 1994. Taxonomy and phylogeny of *Gliocladium* analysed from nuclear large subunit ribosomal DNA sequences. *Mycological Research* **98**, 625-34.

Revell LJ, 2012. phytools: an R package for phylogenetic comparative biology (and other things). *Methods in Ecology and Evolution* **3**, 217-23.

Ronquist F, Huelsenbeck JP, 2003. MrBayes 3: Bayesian phylogenetic inference under mixed models. *Bioinformatics* **19**, 1572-4.

Sutton BC, 1971. *Coelomycetes: The Genus Harknessia, and Similar Fungi on Eucalyptus. IV*. Kew, United Kingdom: Commonwealth Mycological Institute.

Sutton BC, 1980. *The Coelomycetes. Fungi imperfecti with pycnidia, acervuli and stromata*. Kew, United Kingdon: Commonwealth Mycological Institute.

Swofford D, 2003. *PAUP*: phylogenetic analysis using parsimony, version 4.0 b10* Sunderland, Massachusetts: Sinauer Associates, Inc. Publishers.

Verkley G, Dukik K, Renfurm R, Göeker M, Stielow J, 2014. Novel genera and species of coniothyrium-like fungi in *Montagnulaceae* (*Ascomycota*). *Persoonia* **32**, 25-51.

Wang CY, Wang BG, Brauers G, Guan HS, Proksch P, Ebel R, 2002. Microsphaerones A and B, two novel γ-pyrone derivatives from the sponge-derived fungus *Microsphaeropsis* sp. *Journal of Natural Products* **65**, 772-5.

White TJ, Bruns T, Lee S, Taylor J, 1990. Amplification and direct sequencing of fungal ribosomal RNA genes for phylogenetics. *PCR Protocols: A Guide to Methods and Applications* **18**, 315-22.

Wickham H, 2007. Reshaping data with the reshape package. *Journal of Statistical Software* **21**, 1-20.

Wingfield MJ, De Beer ZW, Slippers B, *et al.*, 2012. One fungus, one name promotes progressive plant pathology. *Molecular Plant Pathology* **13**, 604-13.

Woudenberg J, Aveskamp M, De Gruyter J, Spiers A, Crous P, 2009. Multiple *Didymella* teleomorphs are linked to the *Phoma clematidina* morphotype. *Persoonia* **22**, 56-62.

Xiao X, Luo S, Zeng G, *et al.*, 2010. Biosorption of cadmium by endophytic fungus (EF) *Microsphaeropsis* sp. LSE10 isolated from cadmium hyperaccumulator *Solanum nigrum* L. *Bioresource Technology* **101**, 1668-74.

Xie WG, Lewis PO, Fan Y, Kuo L, Chen MH, 2011. Improving marginal likelihood estimation for Bayesian phylogenetic model selection. *Systematic Biology* **60**, 150-60.

Zeileis A, Wiel MA, Hornik K, Hothorn T, 2008. Implementing a class of permutation tests: The coin package. *Journal of Statistical Software* **28**, 1-23.

MATING-TYPE GENE STRUCTURE IN *DIDYMELLA TANACETI* AND THEIR SPATIAL DISTRIBUTION IN PYRETHRUM FIELDS

Tamieka L Pearce[a*], Jason B Scott[a], Frank S Hay[b], Sarah J Pethybridge[b]

[a]Tasmanian Institute of Agriculture, School of Land and Food, University of Tasmania, PO Box 3523 Burnie, Tasmania 7320, Australia; [b]Cornell University, School of Integrative Plant Science, Section of Plant Pathology and Plant-Microbe Biology, Cornell University, Geneva, NY 14456.

*Corresponding author: Tamieka.Pearce@utas.edu.au

Keywords: sexual reproduction, *MAT* genes, *Didymellaceae*, Multiplex-PCR, ascomycetes, tan spot.

This manuscript has been accepted for publication in *Phytopathology.*

Pearce T, Scott J, Hay F, Pethybridge S, *in press*. Mating-type gene structure in *Didymella tanaceti* and their spatial distribution in pyrethrum fields. *Phytopathology*. Doi: 10.1094/PHYTO-01-16-0038-R

FINE SCALED POPULATION GENETIC ANALYSIS OF *DIDYMELLA TANACETI*

Tamieka L. Pearce[a*], Jason B. Scott[a], Frank S. Hay[b], Sarah J. Pethybridge[b].

[a]Tasmanian Institute of Agriculture, School of Land and Food, University of Tasmania, PO Box 3523 Burnie, Tasmania 7320, Australia; [b]Cornell University, School of Integrative Plant Science, Section of Plant Pathology and Plant-Microbe Biology, Cornell University, Geneva, NY 14456.

*Corresponding author: Tamieka.Pearce@utas.edu.au

Keywords: Didymellaceae, high resolution melt, microsatellite development, population genetics, clonal organisms.

5.1 ABSTRACT

Fine scale population analysis of *Didymella tanaceti*, the causal pathogen of tan spot in pyrethrum in Australia, was undertaken using SSR markers and mating-type data. Eight newly designed, polymorphic SSR markers were used to genotype 317 isolates collected in 2012 from two fields in each of Sassafras and Table Cape in Tasmania, Australia. Alleles were discriminated using real-time PCR and high resolution melt analysis. The presumed asexual pathogen, exhibited high average genetic (*uh* = 0.49) and genotypic diversity (*D* = 0.95) within field populations, suggesting individuals have a high adaptive ability. Following clone correction, the mating-type ratios in each field did not significantly deviate from a 1:1 ratio. Even with clone correction, significant linkage disequilibrium was detected in three of the four fields. However, historical gene flow between the isolates of the two mating-types in each field was identified. These results suggested infrequent recombination as part of a mixed mode of reproduction. A large number of multilocus genotypes (MLGs) (*n* = 127) were identified and 50.4% of individuals were contained within 15 MLGs. Of the 45 recurrent MLGs only 20 were found in both Sassafras and Table Cape and 3 found in all four fields. Despite many unique MLGs, there was no genotypic spatial structure at the regional or field scale. Furthermore, spatial autocorrelation analysis indicated no evidence of localised plant to plant spread of genotypes within fields. Similar allele frequencies for each SSR loci were observed in each field and only three private alleles were identified at the field scale, with each only occurring in a single isolate. Evidence of high levels of historical genotypic migration between fields was also detected. These results suggested that the *D. tanaceti* individuals within these populations may have originated from a common genetic source, such as an alternative host or a seed crop. They further suggest that a combination of additional factors, such as high levels of seed borne inoculum, fungicide resistance and/or

increased virulence (derived from the high adaptive potential) may have also contributed to the rapid increase in tan spot incidence.

5.2 INTRODUCTION

Pyrethrum (*Tanacetum cinerariifolium* (Trevir) Sch.Bip) is a perennial *Asteraceae* grown commercially for the extraction of chemical esters called pyrethrins. Pyrethrins, which have insecticidal properties, are concentrated within oil glands on the seed. Australia currently leads global pyrethrum production from approximately 3,000 ha in Tasmania and Victoria. Fields are sown in spring (September to November) from seed. Plants then undergo a juvenile-like growth stage for 6 to 8 months until the following winter (June to August) provides conditions for vernalisation and subsequent bud initiation (Brown & Menary, 1994). Daisy-like flowers are produced on multiple stems per plant annually in late spring to summer (November to December) every year thereafter. Crops often yield two to four annual harvests. Stems are cut and placed in windrows after natural plant senescence, which is followed by seed harvest and pyrethrin extraction.

Tan spot is the most significant foliar disease of pyrethrum in Tasmania (Hay et al., 2015, Pethybridge et al., 2008b). The disease is caused predominately by the ascomycete *Didymella tanaceti* (syn: *Microsphaeropsis tanaceti*) (Pearce, Chapter 3, Pethybridge et al., 2008b) which was first associated with necrotic leaf, stem and bud lesions in 2001 (Pethybridge et al., 2003). Tan spot epidemics typically occur in spring, however temporal shifts associated with high disease prevalence and intensity throughout autumn and winter

have also been observed (Hay et al., 2015, Pethybridge et al., 2008a, Pethybridge et al., 2008b).

Knowledge of the genetic structure of *D. tanaceti* populations is limited, and genetic diversity studies have not been undertaken. However, *D. tanaceti* isolates with reduced sensitivities to fungicides containing difenoconazole and boscalid have been identified (Hay et al., 2015, Pethybridge et al., 2008b). This suggested that *D. tanaceti* field populations may have an increased genetic adaptive potential. Furthermore, a large increase in the number of *D. tanaceti* isolates with insensitivities to boscalid was observed between 2009 and 2011. Therefore, the pathogen population may be rapidly evolving, with a high mutation rate and/or utilises mechanisms which allow rapid distribution of resistance genotypes (Hay et al., 2015).

No sexual stage has been observed for *D. tanaceti*, though related *Didymella* spp. have described sexual stages (Chen et al., 2015). Analysis of *D. tanaceti* for molecular signs of sexual reproduction identified the pathogen as a putative heterothallic species. The *MAT1-1-1* and *MAT1-2-1* genes occupied the same chromosomal position in different isolates (Pearce, Chapter 4). Analysis of the *MAT* gene sequences indicated the two *MAT* genes were functional and may be under selection. However, two *MAT1-1-1* haplotypes (I and II) have been observed which shared 99.6% sequence homology (Pearce, Chapter 4). Field population studies identified equal proportions of *MAT1-1* and *MAT1-2* isolates in fields. Despite these occurrences, the sexual morph of *D. tanaceti* has not been observed or successfully produced *in vitro* (Pearce, Chapter 4). Thus, a primarily asexual reproductive mode was hypothesised for *D. tanaceti*.

Characterising and analysing the amount of genetic variability in *D. tanaceti* field populations would provide an indication of the occurrence and frequency of sexual events in *D. tanaceti*. This may include identifying the level of clonality and genetic relationships between individuals, the occurrence of genetic recombination and the genetic structure and gene flow among populations. Furthermore, knowledge of the structure of genetic diversity of *D. tanaceti* within populations may be of benefit to the pyrethrum industry to estimate the adaptive ability of individuals. This study aimed to analyse the amount and structure of genetic diversity within populations of *D. tanaceti* isolates collected from four geographically separated 12 month old crops. Furthermore, as the mating-type of these isolates were known, it aimed to analyse the amount and structure of genetic diversity in populations of each mating-type to identify evidence of sexual reproduction. For analysis of diversity, a set of polymorphic microsatellite (SSR) markers for *D. tanaceti* were developed.

5.3 MATERIALS AND METHODS

5.3.1 Population sampling

A population of *D. tanaceti* was collected in July/August 2012 from two fields in each of Sassafras, Tasmania, Australia (41° 17' South, 146° 30' East) (S1 and S2), and Table Cape, Tasmania, Australia (40° 56' South, 145° 43' East) (TC1 and TC2). The two regions were separated by ~70 km. The two fields in each of Sassafras and Table Cape were separated by 5.2 and 1.4 km, respectively. The fields were sown between August and October 2011 with seed harvested from four different pyrethrum seed crops. Field S1 was sown with a different pyrethrum variety than S1, TC1, and TC2. Sampling was structured to allow spatial analyses,

with two parallel 50 m transects in each field. Fungal isolations from single lesions on each of four leaves collected from an individual pyrethrum plant at 0.5 m intervals along each transect were undertaken as described by Pearce (Chapter 4). A single *D. tanaceti* culture was randomly selected per sampling unit and stored at -80°C.

5.3.2 DNA extraction of isolates

For extraction of genomic DNA, the isolates were recovered from -80°C onto potato dextrose agar (PDA; Amyl Media) and incubated in the dark at 21°C for 7 d. Petri plates containing ~20 mL of 2% (*w/v*) malt extract broth (MEB; Oxoid Ltd.) were inoculated with mycelium scrapped from the top of the growing cultures and incubated at ~20°C on an orbital shaker (54 rpm) for 12 d. The mycelial mats were blotted with sterile paper towel and ground in liquid nitrogen. DNA was extracted from the ground mycelia using the DNeasy Plant Mini Kit (QIAGEN), quantified using a High Sensitivity Double Stranded DNA QUBIT kit (Life Technologies) and used as the template for polymerase chain reaction (PCR).

5.3.3 Mating-type of isolates

The mating-type of each isolate in the 2012 collected population was determined previously by Pearce (Chapter 4) using a *MAT*-specific multiplex PCR assay. The two identified haplotypes of *MAT1-1-1* were differentiated using a restriction enzyme digestion.

5.3.4 Multilocus genotyping

The open source C++ library QDD v1.3 (Meglécz et al., 2010, Rozen & Skaletsky, 2000) was used to screen 135,404 sequences (average length: 413 base pair (bp)) of *D. tanaceti* genomic DNA produced from high throughput DNA shotgun 454 sequencing (Pearce, Chapter 4) for SSR loci. Putative loci, containing di- to tetra- repeat motifs and a minimum of 5 repeats in the sequence data were selected. Primer 3 (Meglécz et al., 2010, Rozen & Skaletsky, 2000) was used to designed PCR primers to flank the loci and amplify markers with a product size < 290 bp.

A test population of *D. tanaceti* (*n* = 35; Table 5.1) collected from fields in Tasmania between 2004 and 2014 was used to evaluate the markers. Genomic DNA was extracted from the isolates as described previously. Each marker was analysed using real-time PCR followed by high resolution melt (HRM) analysis to confirm consistency in amplification and to identify polymorphic loci. Real-time PCR and HRM were undertaken in a Rotor-Gene Q real-time PCR machine (QIAGEN). Reaction mixes (10 µL) contained 2 × Type-it HRM buffer (QIAGEN), 0.7 µM of each primer and 2 ng of genomic DNA. Reaction conditions were an initial denature of 5 min at 95°C, followed by 40 cycles of denaturation at 95°C for 10 s, annealing at 55°C or 57°C for 30 s and extension at 72°C for 10 s. Amplified products were subjected to HRM using 0.01°C increments from 65°C to 95°C with a 10 s hold at each temperature prior to data acquisition. Samples were run in duplicate.

Runs from each marker were analysed in the Rotor Gene ScreenClust HRM software v1.10.1.2 (QIAGEN) (Reja et al., 2010). The raw melt data was analysed to confirm the amplification of only a single product. The data was normalised within regions spanning 1°C

prior to and following the melt curve transition. An "unsupervised" analysis was used to partition the data into clusters (Reja et al., 2010). To verify that individuals within each identified cluster had unique melt profiles, indicating polymorphisms, melt analysis of the data was also undertaken using the Rotor-Gene Q Series software (QIAGEN). For each marker, the SSR loci of representative isolates of each cluster were sequenced to identify if the variation detected was due to polymorphisms within the SSR loci. PCRs for loci sequencing were performed in a C1000 thermocycler (BioRad). PCR mixtures contained 1 × TopTaq polymerase (QIAGEN), 1 × PCR buffer, 1 × CoralLoad, 1.5 mM $MgCl_2$, 0.7 µM of each primer, 200 µM of each dNTP (Bioline) and 3 ng of DNA. PCR amplification included denaturation at 94°C for 3 min, followed by 30 cycles of denaturation at 94°C for 15 s, annealing at 55°C for 15 s and extension at 72°C for 20 s, followed by 72°C for 5 min on the final cycle. Amplified products were analysed by gel electrophoresis in a 1.5% (w/v) agarose gel containing GelRed® (Biotium Inc.) in 1 × TAE buffer. Products were prepared for sequencing using the UltraClean PCR Clean-Up kit (Mo Bio Laboratories Inc.). The amplicons were sequenced in one direction with a single primer to provide coverage of the SSR loci, at the Australian Genome Research Facility (AGRF; Melbourne, Australia) using Big Dye Terminator v3.1 chemistry and capillary separation on an AB 3730xl DNA Analyser (Applied Biosystems Inc.). Sequences for each marker were aligned using MAFFT v7.017 (Katoh et al., 2002) in Geneious v7.1.0 (Biomatters Ltd.) to identify polymorphisms in the number of SSR repeats (Fig. 5.1).

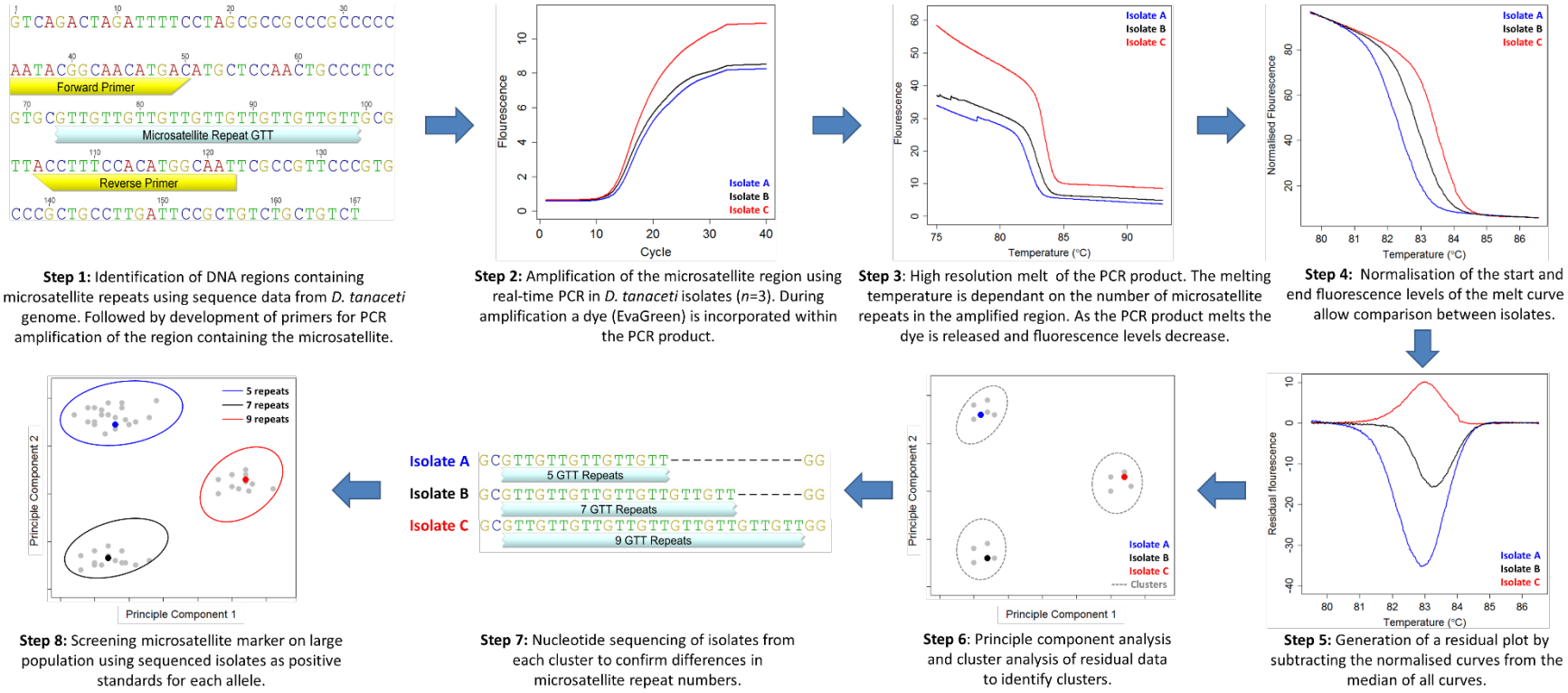

Step 1: Identification of DNA regions containing microsatellite repeats using sequence data from *D. tanaceti* genome. Followed by development of primers for PCR amplification of the region containing the microsatellite.

Step 2: Amplification of the microsatellite region using real-time PCR in *D. tanaceti* isolates (*n*=3). During amplification a dye (EvaGreen) is incorporated within the PCR product.

Step 3: High resolution melt of the PCR product. The melting temperature is dependant on the number of microsatellite repeats in the amplified region. As the PCR product melts the dye is released and fluorescence levels decrease.

Step 4: Normalisation of the start and end fluorescence levels of the melt curve to allow comparison between isolates.

Step 5: Generation of a residual plot by subtracting the normalised curves from the median of all curves.

Step 6: Principle component analysis and cluster analysis of residual data to identify clusters.

Step 7: Nucleotide sequencing of isolates from each cluster to confirm differences in microsatellite repeat numbers.

Step 8: Screening microsatellite marker on large population using sequenced isolates as positive standards for each allele.

Fig. 5.1. Workflow diagram of microsatellite marker development in *Didymella tanaceti*.

5.3.5 Population screen with selected SSR markers

Eight polymorphic SSR markers, of which the loci were able to be differentiated via HRM and cluster analysis (Table 5.2), were used to genotype the *D. tanaceti* population collected in 2012 (n = 317). Real-time PCR was as previously outlined, with the exception of only 35 amplification cycles used. HRM used a melting increment of 0.1°C and specific melting ranges for each marker (Table 5.2). Representative isolates for each known allele (known-genotype) from the test population were included in each run for each marker. To allow individual runs for each marker to be analysed concurrently, three replicates of a control isolate were also included in each run as standards.

5.3.6 HRM allele calling

Prior to analysis, the raw fluorescence data of each run was examined in the Rotor-Gene Q Series software to detect isolates with poor amplification or abnormalities in the amplification or melt curves (Qiagen, 2014). Identified isolates were removed from further analyses and real-time PCR and HRM repeated. Analysis of the data for allele assignment was undertaken in R v3.1.0 (R Core Team, 2014). The raw fluorescence melt data was extracted from the HRM file using the R package *XML* (Lang, 2015). For each run, the raw fluorescence HRM data of each isolate was normalised by applying curve scaling to a line of best fit (LOBF) (Reja et al., 2010). The range of the normalisation regions used to fit the LOBF prior to and following the melt curve transition varied for each marker (Table 5.2). These regions were selected following analysis of varying combinations of normalisation regions spanning 0.5 to 2.0°C. Selection was based on the range that best grouped the known-genotype isolates for each marker into discrete clusters. The normalized melt curve of each isolate was differentiated to accentuate the rate of change. Within each run, the three replicates of the

control isolate were used to calculate a composite average normalised control curve. The composite average normalised control curve was subtracted from each of the individual normalized, differentiated isolate curves to produce residual data for each isolate. For each marker the residual data from all the isolates in each run were combined and analysed concurrently using principal components analysis (PCA) and partitioning around medoids (PAM) (Sergios & Konstantinos, 2006, Kaufman & Rousseeuw, 1987) for allele discrimination.

The initial analysis for allele discrimination used an "unsupervised" mode to identify any new putative genotypes. Known-genotype samples were utilised as "pseudo-unknowns" in each run to confirm correct identification in the combined data set. For each marker, a euclidean distance matrix was computed from the residual data of all isolates. The number of clusters used to partition the data was estimated based on the distance matrix, via PAM and 100 Monte Carlo bootstraps, using the Gap statistic computed with the *clusGap* function in the package *Cluster* (Maechler et al., 2015). Representative isolates of any previously unidentified clusters or outliers to clusters were selected and the SSR loci sequenced, as described previously, to confirm any putative new alleles. These individuals were then employed as known-genotype isolates in the subsequent analysis.

A "supervised" mode of cluster analysis was subsequently undertaken using a PAM based clustering. The number of medoids used to cluster the data was equal to the number of known alleles for each marker. Principal component analysis was performed using the function *princomp* on the euclidean distance matrix, calculated from the residual data.

Table 5.1. *Didymella tanaceti* isolates included in the test population for microsatellite marker selection.

Isolate[a]	Year collected	Origin[b]
TAS 041-0042	2004	Forth
TAS 041-0050	2004	Montumana
TAS 041-0047	2004	Penguin
BRIP 61992	2004	Penguin
TAS 041-0049	2004	Montumana
TAS 041-0079	2004	Table Cape
TAS 041-0064	2004	Table Cape
BRIP 61999	2005	Kindred
TAS 041-0071	2005	Sassafras
TAS 041-0073	2005	Wesley Vale
TAS 041-0076	2005	Sassafras
TAS 041-0052	2005	Table Cape
TAS 041-0054	2005	Wynyard
TAS 041-1350	2009	Don
TAS 041-1340	2009	Forth
TAS 041-1333	2009	Howth
TAS 041-1332	2009	Penguin
TAS 041-1343	2009	Burnie
TAS 041-1344	2009	Wesley Vale
TAS 041-1341	2009	Don
TAS 041-1348	2009	Wesley Vale
BRIP 61994	2009	Penguin
TAS 041-0010	2010	Don
TAS 041-0025	2010	Penguin
TAS 041-0032	2010	Penguin
TAS 041-0003	2010	Howth
BRIP 61993	2010	Wesley Vale
TAS 041-0014	2010	Wesley Vale
TAS 041-0020	2010	Wesley Vale
TAS 041-0001	2010	Don
TAS 041-0028	2010	Kindred
TAS 041-0038	2010	Table Cape
BRIP 61988	2012	Sassafras
BRIP 61990	2012	Sassafras
BRIP 61991	2012	Table Cape

[a] TAS: Tasmanian Institute of Agriculture fungal collection, Tasmania, Australia; BRIP: Queensland Plant Pathology herbarium collection, Brisbane, Australia.
[b] Region in Tasmania, Australia.

Table 5.2. Microsatellite (SSR) primers sequences and conditions for amplification and analysis used in this study.

SSR	Primer sequence (5'– 3')	Amplicon length (base pair)	Motif	Annealing temperature (°C)[a]	Melting temperature (°C)[b]	Normalisation regions		SSR repeats observed
						Left boundary (°C)[c]	Right boundary (°C)[d]	
SSR05	F: ATGCCTTGTGGATCTCGACT R: GTGACTGTGCCGCTATCTGA	142 – 160	TCG	55	78 – 92	82.0 – 82.5	88.0 – 89.0	7, 10, 11, 13
SSR32	F: ATTGCTCGACTGGAAAGCAT R: TGGGCATAACCTCTCGAATC	190 – 199	TTG	55	80 – 92	83.5 – 84.5	88.0 – 89.0	5, 7, 8
SSR62	F: CAAGTCTGCTGGTCTTGCAC R: CTGCGACTCGTATCCTTGGT	242 – 257	CAG	55	80 – 92	83.5 – 84.5	88.5 – 89.5	6, 8, 9, 11
SRR64	F: CCAGGTGCAGATGTCCCC R: TCGTATGCTACACGAATCGC	109 – 124	GCA	55	81 – 93	84.0 – 85.0	90.0 – 91.0	8, 9, 13
SSR53	F: GTCGGCTTGGCTCATGTAGT R: GTCCCCAGCAACACATTGAT	77 – 86	TGC	55	77 – 92	81.0 – 82.5	88.5 – 89.5	7, 8, 10
SSR54	F: GTGCAATACGGCAACATGAC R: GAATTGCCATGTGGAAAGGT	107-143	TTGC	55	76 – 92	79.5 – 80.5	89.5 – 90.5	6, 7, 9, 10, 13
SSR58	F: AGTCGTTCTGATACGTGCCC R: ACTTCTCCATGTACCACGCC	252 – 315	GCT	55	84 – 95	85.5 – 86.5	93.0 – 94.0	5, 7, 13, 26
SSR44	F: GGTCGGACATGACGACTG R: GCGACTGTCAGGCAGTGA	152 – 158	AGC	57	87 – 95	88.5 – 89.5	93.0 – 93.5	8, 9, 10

[a] Annealing temperature used for real-time PCR.
[b] Melt range temperature used for high resolution melt (HRM) of real-time PCR products.
[c] Left boundary temperature range for normalisation of HRM fluorescence data.
[d] Right boundary temperature range for normalisation of HRM fluorescence data.

The PCA scores of the known-genotype isolates for each allele were analysed and the isolate whose average PCA scores dissimilarity to each of the other known-genotype isolates of that allele was the smallest was selected as the medoid for that allele. The distance between each isolate and the selected medoids for each allele was calculated by squaring the difference between the PCA scores of each isolate and the PCA scores of each of the selected medoids. Each of these obtained PCA scores were then weighted according the proportion of variance obtained from each PCA score, summed and square rooted to obtain final distance measurements between each isolate and the selected medoids for each allele. For each isolate the closest medoid was selected as the allele of that isolate. For some alleles, variation in the distribution of isolates within clusters required the inclusion of multiple medoids per alleles to cluster all the known-genotype isolates correctly. The majority of the additional medoids were chosen to be located around cluster boundaries to allow clear separation of allele clusters. In addition, where necessary, visual examination of the residual plots and HRM melt peak curves was used to assist allele calls. Isolates which bordered between two clusters and had similar distance to two medoids were re-amplified and analysed in additional runs and/or the SSR loci of these isolates was sequenced and the isolate used as additional known-genotype isolates in analyses.

5.3.7 Genotypic data analysis

The hierarchal sampling method imposed for the collection of the 2012 *D. tanaceti* isolates resulted in two regional populations (Sassafras and Table Cape), which were further differentiated as four field populations (S1, S2, TC1 and TC2). For analysis of population diversity statistics and gene flow the *MAT1-1* and *MAT1-2* isolates in each region and/or field were also examined and compared. Due to the low number of *MAT1-1* isolates of the second

haplotype (*MAT1-1* (II)) within the populations *(n* = 5; Supplementary Table 5.1), only *MAT1-1* haplotype I isolates (*MAT1-1* (I)) were included in these analyses. However, for the calculation of the minimum spanning network (MSN), both *MAT1-1* haplotypes were included.

Within each population, two data sets were generated for analysis. The first contained all isolates within each population (uncorrected data set). The second data set was constructed to minimise bias introduced by the clonality observed in the uncorrected data set. Isolates with the same combination of alleles at each locus (genotype) and the same mating-type were considered to be clones. The clone corrected dataset included one member of each MLG for each mating-type by population.

5.3.7.1 SSR marker diversity

For each SSR locus, the number and frequency of alleles in each uncorrected population was calculated. Private alleles (found in only one population) were also identified. Furthermore, for each locus the polymorphic informative content (PIC) (Botstein et al., 1980) and the effective number of alleles (ENA) (Kimura & Crow, 1964) were calculated for the overall uncorrected dataset in R. The PIC was defined as $1-\text{sum}((Ai)^2)$ and ENA as $1/\text{sum}((Ai)^2)$; where Ai is the frequency of the i^{th} allele of the locus.

5.3.7.2 Population diversity

For the overall uncorrected and clone corrected populations the clonal fraction was calculated as 1- (*nMLG*/*N*); where *nMLG* was the number of MLGs and *N* was the number of samples in the population (Zhan et al., 2003). Nei's unbiased gene diversity (*uh*) was calculated for the uncorrected and clone corrected regional and field populations, and the overall datasets by weighting Nei's genetic diversity (*h)* by sample size (Nei, 1973) in GenAlEx v6.5 (Peakall & Smouse, 2006, Peakall & Smouse, 2012). This index is the probability that at a given locus, two randomly drawn alleles from the gene pool are identical. Multilocus genotypic diversity indices were calculated for the uncorrected regional and field populations, and the overall dataset using the R program *Poppr* v2.0 (Kamvar et al., 2015, Kamvar et al., 2014). The number and frequency of each MLG within each population was calculated. To account for differences in samples sizes and allow comparisons between the populations, the number of expected genotypes (eMLG = genotypic richness (*R*)) in each population corresponding to the smallest sample size (*n*) of all populations being compared, was approximated based on rarefaction curves using 1,000 bootstrapped samples (Grunwald et al., 2003). To evaluate the distribution of genotypes within each population, genotypic evenness was calculated using the index, E_5 (Ludwig & Reynolds, 1988). E_5 converges to 0 when a population consists of a single genotype and is equal to 1 when all genotypes occur at the same frequency (Ludwig & Reynolds, 1988). Genotypic diversity was calculated using Simpson's index (*D*) (Simpson, 1949), which estimates the probability that two randomly selected individuals would have a different MLG, and Stoddard and Taylor's index (*G*) (Stoddart & Taylor, 1988). To compare the genotypic diversity indices (*D* and *G*) within populations of different sizes, the indices were estimated following random subsampling of the data using rarefaction in *Poppr* with 1,000 jack-knife replicates. The number of samples drawn in each replicate was equal to the smallest sample size of all populations being compared. In addition, genetic diversity and the

multilocus genotypic indices were calculated and compared for the *MAT1-1* (I) and *MAT1-2* isolates in each regional and field population and the overall dataset.

5.3.7.3 Analysis of random mating

To test if the recurrent MLGs in the field populations originated independently from sexual reproduction, GENCLONE v2.0 (Aranud-Haond & Belkhir, 2007) was used to calculate the probability of observing *n* copies of a MLG in a sample of size *N*, (P_{sex}), for each recurrent MLG (significance determined at $P_{sex} < 0.05$). For the purpose of this analysis, clonality referred to all members of a MLG originating asexually from a common ancestor (Gregorius, 2005). As individuals with the same MLG, but different mating-type genes have not originated from the same common ancestor, MLGs were calculated with the inclusion of the mating-type data for this analysis. If P_{sex} of a multi-copy MLG at $n = 2$ was significant, then all copies of that MLG could be considered to be the product of clonal reproduction. If P_{sex} was significant for some $n > 2$, then the hypothesis that more than n-1 clones exist within n copies of that MLG could be rejected (Gregorius, 2005).

Multilocus linkage disequilibrium was tested using the standardized index of association ($\bar{r}_d$) (Agapow & Burt, 2001), implemented using *Poppr*, for the regional and field populations, using both the uncorrected and clone corrected data sets. A null distribution of values expected for a randomly mating population was calculated from 9,999 permutations. Significance of the obtained $\bar{r}_d$ value was determined from a one-sided *P* value under a null hypothesis of random association of alleles. Linkage disequilibrium between loci pairs was tested under a null hypothesis of independent allele association between loci using an exact *G*

test (Fisher's test) procedure implemented in GENEPOP v4.6 (Rousset, 2008). Markov chain parameters included 10,000 dememorization steps, 1,000 batches, and 5,000 iterations per batch. To adjust the resulting *P*-value distribution for multiple tests, the false discovery rate (FDR) procedure (Benjamini & Hochberg, 1995) was implemented in *R*.

5.3.7.4 Population structure and differentiation

Analysis of molecular variance (AMOVA) was conducted to determine the partitioning of genetic variation between and within the two regional and four field populations (Excoffier et al., 1992) for the uncorrected and clone corrected datasets using GenAlEx. In addition, partitioning of genetic variation between and within the two mating-type populations was also examined. For analysis of the mating-type populations, the haplotype II *MAT1-1* isolates were excluded. The distance matrices were constructed using the haploid-SSR distance calculation, which assumes as stepwise mutation model. Significance of differentiation between populations was tested using a null distribution of variance (i.e. a random population) computed from 9,999 random permutations of the sample matrices (Excoffier et al., 1992).

To identify clusters of similar genotypes within the field transects, spatial autocorrelation (Smouse & Peakall, 1999) was performed with the uncorrected field datasets in GenAlEx. Geographic and genetic distance matrices, summed over all loci under the assumption of independence, were calculated for all pairs of isolates within the two 50 m transects within each field. For each field, multiple analyses were performed using even distance classes of sizes ranging from the minimum to the maximum distance of sampling. A correlation coefficient, *r*, between linear genetic and geographic distances was calculated for all pairs of

isolates within the geographic distance classes and 95% confidence intervals of *r* calculated from 999 bootstrap replicates. Permutations (n = 999) were used to generate 95% confidence intervals about the null hypothesis of no spatial structure by random shuffling of all individuals among the geographical locations. For each distance class, *r* was considered statistically significant if it exceeded the 95% confidence interval around the null hypothesis and if the 95% confidence intervals around *r* did not intercept 0. To assess the effect of the different distance classes on spatial autocorrelation, isolates were pooled into successively larger classes (e.g. 0 – 1, 0 – 2, 0 – 5 m etc.) and the results of the first distance bin of each plotted as a composite graph.

To determine if significant relationships existed between the genetic and physical distance of isolates within transects, Mantel tests for matrix correspondence (Mantel, 1967, Smouse et al., 1986) were conducted in GenAlEx. The correlation coefficient, R_{xy}, was calculated and *P* values determined by comparison to the frequency distribution produced from 999 random permutations.

A MSN was conducted to evaluate the relationship between MLG groups and population structure with respect to fields and the mating-type of isolates. A MSN was constructed on the overall uncorrected dataset based on Bruvo's distance (Bruvo et al., 2004). Bruvo's method uses a stepwise mutation model to calculate genetic distance of the individuals using microsatellite data. The MSN was implemented using *Poppr* with reticulation to allow population structure to be more readily detectable (Kamvar et al., 2015).

5.3.7.5 Gene flow

Gene flow among fields was estimated by performing a maximum likelihood based analysis in Migrate-N v3.1.11 (Beerli, 2009, Beerli & Felsenstein, 2001) to estimate Θ (the number of *D. tanaceti* immigrants per generation), *M* (mutation-scaled immigration rate), and the amount and direction of gene flow between the four fields. The mutation rate for each locus was estimated from the data, as opposed to assuming a constant rate for each locus. A continuous Brownian motion model was used and each field was able to send and receive migrants. Data was analysed using 10 short chains with 1,000 samples and 20 sampling increments and 3 long chains with 10,000 samples and 20 sampling increments. Static heating was active and the default program temperatures were used. Three independent runs were conducted and the estimates of Θ and *M* presented as the mean and range of means from the three runs. In addition, within each field gene flow between isolates of the two mating-types was also estimated.

5.4 RESULTS

5.4.1 SSR marker diversity

Twenty seven SSR markers were screened against the test population of *D. tanaceti* isolates collected between 2004 and 2012. Sixteen markers did not contain variation in the number of SSR loci repeats. However, six of these markers contained single nucleotide polymorphisms (SNPs) adjacent to the SSR loci which were able to be detected using HRM. Of the eleven markers with variability in the number of SSR repeats, the alleles of two markers could not be differentiated via HRM, and one contained variation in only one isolate of the test

population. Marker SSR54, which was polymorphic, also contained a SNP adjacent to the SSR motif. However, combinations of this SNP with each of the SSR alleles were able to be identified via HRM analysis and therefore this marker was able to be included for analysis of the populations. The SNP was not included in any subsequent analyses.

A total of 317 *D. tanaceti* isolates were genotyped from the 2012 population with the eight microsatellite markers (Table 5.3). Within each population all markers were polymorphic, with the number of alleles per locus ranging from 3 to 5 and averaging 3.62 (Table 5.2; Fig. 5.2). The PIC averaged 0.50 across all markers and ranged from 0.32 to 0.62 (Fig. 5.2. The ENA for each marker ranged from 1.47 to 2.65 and averaged 2.04 (Fig. 5.2). Four private alleles were identified (Supplementary Table 5.1). For marker SSR05, an allele consisting of ten repeats was only found in the Sassafras population, but occurred in both field S1 and S2 (Supplementary Table 5.1). Private alleles consisting of only single isolates were also identified for markers SSR62 (6 repeats) and SSR64 (13 repeats) in S1 and SSR05 (13 repeats) in S2. No additional private alleles were identified when the *MAT1-1* (I) and *MAT1-2* isolates of the field, region and overall populations were examined (Supplementary Table 5.1).

5.4.2 Population diversity

Within the overall uncorrected dataset 127 MLGs were identified, resulting in 59.9% clonality. Of these, 63 and 44 MLGs were unique to the Sassafras and Table Cape populations, respectively. Eighty two of the 127 MLGs (63.8%) were singleton (Table 5.3). A number of predominate MLGs were identified, with 32.4% of isolates contained within six

MLGs and 50.4% contained within fifteen MLGs. Within each region only thirteen and eleven MLGs occurred within both fields at Sassafras and Table Cape, respectively (Fig. 5.3a & 5.3b). Additionally, only three MLGs (MLG 28, MLG 61 and MLG 116) were found in each of the four fields (Fig. 5.3a & 5.3b). The clone corrected dataset contained 145 MLGs, resulting in 54.3 % clonality (Table 5.3). The majority of the 45 recurrent MLGs consisted solely of *MAT1-1* (I) isolates (14 MLGs) or *MAT1-2* isolates (13 MLGs) (Fig. 5.3a & 5.3b). These included three of the dominant MLG groups (MLG 61, MLG 58 and MLG 118; Fig. 5.3a & 5.3b). Singleton MLGs were identified for each of the 5 *MAT1-1* (II) isolates.

Gene diversity (*uh*) was high and ranged from 0.47 to 0.52 and 0.50 to 0.56 for the uncorrected and clone corrected population datasets, respectively. The number of MLGs in each uncorrected population increased with sample size (Table 5.3). Comparison of richness using rarefaction, indicated that based on a population size of 142 (e$MLG_{n=142}$) the Sassafras population had higher richness (71.9) than the Table Cape population (64.0) (Table 5.3). However, genotypic diversity ($G_{n=142}$) and evenness (E_5) were higher in the Table Cape population (Table 5.3). Genotypic diversity based on Simpson's index (*D*) was slightly higher in the Table Cape population (0.96) than for the Sassafras population (0.97) (Table 5.3). Comparison of the four fields based on a sample size of 42, identified even richness ($eMLG_{n=42}$) in the two fields in Table Cape (27.3 and 27.0), while fields S1 and S2 at Sassafrass had the highest (29.6) and lowest (24.7) richness of the four fields, respectively. Evenness (E_5) was similar for the two fields in each region, but was higher for the two fields at Table Cape (0.75 and 0.77; Table 5.3) than for the two fields at Sassafras (0.62 and 0.67; Table 5.3). Genotypic diversity based on $G_{n=42}$ was similar in S1 (20.2) and TC1 (20.0), but

was lower for S2 (14.6) and TC2 (17.3) (Table 5.3). However, genotypic diversity based on $D_{n=42}$ was very similar for all four fields and ranged from 0.93 to 0.95.

The number of MLGs identified for the *MAT1-1* (I) and *MAT1-2* isolates in each regional and field population was similar, and also represented the number of *MAT1-1* (I) and *MAT1-2* isolates in the clone corrected dataset. Comparison of the *MAT1-1* (I) and *MAT1-2* isolates in each regional and field population identified private MLGs which were only found in *MAT1-1* (I) and *MAT1-2* isolates (Table 5.4; Fig. 5.3a & 5.3b). A similar number of isolates with singleton MLGs were identified for *MAT1-1* (I) and *MAT1-2* isolates in each regional and field population. Evenness (E_5) varied for the *MAT1-1* (I) and *MAT1-2* isolates across each of the populations, but was generally consistent for the *MAT1-1* (I) and *MAT1-2* isolates in each population. However, the *MAT1-1*(I) isolates in Table Cape and TC2 had higher evenness (0.80 and 0.95) than the *MAT1-2* isolates (0.68 and 0.75). In all the fields, except S1, the *MAT1-1* (I) isolates had higher genotypic diversity (when comparing populations of equal size), evenness and lower gene diversity than the *MAT1*-2 isolates, though some of the differences were minimal (Table 5.4).

5.4.3 Analysis of random mating

The inclusion of the mating-type data for the calculation of MLG groups in each field, for analysis of P_{sex} resulted in 70, 37, 52 and 29 MLGs for S1, S2, TC1 and TC2, respectively (Table 5.3). Of these, 13, 11, 16 and 6 MLGs were recurrent for each field, respectively, and used to analyse P_{sex}. A clonal origin was only supported for isolates within 4, 2, 3 and 2

MLGS within each field, respecitevly ($P < 0.05$ at $n = 2$). The isolates in the remaining recurrent MLGs were supported to be derived from more than 1 ancestor ($P < 0.05$ at $n > 2$).

Analysis of a multi-locus disequilibrium in both the uncorrected and clone corrected data sets for each of the regional and field populations resulted in rejection of the null hypothesis of random association of alleles ($P \leq 0.042$; Table 5.3). In addition, extensive pairwise linkage disequilibrium between loci was evident in all populations and overall for the uncorrected dataset. The number of linked loci in each population decreased in the clone corrected dataset (Table 5.3).

5.4.4 Population structure and differentiation

AMOVA results from the hierarchical examination of regional and field populations indicated that 99.53% of the total genetic variation was attributed to genetic differences within fields (Table 5.5). Comparative analysis of the clone corrected regional and field populations dataset resulted in similar distributions of genetic variation for each hierarchy. A negative variance (σ) component was identified among the regions for the uncorrected and clone corrected data set, indicating an absence of genetic structure at that hierarchy level. Significant differences were not found among regions among fields within regions or among field populations for the uncorrected and clone corrected datasets ($P \geq 0.107$; Table 5.6) . Phi (Φ) values were low and ranged from -0.002 – 0.0050 and -0.021 – 0.022 for the uncorrected and clone corrected dataset hierarchies, respectively (Table 5.6). AMOVA results from analysis of the two mating-type populations indicated that only 1.46% of the total genetic variation were attributed to genetic differences between the mating-types (Table 5.5).

Significant testing indicted that for the uncorrected dataset the there was a significant difference between the two mating-type populations (P = 0.42). However, after clone correction to remove bias within the data set, there was no significant difference between the two mating-type populations (P = 0.326; Table 5.6).

Analysis of spatial autocorrelation identified that isolates within the two transects in each field were not genetically spatially autocorrelated; r was effectively 0 for the first bin of each distance class tested and the null hypothesis of no autocorrelation could not be rejected (Fig. 5.4). Mantel tests showed no significant correlation between genetic and geographical distance in in each field ($0.17 \leq P \geq 0.4$, $-0.04 \leq R_{xy} \geq 0.00$).

The MSN based on Bruvo's distance with reticulation identified five clusters of MLGs. Each cluster of MLGs failed to group individual isolates according to population. Each cluster included isolates from each of the four fields (Fig. 5.5a), and both *MAT1-1* (I) and *MAT1-2* isolates (Fig. 5.5b). The dominant MLGs (≥ 5 members) were distributed between the five cluster groups (Fig. 5.5a & 5.5b).

5.4.5 Gene flow

Maximum likelihood based analysis of gene flow between the fields identified that all field populations were well connected in both directions. The relative mutation rates used in the field analyses, identified from the data, ranged from 0.86 – 1.30 across the loci. The average value of the mutation-scaled population size (Θ) of each population from three runs varied

between 0.11 – 0.82 for the four fields (Table 5.7). All values of the mutation-scaled immigration rate (*M*) were greater than 1, indicating that the effect of migration (*m*) was larger than the effect of mutation (μ) (Table 5.7). Additionally, within each field gene flow between the *MAT1-1* (I) and *MAT1-2* isolates in both directions was detected. The average value of M from the three runs for each field was greater than 1 and similar in magnitude for movement in both directions.

5.5 DISCUSSION

To best of our knowledge this is the first study to examine the genotypic population structure of *D. tanaceti*, the causal agent of tan spot in pyrethrum. The *D. tanaceti* isolates examined represented the pathogen populations 12 months after crops were planted, for four different fields in two geographically separated (70 km) regions in Tasmania. Transmission of tan spot had previously been attributed to a combination of localised plant to plant and within plant transmission via splash dispersal of *D. tanaceti* conidia, and crop to crop transmission via seed borne inoculum (Pethybridge et al., 2006). The contribution of long range dispersal via ascospores was unknown. The incidence of *D. tanaceti* within each of the sampled fields was high (21 to 54% of sampling units within each field) and provided a sufficient number of individuals for population analysis (Hale et al., 2012). Both regional and field populations exhibited high genetic and genotypic diversity, indicating the pathogen populations may have a high adaptive ability (McDonald & Linde, 2002, Zhang et al., 2013). While gene diversity is not affected by the pathogen mating systems, high genotypic diversity is often associated with sexual reproduction, as sexual reproduction creates many new genotypes (McDonald, 1997). Despite the occurrence of significant linkage disequilibrium in the majority of the

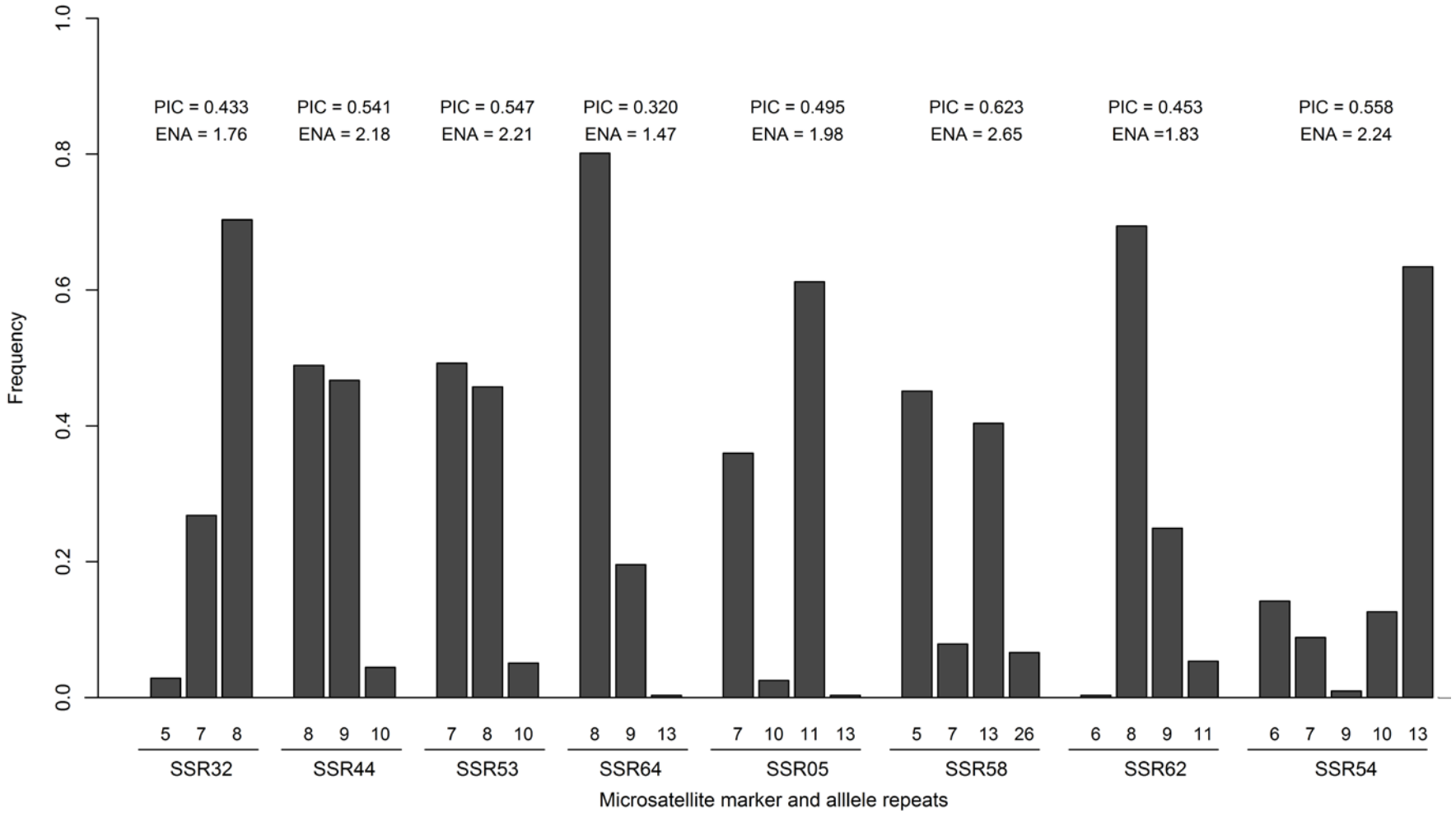

Fig. 5.2. Frequency of alleles of each microsatellite marker in the *Didymella tanaceti* population (*n* = 317) collected in 2012. The polymorphic information content (PIC) (Botstein et al., 1980) and effective number of alleles (ENA) (Kimura & Crow, 1964) of each marker are presented above the frequency chart.

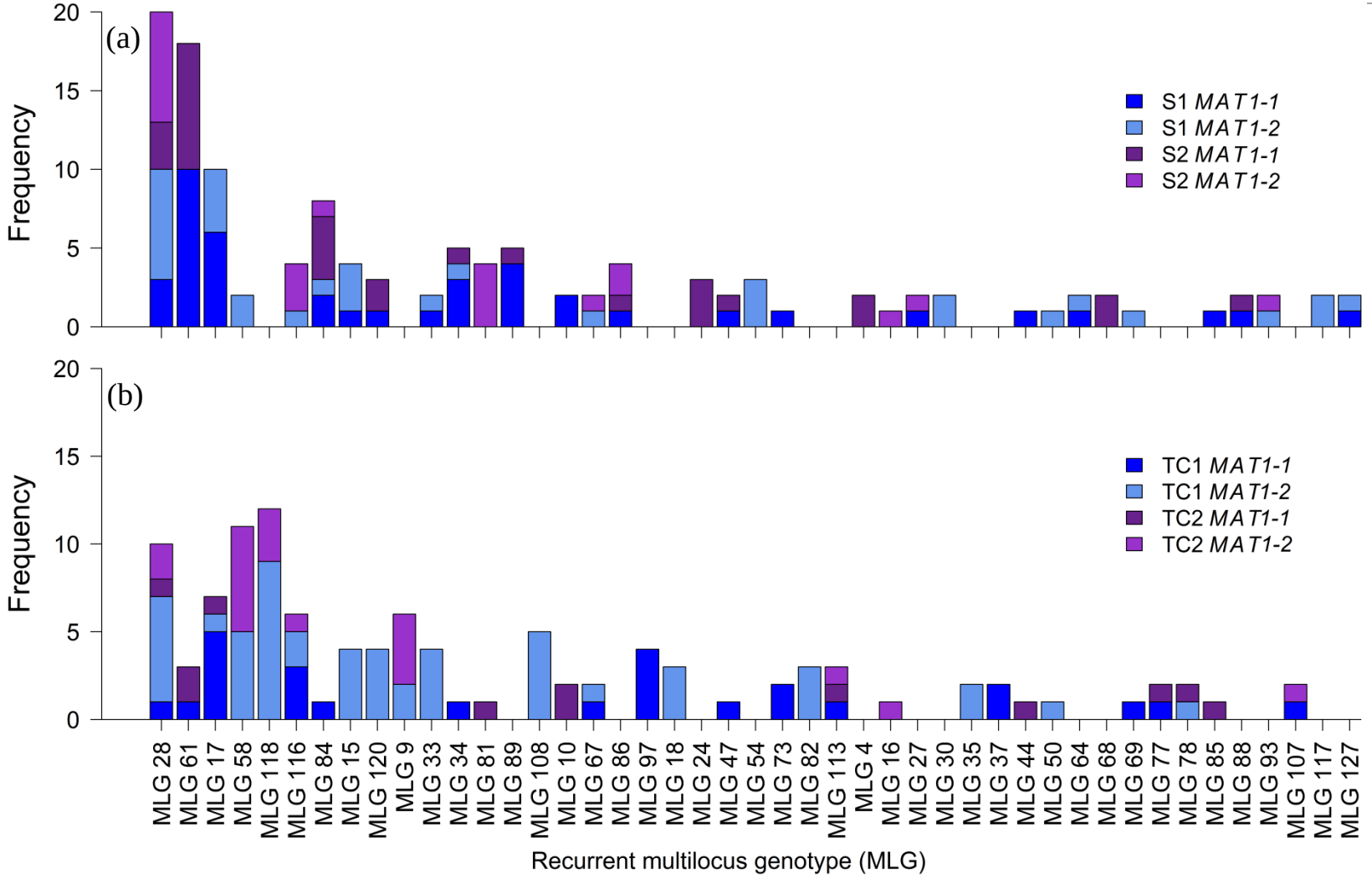

Fig. 5.3. Frequency of the 45 recurrent multilocus genotypes (MLGs) identified in the *Didymella tanaceti* population collected in 2012. (a) *MAT1-1* and *MAT1*-2 isolates in fields S1 and S2 located in Sassafras, Tasmania; (b) *MAT1-1* and *MAT1*-2 isolates in fields TC1 and TC2 located in Table Cape, Tasmania.

Table 5.3. Diversity and linkage disequilibrium statistics for each regional and field population, and overall for the uncorrected and clone correct datasets collected in 2012.

Population[a]	Uncorrected[b] Index[d]												Clone Corrected[c] Index				
	N	MLG	$MLG_{n=1}$	eMLG	E_5	*G*	$G_{n=}$	*D*	$D_{n=}$	*uh*	$\bar{r}_d$	*P* value	NLL	MLG_{CC}	*uh*	$\bar{r}_d$	*P* value	NLL
Regional																		
Sassafras	175	83	56	71.9	0.53	26.8	26.2	0.96	0.96	0.50	0.081	<0.0001	27	93	0.56	0.039	<0.0001	14
Table Cape	142*	64	41	64.0	0.67	29.5	29.5	0.97	0.97	0.48	0.051	<0.0001	20	71	0.51	0.019	0.0033	5
Field																		
S1	109	62	47	29.6	0.62	26.9	20.2	0.96	0.95	0.52	0.076	<0.0001	20	70	0.56	0.036	<0.0001	9
S2	66	34	24	24.7	0.67	16.3	14.6	0.94	0.93	0.47	0.107	<0.0001	16	37	0.55	0.056	0.0002	2
TC1	100	48	31	27.3	0.75	26.7	20	0.96	0.95	0.47	0.054	<0.0001	19	52	0.50	0.024	0.0067	4
TC2	42*	27	20	27.0	0.77	17.3	17.3	0.94	0.94	0.51	0.052	<0.0001	7	29	0.51	0.020	0.0419	0
Overall	317	127	82	127.0	0.52	37.1	NC[f]	0.97	NC	0.50	NC	NC	NC	145	0.55	NC	NC	NC

[a] Regional populations = two regions in Tasmania, Australia; Field = four field populations, S1 and S2 were located in Sassafras, TC1 and TC2 were located in Table Cape; Overall = all isolates.

[b] Contains all individuals in each population.

[c] Contains one member of each multilocus genotype (MLG) for each mating-type in each population.

[d] *N* = number of individuals; MLG = number of multilocus genotypes (MLGs); $MLG_{n=1}$ = number of singleton MLGs; eMLG = expected number of MLGs after rarefaction (Grunwald et al., 2003); E_5 = genotypic evenness (Ludwig & Reynolds, 1988); *G* = Stodart and Taylor's index of genotypic diversity (Stoddart & Taylor, 1988); $G_{n=}$ = Stodart and Taylor's index of genotypic diversity based on bootstrapping where the number of samples drawn in each replicate was equal to the smallest sample size of all population being compared (indicated by *); *D* = Simpson's index of genotypic diversity (Simpson, 1949); $D_{n=}$ = Simpson's index of genotypic diversity based on bootstrapping, where the number of samples drawn in each replicate was equal to the smallest sample size of all population being compared (indicated by *); *uh* = Nei's unbiased haploid genetic diversity (Nei, 1973); $\bar{r}_d$ = standardized index of association (Agapow & Burt, 2001); *P* value = significance of the observed $\bar{r}_d$ value from 9,999 permutations; NLL = number of linked loci.

[e] MLG_{CC} = number of MLGs reserved in the clone corrected dataset.

[f] NC = not calculated.

Table 5.4. Diversity statistics for *MAT1-1* and *MAT1-2* isolates in the regional, field and overall populations collected in 2012.

Population[a]	Mating-type[b]	Index[c]										
		N	MLG	$MLG_{n=1}$	$MLG_{private}$	eMLG	E_5	*G*	$G_{n=}$	*D*	$D_{n=}$	*uh*
Regional												
Sassafras	*MAT1-1*	95	46	27	27	39.0	0.55	16.5	16.1	0.94	0.94	0.53
	MAT1-2	75*	42	24	24	42.0	0.58	17.6	17.6	0.94	0.94	0.47
Table Cape	*MAT1-1*	54*	36	23	18	36.0	0.80	24.3	24.3	0.96	0.96	0.42
	MAT1-2	88	35	18	20	25.7	0.68	15.7	14.4	0.94	0.93	0.50
Field												
S1	*MAT1-1*	59	36	25	17	30.0	0.64	16.8	16.0	0.94	0.94	0.53
	MAT1-2	47*	31	19	17	31.0	0.74	18.6	18.6	0.95	0.95	0.50
S2	*MAT1-1*	36	19	11	10	16.2	0.72	10.6	10.1	0.90	0.90	0.45
	MAT1-2	28*	16	11	7	16.0	0.70	8.7	8.7	0.89	0.89	0.49
TC1	*MAT1-1*	37*	26	19	13	26.0	0.79	17.3	17.3	0.94	0.94	0.44
	MAT1-2	63	26	12	14	19.5	0.78	15.3	13.3	0.94	0.92	0.51
TC2	*MAT1-1*	17*	15	11	5	15.0	0.95	13.8	13.8	0.93	0.93	0.47
	MAT1-2	25	14	9	6	10.7	0.75	8.3	7.6	0.88	0.86	0.49
Overall	*MAT1-1*	149*	72	50	45	72.0	0.54	24.4	24.4	0.96	0.96	0.50
	MAT1-2	163	68	45	44	64.1	0.57	23.1	22.8	0.96	0.96	0.50

[a] Regional = two regional populations in Tasmania, Australia; Field = four field populations; S1 and S2 were located in Sassafras, TC1 and TC2 were located in Table Cape.; Overall = all isolates.

[b] Mating-type: *MAT1-1* = individuals with a haplotype I *MAT1-1* mating-type; *MAT1-2* = individuals with a *MAT1-2* mating-type.

[c] *N* = number of individuals; MLG = number of multilocus genotypes (MLGs); $MLG_{n=1}$ = number of singleton MLGs; $MLG_{private}$ = number of MLGs only found in the population/mating-type ; eMLG = expected number of MLGs after rarefaction (Grunwald et al., 2003); E_5 = genotypic evenness (Ludwig & Reynolds, 1988); *G* = Stodart and Taylor's index of genotypic diversity (Stoddart & Taylor, 1988); $G_{n=}$ = Stodart and Taylor's index of genotypic diversity based on bootstrapping where the number of samples drawn in each replicate was equal to the smallest sample size of the two populations being compared indicated by *; *D* = Simpson's index of genotypic diversity (Simpson, 1949); $D_{n=}$ = Simpson's index of genotypic diversity based on bootstrapping, where the number of samples drawn in each replicate was equal to the smallest sample size of the two populations being compared (indicated by *); *uh* = Nei's unbiased haploid genetic diversity (Nei, 1973).

Table 5.5. Analysis of molecular variance (AMOVA) for uncorrected and clone corrected datasets.

	Uncorrected dataset[a]					Clone corrected dataset[b]				
	df	Sum of squares	Mean SS	Variance (σ)	Variation (%)	*df*	Sum of squares	Mean SS	Variance (σ)	Variation (%)
Region and field population[c]										
Among regions	1	48.75	48.75	0 (-0.10)[d]	0	1	11.06	11.06	0 (-1.21)[d]	0
Among fields within regions	2	122.56	61.28	0.22	0.47	2	226.27	113.14	1.3	2.21
Within fields	313	14393.13	45.98	45.99	99.53	184	10571.87	57.46	57.46	97.79
Total	316	14564.44	156.01	46.21	100	187	10809.21	181.66	58.76	100
Mating-type population[e]										
Among Mating-types	1	148.39	148.39	0.67	1.46	1	61.84	61.84	0.04	0.06
Within Mating-types	310	13916.90	44.89	44.89	98.54	138	8211.55	59.50	59.50	99.94
Total	311	14065.29	193.28	45.56	100	139	8273.39	121.34	59.54	100

[a] Contains all individuals in each population.

[b] For Regions and field population analysis the clone corrected dataset contained one member of each multilocus genotype for each mating-type in each field population. For Mating-types analysis the clone corrected dataset contained one member of each multilocus genotype for each mating-type in total population.

[c] Hierarchical AMOVA, partitioning total genetic variance into the following components: among the two regional populations (Sassafras and Table Cape), among the two field populations in each region and within the four fields collected in 2012

[d] Negative variance (σ) converted to 0, negative value in parenthesis.

[e] Partitioning total genetic variance into the following components among the two mating-types and within the two mating-types. Includes only haplotype I *MAT1-1* and *MAT1-2* isolates.

Table 5.6. Analysis of molecular variance (AMOVA) output for testing significance for the uncorrected and clone corrected datasets

	Uncorrected dataset[a]		**Clone corrected dataset**[b]	
	Phi (Φ)	*P*[c]	Phi (Φ)	*P*
Region and field population				
Among regions	-0.002	0.625	-0.021	0.939
Among fields within regions	0.005	0.243	0.022	0.107
Among fields	0.002	0.280	0.002	0.335
Mating-type population[d]				
Among mating-types	0.015	0.042	0.001	0.326

[a] Contains all individuals in each population.

[b] For Among regions, Among fields within regions and Among fields analysis the clone corrected dataset contained one member of each multilocus genotype for each mating-type in each field population. For Among mating-types analysis the clone corrected dataset contained one member of each multilocus genotype for each mating-type in total population.

[c] Significance of differentiation was tested using a null distribution of variance from 9,999 random permutations (Excoffier et al., 1992).

[d] Includes only haplotype I *MAT1-1* and *MAT1-2* isolates.

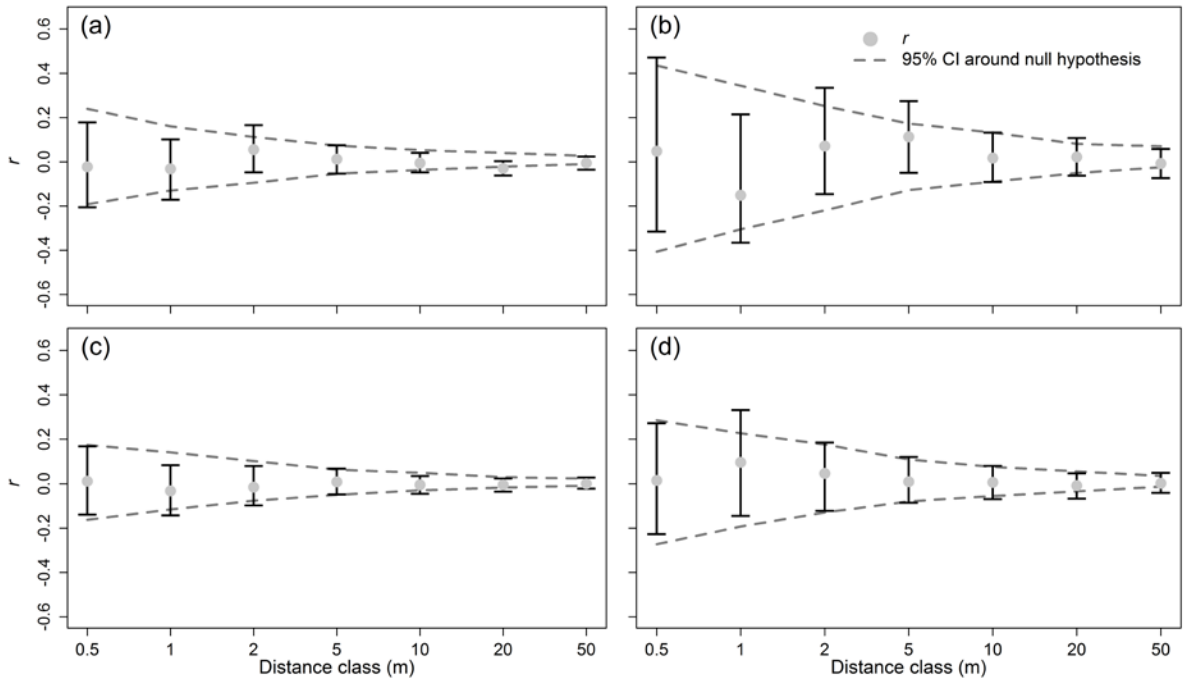

Fig. 5.4. Composite graphs of the first distance bin of increasing distance class sizes (*n* = 7) from analysis of spatial autocorrelation for all pairs of isolates within each of the two 50 m transects in each field; (a) field S1; (b) field S2; (c) field TC1; (d) field TC2.
Dashed lines indicate the 95% confidence intervals about the null hypothesis of no spatial structure for the combined data set from 999 permutations. Error bars bound the 95% confidence interval of *r* were determined by 1,000 bootstrap replicates.

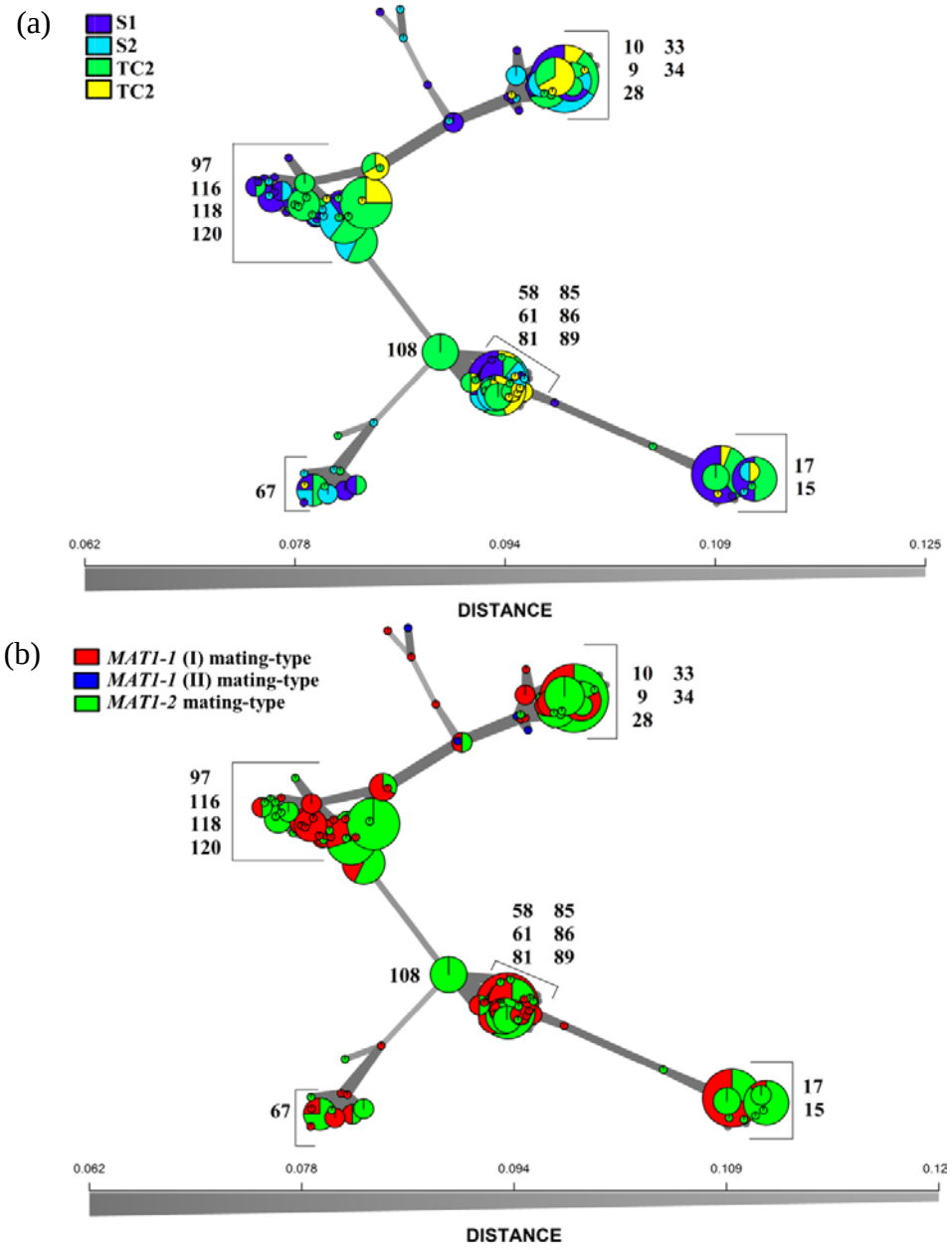

Fig. 5.5. Minimum spanning networks of the relationship between multilocus genotypes (MLGs) allowing reticulation. Each node represents a MLG and is characterized by a pie chart to identify the contributed to each MLGs from (a) isolates from fields S1, S2, TC1 and TC2; (b) *MAT1-1* (haplotype I), *MAT1-1* (haplotype II) and *MAT1-2* isolates. Distances between MLGs was estimated using Bruvo's distance (Bruvo et al., 2004). The size of each node is scaled to represent the number of individuals in each MLG. The numbers next to each cluster indicate which MLG groups (containing ≥ 5 members) are located in each cluster. The scale bar indicates the edge weight and is scaled proportional To the inverse of the observed distance, such that the line becomes thicker for more related nodes.

Table 5.7. Gene flow between the four field populations collected in 2012.

Source population	Θ[b]	*M*[a] estimates for sink population			
		S1	S2	TC1	TC2
S1	0.82 (0.79-0.84)[c]	-	39.66 (34.6-44.7)	14.50(10.2-19.7)	47.35 (46.1-48.4)
S2	0.24 (0.24-0.24)	20.63 (19.0-23.2)	-	43.86 **(**39.6-50.1)	34.28 (24.1-42.8)
TC1	0.11 (0.09-0.12)	5.33 (4.3-6.2)	39.80(35.0-45.1)	-	31.49 (30.9-32.5)
TC2	0.90 (0.85-0.95)	23.3 (20.0-28.3)	33.45 (30.7-37.3)	49.55 (42.6-57.0)	-

[a] M = scaled number of migrants (m/μ; where m = immigration rate and μ = mutation rate per locus).

[b] Θ = number of immigrants per generation ($2Ne\mu$; where Ne is the effective population size).

[c] The mean maximum likelihood estimates and range in parentheses observed in three independent analyses in Migrate-N for the mutation-scaled population size.

populations, several analyses indicated that sexual reproduction might occur, but may be infrequent. Analysis of the entire population identified 127 MLGs. Of the 45 recurrent MLGs, 20 were found in both regions but only 3 were found in all four fields. The three found in all four fields included the two most frequent MLGs in the overall population. Thus, these MLGs may represent historically dominant MLG groups. The majority of the MLGs were only represented by a single isolate. However, most of the singleton MLGs appeared to be due to re-shuffling of alleles at each locus, rather than via mutation. This was evident by the lack of occurrence of private alleles and the similar allele frequencies for each marker in each of the populations (Supplementary Table 5.1). Further evaluation of the single isolates containing the private alleles for the markers SSR05 and SSR62 identified that they contained the second haplotype of the *MAT1-1-1* gene. The second haplotype of *MAT1-1-1* was proposed to have evolved via genetic drift and contained several mutations (Pearce, Chapter 4). Furthermore, each of the five *MAT1-1* haplotype II isolates had unique singleton MLGs and were identified within the margins of the MSN, suggesting they were the result of rare mutation events or migrated from locations containing different genotypes (Goss et al., 2009).

Didymella tanaceti is a heterothallic species with previous analysis of the populations genotyped in this study identifying an equal proportions of *MAT1-1* or *MAT1-2* isolates in in all fields, except TC1 (Pearce, Chapter 4). Following clone correction of the populations in this study, the ratio of *MAT1-1* to *MAT1-2* isolates in each regional, field and the overall population was consistent with a 1:1 ratio (data not shown). A 1:1 distribution of *MAT* isolates is consistent with reproduction occurring in previously presumed asexual heterothallic species (Groenewald et al., 2008; Linde et al., 2003). Furthermore, we propose that if sexual reproduction was absent, genetic interaction between isolates of each mating-

type would be limited. This would result in *MAT1-1* and *MAT1-2* populations of D. tanaceti diverging via genetic drift, as individuals of the same mating-type would not be permitted to recombine with each other via meiosis (reshuffling of loci may potentially occur as part of a parasexual cycle). This would lead to random changes in the allele frequencies for neutral loci, such as SSR markers, in the populations of each mating-type (McDonald, 1997). However, little evidence of this was found in this study. Forty percent of the recurrent MLGs contained isolates of each mating-type. The chance of two isolates of different mating-types evolving the same combinations of alleles at 8 polymorphic SSR loci would be low. We also identified isolates with the same MLG and different mating-types which contained rare alleles (frequency < 0.07). Furthermore, calculation of Psex indicated that that the majority of isolates with the same MLG and mating-type in each field were not true clones and had evolved independently from at least two ancestors. This was further supported by evidence of historical gene flow between the *MAT1-1* and *MAT1-2* isolates in each field and the lack of additional private alleles within isolates of each mating-type. The results obtained from analysing the mating-type populations are consistent with that expected under a mixed reproductive system, with some genotypes being recombined between the mating-types and some specific to each mating-type.

Analysis of the fields in this study identified significant linkage disequilibrium within all populations, except for the clone corrected population from field TC2. While linkage disequilibrium is expected in populations that do not undergo regular sexual reproduction, it can also be attributed to other factors (Falush et al., 2003, Brewer et al., 2012). Linkage disequilibrium may be observed due to physical linkage of the SSR loci (Xu, 2006). The full genome of *D. tanaceti* is not currently available, but is part of ongoing work which once

complete will allow the physical distance between the SSR loci to be examined. Linkage disequilibrium in populations can also result due to admixture within the examined populations (Milgroom, 1996, Brewer & Milgroom, 2010). However, Mantel tests and analysis of spatial autocorrelation showed no evidence of spatially aggregated genetic clusters in any of the fields in this study. This supported the analysis of the populations at a field spatial scale and indicated that smaller field subpopulations were not being analysed as one single population. However, it is also proposed that a sampling scale < 0.5 m, such as within the same plant and or neighbouring plants, may be worth investigating in future studies. Despite being used extensively as an indicator of clonal reproduction, the occurrence of linkage disequilibrium does not exclude the occurrence of sexual reproduction. Linkage disequilibrium has been observed in a number of pathogens populations with known mixed modes of reproduction, in which a sexual cycle is followed by multiple rounds of asexual reproduction (Dale et al., 2011, Brewer et al., 2012, Bogacki et al., 2010). It has been suggested that specific factors are required for sexual reproduction in *D. tanaceti* (Pearce, Chapter 4), and therefore sexual reproduction may only occur infrequently. As linkage disequilibrium between unlinked loci can only decay by a maximum of 50% with recombination from each sexual generation, it may take several sexual recombination events for the disequilibrium to be eliminated (Ardlie et al., 2002). It may also be possible that the populations were sampled prior to the occurrence of conditions conducive for sexual reproduction.

Analysis of the genetic population structure using a MSN identified five clusters. However, the inferred clusters did not represent geographical populations, or *MAT1-1* (I and II) and *MAT1-2* isolates, but instead consisted of isolates admixed from all populations and mating-

types. MLGs consisting of isolates of only one mating-type and those containing both mating-types were identified as closely related within the MSN. Furthermore, each cluster contained a proportion of singleton and recurrent MLG groups, indicating a stepwise mutation process between the singleton MLGs and the MLGs which contained multiple isolates. Furthermore, evidence of population structure was also absent at a regional or field levels using AMOVA with 97.99% of the total genetic variation attributed to genetic differences within fields. The lack of differentiation may be due to the identified gene flow between populations (McDermott & McDonald, 1993).

The lack of significance of the Mantel correlations and spatial autocorrelation tests indicated that isolates sampled within short distances were as similar to each other as expected by random. Thus, within each transect plant to plant spread of clonal genotypes was minimal. The random distribution of genotypes within each transect was more consistent with either seed-borne transmission, a random movement of different genotypes through airborne ascospores or medium range dispersal of conidia (Kohn, 1995). Furthermore, the combined lack of significant population structure between fields, similar allele frequencies for each marker within each field, low frequency of private alleles, and suggested historical gene flow between each of the field populations suggest that the *D. tanaceti* isolates within these populations may have originated from a common genetic pool, such as an alternative host or common seed crop.

HRM analysis was employed as an efficient, accurate and cost-effective alternative to fragment length electrophoresis based methods for differentiating alleles of the SSR markers used in this study (Arthofer et al., 2011, Distefano et al., 2012). The additional advantage of

HRM, in the detection of polymorphisms within or adjacent to the SSR loci, was also observed in this study. For the marker SSR44, two of the alleles differed in repeat length due to a single base substitution in the final repeat unit, resulting in interruption of the synthesis of an exact repeat, and a resultant decreased number of repeats of the SSR motif in these isolates. Thus, fragment length analysis would not have differentiated isolates containing 8 or 9 repeats of the SSR motif for this marker. Furthermore, a substitution (A to G) outside of the SSR loci in the marker SSR54 was able to be detected using HRM. The inability of HRM to differentiate alleles of two of the polymorphic SSR markers identified is proposed to be due to the size of the real-time PCR product of these markers concealing the impact of the increased repeat numbers on the melting temperature of the product. Discrimination between alleles, especially those differing by a single repeat, was more prominent for SSR markers with smaller product sizes. Therefore, re-designing the PCR primers of these two markers, as well as some of the larger markers used in this study, such that they are more proximate to the SSR motif, may be beneficial for future work.

The occurrence of *D. tanaceti* has greatly increased over the past decade resulting in increased tan spot incidence and severity in pyrethrum crops (Hay et al., 2015). The results from this study imply that that the rapid expansion may not have been due to an increase in the number of clonal individuals. Instead, it is most likely due to the development of a genetically diverse population, through mutation and infrequent sexual recombination. Future studies temporally analysing genetic variation and distribution of *D. tanaceti* populations over the last decade would be beneficial. They may assist in pinpointing the timeline of the development of the increase in genetic and determining the original source of introduction of *D. tanaceti* and/or alternative hosts. They may further aid in identifying

historical selective sweeps or selection pressures, such as the introduction of new fungicides or pyrethrum varieties. We further propose that the evidence of infrequent sexual reproduction, as a means of providing long distance pathogen transmission, and minimal clonal patterns of transmission within fields may indicated additional factors, such as fungicide resistance, increased seed borne inoculum or increased virulence may have contributed to the rapid increase in disease incidence. *Didymella tanaceti* individuals with decreased sensitivity to boscalid have already been identified (Hay et al., 2015) and the results within this study indicated that the pathogen population may have an increased adaptive potential due to high genotypic diversity.

5.6 ACKNOWLEDGEMENTS

The authors wish to thank Pattie Weichelt, Craig Palmer, Stacey Pilkington and Phil Gardam (Tasmanian Institute of Agriculture; University of Tasmania, Australia) for assisting with the collection of isolates used in this study. Support for this research was generously provided by Botanical Resources Australia (Agricultural Services Pty. Ltd.). The first author was awarded the University of Tasmania's Australian Postgraduate Award and the Cuthbertson Elite Tasmania Graduate Research Scholarship, which supported this research.

5.7 REFERENCES

Agapow P-M, Burt A, 2001. Indices of multilocus linkage disequilibrium. *Molecular Ecology Notes* **1**, 101-2.

Aranud-Haond S, Belkhir K, 2007. GENCLONE: a computer program to analyse genotypic data, test for clonality and describe spatial clonal organization. *Molecular Ecology Notes* **7**, 15-7.

Ardlie KG, Kruglyak L, Seielstad M, 2002. Patterns of linkage disequilibrium in the human genome. *Nature Reviews Genetics* **3**, 299-309.

Arthofer W, Steiner FM, Schlick-Steiner BC, 2011. Rapid and cost-effective screening of newly identified microsatellite loci by high-resolution melting analysis. *Molecular Genetics and Genomics* **286**, 225-35.

Beerli P, 2009. How to use migrate or why are Markov chain Monte Carlo programs difficult to use. In: Bertorelle G, Bruford MW, Hauffe HC, Rizzoli A, Vernesi C, eds. *Population Genetics for Animal Conservation.* Cambridge, UK: Cambridge University Press, 42-74.

Beerli P, Felsenstein J, 2001. Maximum likelihood estimation of a migration matrix and effective population sizes in n subpopulations by using a coalescent approach. *Proceedings of the National Academy of Sciences* **98**, 4563-8.

Benjamini Y, Hochberg Y, 1995. Controlling the false discovery rate: A practical and powerful approach to multiple testing. *Journal of the Royal Statistical Society. Series B (Methodological)* **57**, 289-300.

Bogacki P, Keiper FJ, Oldach KH, 2010. Genetic structure of South Australian *Pyrenophora teres* populations as revealed by microsatellite analyses. *Fungal Biology* **114**, 834-41.

Botstein D, White RL, Skolnick M, Davis RW, 1980. Construction of a genetic linkage map in man using restriction fragment length polymorphisms. *American Journal of Human Genetics* **32**, 314.

Brewer MT, Frenkel O, Milgroom MG, 2012. Linkage disequilibrium and spatial aggregation of genotypes in sexually reproducing populations of *Erysiphe necator*. *Phytopathology* **102**, 997-1005.

Brewer MT, Milgroom MG, 2010. Phylogeography and population structure of the grape powdery mildew fungus, *Erysiphe necator*, from diverse *Vitis* species. *BMC Evolutionary Biology* **10**, 268.

Brown PH, Menary RC, 1994. Flowering in pyrethrum (*Tanacetum cinerariaefolium* L) .1. Environmental requirements. *Journal of Horticultural Science* **69**, 877-84.

Bruvo R, Michiels NK, D'souza TG, Schulenburg H, 2004. A simple method for the calculation of microsatellite genotype distances irrespective of ploidy level. *Molecular Ecology* **13**, 2101-6.

Chen Q, Jiang JR, Zhang GZ, Cai L, Crous PW, 2015. Resolving the Phoma enigma. *Studies in Mycology* **82**, 137-217.

Dale AL, Lewis KJ, Murray BW, 2011. Sexual reproduction and gene flow in the pine pathogen *Dothistroma septosporum* in British Columbia. *Phytopathology* **101**, 68-76.

Distefano G, Caruso M, La Malfa S, Gentile A, Wu S-B, 2012. High resolution melting analysis is a more sensitive and effective alternative to gel-based platforms in analysis of SSR – An example in citrus. *PLoS One* **7**, e44202.

Excoffier L, Smouse PE, Quattro JM, 1992. Analysis of molecular variance inferred from metric distances among DNA haplotypes: application to human mitochondrial DNA restriction data. *Genetics* **131**, 479-91.

Falush D, Stephens M, Pritchard JK, 2003. Inference of population structure using multilocus genotype data: Linked loci and correlated allele frequencies. *Genetics* **164**, 1567-87.

Goss EM, Larsen M, Chastagner GA, Givens DR, Gruenwald NJ, 2009. Population genetic analysis infers migration pathways of *Phytophthora ramorum* in US nurseries. *PLoS Pathogens* **5**, e1000583.

Gregorius H, 2005. Testing for clonal propagation. *Heredity* **94**, 173-9.

Grunwald NJ, Goodwin SB, Milgroom MG, Fry WE, 2003. Analysis of genotypic diversity data for populations of microorganisms. *Phytopathology* **93**, 738-46.

Hale ML, Burg TM, Steeves TE, 2012. Sampling for microsatellite-based population genetic studies: 25 to 30 individuals per population is enough to accurately estimate allele frequencies. *PLoS One* **7**, e45170.

Hay FS, Gent DH, Pilkington SJ, Pearce TL, Scott JB, Pethybridge SJ, 2015. Changes in distribution and frequency of fungi associated with a foliar disease complex of pyrethrum in Australia. *Plant Disease* **99**, 1227-35.

Kamvar ZN, Brooks JC, Grünwald NJ, 2015. Novel R tools for analysis of genome-wide population genetic data with emphasis on clonality. *Frontiers in Genetics* **6**, 1-10.

Kamvar ZN, Tabima JF, Grünwald NJ, 2014. Poppr: an R package for genetic analysis of populations with clonal, partially clonal, and/or sexual reproduction. *PeerJ* **2**, e281.

Katoh K, Misawa K, Kuma K-I, Miyata T, 2002. MAFFT: a novel method for rapid multiple sequence alignment based on fast fourier transform. *Nucleic Acids Research* **30**, 3059-66.

Kaufman L, Rousseeuw PJ, 1987. Clustering by means of medoids. In: Dodge Y, ed. *First International Conference on Statistical Data Analysis Based on the L1-Norm and Related Methods.* Neuchâtel, Switzerland, 405-16.

Kimura M, Crow JF, 1964. The number of alleles that can be maintained in a finite population. *Genetics* **49**, 725.

Kohn L, 1995. The clonal dynamic in wild and agricultural plant-pathogen populations. *Canadian Journal of Botany* **73**, 1231-40.

Lang DT, 2015. *XML: Tools for parsing and generating XML within R and S-Plus. R package version 3.98-1.3*.

Ludwig JA, Reynolds JF, 1988. *Statistical ecology: A primer in methods and computing*. New York, USA: John Wiley & Sons.

Maechler M, Rousseeuw P, Struyf A, *et al.*, 2015. *Cluster: Cluster analysis basics and extensions V. v2.0.3*.

Mantel N, 1967. The detection of disease clustering and a generalized regression approach. *Cancer Research* **27**, 209-20.

Mcdermott JM, Mcdonald BA, 1993. Gene flow in plant pathosystems. *Annual Review of Phytopathology* **31**, 353-73.

Mcdonald BA, 1997. The population genetics of fungi: tools and techniques. *Phytopathology* **87**, 448-53.

Mcdonald BA, Linde C, 2002. Pathogen population genetics, evolutionary potential, and durable resistance. *Annual Review of Phytopathology* **40**, 349-79.

Meglécz E, Costedoat C, Dubut V, *et al.*, 2010. QDD: a user-friendly program to select microsatellite markers and design primers from large sequencing projects. *Bioinformatics* **26**, 403-4.

Milgroom MG, 1996. Recombination and the multilocus structure of fungal populations. *Annual Review of Phytopathology* **34**, 457-77.

Nei M, 1973. Analysis of gene diversity in subdivided populations. *Proceedings of the National Academy of Sciences* **70**, 3321-3.

Peakall R, Smouse PE, 2006. GenAlEx 6: genetic analysis in Excel. Population genetic software for teaching and research. *Molecular Ecology Notes* **6**, 288-95.

Peakall R, Smouse PE, 2012. GenAlEx 6.5: genetic analysis in Excel. Population genetic software for teaching and research - an update. *Bioinformatics* **28**, 2537-9.

Pearce T, Chapter 3. Tan spot of pyrethrum is caused by a *Didymella* species complex. In. *Population biology of the tan spot pathogen of pyrethrum, PhD thesis.* University of Tasmania, 106-44.

Pearce T, Chapter 4. Mating-type gene structure in *Didymella tanaceti* and their spatial distribution in pyrethrum fields. In. *Population biology of the tan spot pathogen of pyrethrum, PhD thesis.* University of Tasmania, 145-80.

Pethybridge S, Hay F, Groom T, 2003. Seasonal fluctuations in fungi associated with pyrethrum foliage in Tasmania. *Australasian Plant Pathology* **32**, 223-30.

Pethybridge SJ, Hay F, Jones S, Wilson C, Groom T, 2006. Seedborne infection of pyrethrum by *Phoma ligulicola*. *Plant Disease* **90**, 891-7.

Pethybridge SJ, Hay FS, Esker PD, *et al.*, 2008a. Diseases of pyrethrum in Tasmania: challenges and prospects for management. *Plant Disease* **92**, 1260-72.

Pethybridge SJ, Jones SJ, Shivas RG, Hay FS, Wilson CR, Groom T, 2008b. Tan spot: A new disease of pyrethrum caused by *Microsphaeropsis tanaceti* sp. nov. *Plant Pathology* **57**, 1058-65.

Qiagen, 2014. *Rotor-Gene Q User Manual V. 4.0* https://www.qiagen.com/au/resources/resourcedetail?id=58d4a7d9-287f-4b01-85c3-5cb83db2228b&lang=en: Qiagen.

R Core Team, 2014. *R: A language and environment for statistical computing V. 3.0.1* Vienna, Austria.: R Foundation for Statistical Computing.

Reja V, Kwok A, Stone G, *et al.*, 2010. ScreenClust: Advanced statistical software for supervised and unsupervised high resolution melting (HRM) analysis. *Methods* **50**, S10-S4.

Rousset F, 2008. GENEPOP '007: A complete re-implementation of the GENEPOP software for Windows and Linux. *Molecular Ecology Resources* **8**, 103-6.

Rozen S, Skaletsky H, 2000. Primer3 on the WWW for general users and for biologist programmers. In: Krawetz S, Misener S, eds. *Bioinformatics Methods and Protocols: Methods in Molecular Biology.* Totowa, NJ,: Humana Press, 365-86.

Sergios T, Konstantinos K, 2006. *Pattern Recognition*. Orlando, Florida: Academic Press, Inc.

Simpson EH, 1949. Measurement of diversity. *Nature* **163**, 688.

Smouse PE, Long JC, Sokal RR, 1986. Multiple regression and correlation extensions of the Mantel test of matrix correspondence. *Systematic Zoology* **35**, 627-32.

Smouse PE, Peakall R, 1999. Spatial autocorrelation analysis of individual multiallele and multilocus genetic structure. *Heredity* **82**, 561-73.

Stoddart JA, Taylor JF, 1988. Genotypic diversity: estimation and prediction in samples. *Genetics* **118**, 705-11.

Xu J, 2006. Fundamentals of fungal molecular population genetic analyses. *Current Issues in Molecular Biology* **8**, 75-89.

Zhan J, Pettway R, Mcdonald B, 2003. The global genetic structure of the wheat pathogen *Mycosphaerella graminicola* is characterized by high nuclear diversity, low mitochondrial diversity, regular recombination, and gene flow. *Fungal Genetics and Biology* **38**, 286-97.

Zhang Y, Qiao M, Xu J, Cao Y, Zhang K-Q, Yu Z-F, 2013. Genetic diversity and recombination in natural populations of the nematode trapping fungus *Arthrobotrys oligospora* from China. *Ecology and Evolution* **3**, 312-25.

Supplementary Table 5.1. Frequency of each microsatellite (SSR) allele for each regional and field population, *MAT1-1* and *MAT1-2* isolates and overall in the 2012 collected population.

		Population[a]									
		Regional		Field				Mating-type			
SSR marker	Repeats of motif	Sassafrass	Table Cape	S1	S2	TC1	TC2	*MAT 1-1* (I)	*MAT 1-1* (II)	*MAT 1-2*	Overall
SSR05	7	0.366	0.352	0.404	0.303	0.350	0.357	0.289	0.600	0.417	0.360
SSR05	10	0.046	0.000	0.055	0.030	0.000	0.000	0.040	0.200	0.006	0.025
SSR05	11	0.583	0.648	0.541	0.652	0.650	0.643	0.671	0.000	0.577	0.612
SSR05	13	0.006	0.000	0.00	0.015	0.000	0.000	0.000	0.200	0.000	0.003
SSR53	7	0.446	0.549	0.468	0.409	0.620	0.381	0.362	1.000	0.595	0.492
SSR53	8	0.520	0.380	0.495	0.561	0.310	0.548	0.550	0.000	0.387	0.457
SSR53	10	0.034	0.070	0.037	0.030	0.070	0.071	0.087	0.000	0.018	0.050
SSR64	8	0.800	0.803	0.780	0.833	0.840	0.714	0.765	1.000	0.828	0.801
SSR64	9	0.194	0.197	0.211	0.167	0.160	0.286	0.235	0.000	0.166	0.196
SSR64	13	0.006	0.000	0.009	0.000	0.000	0.000	0.000	0.000	0.006	0.003
SSR58	5	0.429	0.479	0.440	0.409	0.480	0.476	0.376	0.800	0.509	0.451
SSR58	7	0.086	0.070	0.110	0.045	0.090	0.024	0.107	0.000	0.055	0.079
SSR58	13	0.406	0.401	0.394	0.424	0.370	0.476	0.443	0.000	0.380	0.404
SSR58	26	0.080	0.049	0.055	0.121	0.060	0.024	0.074	0.200	0.055	0.066
SSR62	6	0.006	0.000	0.009	0.000	0.000	0.000	0.000	0.200	0.000	0.003
SSR62	8	0.674	0.718	0.615	0.773	0.730	0.690	0.758	0.400	0.644	0.694
SSR62	9	0.229	0.275	0.257	0.182	0.260	0.310	0.215	0.400	0.276	0.249
SSR62	11	0.091	0.007	0.119	0.045	0.010	0.000	0.027	0.000	0.080	0.054
SSR54	6	0.149	0.134	0.138	0.167	0.110	0.190	0.181	0.000	0.110	0.142
SSR54	7	0.109	0.063	0.101	0.121	0.070	0.048	0.114	0.800	0.043	0.088
SSR54	9	0.011	0.007	0.009	0.015	0.010	0.000	0.013	0.000	0.006	0.009
SSR54	10	0.103	0.155	0.110	0.091	0.140	0.190	0.074	0.000	0.178	0.126
SSR54	13	0.629	0.641	0.642	0.606	0.670	0.571	0.617	0.200	0.663	0.634
SSR32	5	0.046	0.007	0.064	0.015	0.000	0.024	0.020	0.800	0.012	0.028
SSR32	7	0.189	0.366	0.202	0.167	0.320	0.476	0.195	0.200	0.337	0.268
SSR32	8	0.766	0.627	0.734	0.818	0.680	0.500	0.785	0.000	0.650	0.703
SSR44	8	0.560	0.401	0.569	0.545	0.360	0.500	0.644	0.200	0.356	0.489
SSR44	9	0.371	0.585	0.358	0.394	0.620	0.500	0.309	0.400	0.613	0.467
SSR44	10	0.069	0.014	0.073	0.061	0.020	0.000	0.047	0.400	0.031	0.044
Population size		175	142	109	66	100	42	149	5	163	317

[a] Regional populations = 2 regional populations in Tasmania, Australia; Field populations = S1 and S2 were located in Sassafras, TC1 and TC2 were located in Table Cape; Mating-type: *MAT1-1* (I) = individuals with a haplotype I *MAT1-1* mating-type; *MAT1-1(II)* = individuals with a haplotype II *MAT1-1* mating-type; *MAT1-2* = individuals with a *MAT1-2* mating-type; Overall = all isolates.

CHARACTERISATION OF BOSCALID SENSITIVITY IN *DIDYMELLA TANACETI*

Tamieka L Pearce[a*], Jason B Scott[a], Calum R Wilson[b], Frank S Hay[c], Sarah J Pethybridge[c]

[a]Tasmanian Institute of Agriculture, School of Land and Food, University of Tasmania, PO Box 3523 Burnie, Tasmania 7320, Australia; [b]Tasmanian Institute of Agriculture, School of Land and Food, University of Tasmania, Private Bag 98, Hobart, Tasmania 7001 Australia ; [c]Cornell University, School of Integrative Plant Science, Section of Plant Pathology and Plant-Microbe Biology, Cornell University, Geneva, NY 14456.

*Corresponding author: Tamieka.Pearce@utas.edu.au

Keywords: ascomycetes, *Didymellaceae*, fungicide resistance, high resolution melt, succinate dehydrogenase inhibitor, *SDHB*.

6.1 ABSTRACT

Didymella tanaceti is a fungal pathogen that causes tan spot of pyrethrum in Tasmania, Australia. Within the past decade, tan spot has progressed from a minor foliar disease to the predominant disease throughout spring. Disease control has been based, in part, on applications of boscalid, a succinate dehydrogenase inhibiting fungicide. Previously, resistance to boscalid was identified in a small number of *D. tanaceti* isolates collected between 2009 and 2011. The succinate dehydrogenase subunit B (*SDHB*) gene of a subset of these isolates (n = 48) was partially sequenced to identify the molecular mechanisms associated with reduced sensitivity. Comparison of the *SDHB* sequences of sensitive and resistant isolates revealed that a decreased sensitivity to boscalid was associated with the substitution of a highly conserved histidine residue at codon 277 with either tyrosine (H277Y) or arginine (H277R). In addition, an isoleucine to valine (I279V) substitution occurred in some isolates at codon 279, but did not correlate with a decreased sensitivity to boscalid. However, isolates with a resistant phenotype, but no mutations in the *SDHB* gene were also identified, indicating mutations in the succinate dehydrogenase subunit C (*SDHC*) and D (*SDHD*) genes, or some other mechanisms may also occur in *D. tanaceti*. A high resolution melt analysis assay was developed to allow rapid detection of the identified *SDHB* mutations. This assay was subsequently used to genotype a *D. tanaceti* population collected in 2012. A subset of isolates within this population (n = 23) were characterised by testing the *in vitro* growth response to varying concentrations of boscalid to verify the range of sensitivities associated with the SDHB substitutions. Within the 2012 population, the H277Y substitution was the most dominant, occurring in 52.3% of isolates, while the H277R substitution occurred in 9.3% of isolates. The results indicated that the majority of isolates contained mutations in the *SDHB*. The implications of boscalid resistance in field populations are discussed.

6.2 INTRODUCTION

The perennial nature of pyrethrum (*Tanacetum cinerariifolium)* permits pathogen populations to undergo polyetic disease epidemics throughout the life of the crop. If disease levels become severe and impact on pyrethrum production and profitability, early termination of the crop may be necessary. To prevent this, efficient disease control is necessary to decrease pathogen inoculum during periods which are conducive to infection. Practices such as reducing planting density, site selection and strategic irrigation are used to decrease the incidence of fungal disease (Pethybridge & Hay, 2001, Pethybridge et al., 2008a). However, the pyrethrum industry remains reliant on fungicides for disease control.

One of the risks associated with the use of fungicides for disease control is that fungi may develop resistance to the chemical. This results in individuals within populations with heritable, reduced sensitivity to the fungicide and a subsequent decrease in effectiveness of this method of disease control. Resistance develops from the mutation of genes, involved in the cellular mechanisms associated with the mode of action of the fungicide (Ma & Michailides, 2005, Brent et al., 1998). Resistance can be described as qualitative (individuals are either sensitive or highly resistant) or quantitative (there is a broad range in sensitivities between individuals) (Deising et al., 2008).

Fungicides are placed into different fungicide group codes (FRAC codes) according to their mode of action (FRAC, 2015). Fungicides with a single-site mode of action (e.g. boscalid and cyprodinil) are more susceptible to the development of resistance than those with a multi-site mode of action (e.g. chlorothalonil) (Deising et al., 2008). Furthermore, individuals with resistance to one member of a FRAC code may exhibit cross-resistance to other fungicides

within the same FRAC code, despite not being directly exposed to the other fungicides, due to sharing the same mode of action. Fungicide resistance can be identified by quantifying fungal growth, germination or spore production in response to varying concentrations of fungicide *in vitro*.

Boscalid (Filan®; Nufarm Ltd.; FRAC code 7) was introduced into the pyrethrum spring fungicide program in 2005 to control the dominant fungal pathogen at that time: *Stagonosporopsis tanaceti* (Pethybridge & Wilson, 1998, Vaghefi et al., 2012). Prior to the introduction of boscalid, control of *S. tanaceti* had been based on the use of azoxystrobin (Amistar®; Syngenta Ltd.; FRAC code 11) and difenoconazole (Score®; Syngenta Ltd.; FRAC code 3). Post-2005, the spring fungicide program utilised boscalid and azoxystrobin, with the incorporation of cyprodinil (Chorus®; Syngenta Ltd.; FRAC code 9) in 2009 providing an alternative fungicide group for control. A number of mechanisms to prevent, or at least delay, the occurrence of resistance was were implemented by the pyrethrum industry. These included restricting the number of individual fungicide applications to a maximum of two per season and tank mixing of fungicides with single-site modes of action with the multi-site protectant chlorothalonil (Bravo®; Syngenta Ltd.; FRAC code M5). An additional benefit of the use of boscalid, azoxystrobin and cyprodinil from 2009 was that they provided control of *Didymella tanaceti* (syn: *Microsphaeropsis tanaceti*), at the time a minor pathogen of pyrethrum causing tan spot (Pearce, Chapter 3, Pethybridge et al., 2008b). However by 2012, tan spot had become the dominant fungal disease in pyrethrum (Hay et al., 2015). It has been proposed that the rapid increase in disease incidence and severity associated with *D. tanaceti* from 2006 to 2012 could be at least partially attributed to a decreased sensitivity to fungicides providing *D. tanaceti* with a competitive advantage over susceptible species (Hay

et al., 2015, Pethybridge et al., 2008b). Previous, *in vitro* fungicide testing of field isolates of *D. tanaceti* identified that isolates remained sensitive to azoxystrobin and cyprodinil (Hay et al., 2015, Pethybridge et al., 2008b). However, *in vitro* testing of *D. tanaceti* field isolates collected in 2009 and 2011 identified the presence of a boscalid-resistant phenotype. Furthermore, the majority of *D. tanaceti* isolates collected in 2011 from fields with severe foliar disease, had EC_{50} values above 50.0 µg a.i./mL of boscalid (Hay et al., 2015).

Boscalid was commercially released in 2003 and is a pyridine-carboxamide fungicide that acts as a succinate dehydrogenase inhibitor (SDHI). Succinate dehydrogenase is an enzyme necessary for cellular respiration (Hägerhäll, 1997) and is constructed from four nuclear encoded protein subunits; SDHA, SDHB, SDHC and SDHD (Horsefield et al., 2006, Avenot & Michailides, 2010, Huang & Millar, 2013). The SDHB subunit contains three iron-sulphur clusters (2Fe-2S, 4Fe-4S and 3Fe-4S) which transfer electrons for the reduction of ubiquinone. The ubiquinone binding site (Q-site) is formed by the interface of the SDHB, SDHC and SDHD subunits (Hägerhäll, 1997, Horsefield et al., 2006, Scalliet et al., 2012, Fraaije et al., 2012). Boscalid inhibits ubiquinone reduction by binding to the Q-site, restricting cellular respiration and resulting in cell death. Mutations within each of the subunits have been correlated with boscalid resistance within field isolates and laboratory-induced mutants of different fungal species (Avenot & Michailides, 2010, Sierotzki & Scalliet, 2013). However, a conserved histidine (H) residue in the third iron-sulphur complex (3Fe-4S) within the SDHB subunit was proposed to play a central role in ubiquinone binding and reduction and is essential for the attachment of boscalid (Fraaije et al., 2012, Horsefield et al., 2006). In ascomycetes, boscalid resistance has been associated with mutations in the *SDHB* resulting in the substitution of this conserved histidine residue with tyrosine (Y),

arginine (R) or leucine (L) (Avenot et al., 2012, Miyamoto et al., 2010, Avenot et al., 2008, Veloukas et al.). Boscalid resistance in *Botrytis cinerea* has also been associated with substitutions (P225F and N230I) in the second iron-sulphur complex (4Fe-4S) (Veloukas et al., 2011, Yin et al., 2011).

The mutations associated with boscalid resistance in *D. tanaceti* have not been identified. Current methods of detecting resistant isolates rely on *in vitro* testing of fungal growth responses to varying concentrations of boscalid. This process is labour intensive which restricts the number of isolates which can be screened. While it is hypothesised that mutations in each of the SDH subunits, or other regions, may be associated with a boscalid resistant phenotype, this study initiated the examination of SDH mutations via focussing on the SDHB subunit. It aimed to evaluate the correlation between mutations in the *SDHB* gene and proposed boscalid phenotypes by examining the *SDHB* gene of isolates collected from 2009 – 2011 with varied responses to boscalid *in vitro*. Further, a genotyping assay using high resolution melt (HRM) analysis was developed and verified as a means of rapidly differentiating the *SDHB* alleles identified. The protocols developed were then used to establish the proportion of *D. tanaceti* field isolates collected in 2012 which contained each of the *SDHB* alleles.

6.3 MATERIALS AND METHODS

6.3.1 Identification of the *SDHB* alleles associated with boscalid in-sensitivity

6.3.1.1 In vitro *testing of boscalid response*

Commercial grade boscalid (Filan®; 50% active ingredient (a.i)) was dissolved in distilled water and made up to 75% (v/v) ethanol to provide a stock solution of 50 mg a.i/mL. From the initial stock solution dilutions in autoclaved deionised water produced additional stock solutions of: 25, 2.5, 0.25 and 0.025 mg a.i/mL. Autoclaved potato dextrose agar (PDA; Amyl Media) was cooled to 55°C and sufficient volumes of stock solution added to obtain final boscalid concentrations of: 0.01, 0.05, 0.5, 5, 50 and 250 µg a.i/mL. No fungicide was added to the non-amended control concentration (0 µg a.i/mL). Approximately 20 mL of the amended PDA was added to plastic petri plates (90 mm diameter). The concentration of ethanol within each plate did not exceed 0.38% (v/v). A 7 mm diameter plug taken from the margin of an actively growing colony of each *D. tanaceti* isolate was placed onto plates of each fungicide concentration in triplicate and incubated at 21°C in the dark. Mycelial growth was measured across two perpendicular lines for each replicate plate of each fungicide concentration after 9 d incubation. For each isolate the average colony radius was calculated for each fungicide concentration and expressed as a proportion of the average radius of the non-amended controls. Data was analysed in R v3.1.3 (R Core Team, 2015). For isolates with complete growth inhibition at the boscalid concentrations tested, the package *drc* (Ritz & Streibig, 2005) was used to fit a dose response model. The model used an exponential decay function, and was used to calculate the effective dose required for a 50% reduction in in growth. EC_{50} discriminatory dose ranges were also calculated for all isolates as the concentration range at which radial growth was reduced to $\leq$ 50% of the non-amended controls. Additional R packages used for data manipulation and graphing included *reshape* (Wickham, 2007) and *lattice* (Deepayan, 2008).

6.3.1.2 Isolates for detection of the SDHB *alleles associated with boscalid resistance*

To identify the molecular mechanisms associated with boscalid in-sensitivity a subset (*n* = 48) of *D. tanaceti* isolates collected from 2009 – 2011 of known boscalid sensitivity were selected (Table 6.1). The EC_{50} discriminatory boscalid concentration range of these isolates had been previously identified from *in vitro* testing (Hay *et al.,* 2015; F. Hay, unpublished data; Table 6.1). This work followed the protocol outlined previously, except a reduced range of boscalid concentrations were used (0, 0.05, 0.5, 5, and 50 µg a.i/mL). Based on the EC_{50} ranges these isolates were initially characterised into four distinct phenotypes consisting of sensitive (S; EC_{50} range 0 – 0.5 µg a.i/mL), moderately resistant (MR; EC_{50} range 0.5 – 5.0 µg a.i/mL), resistant (R; EC_{50} range 5.0 – 50 µg a.i/mL) and highly resistant (HR: EC_{50} range > 50 µg a.i/mL) isolates (Table 6.1).

To validate the proposed boscalid phenotype EC_{50} ranges and examine their correlation with the identified *SDHB* alleles, a subset (*n* = 23; Table 6.2) of *D. tanaceti* isolates were randomly selected from a population collected in July/August 2012 (*n* = 323). Isolates were collected from two fields in each of Sassafras, Tasmania, Australia (41° 17' South, 146° 30' East) (S1 and S2), and Table Cape, Tasmania, Australia (40° 56' South, 145° 43' East) (TC1 and TC2). Within each field two parallel 50 m transects were sampled at 0.5 m intervals and *D. tanaceti* isolates identified, isolated, stored and the genomic DNA extracted as described by Pearce (Chapter 4). *In vitro* fungicide testing and data analysis followed the protocol outlined previously and included a wider range of boscalid concentrations than tested by Hay et al. (2015).

.3.1.3 Amplification and sequencing of the SDHB *gene*

A custom *D. tanaceti* database was derived from nucleotide sequence data obtained from 454 genomic sequencing of *D. tanaceti* strain BRIP 61988 (Pearce, Chapter 4). This custom nucleotide database was used to search for orthologues of an *SDHB* gene in *D. tanaceti*. A discontinuous megablast in Geneious v7.1 (Biomatters Ltd.), with the complete *SDHB* gene of *Alternaria alternata* isolate 1178-W1 (GenBank acc: EU178851) identified a 416 base pair (bp) fragment within the custom *D. tanaceti* nucleotide database with high similarity to the 3' end of an *SDHB* gene. In addition, a discontinuous megablast of a custom nucleotide database of *S. tanaceti* derived from 100 bp pair end sequence reads (assembly size ~40.8 Mbp) (Vaghefi et al., 2015, Wingfield et al., 2015) with EU178851 identified a complete *SDHB* gene. Due to their close phylogenetic relationship (Pearce, Chapter 3), the putative *SDHB* gene of *S. tanaceti* was used as a reference sequence for primer design to amplify the *D. tanaceti SDHB* and for species comparison of the *SDHB* gene and protein characteristics. MAFFT v7.017 (Katoh et al., 2002) was used to align the *D. tanaceti SDHB* fragment, putative *S. tanaceti SDHB* gene, complete *SDHB* genes of *A. alternata*, *A. solani* (KC517310), *Corynespora cassiicola* (AB548738), *Mycosphaerella graminicola* (JF916687) and cDNA sequence of the *SDHB* of *Stagonosporopsis cucurbitacearum* (HQ156460). The alignment was used to identify highly conserved coding regions proximate to the *SDHB* start and stop codons. Polymerase chain reaction (PCR) primers were designed to target these regions using Primer3 v2.3.4 (Untergasser et al., 2012, Koressaar & Remm, 2007) and Netprimer (Premier Biosoft International, http://www.premierbiosoft. com/ netprimer/index.html).

The partial *SDHB* of *D. tanaceti*, including coverage of the three iron-sulphur units, was amplified and sequenced for the 48 *D. tanaceti* isolates of known boscalid EC_{50} range (Table

6.1) from the 2009 – 2011 population and the 23 *D. tanaceti* isolates from the 2012 population with the primers SDHB-F (5'- ACGCACTTTTGCTCGTCTGGCTAC -3') and SDHB-R2 (5'- CATGCTCTTCTTGATCTCRGC -3'). PCR reactions were performed in a C1000 thermocycler (BioRad) in a total volume of 20 µL. Reaction mixes contained 1 × TopTaq polymerase (QIAGEN), 10 × PCR buffer, 10 × CoralLoad, 0.2 µM of each primer, 200 µM of each dNTP (Bioline) and 3 ng of genomic DNA. Conditions for amplification were an initial denaturation of 5 min at 94°C, followed by 30 cycles of denaturation at 94°C for 30 s, annealing at 56°C for 30 s and extension at 72°C for 1 min, with a final elongation of 72°C for 5 min on the last cycle. Amplified products were visualised via gel electrophoresis using a 1.5% (w/v) agarose gel pre-stained with GelRed^{TM} (Biotium Inc.) in 1 × TAE buffer. PCR products were prepared for sequencing using the UltraClean PCR-clean up kit (Mo Bio Laboratories Inc.), according to the manufacturer's instructions and sequenced in both directions at the Australian Genome Research Facility (AGRF; Melbourne, Australia) using Big Dye Terminator v3.1 chemistry and capillary separation on an AB 3730xl DNA Analyser (Applied Biosystems).

The consensus sequence of the *SDHB* gene of each isolate was obtained from assembly of the forward and reverse sequences in Geneious. The consensus sequences of each isolate were then aligned using MAFFT to identify polymorphisms between isolates. The coding sequence of the *D. tanaceti SDHB* was inferred following alignment of the consensus sequences to EU178851 and AB548738. The amplicons were compared to those within GenBank using BLASTn (Agarwala et al., 2015, Benson et al., 2015) to confirm the region as homologous to a *SDHB* gene and BLASTp (Altschul et al., 1997, Altschul et al., 2005) against the conserved domain database (CDD) (Marchler-Bauer et al., 2015).

The phenotypes associated with each of the identified polymorphisms were evaluated to identify correlation between amino acid substitutions and phenotype for the 2009 – 2011 and 2012 populations.

6.3.2 Development of a high resolution melt (HRM) assay for *SDHB* allele detection

Based on analysis of the *SDHB* gene sequence data obtained for *D. tanaceti*, polymorphisms resulting in amino acid changes within the third conserved cysteine region associated with the third iron-sulphur unit (3Fe-4S) were identified. To allow rapid identification of the polymorphisms, the primer pair SDHB-3C-HRM-F1 (5'- CTCAACAACAGCATGAGCTT G -3') and SDHB-3C-MT-HRM-R (5'- CAGCGCAGGGTTAAGTCC -3') was designed, to amplify an 85 bp product containing the polymorphic region. The program uMELT (Dwight et al., 2011) was used to predict the discrimination of *SDHB* alleles of the resultant PCR product using an *in silico* HRM algorithm for each known allele.

To confirm the discrimination capacity of alleles via HRM analysis, a subset (n = 10) of the sequenced *D. tanaceti* isolates, including three of each known allele were analysed via real-time PCR, followed by HRM. PCR amplification and HRM analysis were undertaken in a Rotor-Gene Q real-time PCR machine (QIAGEN). Reaction mixes contained 2 × Type-it HRM buffer (QIAGEN), 0.7 µM of each primer, 2 ng of genomic DNA and sufficient nuclease free water to produce a final reaction volume of 10 µL. Conditions for amplification were an initial denaturation of 5 min at 95°C, followed by 40 cycles of denaturation at 95°C for 10 s, annealing at 50°C for 30 s and extension at 72°C for 10 s. Data acquisition occurred following the extension phase of each cycle. Amplified products were

Table 6.1. Boscalid growth response and amino acids encoded by polymorphic codons of the succinate dehydrogenase B subunit gene of the 2009 – 2011 collected *Didymella tanaceti* isolates.

Strain[a]	Year collected	Location[b]	EC_{50} range (µg a.i/mL)[c]	Phenotype[d]	Amino acid at codon 277[e]	Amino acid at codon 279[e]
F50607A	2009	Kindred	0 – 0.05	S	H	I
F50607B	2009	Kindred	0 – 0.05	S	H	I
F52010A	2009	Kindred	0 – 0.05	S	H	I
041-0002	2010	Don	0 – 0.05	S	H	I
041-0011	2010	Don	0 – 0.05	S	H	I
041-0013	2010	Don	0 – 0.05	S	H	I
041-0028	2010	Kindred	0 – 0.05	S	H	I
041-0034	2010	Penguin	0 – 0.05	S	H	I
041-0005	2010	Cuprona	0.05 – 0.5	S	H	I
041-0010	2010	Don	0.05 – 0.5	S	H	I
041-0012	2010	Don	0.05 – 0.5	S	H	I
041-0026	2010	Don	0.05 – 0.5	S	H	I
041-0032	2010	Penguin	0.05 – 0.5	S	H	I
041-0039	2010	Table Cape	0.05 – 0.5	S	H	V
041-0035	2010	unknown	0.5 – 5	MR	H	I
041-0036	2010	Table Cape	0.5 – 5	MR	H	I
041-0038	2010	Table Cape	0.5 – 5	MR	H	I
041-0024	2010	Cuprona	0.5 – 5	MR	R	I
041-0031	2010	Penguin	0.5 – 5	MR	R	I
041-0003	2010	Howth	0.5 – 5	MR	Y	I
041-0020	2010	Wesley Vale	0.5 – 5	MR	Y	I
041-0027	2010	Wesley Vale	5 – 50	R	H	I
041-0018	2010	Cuprona	5 – 50	R	R	I
041-0004	2010	Howth	5 – 50	R	Y	I
041-0009	2010	Howth	5 – 50	R	Y	I
041-0015	2010	Howth	5 – 50	R	Y	I
041-0041	2010	Table Cape	5 – 50	R	Y	I
CF196	2011	Stowport	5 – 50	R	H	I
CF30	2011	Forest	5 – 50	R	R	I
CF78	2011	Forest	5 – 50	R	R	I
041-0007	2010	Don	> 50	HR	H	I
041-0016	2010	Wesley Vale	> 50	HR	H	I
041-0025	2010	Penguin	> 50	HR	H	I
041-0040	2010	Table Cape	> 50	HR	H	I
041-0001	2010	Don	> 50	HR	Y	I
041-0022	2010	Wesley Vale	> 50	HR	Y	I
041-0023	2010	Wesley Vale	> 50	HR	Y	I
CF149	2011	Kindred	> 50	HR	H	I
CF34	2011	Forest	> 50	HR	H	I
CF54	2011	Forest	> 50	HR	H	I
CF55	2011	Forest	> 50	HR	H	I
CF103	2011	Forest	> 50	HR	Y	I
CF142	2011	Gawler	> 50	HR	Y	I
CF143	2011	Gawler	> 50	HR	Y	I
CF200	2011	Stowport	> 50	HR	Y	I
CF39	2011	Forest	> 50	HR	Y	I
CF56	2011	Forest	> 50	HR	Y	I
CF88	2011	Kindred	> 50	HR	Y	I

[a] Isolates stored in the Tasmanian Institute of Agriculture fungal collection, Tasmania, Australia. All isolates originally recovered from pyrethrum leaves.

[b] Location in Tasmania, Australia.

[c] EC_{50} discriminatory dose range calculated as the concentration range in which radial growth was reduced to ≤50% of the non-amended controls identified by Hay et al. (2015) and F. Hay (unpublished data).

[d] S= susceptible, MR= moderately resistant, R= resistant, HR= highly resistant.

[e] Amino acid: H = histidine (wild type); Y = tyrosine; R = arginine; I = isoleucine (wild type); V = valine.

melted to confirm the amplification of a single amplicon and the ability to differentiate the *SDHB* alleles. Products were melted in 0.2°C intervals from 76 to 90°C with a 10 s hold at each temperature prior to data acquisition. The data was analysed in the Rotor-Gene Q series software (QIAGEN) to confirm the occurrence of discrete melt curves for each allele.

6.3.3 *SDHB* allele frequency in the 2012 field populations

The *SDHB* HRM assay was used to genotype the entire population of *D. tanaceti* collected in 2012. Within the HRM analysis the subset of sequenced isolates from the 2012 population were employed as "pseudo unknowns" to validate the identification of alleles. Real-time PCR and HRM were undertaken as previously described. Within each run, three isolates of each known allele were selected from the 2009 – 2011 population and included as known-genotype isolates (employed as positive controls). Due to a small difference in the melting temperature of the PCR product of two of the identified alleles, data analysis of each run was undertaken in the Rotor-Gene Q series software and the Rotor Gene ScreenClust HRM software v1.10.1.2 (QIAGEN) (Reja et al., 2010) to assist with the genotyping of the two alleles. Within each run, quantitation analysis of the cycling green channel with dynamic tube and slope correction was used to recognise isolates with poor amplification efficiency. Isolates with a cycling threshold (CT) value greater or lower than the median CT value of all isolates in the run +/- 1.5 CT were removed from further analyses. Real-time PCR amplification and HRM were repeated for these isolates to obtain sufficient amplification. For analysis of each run in the ScreenClust software, data was normalised within left boundaries (78°C – 79°C) and right boundaries (86°C – 87°C). An "unsupervised" analysis, using *K*-means and the known-genotype isolates employed as pseudo-unknowns, was used to identify any new putative genotypes, which would separate into discrete clusters or appear as

outliers within clusters. The number of clusters and principle components (PC) were determined using the gap statistic (Tibshirani et al., 2001). Samples were genotyped using the "supervised" mode. The known-genotype isolates were used to calculate a cluster distribution using linear discriminant analysis (LDA), with the centre of each cluster equal to the mean of the known-genotype isolates of each identified genotype. The number of PC was selected using cross-validation to find the number of PC that produced the lowest number of misclassifications. For each isolate the probability of belonging to each genotype cluster was calculated (Reja et al., 2010). Allelic discrimination in the Rotor Gene-Q series software used melt curve analysis of the HRM channel (*d*F/*d*T against temperature). A threshold fluorescence level, 0.5 units above the baseline fluorescence, was selected to distinguish a single melt peak (max *d*F/*d*T value) per isolate. Peak bins for each allele were identified from the melt peaks of the known-genotype isolates. For each isolate the melting peak was calculated and the closest allele peak bin identified to determine the isolate genotype. Allele calls from Rotor Gene-Q series and ScreenClust analysis were compared for each isolate. Furthermore, the allele calls for the subset of sequenced isolates from the 2012 population were analysed to confirm that they were correct. The proportion of isolates with each of the identified *SDHB* mutations were calculated for each of the four fields and the overall population.

6.4 RESULTS

6.4.1 Identification of the *SDHB* alleles associated with boscalid resistance

PCR amplification and sequencing with primers SDHB-F/SDHB-R2 resulted in a 965 bp product in the *D. tanaceti* isolates sequenced. Based on comparison to the 416 bp *SDHB* fragment of *D. tanaceti* obtained from the custom nucleotide database of *D. tanaceti* (covering the 3' end of *D. tanaceti SDHB* gene) and the *SDHB* gene of other species, the entire *SDHB* gene of *D. tanaceti* was predicted to be 1,033 bp in length (Fig. 6.1). BLASTn identified the *SDHB* gene of *D. tanaceti* to be highly similar to the *SDHB* genes of *A. alternata* and *A. solani*. The *D. tanaceti SDHB* gene was arranged in three exons and was predicted to encode a protein of 306 amino acids (Fig. 6.1). Gene intron splice sites were identical to *A. alternata*, with the exception of an intron located 6 bp upstream from the first conserved cysteine region in *A. alternata*, which was absent in *D. tanaceti*. This intron also occurred in *A. solani*, *M. graminicola*, and *C. cassiicola* (Fig. 6.1 & Fig. 6.2). The amino acids proximate to the splice site were identical in these species, and also occurred in *D. tanaceti* (Fig. 6.2). Furthermore, the structural arrangement of the *SDHB of D. tanaceti* was identical to the putative *SDHB* identified for *S. tanaceti*. BLASTp analysis of the encoded SDHB protein identified protein domains, including a 2Fe-2S iron-sulphur cluster binding domain (Conserved Protein Domain accession = pfam13085) and a 4Fe-4S di-cluster domain (CPD = pfam13534), which were characteristic of an SHDB protein. Comparison of the encoded SDHB protein sequence of *D. tanaceti* with other fungal species showed high amino acid conservation of the three cysteine rich clusters, associated with the iron-sulphur centres (Fig. 6.2).

MAFFT alignment of the encoded SDHB protein of *D. tanaceti* isolates identified two polymorphic amino acid residues located within the third conserved cysteine region. A histidine (CAC) to tyrosine (TAC) (H277Y), or arginine (CGC) (H277R), substitution occurred at codon 277, and an isoleucine (ATT) to valine (GTT) (I279V) substitution occurred at codon 279. Isolates with compound substitutions at codons 277 and 279 were not found.

Within the isolates selected from 2009 – 2011, 27 contained a histidine (H277, wild type; (WT)), 16 contained a tyrosine (H277Y) and 5 contained arginine (H277R) at codon 277 (Table 6.1 & 6.3). A single isolate was identified with an isoleucine to valine substitution at codon 279 (I279V), but contained a histidine at 277 (H277). In addition, the fourteenth nucleotide of the second intron of 15 *D. tanaceti* isolates contained an adenine (A) to guanine (G) transition Evaluation of the boscalid phenotypes and the associated substitutions at codons 277 and 279 identified that all isolates characterised as exhibiting a boscalid sensitive phenotype (S; EC_{50} range of 0 — 0.5 µg a.i/mL) contained a H277 (WT). Additionally, one isolate with a boscalid sensitive phenotype contained an I279V substitution (Table 6.1 & 6.3). However, some of the isolates with a moderately resistant (MR; EC_{50} range 0.5 – 5 µg a.i/mL L), resistant (R; EC_{50} range 5 – 50 µg a.i/mL) and highly resistant (HR; EC_{50} range > 50 µg a.i/mL) phenotype also exhibited a WT *SDHB* gene (Table 6.1 & 6.3). Isolates with a H277R substitution (n = 5) were mainly associated with an R phenotype, though 2 isolates had an MR phenotype (Table 6.1 & 6.3). Of the isolates with a H227Y substitution (n = 16), 10 had an HR phenotype, 4 had an R phenotype and 2 had a MR phenotype (Table 6.1 & 6.3).

6.4.1.1 Validation of boscalid sensitivities associated with phenotypes

The *SDHB* gene sequences of the 23 randomly selected *D. tanaceti* isolates from the 2012 population were identical in structure to the *SDHB* gene identified in the 2009 – 2011 isolates. No additional mutations or combinations of mutations leading to substitutions were identified. Of the 23 isolates, 8 contained a H277 (WT), 13 contained a H277Y substitution and 2 contained H277R substitution (Table 6.2 & 6.3). A single isolate was identified with an I279V substitution (also contained a H277). The A to G transition in the second intron occurred in 5 isolates. *In vitro* boscalid fungicide testing identified no isolates with an EC_{50} range within the lowest tested concentration (0 – 0.01 µg a.i/mL) (Table 6.2 & 6.3). Complete inhibition of mycelial growth at particular boscalid concentrations was only identified for three *D. tanaceti* isolates (Table 6.2). Isolates 041-0231, 041-0227 and 041-0335 were completely inhibited (0% growth) at 5, 50 and 250 µg a.i/mL, respectively (Table 6.2). Modelled EC_{50} values were only calculated for isolates for which growth was completely inhibited at the tested boscalid concentrations. The dose response modelled EC_{50} estimates of these isolates where within the EC_{50} range estimates (Table 6.2). The radial growth of the remaining isolates was not completely inhibited at any of the boscalid concentrations, though radial growth of each isolate was reduced compared to the non-amended control, and was < 50% of the average plate growth of the control at 250 µg a.i/mL (Table 6.2).

Evaluation of the boscalid phenotypes and the associated substitutions at codons 277 and 279 identified that the isolates characterised as exhibiting a boscalid sensitive phenotype contained a H277 (WT) or an I279V substitution (Table 6.2 & 6.3). However, some of the

isolates with a MR, R and HR phenotype also exhibited a WT *SDHB* gene (Table 6.2 & 6.3). Furthermore, isolates 041-0354 and BRIP 61990, which shared the highest relative growth at 250 µg a.i/mL and a WT *SDHB* gene, both had an HR phenotype (Table 6.2). H277Y substitutions were identified in 13 isolates. Of these, 11 had an R phenotype and the remainder had an HR phenotype (Table 6.2 & 6.3). H277R substitutions were identified in 2 isolates which had conflicting *in vitro* results. One of these isolates had an MR phenotype, while the other had an HR phenotype (Table 6.2).

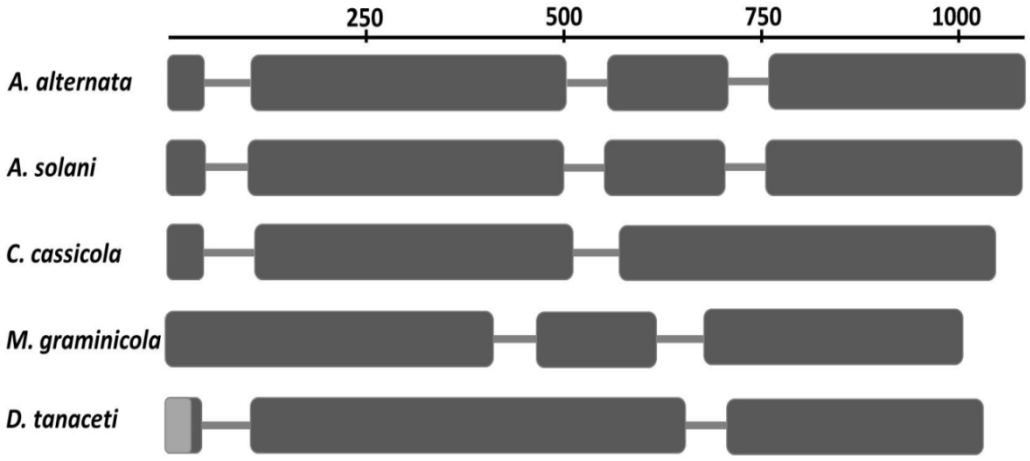

Fig. 6.1. **Structural arrangement of the *succinate dehydrogenase subunit B* gene of *Didymella tanaceti*, *Mycosphaerella graminicola* (GenBank acc: JF916687), *Corynespora cassiicola* (AB548738), *Alternaria solani* (KC517310) and *A. alternata* (EU178851).** Squares indicate exons. Lines connecting the squares indicate introns. The size of the light grey shaded region in the first exon of *D. tanaceti* is predicted from alignment with other fungal species. The scale bar indicates gene length (base pair).

Table 6.2. Boscalid response and amino acids encoded by polymorphic codons of the succinate dehydrogenase B subunit gene of the 2012 collected *Didymella tanaceti* isolates.

Isolate code[a]	Growth percentage of the negative control (0 µg a.i/mL) (%) Boscalid concentration (µg a.i/mL)							EC_{50} range (µg a.i/mL)[b]	EC_{50} estimate ± SE (µg a.i/mL)[c]	Phentoype[d]	Amino acid at codon 277[e]	Amino acid at codon 279[e]
	0	**0.01**	**0.05**	**0.5**	**5**	**50**	**250**					
041-0231	100	82.39	33.45	2.817	0	0	0	0.01–0.05	0.03 ± 0.00	S	H	I
041-0227	100	93.27	82.15	27.61	2.694	0	0	0.05–0.5	0.27 ± 0.02	S	H	V
041-0335	100	102.0	92.82	73.30	22.84	15.10	0	0.5–5	2.13 ± 0.62	MR	H	I
041-0252	100	103.1	100.0	77.17	22.83	8.66	6.30	0.5–5	NA[f]	MR	R	I
041-0297	100	100.8	98.06	75.97	53.10	14.34	12.79	5–50	NA	R	H	I
041-0242	100	102.2	98.53	85.29	71.69	34.19	17.28	5–50	NA	R	Y	I
041-0201	100	99.42	101.0	93.64	70.52	28.90	18.50	5–50	NA	R	H	I
041-0150	100	100.7	102.2	92.13	62.17	26.59	19.10	5–50	NA	R	Y	I
041-0095	100	103.2	100.4	85.43	55.87	27.13	21.05	5–50	NA	R	Y	I
041-0287	100	97.49	97.13	88.17	77.78	34.41	21.15	5–50	NA	R	Y	I
BRIP 61988	100	99.25	95.9	87.31	69.78	38.43	22.01	5–50	NA	R	Y	I
041-0116	100	100.8	93.28	94.07	71.54	39.92	25.69	5–50	NA	R	Y	I
041-0214	100	98.08	95.4	90.04	63.98	42.15	27.97	5–50	NA	R	Y	I
041-0370	100	102.9	103.3	93.80	76.03	48.35	28.10	5–50	NA	R	H	I
041-0176	100	109.4	110.3	100.9	82.48	43.16	30.34	5–50	NA	R	Y	I
041-0383	100	113.6	113.6	89.49	75.88	45.53	30.74	5–50	NA	R	Y	I
041-0352	100	100.7	100.0	88.26	69.75	46.98	31.32	5–50	NA	R	Y	I
041-0374	100	101.9	102.7	93.13	77.48	48.47	33.21	5–50	NA	R	Y	I
041-0414	100	104.0	103.6	85.89	67.74	50.40	25.00	50–250	NA	HR	R	I
041-0408	100	104.5	104.9	86.23	83.00	58.70	33.60	50–250	NA	HR	Y	I
041-0325	100	97.53	98.59	87.99	74.91	51.94	33.92	50–250	NA	HR	Y	I
041-0354	100	104.6	105.7	92.37	79.77	51.91	46.18	50–250	NA	HR	H	I
BRIP 61990	100	101.2	103.1	94.23	83.08	57.31	47.69	50–250	NA	HR	H	I

[a] Isolates stored in the Tasmanian Institute of Agriculture fungal collection, Tasmania, Australia. Isolates with BRIP codes also stored at the Queensland Plant Pathology herbarium collection, Brisbane, Australia. All isolates originally recovered from Tasmanian pyrethrum leaves.
[b] EC_{50} discriminatory dose range calculated as the boscalid concentration range in which radial growth was reduced to ≤50% of the non-amended controls (0 µg a.i/mL).
[c] Estimated effective dose ± the standard error (SE) required for a reduction in radial growth of 50% calculated from a dose response model, using an exponential decay function.
[d] S= susceptible, MR= moderately resistant, R= resistant, HR= highly resistant.
[e] Amino acid codes: H = histidine (wild type); Y = tyrosine; R = arginine; I = isoleucine (wild type); V = valine.
[f] NA = not applied due to a lack of sufficient data points to provide accurate model.

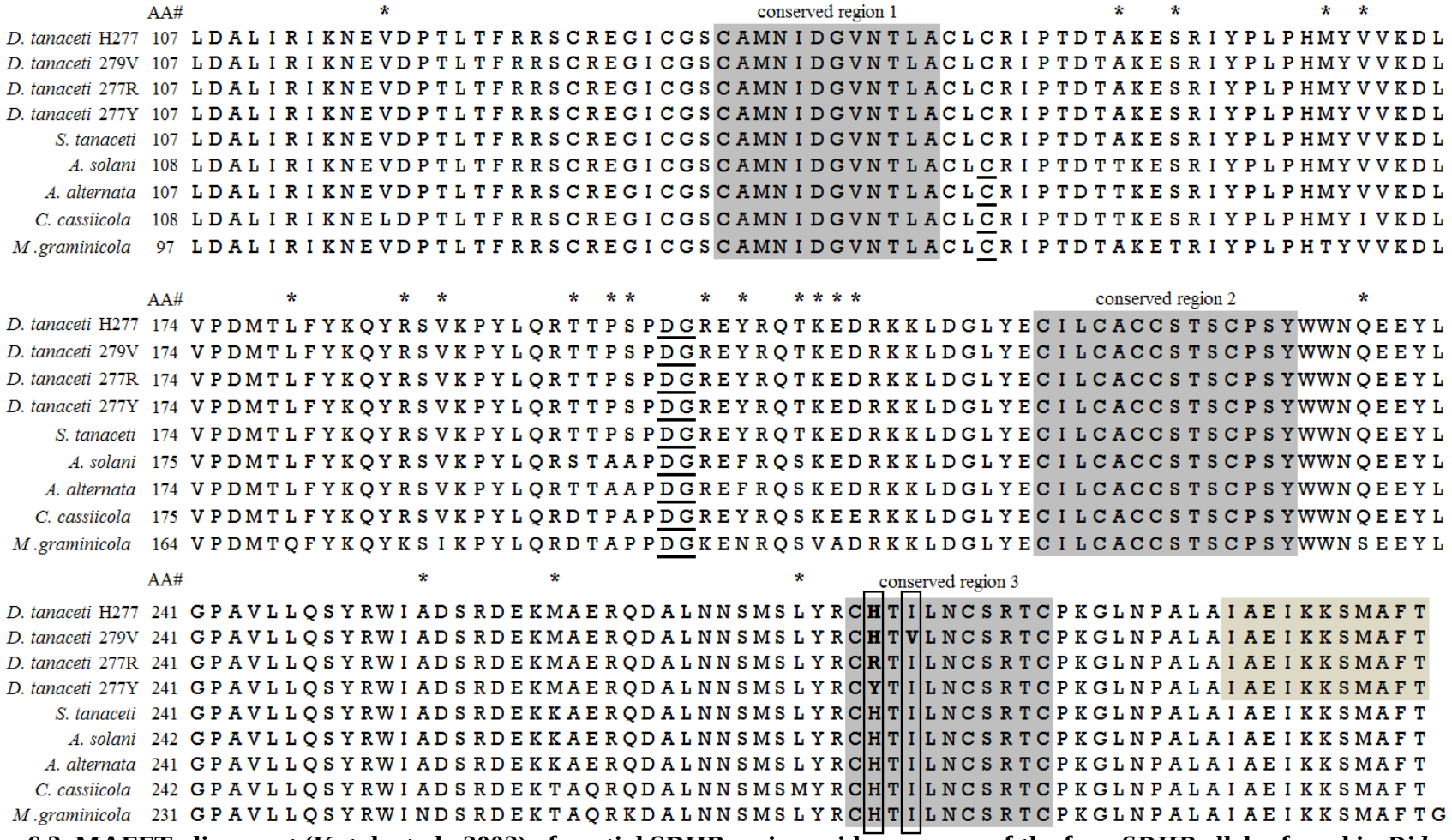

Fig. 6.2. MAFFT alignment (Katoh et al., 2002) of partial SDHB amino acid sequences of the four *SDHB* alleles found in *Didymella tanaceti* (KT591176 – KT591179) with wild type (boscalid susceptible) amino acid sequences of *Stagonosporopsis tanaceti*, *Alternaria solani* (GenBank acc: KC517310), *A. alternata* (EU178851), *Corynespora cassiicola* (AB548738) and *Mycosphaerella graminicola* (JF916687). Reference amino acid numbers relative to each species are located to the left of the alignments. Underlined regions indicate the location of intron splice sites. Asterisks above the alignment indicate polymorphic codons. The dark grey shaded regions indicate the three conserved cysteine regions. Black boxes indicate the amino acid substitutions in the conserved regions which are found at codons 277 and 279 in *D. tanaceti*. The light grey shaded boxes indicate the amino acids inferred from sequence data of *D. tanaceti* strain BRIP 61988.

Table 6.3. Percent of *Didymella tanaceti* isolates of each *SDHB* allele for each EC_{50} range for the subsets of the 2009 – 2011 and 2012 populations.

Population	amino acid at codon 277 + 279[a]	*N*[b]	EC_{50} range[c] (µg a.i/mL)							
			0 – 0.01	0.01-0.05	0 – 0.05	0.05 – 0.5	0.5 – 5	5 – 50	> 50	50 – 250
2009 – 2011[d]		48	S	S	S	S	MR	R	HR	HR
	H + I	26	NT[e]	NT	30.8[f]	19.2	11.5	7.7	30.8	NT
	R + I	5	NT	NT	0	0	40	60	0	NT
	Y + I	16	NT	NT	0	0	12.5	25	62.5	NT
	H + V	1	NT	NT	0	100.0	0	0	0	NT
2012		23								
	H + I	7	0	14.3	NA[g]	0	14.3	28.6	NA	42.9
	R + I	2	0	0	NA	0	50	0	NA	50
	Y + I	13	0	0	NA	0	0	84.6	NA	15.4
	H + V	1	0	0	NA	100.0	0	0	NA	0

[a] Amino acid codes: H = histidine (wild type); Y = tyrosine; R = arginine; I = isoleucine (wild type); V = valine.
[b] *N* = number of isolates in each subset of populations and for each *SDHB* allele in each population.
[c] EC_{50} discriminatory dose range calculated as the boscalid concentration range in which radial growth was reduced to ≤50% of the non-amended controls.
[d] EC_{50} ranges of the 2009 – 2011 isolates identified by Hay et al. (2015) and F. Hay (unpublished data).
[e] NT = upper or lower concentrations of range not included in tested concentration range.
[f] Percent of isolates of each *SDHB* allele for each EC_{50} range.
[g] NA= not applicable as concentration range occurred in additional ranges tested.

6.4.2 *SDHB* allele frequencies in the 2012 field populations

6.4.2.2 Genotyping the 2012 population with the SDHB *HRM assay*

The *SDHB* HRM assay was able to detect and differentiate the three known alleles at codon 277 (Fig. 6.3a) and the two known alleles at codon 279 (Fig. 6.3b). No novel alleles were detected from HRM analysis of the 2012 collected population. Representatives sequences of each *SDHB* allele were deposited in GenBank (accessions: KT591176 – KT591179). The Rotor Gene-Q series software and ScreenClust HRM software produced consistent results for the identification of isolates with H277 (WT) or a H277Y substitution. The "pseudo unknown" isolates from the 2012 population containing these substitutions were also correctly identified. However, the melt profiles of the H277R and the I279V substitutions were similar (Fig. 6.3c), with the melt peaks separated by < 0.1°C. Thirty isolates within the 2012 *D. tanaceti* population were identified with a melt peak and normalised curve/clusters indicative of a H277R or I279V substitution. Analysis of these isolates concurrently in two subsequent runs also failed to clearly distinguish H277R from H279V isolates. Some samples exhibited intermediate melt peaks, resulting in non-distinct clusters, and the results for some isolates were unable to be replicated over the two runs or for multiple sample replicates in the same run. Sequencing the *SDHB* of these isolates, as previously described with SDHB-F and SDHB-R2 identified 25 isolates with a H277R and 5 isolates with an I279V substitution.

The HRM assay indicated that the majority of isolates within each field of the 2012 population contained a mutation in the *SDHB* gene (Table 6.4). The H277Y substitution was the most dominate, occurring in 38.2 and 58.0% of isolates from the two fields at Sassafras, and 47.6 and 57.4% of isolates from the two fields at Table Cape, respectively (Table 6.4).

The incidence of the H277R substitution was higher in the two fields at Table Cape (9.5 and 10.9%; Table 6.4) than the two fields at Sassafras (4.5 and 5.9%; Table 6.4). The I279V substitution only occurred in five isolates collected from field S2. The proportion of isolates with a mutation in the *SDHB* ranged from 44.1 – 68.3% per field and was 59.7% for the overall population (Table 6.4).

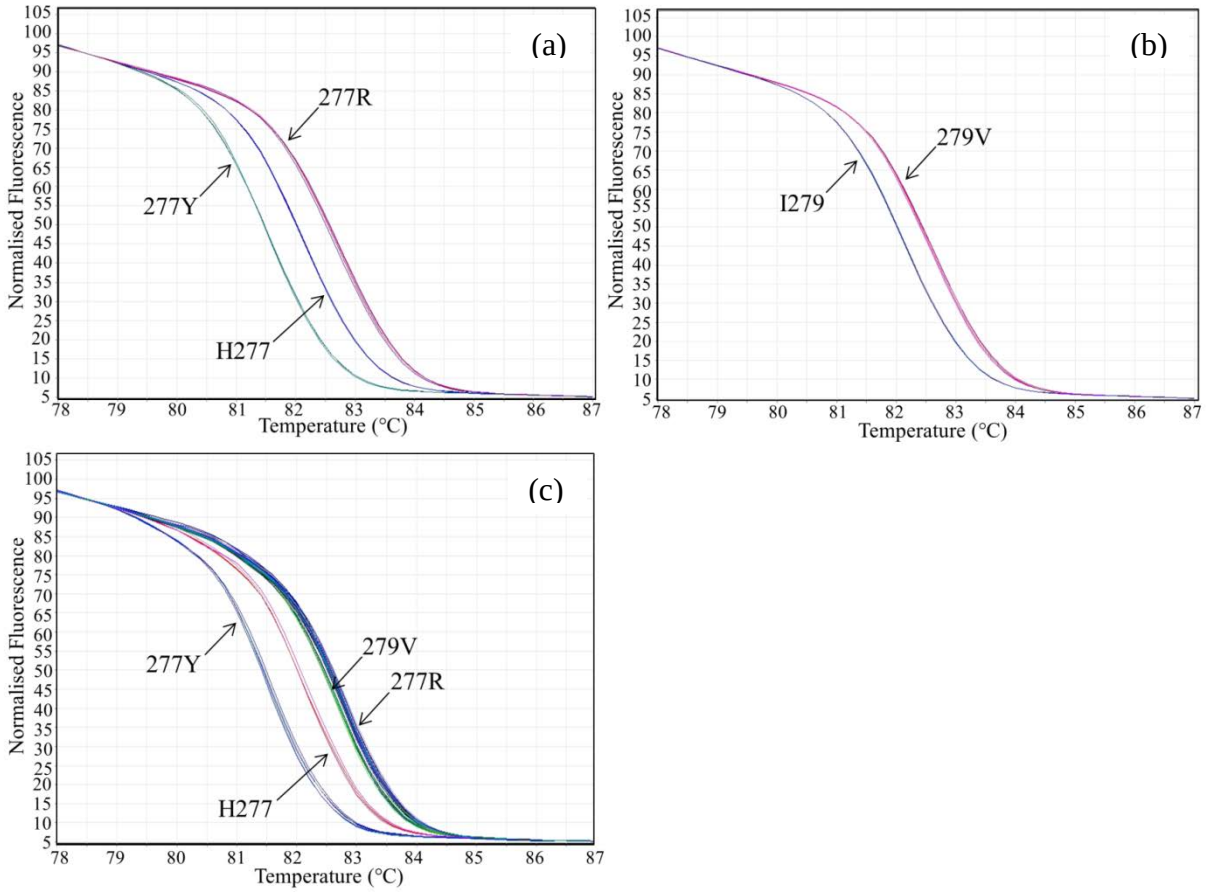

Fig. 6.3. High resolution melt analysis for the detection of polymorphisms in the third conserved cysteine region of the succinate dehydrogenase B subunit gene (*SDHB*) of *Didymella tanaceti*. (a) Normalized fluorescent data of polymorphisms resulting in amino acid substitutions at codon 277: Y = tyrosine; H = histidine and R = arginine**; (b) normalized fluorescent data of polymorphisms resulting in amino acid substitutions at codon 279**: I = isoleucine and V = valine**; (c) fluorescent data of all known *SDHB* alleles.**

Table 6.4. Percentage of field isolates of *Didymella tanaceti* collected in 2012 of each succinate dehydrogenase B subunit (*SDHB*) allele identified by high resolution melt analysis.

Region	Field	*N*	Amino acid at codon 277 (%)[a]			Amino acid at codon 279 (%)[a]		*SDHB* substitution (%) [g]
			H277[b]	277R[c]	277Y[d]	I279[e]	279V[f]	
Sassafras	S1	112	37.5	4.5	58.0	100.0	0	62.5
Sassafras	S2	68	55.9	5.9	38.2	92.7	7.3[h]	44.1
Table Cape	TC1	101	31.7	10.9	57.4	100.0	0	68.3
Table Cape	TC2	42	42.9	9.5	47.6	100.0	0	57.1
Total		323	40.3	7.4	52.3	98.5	1.5	59.7

[a] Percent of isolates.
[b] Histidine at amino acid 277 (wild type).
[c] Tyrosine substitution at amino acid 277.
[d] Arginine substitution at amino acid 277.
[e] Isoleucine at amino acid 279 (wild type).
[f] Valine substitution at amino acid 279.
[g] Percent of isolates with a H277R or H277Y substitution.
[h] Isolates with a I279V substitution at codon 279 contained a histidine at codon 277.

6.5 DISCUSSION

The results from this study provided a first step in characterising mutations in the SDH subunits associated with a boscalid resistant phenotype in *D. tanaceti*. Substitutions of the conserved histidine residue (H277) within the third conserved cysteine rich region of the *SDHB* with tyrosine (H277R) or arginine (H277Y) were associated with decreased boscalid sensitivity (EC_{50} > 0.5 µg a.i/mL) in *D. tanaceti* in this study. No isolates with a boscalid

susceptible phenotype (EC_{50} 0.0 – 0.5 µg a.i/mL) were associated with these substitutions. Thus, until more data from analysing additional isolates or gene regions, or from mutation studies becomes available, the boscalid susceptible phenotype will stand to encompass isolates with an EC_{50} range of 0.0 – 0.5 µg a.i/mL. The H277Y substitution was the most frequent substitution observed in the subsets of 2009 – 2011 and 2012 isolates selected for *in vitro* fungicide testing. Both the H277Y and H277R substitutions were associated with isolates exhibiting moderately resistant, resistant and highly resistant phenotypes. However, the association of isolates with a WT *SDHB* gene for each of the moderately resistant, resistant and highly resistant phenotypes restricted the ability to correlate the H277Y and H277R substitutions with the resistant phenotypes. Based on these findings, the proposed hypothesis is that the isolates with a MR, R, or HR phenotype and a WT *SDHB* gene contain mutations associated with resistance in other regions, such as the *SDHC* and *SDHD* genes. Additional research would need to be undertaken to test this hypothesis. Additionally, such research would allow a more thorough analysis of the mutations associated with the proposed boscalid resistant phenotypes to be carried out.

The H277Y and H277R substitutions have been identified to be associated with boscalid resistance in a range of other fungal species. It is proposed that they alter the structure of the Q-site, resulting in decreased efficiency of boscalid binding (Avenot & Michailides, 2010, Scalliet et al., 2012). Furthermore mutagenesis studies have shown that H272Y and H272R in *B. cinerea* (corresponding to *D. tanaceti* 277) and H267Y in *M. graminicola* (corresponding to *D. tanaceti* 277) confer resistance to boscalid (Fraaije et al., 2012, Laleve et al., 2014).

The occurrence of moderate, resistance and highly resistant phenotypes for *D. tanaceti* isolates with H277R and H277Y substitutions may indicate that compound mutations in the three subunits (*SDHB*, *SDHC* and *SDHD*) may also occur simultaneously in isolates, which could affect the fungicide response compared to single mutations (Fraaije et al., 2012). Mutations in the *SDHC* and *SDHD* genes associated with fungicide resistance have been identified in a number of pathogens. (Miyamoto et al., 2010, Avenot et al., 2009, Gudmestad et al., 2013, Avenot & Michailides, 2010). Several studies have shown that mutations in the succinate dehydrogenase complex can also result in differential cross-resistance to fungicides in the SDHI group (FRAC code 7) (Sierotzki & Scalliet, 2013). For example, Avenot et al. (2012) identified boscalid resistant isolates of *S. cucurbitacearum* with SDHB H277Y and H277R substitutions, to be as sensitive to the SDHI fungicide penthiopyrad as isolates with a WT SDHB. However in *A. alternata,* a H134R substitution in the SDHC has been shown to confer cross-resistance to all tested SDHI fungicides (Sierotzki et al., 2011). Preliminary work has indicated that isolates of *D. tanaceti* collected from pyrethrum fields with fungicide control failures, which were resistant to boscalid, were sensitive to the SDHI fungicide fluopyram in *in vitro* amended agar plate tests (F. Hay, pers. comm.). This indicated that SDHI fungicides other than boscalid may still be useful for the control of *D. tanaceti*. Identifying the occurrence of mutations in the *SDHC* and *SDHD* genes of *D. tanaceti* would be beneficial to provide the pyrethrum industry with further information relating to whether other SDHI fungicides might be utilised for pyrethrum disease control or if the introduction of a SDHI fungicide may lead to rapid selection of resistance in *D. tanaceti* to the new SDHI.

To the best of our knowledge, the I279V substitution, identified in a small proportion of *D. tanaceti* isolates, has only been induced in laboratory studies in isolates of *M. graminicola*

following UV mutagenesis and selection on carboxin amended media (Scalliet et al., 2012, Fraaije et al., 2012). Therefore, this is the first identification of field isolates of an ascomycete with an I279V substitution. This amino acid residue is considered to be important in forming the docking cavity for the fungicide and forms van der Waals interactions with the acid component of carboxamides (pyridine for boscalid) (Scalliet et al., 2012). However, this substitution was associated with a boscalid susceptible phenotype in this study, which is consistent with other findings for *M. graminicola* (Fraaije et al., 2012, Scalliet et al., 2012). It is proposed that valine, which differs from isoleucine by the addition of a methyl group, compensated for some of the lipophilic interactions performed by the isoleucine (Scalliet et al., 2012). However, isolates with an I279V substitution may be less sensitive to carboxin than I279 isolates (Scalliet et al., 2012, Fraaije et al., 2012). The five isolates from the 2012 sampled populations with a valine substitution at position 279 were all identified in field S2 at Sassafras. Previous characterisation of these five isolates had identified that four contained a *MAT1-2-1* mating-type gene (Pearce, Chapter 4) and had an identical microsatellite marker profile produced from eight polymorphic markers (Pearce, Chapter 5). The remaining isolate contained a *MAT1-1-1* mating-type gene and was different to these isolates at two of the microsatellite marker loci. It was therefore proposed that this mutation has arisen independently on at least two separate occasions or that it has been distributed via recombination as part of a sexual reproduction cycle.

High resolution melt analysis has been used for a number of fungal pathogens to detect mutations associated with fungicide resistance (Chatzidimopoulos et al., 2014, Curvers et al., 2015). However, each of these studies has only dealt with the need to detect changes within a single codon. As the H277R and I279V substitutions resulted in different responses to

boscalid *in vitro*, it is important that these substitutions are able to be differentiated without the need to sequence the *SDHB* gene of isolates. Therefore, it is proposed for future work, rather than sequencing the *SDHB* of all putative H277R and I279V isolates, that the PCR products from real-time PCR amplification are digested with the restriction enzyme *TaaI* (*HpyCH4II*). This enzyme recognises CAN^GT sites and thus would digest products with an ATT (I) to GTT (V) mutation at codon 279. High resolution melt analysis could also be used to detect mutations with the *SDHC* and *SDHD* genes which are associated with resistance.

Based on the HRM screen, 59.7% of *D. tanaceti* field isolates from four separate fields sampled in 2012 contained mutations in the *SDHB* gene. While this screen cannot be used to identify the percentage of isolates resistant to boscalid it provides an adequate screening method to be able to rapidly identify the mutations within individuals. It may be used to identify more individuals of lower frequency mutations such as the I279V and H277R for additional boscalid plate testing *in vitro*. As the 2012 fields were first harvest crops that had not received an application of boscalid prior to sampling, it is proposed that the mutated isolates may have been introduced to, rather than produced in the fields. As *D. tanaceti* is a seed-borne pathogen (Pethybridge et al., 2006) and pyrethrum is a perennial crop, seed-borne isolates may have been exposed to multiple applications of boscalid over the life of the seed crops, and developed resistance prior to seed infection and dissemination into the 2011 planted crops. Furthermore, the seed used to plant field S1 in Sassafras was from a crop harvested in the summer of 2006/2007, and assuming a large amount of infection is seed-borne, this suggested that boscalid insensitive isolates were present at relatively high levels in 2006/2007. Rapid development of reduced sensitivity to boscalid has also occurred in *A. alternata* (Avenot et al., 2008) and *C. cassiicola* (Miyamoto et al., 2009) with resistant isolates detected within two and three years of boscalid introduction, respectively.

Despite implementation of best management practices by the pyrethrum industry to limit the development of fungicide resistance, the high proportion of *D. tanaceti* isolates within the 2012 characterised population containing *SDHB* mutations, which have shown to be causative of boscalid resistance in other species and the finding that only 9.7% of isolates from the subset of the 2012 population had a boscalid sensitive phenotype, indicated that boscalid resistance in *D. tanaceti* may have contributed to the rapid increase in the frequency and incidence of tan spot. However, other pyrethrum pathogens, including *S. tanaceti* exhibit no evidence of a reduced sensitivity to boscalid (Hay et al., 2015), indicating that the imposed management strategies are working for some species. Furthermore, it could be argued that *S. tanaceti* has had longer exposure to and selection pressure imposed from boscalid than *D. tanaceti*, as the *S. tanaceti* pathogen incidence was higher relative to *D. tanaceti* following the period of boscalid introduction (Pethybridge et al., 2007, Pethybridge et al., 2006). This suggests that a low proportion of *D. tanaceti* already had resistance to SDHI fungicides or that *D. tanaceti* has the ability to rapidly evolve. Analysis of *D. tanaceti* populations has identified high genetic variation among individuals, inferring a high adaptive ability (Pearce, Chapter 5). Furthermore, while no evidence of a sexual cycle in *S. tanaceti* has been found (Vaghefi et al., 2015), a sexual cycle in *D. tanaceti* cannot be dismissed (Pearce, Chapter 4). The implications of a sexual cycle in *D. tanaceti* would allow long range dispersal mechanisms and genetic recombination, which may have contributed to the development of resistance. In 2015, boscalid was removed from the spring fungicide program due to concerns with control failures (T. Groom, pers. comm.).

Overall this study has initiated the characterisation of the molecular basis of boscalid resistance in *D. tanaceti*. Identifying and sequencing orthologues of the *SDHC* and *SDHD* genes of *D. tanaceti* would be beneficial to further aid the characterisation. Furthermore, this

would allow identification of specific mutations which could then be targeted for in a site-specific mutagenesis study to confirm which mutations confer boscalid resistance. It would also identify the occurrence of any isolates with compound mutations in the *SDHB, SDHC* and *SDHD* genes and provide the pyrethrum industry with further information on the potential for cross-resistance within the SDHI group of fungicides. In addition, examining the associated fitness of *D. tanaceti* isolates with particular substitutions and the rate of development of resistance in the presence of the selection pressure imposed from fungicides would assist with developing future strategies to minimise the development of resistance. The HRM assay developed in this study has been shown to be an effective method to rapidly screen the frequency of SDHB alleles of isolates in large populations. It will provide a method to evaluate how the distribution of *SDHB* alleles changes with the removal of boscalid from the pyrethrum fungicide program

6.6 ACKNOWLEDGEMENTS

The authors wish to thank Pattie Weichelt, Craig Palmer, Stacey Pilkington and Phil Gardam (Tasmanian Institute of Agriculture; University of Tasmania, Australia) for assisting with the collection of isolates used in this study. Support for this research was generously provided by Botanical Resources Australia (Agricultural Services Pty. Ltd.) and the Commonwealth Government through the Australian Research Councils Linkage funding scheme (project number LP130100739). The first author received the University of Tasmania's Australian Postgraduate Award and the Cuthbertson Elite Tasmania Graduate Research Scholarship, which also supported this research.

6.7 REFERENCES

Agarwala R, Barrett T, Beck J, *et al.*, 2015. Database resources of the National Center for Biotechnology Information. *Nucleic Acids Research* **43**, 6-17.

Altschul SF, Madden TL, Schäffer AA, *et al.*, 1997. Gapped BLAST and PSI-BLAST: a new generation of protein database search programs. *Nucleic Acids Research* **25**, 3389-402.

Altschul SF, Wootton JC, Gertz EM, *et al.*, 2005. Protein database searches using compositionally adjusted substitution matrices. *Febs Journal* **272**, 5101-9.

Avenot H, Sellam A, Karaoglanidis G, Michailides T, 2008. Characterization of mutations in the iron-sulphur subunit of succinate dehydrogenase correlating with boscalid resistance in *Alternaria alternata* from California pistachio. *Phytopathology* **98**, 736-42.

Avenot H, Sellam A, Michailides T, 2009. Characterization of mutations in the membrane-anchored subunits AaSDHC and AaSDHD of succinate dehydrogenase from *Alternaria alternata* isolates conferring field resistance to the fungicide boscalid. *Plant Pathology* **58**, 1134-43.

Avenot HF, Michailides TJ, 2010. Progress in understanding molecular mechanisms and evolution of resistance to succinate dehydrogenase inhibiting (SDHI) fungicides in phytopathogenic fungi. *Crop Protection* **29**, 643-51.

Avenot HF, Thomas A, Gitaitis RD, Langston Jr DB, Stevenson KL, 2012. Molecular characterization of boscalid and penthiopyrad resistant isolates of *Didymella bryoniae* and assessment of their sensitivity to fluopyram. *Pest Management Science* **68**, 645-51.

Benson DA, Clark K, Karsch-Mizrachi I, Lipman DJ, Ostell J, Sayers EW, 2015. GenBank. *Nucleic Acids Research* **43**, 30-5.

Brent KJ, Hollomon DW, Federation GCP, 1998. *Fungicide resistance: the assessment of risk*. Brussels, Belgium: Fungicide Resistance Action Committee

Chatzidimopoulos M, Ganopoulos I, Madesis P, Vellios E, Tsaftaris A, Pappas A, 2014. High-resolution melting analysis for rapid detection and characterization of *Botrytis cinerea* phenotypes resistant to fenhexamid and boscalid. *Plant Pathology* **63**, 1336-43.

Curvers K, Pycke B, Kyndt T, Vanrompay D, Haesaert G, Gheysen G, 2015. A high-resolution melt (HRM) assay to characterize CYP51 haplotypes of the wheat pathogen *Mycosphaerella graminicola*. *Crop Protection* **71**, 12-8.

Deepayan S, 2008. *Lattice: Multivariate data visualization with R*. New York: Springer.

Deising HB, Reimann S, Pascholati SF, 2008. Mechanisms and significance of fungicide resistance. *Brazilian Journal of Microbiology* **39**, 286-95.

Dwight Z, Palais R, Wittwer CT, 2011. uMELT: prediction of high-resolution melting curves and dynamic melting profiles of PCR products in a rich web application. *Bioinformatics* **27**, 1019-20.

Fraaije BA, Bayon C, Atkins S, Cools HJ, Lucas JA, Fraaije MW, 2012. Risk assessment studies on succinate dehydrogenase inhibitors, the new weapons in the battle to control Septoria leaf blotch in wheat. *Molecular Plant Pathology* **13**, 263-75.

Frac, 2015. FRAC Code List 2015: Fungicides sorted by mode of action. In.: Fungicide Resistance Action Committee.

Gudmestad N, Arabiat S, Miller J, Pasche J, 2013. Prevalence and impact of SDHI fungicide resistance in *Alternaria solani*. *Plant Disease* **97**, 952-60.

Hägerhäll C, 1997. Succinate: quinone oxidoreductases: variations on a conserved theme. *Biochimica et Biophysica Acta* **1320**, 107-41.

Hay FS, Gent DH, Pilkington SJ, Pearce TL, Scott JB, Pethybridge SJ, 2015. Changes in distribution and frequency of fungi associated with a foliar disease complex of pyrethrum in Australia. *Plant Disease* **99**, 1227-35.

Horsefield R, Yankovskaya V, Sexton G, *et al.*, 2006. Structural and computational analysis of the quinone-binding site of complex II (succinate-ubiquinone oxidoreductase) - A mechanism of electron transfer and proton conduction during ubiquinone reduction. *Journal of Biological Chemistry* **281**, 7309-16.

Huang S, Millar AH, 2013. Succinate dehydrogenase: the complex roles of a simple enzyme. *Current Opinion in Plant Biology* **16**, 344-9.

Katoh K, Misawa K, Kuma K-I, Miyata T, 2002. MAFFT: a novel method for rapid multiple sequence alignment based on fast fourier transform. *Nucleic Acids Research* **30**, 3059-66.

Koressaar T, Remm M, 2007. Enhancements and modifications of primer design program Primer3. *Bioinformatics* **23**, 1289-91.

Laleve A, Gamet S, Walker A-S, Debieu D, Toquin V, Fillinger S, 2014. Site-directed mutagenesis of the P225, N230 and H272 residues of succinate dehydrogenase subunit B from *Botrytis cinerea* highlights different roles in enzyme activity and inhibitor binding. *Environmental Microbiology* **16**, 2253-66.

Ma Z, Michailides TJ, 2005. Advances in understanding molecular mechanisms of fungicide resistance and molecular detection of resistant genotypes in phytopathogenic fungi. *Crop Protection* **24**, 853-63.

Marchler-Bauer A, Derbyshire MK, Gonzales NR, *et al.*, 2015. CDD: NCBI's conserved domain database. *Nucleic Acids Research* **43**, D222-D6.

Miyamoto T, Ishii H, Seko T, Kobori S, Tomita Y, 2009. Occurrence of *Corynespora cassiicola* isolates resistant to boscalid on cucumber in Ibaraki Prefecture, Japan. *Plant Pathology* **58**, 1144-51.

Miyamoto T, Ishii H, Stammler G, *et al.*, 2010. Distribution and molecular characterization of *Corynespora cassiicola* isolates resistant to boscalid. *Plant Pathology* **59**, 873-81.

Pearce T, Chapter 3. Tan spot of pyrethrum is caused by a *Didymella* species complex. In. *Population biology of the tan spot pathogen of pyrethrum, PhD thesis.* University of Tasmania, 106-44.

Pearce T, Chapter 4. Mating-type gene structure in *Didymella tanaceti* and their spatial distribution in pyrethrum fields. In. *Population biology of the tan spot pathogen of pyrethrum, PhD thesis.* University of Tasmania, 145-80.

Pearce T, Chapter 5. Fine scaled population genetic analysis of *Didymella tanaceti*. In. *Population biology of the tan spot pathogen of pyrethrum, PhD thesis.* University of Tasmania, 181-226.

Pethybridge S, Hay F, 2001. Influence of *Phoma ligulicola* on yield, and site factors on disease development, in Tasmanian pyrethrum crops. *Australasian Plant Pathology* **30**, 17-20.

Pethybridge S, Wilson C, 1998. Confirmation of ray blight disease of pyrethrum in Australia. *Australasian Plant Pathology* **27**, 45-8.

Pethybridge SJ, Esker P, Dixon P, *et al.*, 2007. Quantifying loss caused by ray blight disease in Tasmanian pyrethrum fields. *Plant Disease* **91**, 1116-21.

Pethybridge SJ, Hay F, Jones S, Wilson C, Groom T, 2006. Seedborne infection of pyrethrum by *Phoma ligulicola*. *Plant Disease* **90**, 891-7.

Pethybridge SJ, Hay FS, Esker PD, *et al.*, 2008a. Diseases of pyrethrum in Tasmania: challenges and prospects for management. *Plant Disease* **92**, 1260-72.

Pethybridge SJ, Jones SJ, Shivas RG, Hay FS, Wilson CR, Groom T, 2008b. Tan spot: A new disease of pyrethrum caused by *Microsphaeropsis tanaceti* sp. nov. *Plant Pathology* **57**, 1058-65.

R Core Team, 2015. *R: A language and environment for statistical computing V. 3.1.3* Vienna, Austria.: R Foundation for Statistical Computing.

Reja V, Kwok A, Stone G, *et al.*, 2010. ScreenClust: Advanced statistical software for supervised and unsupervised high resolution melting (HRM) analysis. *Methods* **50**, S10-S4.

Ritz C, Streibig JC, 2005. Bioassay analysis using R. *Journal of Statistical Software* **12**, 1-22.

Scalliet G, Bowler J, Luksch T, *et al.*, 2012. Mutagenesis and functional studies with succinate dehydrogenase inhibitors in the wheat pathogen *Mycosphaerella graminicola*. *PLoS One* **7**, e35429.

Sierotzki H, Frey R, Morchoisne M, Olaya G, Mosch M, Scalliet G, 2011. Sensitivity of fungal pathogens to SDHI fungicides. In: Dehne HW, Deising HB, Gisi U, Kuck KH, Russell PE, Lyr H, eds. *Modern fungicides and antifungal compounds VI. 16th International Reinhardsbrunn Symposium, Friedrichroda, Germany, April 25-29, 2010.* 179-86.

Sierotzki H, Scalliet G, 2013. A review of current knowledge of resistance aspects for the next-generation succinate dehydrogenase inhibitor fungicides. *Phytopathology* **103**, 880-7.

Tibshirani R, Walther G, Hastie T, 2001. Estimating the number of clusters in a data set via the gap statistic. *Journal of the Royal Statistical Society: Series B (Statistical Methodology)* **63**, 411-23.

Untergasser A, Cutcutache I, Koressaar T, *et al.*, 2012. Primer3 - new capabilities and interfaces. *Nucleic Acids Research* **40**, 1-12.

Vaghefi N, Ades PK, Hay FS, Pethybridge SJ, Ford R, Taylor PW, 2015. Identification of the MAT1 locus in *Stagonosporopsis tanaceti*, and exploring its potential for sexual reproduction in Australian pyrethrum fields. *Fungal Biology* **119**, 408-19.

Vaghefi N, Pethybridge S, Ford R, Nicolas M, Crous P, Taylor P, 2012. *Stagonosporopsis* spp. associated with ray blight disease of *Asteraceae*. *Australasian Plant Pathology* **41**, 675-86.

Veloukas T, Leroch M, Hahn M, Karaoglanidis GS, 2011. Detection and molecular characterization of boscalid-resistant *Botrytis cinerea* isolates from strawberry. *Plant Disease* **95**, 1302-7.

Wickham H, 2007. Reshaping data with the reshape package. *Journal of Statistical Software* **21**, 1-20.

Wingfield BD, Ades PK, Al-Naemi FA, *et al.*, 2015. IMA Genome-F 4: Draft genome sequences of *Chrysoporthe austroafricana*, *Diplodia scrobiculata*, *Fusarium nygamai*, *Leptographium lundbergii*, *Limonomyces culmigenus*, *Stagonosporopsis tanaceti*, and *Thielaviopsis punctulata*. *IMA Fungus* **6**, 233.

Yin YN, Kim YK, Xiao CL, 2011. Molecular characterization of boscalid resistance in field isolates of *Botrytis cinerea* from apple. *Phytopathology* **101**, 986-95.

GENERAL DISCUSSION AND SUGGESTIONS FOR FUTURE RESEARCH

7.1 GENERAL DISCUSSION

This study investigated the causal pathogens of tan spot of pyrethrum in Tasmania, Australia. A population of the dominant pathogen collected from Tasmanian fields was characterised for (i) mating-type; (ii) genetic diversity; and (iii) sensitivity to the fungicide boscalid. These analyses were undertaken to identify underlying mechanisms which may have contributed to the recent increase in frequency and severity of tan spot within fields.

Analysis of five DNA regions, including the complete 5.8S nuclear ribosomal loci, including the two flanking internal transcribed spacers (ITS), and partial sequences of the β-tubulin (*TUB2*), large subunit 28S nrDNA (LSU), actin (*ACT*) and glyceraldehyde-3-phosphate-dehrydogenase (*GAPDH*), indicated that two closely related species cause tan spot in pyrethrum. Genetic differences between the two species were further supported by morphological differences. Phylogenetic analysis using both Bayesian inference and maximum parsimony analysis indicated that the species, which were previously recognised as two haplotypes of *Microsphaeropsis tanaceti* (Pethybridge *et al.*, 2008), were phylogenetically embedded within the genus *Didymella*. Based on these results, the two haplotypes were reclassified as two *Didymella* species; *D. tanaceti* and *D. rosea*. The first tan spot pathogen isolates were stored in the fungal collection at the Tasmanian Institute of Agriculture (TIA) in 2004. Of these, a single *D. rosea* isolate was included, indicating that both species were historically present in pyrethrum and that *D. rosea* is not a recent introduction.

Didymella tanaceti and *D. rosea* can be differentiated by mycelium characteristics and thus can be identified following incubation of infected plant material on water agar (WA). Differences in mycelium morphology are consistent between the two species, but to an untrained eye they could be misidentified as the same species on WA. On PDA, *D. tanaceti* exhibits culture morphology consistent with the initial description of "*M. tanaceti"*. In contrast, *D. rosea* exhibits distinctive colony colours ranging from salmon to peach on top with white aerial mycelium, to saffron to salmon on the reverse with honey pigmented hyphae extending from centre. Pathogens of pyrethrum are commonly identified from plant isolations on WA or subsequently following incubation of hyphal tipped mycelium from WA on PDA. I propose that the lack of historical isolation frequency data for *D. rosea* and the inclusion of only a single isolate in the pathogen database at the TIA pre-2012, is due to a combination of a low frequency of *D. rosea* within pyrethrum fields and isolates with culture morphology characteristic of *D. rosea* not being identified as *M. tanaceti*. For example, the 2012 field populations were collected prior to the morphological characterisation of *D. rosea.* A few cultures with *D. rosea* morphology were identified in the field S2 at Sassafrass, but were discarded from the population as they were not typical of "*M. tanaceti"*. Furthermore, since the morphological characterisation of *D. rosea* in 2012, hundreds of leaf isolations have been undertaken from multiple pyrethrum fields. *Didymella tanaceti* remained the dominant species, with only 40 isolates of *D. rosea* identified. Additionally *D. rosea* has not been associated with infection of pyrethrum seed.

Within the field transects sampled in July/August 2012, *D. tanaceti* was isolated at a high frequency. Furthermore, at some of the sampling units, *D. tanaceti* was identified from lesions on each of the four sampled leaves from each plant. These results indicated that both

fields and plants within the fields had a high incidence of tan spot. A recent study examining the temporal fluctuations in the frequency of *D. tanaceti* identified an increased frequency in pyrethrum crops throughout the winter (April – July) of 2012 (Hay *et al.*, 2015), which may have contributed to the high frequency identified in July/August in this study. Analysis of the field populations for mating-type genes, genetic diversity and boscalid sensitivity identified a lack of population structure among regions, fields or within transects. Gene flow between fields was identified and equal ratios of isolates of each mating-type gene were observed in most of the uncorrected and in each of the clone corrected field populations. Despite these indicators of sexual reproduction, linkage disequilibrium was identified in all fields. The majority of isolates contained mutations in the *SDHB*. While these mutations could not be correlated with a boscalid resistant phenotype (due to some isolates with a WT *SDHB* allele exhibiting a resistant phenotype, which was hypothesised to be due to mutations in additional genes governing resistance), their characterisation was a first step in characterising the molecular mechanism associated with boscalid resistance in *D. tanaceti*.

The increased frequency of tan spot observed has also been associated with a decrease in incidence of *Stagonosporopsis tanaceti* (ray blight) (Hay *et al.*, 2015). Previous studies have evaluated the population biology of *S. tanaceti*. *Stagonosporopsis tanaceti* has many similar disease epidemiology characteristics to *D. tanaceti*. It also contributes to spring and summer disease epidemics and has infected pyrethrum for over 20 years. *Stagonosporopsis tanaceti* is presumed heterothallic (Vaghefi *et al.*, 2015a), and is dispersed via conidia (splash dispersal) and seed-borne inoculum (Pethybridge & Wilson, 1998; Pethybridge *et al.*, 2006). However, a number of differences between the two species have been observed, which are proposed to have impacted on the shift in incidence of the two diseases. For *D. tanaceti*, both

MAT genes have been identified, appear putatively functional and isolates of each mating-type occur in equal ratios within field transects, suggesting that a sexual cycle cannot be dismissed. However, only *S. tanaceti* isolates containing a *MAT1-1-1* gene have been identified. In addition, the *MAT1-1-1* gene of *S. tanaceti* contains a large uncharacteristic insertion and thus *S. tanaceti* is proposed to be restricted to asexual reproduction (Vaghefi *et al.*, 2015a). Population genetic analyses of *S. tanaceti* using SSRs, AFLPs and RAPDs identified lower gene and genotypic diversity, and a higher percentage of clonality than identified for *D. tanaceti* (Pethybridge *et al.*, 2012; Vaghefi *et al.*, 2015b), indicating that *S. tanaceti* may not have as high adaptive ability as *D. tanaceti*. Furthermore, *S. tanaceti* isolates remain sensitive to boscalid (Hay *et al.*, 2015), for which many *D. tanaceti* isolates have resistant phenotypes. The combination of these factors is proposed to have increased inoculum loads of *D. tanaceti* in fields and seeds, relative to *S. tanaceti*, allowing *D. tanaceti* to outcompete *S. tanaceti* in the winter and spring.

To decrease the disease pressure applied from *D. tanaceti*, control mechanisms need to be implemented which decrease the number of individuals in fields and the movement of inoculum into fields. With the potential host range of *D. tanaceti* unknown, controlling the movement of inoculum into fields from seed is the most appropriate action. Additionally, chemical control options need to control boscalid resistant and susceptible isolates of *D. tanaceti*, to decrease the number of individuals in fields, and subsequently the proportion of infected seed. Tan spot control currently relies on spring applications of Amistar® (azoxystrobin; Syngenta; FRAC code 11), Chorus® (cyprodinil; Syngenta; FRAC code 9) and Prosaro® (prothioconazole and tebuconazole; Bayer CropScience; FRAC code 3) combined with the multisite protectant Bravo® (chlorothalonil; Syngenta; FRAC code M5). The

systemic fungicide Switch® (cyprodinil and fludioxonil; Syngenta; FRAC code 12) is used only in first harvest crops. In addition, application of Emblem® (Fluazinam; Crop Care Australasia; FRAC code 29) aims to control the inoculum load of *D. tanaceti* in autumn/winter which contributes to spring disease epidemics. *In vitro* fungicide testing studies have indicated that the current fungicide program should, for the majority, provide control of *D. tanaceti* (F. Hay, unpublished data). However, indications that *D. tanaceti* can evolve rapidly suggest that this cannot be taken for granted and continued monitoring of populations should be undertaken to maintain effective fungicide control of tan spot. In addition, new pyrethrum seed treatments have been introduced to limit the occurrence of *D. tanaceti* infection. One of the seed treatments being utilised is steam sterilisation, which kills the pathogen in the seed and thus provides removal of the pathogen from the system. The tools developed in this thesis will assist in the evaluation of these control methods. If disease pressure continues to remain high, additional mechanisms may need to be developed and adopted for control.

Overall the results from this thesis have highlighted that tan spot is caused by a species complex. *Didymella tanaceti* is a heterothallic pathogen which is proposed to undergo infrequent sexual reproduction, under specific environmental conditions, which has resulted in a genotypically diverse population. The adaptive ability of *D. tanaceti* has resulted in the development of field populations with a high frequency of individuals with resistance to boscalid. Additionally, the sampling process undertaken will aid future sampling efforts by allowing calculation of the minimum number of pathogen samples required to provide a representation of the overall population. Moreover, the development of PCR based assays for

mating-type and fungicide sensitivity testing will aid future studies by decreasing the time required for data collection and increasing the number of individuals able to be examined.

7.2 SUGGESTIONS FOR FUTURE RESEARCH

Additional research is required to further characterise the pathogens associated with tan spot and extend on the results obtained from this thesis. Potential areas include:

1. *Further characterisation of* Didymella rosea.

This thesis identified two sister species that are associated with tan spot of pyrethrum. However, in this project *D. rosea* was only characterised morphologically *in vitro* and molecularly for five barcode genes. Characterising the structure of the mating-type genes, phenotypic response to boscalid and genetic diversity could potentially be undertaken. Due to the close relatedness with *D. tanaceti*, some of the tools developed in this thesis may be able to be transferred to *D. rosea.* Such studies may help elucidate reasons for the large differences in the isolation frequency of the two species. Furthermore, it would allow the potential risk of *D. rosea* developing into a major pathogen of pyrethrum to be evaluated. However, prior to these studies being undertaken a population of *D. rosea* from multiple geographical regions over different time periods should be collected. Furthermore,

quantifying differences in virulence and survival under a range of conditions between *D. tanaceti* and *D. rosea* should also be undertaken.

2. *Production of the sexual morph of* D. tanaceti.

Despite the inability to induce the sexual morph of *D. tanaceti* is this thesis, several indicators of the occurrence of cryptic/infrequent sexual reproduction were identified. Only a limited number of conditions were able to be evaluated in this thesis to induce the sexual morph. Testing additional growth media, temperature and lighting conditions should be undertaken. Additionally, future genetic evaluation of fields sampled frequently over a temporal scale may identify specific periods during which recombination occurs, which may assist in identifying the necessary conditions to induce the sexual morph. Furthermore, the ability to induce a sexual morph would allow the functionality of the haplotypes of *MAT1-1* identified in this thesis to be confirmed.

3. *Identification of the host range of the tan spot pathogens.*

Genetic analysis of *D. tanaceti* with the developed microsatellite markers in this thesis identified gene flow and similar allele frequencies between field populations. One potential explanation for this is a common origin of isolates, such as an alternative host. An alternative host, providing inoculum for disease in pyrethrum, has also been proposed as a mechanism for the recently observed increase in diseased frequency and severity. Identification of the potential and actual host range of both tan spot pathogens is warranted. The potential host range could be identified from inoculation of plant species with mycelium or conidia *in vitro*.

The actual host range could be inferred from the collection of putative hosts from the field, followed by fungal isolations.

4. *Complete the molecular characterisation of boscalid resistance in* D. tanaceti.

This thesis identified two mutations in the *SDHB* gene, which encodes the SDHB subunit of the succinate dehydrogenase (SDH) enzyme, which correlated with boscalid resistance in isolates of *D. tanaceti*. As isolates with a resistant phenotype, but no mutations in the *SDHB* gene were also identified, mutations in the succinate dehydrogenase subunit C (*SDHC*) and D (*SDHD*) genes may also occur in *D. tanaceti*. Sequencing the *SDHC* and *SDHD* genes for the 48 isolates for which the *SDHB* was characterised would provide a molecular "SDH profile" for each isolate. Comparison of this "profile" to the *in vitro* (phenotypic) response to boscalid would identify the effect of singular and/or compound mutations on the response to boscalid. Subsequently, PCR based assays (such as the high resolution melt assay developed in this thesis) could be developed to allow rapid identification of *SDHC* and *SDHD* alleles governing resistance.

5. *Determine the stability of mutations governing boscalid resistance*

The high proportion of boscalid resistant individuals with the field populations characterised in this thesis indicated that applications of boscalid to these fields would have provided minimal disease control. The implications of the removal of boscalid from the fungicide program are unknown. Studies evaluating both the fitness of isolates with the identified mutations in the SDH subunits, and the stability of the mutations following generations without the fungicide selection pressure are warranted. The *SDHB* HRM assay developed in this project could be employed to monitor mutations. However, the development of a real-

time PCR assay, most likely probe-based, could quantify changes in the mutation frequency of the SDH genes. It could be used to detect changes in mycelium or conidia of single strain cultures in the presence or absence of the fungicide or to analyse field populations by screening DNA extracts containing multiple individuals of *D. tanaceti*.

6. *Temporal examination of populations*

The populations sampled and characterised in this thesis provided analysis of *D. tanaceti* populations at a single time period in two regions. Future studies are warranted to address temporal fluctuations, either historical or future, for multiple aspects examined in this thesis. There exits two current opportunities to examine temporal changes in *D. tanaceti*. Firstly, the field transects which were intensively sampled in July/August 2012, to provide the populations examined in this thesis, were also re-sampled in November 2012. In the period between the samplings, fields received the standard spring fungicide program. Characterising the population sampled in November for the proportion of each mating-type and *SDHB* alleles, and genetic diversity, using the marker systems developed in this project should be undertaken. This would provide a fine scale temporal comparison within fields, allowing the effects of spring epidemics, fungicide application and migration of individuals to be identified. Secondly, within the fungal strain collection at TIA, *D. tanaceti* isolates from a range of geographical locations have been collected and stored in 2004, 2006, 2009 – 2015, which provides the ability to evaluate historical population changes. Furthermore, analysis of isolates collected pre-2012 may pinpoint the periods of boscalid resistance development or increases in genetic diversity. Specific evaluation of the thirty-eight *D. tanaceti* isolates stored in 2004 may infer how the pathogen was introduced into pyrethrum and the characteristics of the founder population.

7. Population analysis at the plant spatial scale

In this thesis, analysis of the distribution of genotypes of *D. tanaceti* within field transects did not identify any significant spatial aggregation of isolates of the same genotype. This may have been due to a lack of dissemination between plants, plants containing a range of genetic differentiated individuals with random dissemination patterns or spread being limited across the spatial scale sampled. Therefore, it may be beneficial to collect *D. tanaceti* populations at smaller spatial hierarchical scales (i.e. neighbouring plants, within a plant, within leaves on a plant, within lesions on a leaf) to evaluate such relationships. Furthermore, analysis at this scale would allow further evaluation of mating-type ratios and confirm the physical interaction of isolates of each mating-type within plants.

7.3 REFERENCES

Hay FS, Gent DH, Pilkington SJ, Pearce TL, Scott JB, Pethybridge SJ, 2015. Changes in distribution and frequency of fungi associated with a foliar disease complex of pyrethrum in Australia. *Plant Disease* **99**, 1227-35.

Pethybridge S, Wilson C, 1998. Confirmation of ray blight disease of pyrethrum in Australia. *Australasian Plant Pathology* **27**, 45-8.

Pethybridge SJ, Hay F, Jones S, Wilson C, Groom T, 2006. Seedborne infection of pyrethrum by *Phoma ligulicola*. *Plant Disease* **90**, 891-7.

Pethybridge SJ, Jones SJ, Shivas RG, Hay FS, Wilson CR, Groom T, 2008. Tan spot: A new disease of pyrethrum caused by *Microsphaeropsis tanaceti* sp. nov. *Plant Pathology* **57**, 1058-65.

Pethybridge SJ, Scott JB, Hay FS, 2012. Lack of evidence for recombination or spatial structure in *Phoma ligulicola* var. *inoxydabilis* populations from Australian pyrethrum fields. *Plant Disease* **96**, 746-51.

Vaghefi N, Ades PK, Hay FS, Pethybridge SJ, Ford R, Taylor PW, 2015a. Identification of the MAT1 locus in *Stagonosporopsis tanaceti*, and exploring its potential for sexual reproduction in Australian pyrethrum fields. *Fungal Biology* **119**, 408-19.

Vaghefi N, Hay FS, Ades PK, Pethybridge SJ, Ford R, Taylor PWJ, 2015b. Rapid changes in the genetic composition of *Stagonosporopsis tanaceti* population in Australian pyrethrum fields. *Phytopathology* **105**, 358-69.

APPENDICES

APPENDIX 1: DECLARATIONS OF CO-AUTHORSHIP

Experimental chapter I

Article title: TAN SPOT OF PYRETHRUM IS CAUSED BY A *DIDYMELLA SPECIES* COMPLEX

Co-authors: Jason B Scott, Pedro W Crous, Frank S Hay and Sarah J Pethybridge.

Evaluation scale:

1 – has contributed to this work (0-33%)
2 – has made substantial contribution to this work (34-66%)
3 – has made a major contribution to this work (67-100%)

Declaration regarding specific elements	***Extent* (1,2,3)**
1. Formulation/identification of the scientific problem that need to be clarified. This includes a condensation of the problem to specific scientific questions that is judged to be answerable via experiments	3
2. Planning of the experiments and methodology design, including selection of methods and method development	3
3. Involvement in the experimental work	3
4. Presentation, interpretation and discussion in a journal format of the obtained data	3
Overall contribution	3

Signature of the co-authors:

Dr. Jason B. Scott:

Prof. Dr. Pedro W. Crous:

Dr. Frank S. Hay:

Dr. Sarah J. Pethybridge:

Experimental chapter II

Article title: MATING-TYPE GENE STRUCTURE IN *DIDYMELLA TANACETI* AND THEIR SPATIAL DISTRIBUTION IN PYRETHRUM FIELDS

Co-authors: Jason B Scott, Frank S Hay and Sarah J Pethybridge**.**

Evaluation scale:

1 – has contributed to this work (0-33%)
2 – has made substantial contribution to this work (34-66%)
3 – has made a major contribution to this work (67-100%)

Declaration regarding specific elements	***Extent* (1,2,3)**
1. Formulation/identification of the scientific problem that need to be clarified. This includes a condensation of the problem to specific scientific questions that is judged to be answerable via experiments	3
2. Planning of the experiments and methodology design, including selection of methods and method development	3
3. Involvement in the experimental work	3
4. Presentation, interpretation and discussion in a journal format of the obtained data	3
Overall contribution	3

Signature of the co-authors:

Dr. Jason B. Scott:

Dr. Frank S. Hay:

Dr. Sarah J. Pethybridge:

Experimental chapter III

Article title: FINE SCALED POPULATION GENETIC ANALYSIS OF *DIDYMELLA TANACETI*

Co-authors: Jason B Scott, Frank S Hay and Sarah J Pethybridge.

Evaluation scale:

1 – has contributed to this work (0-33%)
2 – has made substantial contribution to this work (34-66%)
3 – has made a major contribution to this work (67-100%)

Declaration regarding specific elements	***Extent* (1,2,3)**
1. Formulation/identification of the scientific problem that need to be clarified. This includes a condensation of the problem to specific scientific questions that is judged to be answerable via experiments	3
2. Planning of the experiments and methodology design, including selection of methods and method development	3
3. Involvement in the experimental work	3
4. Presentation, interpretation and discussion in a journal format of the obtained data	3
Overall contribution	3

Signature of the co-authors:

Dr. Jason B. Scott:

Dr. Frank S. Hay:

Dr. Sarah J. Pethybridge:

Experimental chapter IV

Article title: CHARACTERISATION OF BOSCALID SENSITIVITY IN *DIDYMELLA TANACETI.*

Co-authors: Jason B Scott, Calum R Wilson, Frank S Hay and Sarah J Pethybridge.

Evaluation scale:

1 – has contributed to this work (0-33%)
2 – has made substantial contribution to this work (34-66%)
3 – has made a major contribution to this work (67-100%)

Declaration regarding specific elements	***Extent* (1,2,3)**
1. Formulation/identification of the scientific problem that need to be clarified. This includes a condensation of the problem to specific scientific questions that is judged to be answerable via experiments	3
2. Planning of the experiments and methodology design, including selection of methods and method development	3
3. Involvement in the experimental work	3
4. Presentation, interpretation and discussion in a journal format of the obtained data	3
Overall contribution	3

Signature of the co-authors:

Dr. Jason B. Scott:

Assoc. Prof. Calum R. Wilson:

Dr. Frank S. Hay:

Dr. Sarah J. Pethybridge:

APPENDIX II: *DIDYMELLA TANACETI* ISOLATE CODES, COLLECTION DETAILS, MATING-TYPE, MICROSATELLITE MARKER PROFILE AND AMINO ACIDS AT CODONS 277 AND 279 OF THE SUCCINATE DEHYDROGENASE INHIBITOR SUBUNIT B GENE FOR THE POPULATION COLLECTED IN AUGUST 2012.

Isolate code[a]	Collection details[b]				Mating-type[c]	Microsatellite marker[d]								Amino acid *SDHB*[e]	
	Region	Field	T	Dist (m)		SSR05	SSR53	SSR64	SSR58	SSR62	SSR54	SSR32	SSR44	codon 277	codon 279
						Number of loci repeats[f]									
TAS 041-0080	Sassafras	S1	1	0	*MAT1-1*	10	7	8	5	9	7	5	9	Y	I
TAS 041-0082	Sassafras	S1	1	1	*MAT1-1*	11	8	9	13	8	13	8	8	H	I
TAS 041-0083	Sassafras	S1	1	2	*MAT1-1*	11	?	9	13	8	13	8	8	H	I
TAS 041-0084	Sassafras	S1	1	3	*MAT1-2*	11	8	8	5	11	10	8	8	Y	I
TAS 041-0085	Sassafras	S1	1	3.5	*MAT1-1*	7	8	8	5	9	13	8	8	Y	I
TAS 041-0086	Sassafras	S1	1	5	*MAT1-1*	11	8	9	13	8	13	8	8	Y	I
TAS 041-0087	Sassafras	S1	1	5.5	*MAT1-2*	11	8	9	7	11	13	8	8	Y	I
TAS 041-0088	Sassafras	S1	1	6	*MAT1-2*	11	10	8	13	8	10	8	8	Y	I
TAS 041-0089	Sassafras	S1	1	8	*MAT1-1*	7	7	8	13	8	13	8	8	Y	I
TAS 041-0090	Sassafras	S1	1	9	*MAT1-1*	11	8	8	13	8	7	7	8	R	I
TAS 041-0091	Sassafras	S1	1	9.5	*MAT1-2*	11	8	8	26	8	7	8	8	Y	I
TAS 041-0092	Sassafras	S1	1	10	*MAT1-1*	10	7	8	13	9	7	5	8	Y	I
TAS 041-0093	Sassafras	S1	1	11	*MAT1-1* (II)	7	7	8	5	9	7	5	10	Y	I
TAS 041-0094	Sassafras	S1	1	12.5	*MAT1-2*	7	7	8	13	8	13	8	8	Y	I
TAS 041-0095	Sassafras	S1	1	13.5	*MAT1-1*	11	8	8	26	8	13	7	8	Y	I
TAS 041-0096	Sassafras	S1	1	14.5	*MAT1-2*	7	7	8	5	9	6	8	9	R	I
TAS 041-0097	Sassafras	S1	1	15	*MAT1-2*	11	8	9	13	8	10	8	9	Y	I
TAS 041-0098	Sassafras	S1	1	15.5	*MAT1-2*	7	7	?	5	9	6	8	10	R	I
TAS 041-0099	Sassafras	S1	1	16.5	*MAT1-2*	11	8	9	7	11	10	8	8	H	I
TAS 041-0100	Sassafras	S1	1	17	*MAT1-1*	11	8	8	13	9	13	8	8	H	I
TAS 041-0101	Sassafras	S1	1	17.5	*MAT1-1*	11	8	8	13	9	13	8	8	H	I
TAS 041-0102	Sassafras	S1	1	18	*MAT1-1*	11	8	8	13	9	13	8	8	H	I
TAS 041-0103	Sassafras	S1	1	18.5	*MAT1-1*	7	7	8	5	8	13	8	9	H	I

Appendix II *continued.*

Isolate code[a]	Collection details[b]				Mating-type[c]	Microsatellite marker[d]								Amino acid *SDHB*[e]	
	Region	Field	T	Dist (m)		SSR05	SSR53	SSR64	SSR58	SSR62	SSR54	SSR32	SSR44	codon 277	codon 279
						Number of loci repeats[f]									
TAS 041-0104	Sassafras	S1	1	19	*MAT1-1*	7	8	8	5	8	6	8	8	H	I
TAS 041-0105	Sassafras	S1	1	19.5	*MAT1-2*	7	7	8	13	8	13	7	8	Y	I
TAS 041-0106	Sassafras	S1	1	20.5	*MAT1-1*	7	7	8	5	8	13	8	9	H	I
TAS 041-0107	Sassafras	S1	1	21.5	*MAT1-2*	11	8	13	5	8	6	7	9	H	I
TAS 041-0108	Sassafras	S1	1	22.5	*MAT1-2*	10	7	8	5	9	7	5	9	Y	I
TAS 041-0110	Sassafras	S1	1	23.5	*MAT1-1*	7	7	8	5	8	13	8	9	H	I
TAS 041-0111	Sassafras	S1	1	24	*MAT1-2*	7	7	8	5	9	13	7	9	Y	I
TAS 041-0112	Sassafras	S1	1	24.5	*MAT1-1*	7	7	8	5	8	10	7	9	H	I
TAS 041-0113	Sassafras	S1	1	25.5	*MAT1-2*	7	7	8	13	8	13	7	8	Y	I
TAS 041-0114	Sassafras	S1	1	26	*MAT1-2*	11	8	9	5	11	6	7	9	Y	I
TAS 041-0115	Sassafras	S1	1	26.5	*MAT1-2*	7	7	8	13	8	13	7	8	Y	I
TAS 041-0116	Sassafras	S1	1	27	*MAT1-1*	7	7	9	5	8	13	8	8	Y	I
TAS 041-0118	Sassafras	S1	1	29	*MAT1-1*	11	8	9	13	8	13	8	8	H	I
TAS 041-0119	Sassafras	S1	1	29.5	*MAT1-2*	11	8	9	7	11	10	8	8	Y	I
TAS 041-0120	Sassafras	S1	1	31.5	*MAT1-1*	7	7	8	13	8	13	8	8	R	I
TAS 041-0121	Sassafras	S1	1	32.1	*MAT1-2*	10	?	8	26	11	7	7	10	Y	I
TAS 041-0122	Sassafras	S1	1	33	*MAT1-2*	7	7	8	5	9	13	8	8	Y	I
TAS 041-0123	Sassafras	S1	1	33.5	*MAT1-1*	11	8	8	13	9	13	8	8	Y	I
TAS 041-0124	Sassafras	S1	1	34	*MAT1-1*	7	7	8	13	8	13	8	8	H	I
TAS 041-0125	Sassafras	S1	1	34.5	*MAT1-1*	11	8	8	7	8	10	8	9	Y	I
TAS 041-0126	Sassafras	S1	1	35.5	*MAT1-1*	7	7	8	5	9	13	8	8	Y	I
TAS 041-0127	Sassafras	S1	1	36	*MAT1-2*	7	7	8	5	8	13	8	9	Y	I
TAS 041-0128	Sassafras	S1	1	37	*MAT1-2*	11	8	8	5	8	6	8	9	R	I
TAS 041-0129	Sassafras	S1	1	37.5	*MAT1-1*	11	8	9	13	8	13	8	8	H	I
TAS 041-0130	Sassafras	S1	1	38	*MAT1-1*	10	8	9	13	8	13	8	8	H	I

Appendix II *continued.*

Isolate code[a]	Collection details[b]				Mating-type[c]	Microsatellite marker[d]								Amino acid *SDHB*[e]	
	Region	Field	T	Dist (m)		SSR05	SSR53	SSR64	SSR58	SSR62	SSR54	SSR32	SSR44	codon 277	codon 279
						Number of loci repeats[f]									
TAS 041-0132	Sassafras	S1	1	40.5	*MAT1-1*	11	8	9	13	8	13	8	8	H	I
TAS 041-0133	Sassafras	S1	1	41	*MAT1-1*	7	8	8	5	9	6	7	8	Y	I
TAS 041-0134	Sassafras	S1	1	41.5	*MAT1-1*	11	8	8	7	8	13	7	9	H	I
TAS 041-0135	Sassafras	S1	1	42	*MAT1-1*	11	8	9	13	8	13	8	8	Y	I
TAS 041-0136	Sassafras	S1	1	42.5	*MAT1-1*	7	8	8	5	11	6	7	9	H	I
TAS 041-0137	Sassafras	S1	1	43	*MAT1-1*	11	8	8	13	8	13	8	8	Y	I
TAS 041-0138	Sassafras	S1	1	43.5	*MAT1-1*	7	8	8	5	9	13	8	8	Y	I
TAS 041-0139	Sassafras	S1	1	44	*MAT1-1*	7	7	8	13	8	13	8	8	Y	I
TAS 041-0140	Sassafras	S1	1	44.5	*MAT1-2*	11	8	9	7	11	10	8	8	Y	I
TAS 041-0141	Sassafras	S1	1	45	*MAT1-2*	11	8	9	26	8	13	7	10	Y	I
TAS 041-0142	Sassafras	S1	1	46.5	*MAT1-2*	11	7	8	13	8	13	5	8	H	I
TAS 041-0143	Sassafras	S1	1	47	*MAT1-1*	10	8	8	26	9	7	8	8	H	I
TAS 041-0144	Sassafras	S1	1	47.5	*MAT1-2*	7	7	8	5	8	13	8	9	Y	I
TAS 041-0145	Sassafras	S1	1	48	*MAT1-2*	7	7	8	5	9	6	8	9	Y	I
TAS 041-0146	Sassafras	S1	1	48.5	*MAT1-2*	11	8	8	7	11	6	7	9	H	I
TAS 041-0147	Sassafras	S1	2	0.5	*MAT1-2*	11	7	8	5	9	6	8	9	Y	I
TAS 041-0148	Sassafras	S1	2	1	*MAT1-1*	11	7	8	5	9	13	8	10	H	I
TAS 041-0149	Sassafras	S1	2	1.5	*MAT1-1*	11	8	9	13	8	13	8	8	H	I
TAS 041-0150	Sassafras	S1	2	2	*MAT1-2*	11	8	8	13	8	13	8	8	Y	I
TAS 041-0151	Sassafras	S1	2	2.5	*MAT1-2*	7	7	8	13	8	13	8	8	Y	I
TAS 041-0152	Sassafras	S1	2	4.5	*MAT1-1*	11	10	8	7	8	13	8	8	Y	I
TAS 041-0153	Sassafras	S1	2	5	*MAT1-2*	7	7	8	5	8	13	8	9	Y	I
TAS 041-0154	Sassafras	S1	2	5.5	*MAT1-2*	7	7	8	13	9	6	8	9	H	I
TAS 041-0155	Sassafras	S1	2	6	*MAT1-1*	10	8	8	26	11	7	7	10	Y	I
TAS 041-0156	Sassafras	S1	2	6.5	*MAT1-1* (II)	7	7	8	5	8	13	5	9	Y	I

Appendix II *continued.*

Isolate code[a]	Collection details[b]				Mating-type[c]	Microsatellite marker[d]								Amino acid *SDHB*[e]	
	Region	Field	T	Dist (m)		SSR05	SSR53	SSR64	SSR58	SSR62	SSR54	SSR32	SSR44	codon 277	codon 279
						Number of loci repeats[f]									
TAS 041-0157	Sassafras	S1	2	7	*MAT1-1*	11	8	9	13	8	13	8	8	H	I
TAS 041-0158	Sassafras	S1	2	7.5	*MAT1-2*	11	8	8	5	11	6	7	9	H	I
TAS 041-0159	Sassafras	S1	2	8	*MAT1-2*	7	7	8	5	8	13	8	9	Y	I
TAS 041-0161	Sassafras	S1	2	11	*MAT1-1*	7	7	8	5	9	13	8	8	H	I
TAS 041-0162	Sassafras	S1	2	11.5	*MAT1-1*	7	7	8	13	8	13	8	8	H	I
TAS 041-0163	Sassafras	S1	2	12	*MAT1-1*	11	7	9	5	8	13	8	8	H	I
TAS 041-0164	Sassafras	S1	2	12.5	*MAT1-1*	7	7	8	5	8	13	7	9	Y	I
TAS 041-0165	Sassafras	S1	2	13.5	*MAT1-2*	11	8	8	26	8	13	7	8	Y	I
TAS 041-0166	Sassafras	S1	2	14	*MAT1-1*	11	8	8	7	8	10	8	10	Y	I
TAS 041-0167	Sassafras	S1	2	16.5	*MAT1-2*	11	7	8	13	9	10	8	9	Y	I
TAS 041-0169	Sassafras	S1	2	18	*MAT1-1*	7	7	8	5	9	13	8	8	H	I
TAS 041-0170	Sassafras	S1	2	18.5	*MAT1-2*	11	8	9	13	8	10	8	9	H	I
TAS 041-0171	Sassafras	S1	2	19	*MAT1-1*	11	8	8	13	8	7	8	8	H	I
TAS 041-0172	Sassafras	S1	2	19.5	*MAT1-1*	11	10	8	5	8	13	8	8	H	I
TAS 041-0173	Sassafras	S1	2	20	*MAT1-1*	11	8	8	7	11	7	7	10	Y	I
TAS 041-0174	Sassafras	S1	2	21	*MAT1-2*	11	8	9	13	8	13	7	9	H	I
TAS 041-0175	Sassafras	S1	2	21.5	*MAT1-1*	11	8	8	13	8	13	8	8	Y	I
TAS 041-0176	Sassafras	S1	2	22.5	*MAT1-2*	7	7	8	5	8	13	8	9	Y	I
TAS 041-0177	Sassafras	S1	2	23.5	*MAT1-2*	11	8	8	5	11	6	8	9	Y	I
TAS 041-0178	Sassafras	S1	2	24	*MAT1-2*	11	7	8	5	9	6	8	9	H	I
TAS 041-0179	Sassafras	S1	2	26	*MAT1-1*	7	7	8	13	8	13	8	8	Y	I
TAS 041-0180	Sassafras	S1	2	29.5	*MAT1-2*	7	7	8	5	8	13	8	9	Y	I
TAS 041-0181	Sassafras	S1	2	30	*MAT1-1*	7	7	8	13	8	13	7	8	Y	I
TAS 041-0182	Sassafras	S1	2	30.5	*MAT1-2*	7	7	8	5	8	13	8	9	Y	I
TAS 041-0183	Sassafras	S1	2	31	*MAT1-2*	11	8	9	5	11	10	8	8	Y	I

Appendix II *continued.*

Isolate code[a]	Collection details[b]				Mating-type[c]	Microsatellite marker[d]								Amino acid *SDHB*[e]	
	Region	Field	T	Dist (m)		SSR05	SSR53	SSR64	SSR58	SSR62	SSR54	SSR32	SSR44	codon 277	codon 279
						Number of loci repeats[f]									
TAS 041-0184	Sassafras	S1	2	34	*MAT1-1*	11	7	8	5	9	13	8	9	H	I
TAS 041-0185	Sassafras	S1	2	35.5	*MAT1-1*	11	8	8	13	9	6	8	8	Y	I
TAS 041-0186	Sassafras	S1	2	36.5	*MAT1-2*	11	10	8	5	8	13	8	9	H	I
TAS 041-0187	Sassafras	S1	2	38	*MAT1-2*	11	7	8	5	8	13	8	8	Y	I
TAS 041-0188	Sassafras	S1	2	39	*MAT1-1* (II)	7	7	8	5	6	7	5	10	H	I
TAS 041-0189	Sassafras	S1	2	39.5	*MAT1-1*	7	7	8	5	9	13	7	9	Y	I
TAS 041-0190	Sassafras	S1	2	40	*MAT1-2*	11	8	8	7	8	13	8	8	H	I
TAS 041-0191	Sassafras	S1	2	41	*MAT1-2*	7	7	8	13	8	13	8	8	Y	I
TAS 041-0192	Sassafras	S1	2	43.5	*MAT1-1*	11	8	8	5	8	9	8	9	Y	I
TAS 041-0193	Sassafras	S1	2	44.5	*MAT1-1*	11	8	9	13	8	13	8	8	H	I
TAS 041-0194	Sassafras	S1	2	45	*MAT1-1*	11	8	8	5	8	13	8	10	Y	I
TAS 041-0196	Sassafras	S1	2	46.5	*MAT1-1*	11	8	9	13	8	13	8	8	Y	I
TAS 041-0197	Sassafras	S1	2	47	*MAT1-2*	7	7	8	13	8	13	8	8	Y	I
TAS 041-0198	Sassafras	S1	2	48	*MAT1-1*	11	7	8	7	9	13	8	9	H	I
TAS 041-0200	Sassafras	S2	1	5	*MAT1-1*	11	8	9	13	8	13	8	8	H	I
TAS 041-0201	Sassafras	S2	1	6	*MAT1-1*	11	8	9	7	8	13	8	8	H	I
TAS 041-0202	Sassafras	S2	1	6.5	*MAT1-1*	11	8	9	13	8	13	8	8	R	I
TAS 041-0203	Sassafras	S2	1	7	*MAT1-1*	11	8	8	13	8	9	8	8	H	I
TAS 041-0204	Sassafras	S2	1	9	*MAT1-1*	7	7	8	5	8	13	8	9	H	I
TAS 041-0205	Sassafras	S2	1	11.5	*MAT1-1*	7	7	8	5	8	6	8	9	H	I
TAS 041-0206	Sassafras	S2	1	12.5	*MAT1-2*	7	7	8	13	8	13	7	9	H	I
TAS 041-0208	Sassafras	S2	1	16.5	*MAT1-1*	7	7	8	5	8	13	8	9	H	I
TAS 041-0209	Sassafras	S2	1	17	*MAT1-2*	7	7	8	5	8	13	8	9	H	I
TAS 041-0210	Sassafras	S2	1	18	*MAT1-1*	11	8	8	13	8	13	8	8	H	I
TAS 041-0211	Sassafras	S2	1	18.5	*MAT1-1*	11	8	8	13	8	13	8	8	Y	I

Appendix II *continued.*

Isolate code[a]	Collection details[b]				Mating-type[c]	Microsatellite marker[d]								Amino acid *SDHB*[e]	
	Region	Field	T	Dist (m)		SSR05	SSR53	SSR64	SSR58	SSR62	SSR54	SSR32	SSR44	codon 277	codon 279
						Number of loci repeats[f]									
TAS 041-0212	Sassafras	S2	1	19.5	*MAT1-1* (II)	10	7	8	5	8	7	7	9	Y	I
TAS 041-0214	Sassafras	S2	1	21.5	*MAT1-1*	7	7	8	5	8	13	8	9	Y	I
TAS 041-0215	Sassafras	S2	1	25	*MAT1-2*	11	8	9	26	8	13	7	9	Y	I
TAS 041-0216	Sassafras	S2	1	25.5	*MAT1-1*	11	7	8	5	9	13	8	9	H	I
TAS 041-0217	Sassafras	S2	1	26	*MAT1-1*	10	7	8	26	9	6	7	9	Y	I
TAS 041-0219	Sassafras	S2	1	34.5	*MAT1-2*	7	7	8	5	8	13	8	9	Y	I
TAS 041-0221	Sassafras	S2	1	36.5	*MAT1-2*	7	7	8	5	8	13	8	9	Y	I
TAS 041-0222	Sassafras	S2	1	38.5	*MAT1-1*	11	8	9	13	8	13	8	8	H	I
TAS 041-0223	Sassafras	S2	1	42.5	*MAT1-2*	7	7	8	5	8	13	7	9	H	I
TAS 041-0224	Sassafras	S2	1	43	*MAT1-1*	11	8	9	13	8	13	8	8	Y	I
TAS 041-0227	Sassafras	S2	1	47	*MAT1-2*	11	8	8	13	8	10	8	8	H	V
TAS 041-0229	Sassafras	S2	2	0	*MAT1-2*	11	8	8	5	11	6	8	9	Y	I
TAS 041-0230	Sassafras	S2	2	0.5	*MAT1-2*	11	7	8	5	8	13	8	8	Y	I
TAS 041-0231	Sassafras	S2	2	1	*MAT1-2*	11	8	8	13	8	13	8	8	H	I
TAS 041-0233	Sassafras	S2	2	2.5	*MAT1-2*	11	8	8	13	8	13	7	8	H	I
TAS 041-0234	Sassafras	S2	2	3	*MAT1-1*	11	8	8	13	8	10	7	8	H	I
TAS 041-0235	Sassafras	S2	2	3.5	*MAT1-2*	11	8	8	13	8	10	8	8	H	V
TAS 041-0237	Sassafras	S2	2	5	*MAT1-2*	7	7	8	5	8	13	8	9	Y	I
TAS 041-0238	Sassafras	S2	2	5.5	*MAT1-1*	11	8	8	13	8	13	8	8	H	I
TAS 041-0239	Sassafras	S2	2	6	*MAT1-1*	11	10	8	5	8	13	8	8	Y	I
TAS 041-0241	Sassafras	S2	2	7	*MAT1-1*	11	7	8	26	9	13	8	10	Y	I
TAS 041-0242	Sassafras	S2	2	8	*MAT1-2*	11	8	8	13	9	13	8	9	Y	I
TAS 041-0244	Sassafras	S2	2	11	*MAT1-1*	11	8	9	13	8	13	8	8	H	I
TAS 041-0245	Sassafras	S2	2	11.5	*MAT1-1*	11	8	8	13	9	13	8	8	H	I
TAS 041-0246	Sassafras	S2	2	12	*MAT1-1*	11	8	8	13	9	6	8	8	Y	I

Appendix II *continued.*

Isolate code[a]	Collection details[b]				Mating-type[c]	Microsatellite marker[d]								Amino acid *SDHB*[e]	
	Region	Field	T	Dist (m)		SSR05	SSR53	SSR64	SSR58	SSR62	SSR54	SSR32	SSR44	codon 277	codon 279
						Number of loci repeats[f]									
TAS 041-0248	Sassafras	S2	2	14.5	*MAT1-1*	11	8	9	13	8	13	8	8	H	I
TAS 041-0250	Sassafras	S2	2	17.5	*MAT1-1*	7	7	8	5	8	6	8	9	R	I
TAS 041-0251	Sassafras	S2	2	19.5	*MAT1-1*	11	7	8	5	9	13	8	9	H	I
TAS 041-0252	Sassafras	S2	2	20	*MAT1-1*	7	7	8	5	8	6	7	9	R	I
TAS 041-0253	Sassafras	S2	2	21.5	*MAT1-2*	11	8	8	13	8	10	8	8	H	V
TAS 041-0254	Sassafras	S2	2	25	*MAT1-2*	11	8	8	13	8	10	8	8	H	V
TAS 041-0255	Sassafras	S2	2	26	*MAT1-1*	7	7	8	5	9	13	8	8	H	I
TAS 041-0256	Sassafras	S2	2	27.5	*MAT1-1*	11	8	8	26	9	7	8	8	Y	I
TAS 041-0257	Sassafras	S2	2	29	*MAT1-1* (II)	13	7	8	26	9	7	5	8	H	I
TAS 041-0258	Sassafras	S2	2	29.5	*MAT1-2*	7	7	8	13	9	6	8	8	Y	I
TAS 041-0259	Sassafras	S2	2	30.5	*MAT1-2*	11	8	8	5	11	6	7	10	H	I
TAS 041-0260	Sassafras	S2	2	31.5	*MAT1-2*	11	8	8	13	8	7	8	8	Y	I
TAS 041-0261	Sassafras	S2	2	32	*MAT1-2*	11	8	8	13	8	7	8	8	Y	I
TAS 041-0262	Sassafras	S2	2	34.5	*MAT1-2*	7	8	8	13	8	6	?	8	H	I
TAS 041-0263	Sassafras	S2	2	35	*MAT1-1*	11	8	8	13	8	7	8	8	Y	I
TAS 041-0264	Sassafras	S2	2	35.5	*MAT1-1*	11	8	8	26	9	7	8	8	H	I
TAS 041-0265	Sassafras	S2	2	36.5	*MAT1-2*	11	10	9	7	8	13	8	9	H	I
TAS 041-0266	Sassafras	S2	2	37	*MAT1-1*	7	7	?	5	?	6	7	9	H	I
TAS 041-0267	Sassafras	S2	2	37.5	*MAT1-1*	11	8	9	13	8	13	8	8	H	V
TAS 041-0268	Sassafras	S2	2	38	*MAT1-1*	11	8	9	13	8	13	8	8	H	I
TAS 041-0270	Sassafras	S2	2	42	*MAT1-1*	7	7	8	5	8	6	8	9	H	I
TAS 041-0271	Sassafras	S2	2	42.5	*MAT1-2*	7	7	8	5	8	13	8	9	Y	I
TAS 041-0272	Sassafras	S2	2	43.5	*MAT1-2*	7	7	8	5	8	13	8	9	Y	I
TAS 041-0273	Sassafras	S2	2	44	*MAT1-2*	7	7	8	5	8	13	8	9	Y	I
TAS 041-0274	Sassafras	S2	2	44.5	*MAT1-2*	11	8	8	26	8	7	8	8	H	I

Appendix II *continued.*

Isolate code[a]	Collection details[b]				Mating-type[c]	Microsatellite marker[d]								Amino acid *SDHB*[e]	
	Region	Field	T	Dist (m)		SSR05	SSR53	SSR64	SSR58	SSR62	SSR54	SSR32	SSR44	codon 277	codon 279
						Number of loci repeats[f]									
TAS 041-0275	Sassafras	S2	2	45	*MAT1-2*	11	8	8	7	11	10	8	10	R	I
TAS 041-0276	Sassafras	S2	2	45.5	*MAT1-1*	11	8	8	26	8	13	8	10	H	I
TAS 041-0277	Sassafras	S2	2	46	*MAT1-1*	11	8	8	13	8	13	8	8	Y	I
TAS 041-0279	Sassafras	S2	2	47	*MAT1-2*	11	7	8	5	8	13	8	8	Y	I
TAS 041-0281	Sassafras	S2	2	48	*MAT1-2*	11	7	8	5	8	13	8	8	Y	I
TAS 041-0282	Sassafras	S2	2	49.5	*MAT1-1*	7	8	8	5	8	6	7	9	H	I
TAS 041-0284	Sassafras	S2	2	50	*MAT1-1*	7	8	8	5	8	6	7	9	H	I
TAS 041-0286	Table Cape	TC1	1	0	*MAT1-1*	7	7	8	13	8	13	8	8	H	I
TAS 041-0287	Table Cape	TC1	1	0.6	*MAT1-1*	11	8	8	5	8	10	8	9	Y	I
TAS 041-0288	Table Cape	TC1	1	2	*MAT1-2*	11	7	8	5	9	13	7	9	Y	I
TAS 041-0289	Table Cape	TC1	1	2.5	*MAT1-2*	11	7	8	5	9	13	8	9	R	I
TAS 041-0290	Table Cape	TC1	1	3.5	*MAT1-1*	11	8	8	5	8	10	8	9	Y	I
TAS 041-0291	Table Cape	TC1	1	4.5	*MAT1-2*	11	7	8	5	9	13	8	9	Y	I
TAS 041-0292	Table Cape	TC1	1	5	*MAT1-1*	11	8	8	7	8	10	8	9	Y	I
TAS 041-0293	Table Cape	TC1	1	6	*MAT1-2*	7	7	8	5	9	13	7	9	H	I
TAS 041-0294	Table Cape	TC1	1	7.5	*MAT1-2*	7	7	8	13	8	13	8	8	R	I
TAS 041-0295	Table Cape	TC1	1	7.9	*MAT1-2*	11	7	8	5	9	13	8	9	Y	I
TAS 041-0296	Table Cape	TC1	1	9	*MAT1-2*	7	7	8	5	9	13	8	9	Y	I
TAS 041-0297	Table Cape	TC1	1	9.5	*MAT1-2*	11	8	8	13	8	6	8	8	H	I
TAS 041-0299	Table Cape	TC1	1	10.5	*MAT1-2*	7	8	8	5	8	13	7	8	H	I
TAS 041-0300	Table Cape	TC1	1	11	*MAT1-1*	11	10	9	7	8	13	8	8	R	I
TAS 041-0301	Table Cape	TC1	1	12	*MAT1-2*	7	7	8	13	8	13	7	8	H	I
TAS 041-0302	Table Cape	TC1	1	13	*MAT1-2*	7	8	8	5	9	13	7	8	Y	I
TAS 041-0303	Table Cape	TC1	1	13.5	*MAT1-1*	11	7	8	13	8	6	8	9	Y	I
TAS 041-0304	Table Cape	TC1	1	14.5	*MAT1-1*	11	8	9	26	8	13	8	8	Y	I

Appendix II *continued.*

Isolate code[a]	Collection details[b]				Mating-type[c]	Microsatellite marker[d]								Amino acid *SDHB*[e]	
	Region	Field	T	Dist (m)		SSR05	SSR53	SSR64	SSR58	SSR62	SSR54	SSR32	SSR44	codon 277	codon 279
						Number of loci repeats[f]									
TAS 041-0305	Table Cape	TC1	1	15	*MAT1-1*	11	10	9	13	8	6	8	9	Y	I
TAS 041-0306	Table Cape	TC1	1	15.5	*MAT1-1*	11	8	8	5	8	7	8	8	Y	I
TAS 041-0307	Table Cape	TC1	1	17	*MAT1-1*	11	7	8	13	8	7	8	9	Y	I
TAS 041-0308	Table Cape	TC1	1	17.5	*MAT1-1*	11	10	9	5	8	6	7	9	Y	I
TAS 041-0309	Table Cape	TC1	1	18	*MAT1-2*	11	8	8	13	8	10	8	9	Y	I
TAS 041-0310	Table Cape	TC1	1	19	*MAT1-2*	11	7	8	13	9	13	7	9	Y	I
TAS 041-0311	Table Cape	TC1	1	20	*MAT1-2*	11	7	8	5	9	13	7	9	Y	I
TAS 041-0312	Table Cape	TC1	1	20.5	*MAT1-2*	7	8	8	13	9	13	8	8	H	I
TAS 041-0313	Table Cape	TC1	1	21.5	*MAT1-2*	11	7	8	5	9	13	8	9	Y	I
TAS 041-0314	Table Cape	TC1	1	22	*MAT1-2*	7	7	8	13	8	13	8	9	Y	I
TAS 041-0315	Table Cape	TC1	1	22.5	*MAT1-2*	7	7	8	26	8	13	8	8	H	I
TAS 041-0317	Table Cape	TC1	1	24.5	*MAT1-2*	7	7	8	13	8	13	7	8	Y	I
TAS 041-0318	Table Cape	TC1	1	25	*MAT1-2*	7	7	8	5	8	13	8	9	H	I
TAS 041-0319	Table Cape	TC1	1	25.5	*MAT1-2*	7	7	8	5	8	13	8	9	Y	I
TAS 041-0320	Table Cape	TC1	1	26	*MAT1-1*	11	8	8	5	9	7	8	8	H	I
TAS 041-0322	Table Cape	TC1	1	27.5	*MAT1-2*	7	7	8	5	8	13	7	8	Y	I
TAS 041-0323	Table Cape	TC1	1	29.1	*MAT1-1*	11	8	8	5	8	10	8	9	Y	I
TAS 041-0324	Table Cape	TC1	1	31	*MAT1-2*	11	8	9	13	8	10	8	9	Y	I
TAS 041-0325	Table Cape	TC1	1	32	*MAT1-2*	7	7	8	5	9	13	7	9	Y	I
TAS 041-0326	Table Cape	TC1	1	33	*MAT1-1*	7	7	8	13	8	13	8	8	R	I
TAS 041-0328	Table Cape	TC1	1	35.5	*MAT1-2*	7	7	8	13	8	13	8	9	H	I
TAS 041-0329	Table Cape	TC1	1	36.5	*MAT1-1*	11	7	8	5	8	6	7	9	Y	I
TAS 041-0330	Table Cape	TC1	1	37	*MAT1-1*	11	10	9	5	8	6	8	9	H	I
TAS 041-0331	Table Cape	TC1	1	38	*MAT1-1*	7	7	8	13	8	13	8	8	R	I
TAS 041-0332	Table Cape	TC1	1	38.4	*MAT1-2*	11	7	8	5	8	13	8	8	H	I

Appendix II *continued.*

Isolate code[a]	Collection details[b]				Mating-type[c]	Microsatellite marker[d]								Amino acid *SDHB*[e]	
	Region	Field	T	Dist (m)		SSR05	SSR53	SSR64	SSR58	SSR62	SSR54	SSR32	SSR44	codon 277	codon 279
						Number of loci repeats[f]									
TAS 041-0333	Table Cape	TC1	1	39	*MAT1-2*	11	7	8	5	8	13	8	8	Y	I
TAS 041-0334	Table Cape	TC1	1	39.5	*MAT1-1*	7	7	8	13	8	13	8	8	H	I
TAS 041-0335	Table Cape	TC1	1	40	*MAT1-1*	11	10	8	13	8	13	7	?	H	I
TAS 041-0336	Table Cape	TC1	1	40.4	*MAT1-2*	11	7	8	13	8	13	8	9	R	I
TAS 041-0337	Table Cape	TC1	1	41.5	*MAT1-2*	11	8	9	13	8	10	8	9	Y	I
TAS 041-0338	Table Cape	TC1	1	42	*MAT1-1*	11	7	8	5	8	6	8	9	Y	I
TAS 041-0339	Table Cape	TC1	1	43	*MAT1-2*	11	7	8	13	8	13	8	9	R	I
TAS 041-0340	Table Cape	TC1	1	46	*MAT1-1*	11	8	8	5	8	10	8	9	H	I
TAS 041-0341	Table Cape	TC1	1	47	*MAT1-2*	11	8	8	26	8	7	8	10	Y	I
TAS 041-0342	Table Cape	TC1	1	48.5	*MAT1-2*	7	7	8	13	8	13	8	9	Y	I
TAS 041-0343	Table Cape	TC1	1	49.5	*MAT1-2*	11	7	8	13	8	13	8	9	h	I
TAS 041-0344	Table Cape	TC1	1	50	*MAT1-2*	11	7	8	7	8	13	8	9	R	I
TAS 041-0345	Table Cape	TC1	2	0	*MAT1-2*	11	8	9	13	8	10	8	9	Y	I
TAS 041-0346	Table Cape	TC1	2	1.5	*MAT1-1*	11	10	8	5	8	13	8	8	Y	I
TAS 041-0347	Table Cape	TC1	2	2	*MAT1-2*	11	8	8	13	8	10	8	9	Y	I
TAS 041-0348	Table Cape	TC1	2	2.5	*MAT1-1*	11	7	8	7	8	13	8	8	Y	I
TAS 041-0349	Table Cape	TC1	2	3.5	*MAT1-2*	7	7	8	5	8	13	8	9	H	I
TAS 041-0350	Table Cape	TC1	2	4	*MAT1-2*	11	8	9	13	8	10	8	9	Y	I
TAS 041-0351	Table Cape	TC1	2	4.5	*MAT1-2*	11	7	8	5	9	13	7	9	Y	I
TAS 041-0352	Table Cape	TC1	2	6	*MAT1-2*	7	7	8	5	9	13	7	9	Y	I
TAS 041-0353	Table Cape	TC1	2	8.5	*MAT1-2*	11	7	8	5	9	13	7	9	Y	I
TAS 041-0354	Table Cape	TC1	2	9.5	*MAT1-1*	7	7	8	13	8	13	8	8	H	I
TAS 041-0355	Table Cape	TC1	2	10	*MAT1-1*	11	8	8	7	8	10	8	9	Y	I
TAS 041-0356	Table Cape	TC1	2	10.5	*MAT1-2*	7	7	8	5	8	13	8	9	Y	I
TAS 041-0357	Table Cape	TC1	2	11	*MAT1-2*	7	7	8	5	8	13	8	9	Y	I

Appendix II *continued.*

Isolate code[a]	Collection details[b]				Mating-type[c]	Microsatellite marker[d]								Amino acid *SDHB*[e]	
	Region	Field	T	Dist (m)		SSR05	SSR53	SSR64	SSR58	SSR62	SSR54	SSR32	SSR44	codon 277	codon 279
						Number of loci repeats[f]									
TAS 041-0358	Table Cape	TC1	2	12	*MAT1-1*	11	8	9	13	8	13	8	8	H	I
TAS 041-0359	Table Cape	TC1	2	12.5	*MAT1-2*	11	7	8	5	9	13	7	9	Y	I
TAS 041-0360	Table Cape	TC1	2	13	*MAT1-2*	7	7	9	13	8	13	7	8	Y	I
TAS 041-0361	Table Cape	TC1	2	16.5	*MAT1-2*	7	7	8	5	9	13	7	9	H	I
TAS 041-0362	Table Cape	TC1	2	17	*MAT1-1*	11	7	8	5	8	13	8	8	H	I
TAS 041-0363	Table Cape	TC1	2	17.5	*MAT1-2*	11	8	9	26	8	13	7	10	Y	I
TAS 041-0364	Table Cape	TC1	2	18	*MAT1-2*	11	7	8	13	8	13	8	9	R	I
TAS 041-0365	Table Cape	TC1	2	19	*MAT1-2*	7	7	8	5	8	13	8	9	H	I
TAS 041-0366	Table Cape	TC1	2	19.5	*MAT1-2*	11	8	8	26	8	7	8	8	Y	I
TAS 041-0367	Table Cape	TC1	2	20	*MAT1-2*	7	7	8	5	9	13	8	9	H	I
TAS 041-0368	Table Cape	TC1	2	20.5	*MAT1-2*	7	7	8	13	8	13	7	8	Y	I
TAS 041-0370	Table Cape	TC1	2	21.5	*MAT1-1*	11	8	8	7	11	6	7	9	H	I
TAS 041-0371	Table Cape	TC1	2	22	*MAT1-1*	11	7	8	5	8	13	8	8	R	I
TAS 041-0372	Table Cape	TC1	2	23	*MAT1-1*	11	10	9	7	8	6	7	9	H	I
TAS 041-0373	Table Cape	TC1	2	23.5	*MAT1-1*	11	8	8	13	8	6	7	8	Y	I
TAS 041-0374	Table Cape	TC1	2	24.5	*MAT1-2*	11	8	9	13	8	9	8	9	Y	I
TAS 041-0375	Table Cape	TC1	2	28	*MAT1-2*	11	7	8	5	9	13	7	9	Y	I
TAS 041-0376	Table Cape	TC1	2	29	*MAT1-1*	11	7	8	5	8	13	8	8	H	I
TAS 041-0377	Table Cape	TC1	2	31	*MAT1-2*	11	7	8	5	9	13	7	9	Y	I
TAS 041-0378	Table Cape	TC1	2	32.5	*MAT1-2*	11	8	8	13	8	10	8	9	Y	I
TAS 041-0379	Table Cape	TC1	2	33	*MAT1-1*	7	7	8	5	9	13	8	8	H	I
TAS 041-0380	Table Cape	TC1	2	33.5	*MAT1-1*	7	7	8	5	8	13	8	9	H	I
TAS 041-0381	Table Cape	TC1	2	35.5	*MAT1-2*	11	7	8	13	8	13	8	9	R	I
TAS 041-0383	Table Cape	TC1	2	37.5	*MAT1-2*	11	7	8	5	9	13	7	9	Y	I
TAS 041-0384	Table Cape	TC1	2	38	*MAT1-2*	7	8	8	5	9	13	7	8	Y	I

Appendix II *continued.*

Isolate code[a]	Collection details[b]				Mating-type[c]	Microsatellite marker[d]								Amino acid *SDHB*[e]	
	Region	Field	T	Dist (m)		SSR05	SSR53	SSR64	SSR58	SSR62	SSR54	SSR32	SSR44	codon 277	codon 279
						Number of loci repeats[f]									
TAS 041-0385	Table Cape	TC1	2	38.5	*MAT1-2*	11	7	8	5	9	13	7	9	Y	I
TAS 041-0386	Table Cape	TC1	2	39.5	*MAT1-1*	11	10	9	7	8	6	7	9	H	I
TAS 041-0387	Table Cape	TC1	2	40	*MAT1-2*	11	8	9	13	8	10	8	9	Y	I
TAS 041-0388	Table Cape	TC1	2	41.5	*MAT1-1*	11	7	8	7	8	7	7	9	Y	I
TAS 041-0389	Table Cape	TC1	2	46	*MAT1-2*	7	7	8	13	8	13	7	8	Y	I
TAS 041-0390	Table Cape	TC1	2	47	*MAT1-1*	11	8	8	26	8	7	8	8	H	I
TAS 041-0391	Table Cape	TC1	2	48	*MAT1-1*	11	8	8	13	8	13	8	8	H	I
TAS 041-0392	Table Cape	TC1	2	48.5	*MAT1-2*	7	7	8	5	9	13	7	8	H	I
TAS 041-0394	Table Cape	TC2	1	0	*MAT1-1*	11	7	8	5	8	6	7	9	Y	I
TAS 041-0395	Table Cape	TC2	1	2	*MAT1-2*	11	7	8	5	8	6	7	9	H	I
TAS 041-0396	Table Cape	TC2	1	2.5	*MAT1-2*	11	8	9	13	8	10	8	9	Y	I
TAS 041-0398	Table Cape	TC2	1	6.5	*MAT1-2*	11	7	8	5	8	13	7	9	Y	I
TAS 041-0399	Table Cape	TC2	1	7	*MAT1-1*	7	7	8	5	8	13	8	9	H	I
TAS 041-0400	Table Cape	TC2	1	8.5	*MAT1-1*	11	10	8	7	8	13	8	8	Y	I
TAS 041-0401	Table Cape	TC2	1	10	*MAT1-1*	7	8	8	5	9	13	8	8	Y	I
TAS 041-0402	Table Cape	TC2	1	11.5	*MAT1-2*	11	7	8	5	8	13	8	8	Y	I
TAS 041-0403	Table Cape	TC2	1	12	*MAT1-2*	7	8	8	5	9	13	7	8	H	I
TAS 041-0405	Table Cape	TC2	1	16	*MAT1-2*	11	8	9	13	8	10	8	9	H	I
TAS 041-0407	Table Cape	TC2	1	20	*MAT1-1*	11	8	9	13	8	13	8	8	R	I
TAS 041-0408	Table Cape	TC2	1	24.5	*MAT1-2*	11	8	9	13	8	10	8	9	Y	I
TAS 041-0409	Table Cape	TC2	1	25.5	*MAT1-1*	11	8	8	13	8	6	8	8	Y	I
TAS 041-0410	Table Cape	TC2	1	26	*MAT1-2*	7	8	8	5	9	13	7	8	Y	I
TAS 041-0411	Table Cape	TC2	1	27	*MAT1-1*	11	8	9	26	9	7	8	8	H	I
TAS 041-0412	Table Cape	TC2	1	28	*MAT1-2*	7	7	8	5	9	10	7	9	Y	I
TAS 041-0414	Table Cape	TC2	1	29.5	*MAT1-2*	7	7	8	13	9	13	7	8	R	I

Appendix II *continued.*

Isolate code[a]	Collection details[b]				Mating-type[c]	Microsatellite marker[d]								Amino acid *SDHB*[e]	
	Region	Field	T	Dist (m)		SSR05	SSR53	SSR64	SSR58	SSR62	SSR54	SSR32	SSR44	codon 277	codon 279
						Number of loci repeats[f]									
TAS 041-0415	Table Cape	TC2	1	31	*MAT1-2*	7	7	8	5	8	13	8	9	H	I
TAS 041-0416	Table Cape	TC2	1	32.5	*MAT1-2*	11	8	9	13	8	10	8	9	R	I
TAS 041-0418	Table Cape	TC2	1	36	*MAT1-2*	11	7	8	5	9	13	7	9	Y	I
TAS 041-0419	Table Cape	TC2	1	38	*MAT1-2*	11	7	8	13	8	6	8	9	Y	I
TAS 041-0421	Table Cape	TC2	1	41.5	*MAT1-1*	11	8	8	13	8	10	8	8	Y	I
TAS 041-0422	Table Cape	TC2	1	42	*MAT1-2*	11	8	8	13	9	6	7	8	Y	I
TAS 041-0423	Table Cape	TC2	1	44	*MAT1-2*	11	8	9	13	8	10	8	9	H	I
TAS 041-0424	Table Cape	TC2	1	45.5	*MAT1-2*	7	7	8	13	8	13	7	9	R	I
TAS 041-0426	Table Cape	TC2	2	0.5	*MAT1-2*	7	7	9	5	8	13	7	9	H	I
TAS 041-0427	Table Cape	TC2	2	1	*MAT1-1*	11	10	9	5	8	13	7	8	H	I
TAS 041-0428	Table Cape	TC2	2	6	*MAT1-2*	11	7	8	5	9	13	7	9	Y	I
TAS 041-0429	Table Cape	TC2	2	7.5	*MAT1-1*	7	7	8	13	8	13	8	8	H	I
TAS 041-0431	Table Cape	TC2	2	8.5	*MAT1-1*	11	8	8	13	8	6	7	8	Y	I
TAS 041-0432	Table Cape	TC2	2	11	*MAT1-2*	11	8	9	13	8	10	8	9	H	I
TAS 041-0434	Table Cape	TC2	2	12	*MAT1-2*	7	8	8	5	9	13	7	8	H	I
TAS 041-0435	Table Cape	TC2	2	12.5	*MAT1-1*	11	8	8	13	8	7	7	8	H	I
TAS 041-0439	Table Cape	TC2	2	20	*MAT1-2*	7	7	8	5	8	13	8	9	H	I
TAS 041-0440	Table Cape	TC2	2	23	*MAT1-1*	7	8	8	5	9	13	8	8	Y	I
TAS 041-0441	Table Cape	TC2	2	25.5	*MAT1-1*	11	10	8	13	8	6	7	9	H	I
TAS 041-0442	Table Cape	TC2	2	26.5	*MAT1-1*	11	8	8	13	8	6	5	8	Y	I
TAS 041-0447	Table Cape	TC2	2	36.5	*MAT1-2*	7	8	8	5	8	13	8	9	H	I
TAS 041-0454	Table Cape	TC2	2	47	*MAT1-2*	11	7	8	5	9	13	7	9	Y	I
TAS 041-0455	Table Cape	TC2	2	47.5	*MAT1-1*	11	8	9	13	8	13	7	8	H	I
TAS 041-0456	Table Cape	TC2	2	48.5	*MAT1-2*	7	8	8	5	9	13	7	8	H	I
TAS 041-0457	Table Cape	TC2	2	48	*MAT1-1*	11	8	9	13	8	13	8	8	Y	I

[a] Isolates stored in the Tasmanian Institute of Agriculture fungal collection, Tasmania, Australia. All isolates originally recovered from Tasmanian pyrethrum leaves in July/August 2012.

[b] Region = region in Tasmania from which fields were sampled; Field = S1 and S2 were located in Sassafras, Tasmania and TC1 and TC2 were located in Table Cape, Tasmania; T= transect number (two per field) ; Dist = distance (m) along the 50 m transect in which individuals were located.

[c] *MAT1-1* = contains haplotype I of *MAT1-1-1* mating type gene; *MAT1-1* (II) = contains haplotype II of *MAT1-1-1* mating type gene; *MAT1-2* = contains *MAT1-2-1* mating type gene.

[d] Microsatellite markers used to genotype the population.

[e] Amino acid codes; codon 277: H = histidine (wild type); Y = tyrosine; R = arginine; codon 279: I = isoleucine (wild type); V = valine. (

[f] Genotyped using high resolution melt analysis.